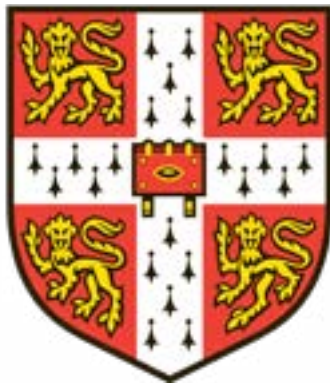


The hormonal regulation of PIN protein localisation and its relevance to shoot architecture



Anthony John Bridgen

Department of Plant Sciences
University of Cambridge

This thesis is submitted for the degree of
Doctor of Philosophy

Gonville and Caius College

March 2022

For my father

~

Bertram John Bridgen

A proud man

"I saw my life branching out before me like the green fig tree in the story. From the tip of every branch, like a fat purple fig, a wonderful future beckoned and winked. One fig was a husband and a happy home and children, and another fig was a famous poet and another fig was a brilliant professor, and another fig was Ee Gee, the amazing editor, and another fig was Europe and Africa and South America, and another fig was Constantin and Socrates and Attila and a pack of other lovers with queer names and offbeat professions, and another fig was an Olympic lady crew champion, and beyond and above these figs were many more figs I couldn't quite make out."

Declaration

This thesis is the result of my own work and includes nothing which is the outcome of work done in collaboration except as declared in the preface and specified in the text. It is not substantially the same as any work that has already been submitted before for any degree or other qualification except as declared in the preface and specified in the text. It does not exceed the prescribed word limit for the Biology Degree Committee.

Anthony John Bridgen

March 2022

Acknowledgements

Ottoline Leyser for her insightful feedback, benevolent counsel and sage advice throughout the years, not to mention the many weekends spent reading my thesis.

Edwige Moyroud for her kindness and support in all things and to all people. Also for providing vast quantities of cake at every opportunity.

Sally Ward for her wisdom as acting oracle of the lab and patience for my many questions, as well as for being the glue that holds the group together.

Zoe Nahas for her knowledge of R and boundless enthusiasm for science.

Stephanie Smith, for her good heart, support through tough times and honest opinions on life and the lab.

Tanya Waldie for introducing me to many of the experimental systems used here.

Hugo Tavares for his help with all things graphical and statistical, without whom many of the figures in this thesis would be a lot uglier.

My dear wife Laurelin Middelkoop for bringing me through the darkest of times and being by my side always.

May Yeo, Colleen Drapek & Jemma Salmon, my lab ladies, for the pastry and the perspective.

Saba Shirvani, my Persian Queen, for the tahdig and making sure we never let standards slip.

David Hoey for many a wee dram after a hard day's night.

My mama for teaching me that I could do anything I set my mind to and giving me space to learn what I wanted, in the way I wanted.

Anna & Adam for setting good examples and providing copious amounts of wine, help and advice throughout.

My grandmama, for the many happy days gardening which planted the seed for my interest in plants.

All members of the Leyser lab for their assistance, advice and materials.

All those who have supported me in ways small and large, personally and academically, and who are too innumerable to name.

Abstract

Shoot branching plasticity relies on integration of diverse signals to regulate the activity of buds, which is partially mediated through auxin transport by PINs and the regulation thereof. Whilst PIN behaviour has been well characterised, the mechanisms by which PINs sense and respond to auxin, strigolactone and cytokinin remain unknown. In this thesis I investigate the regulation of PIN polarity in response to these hormones, presenting evidence of an age-dependent aspect to PIN1 behaviour. I then demonstrate that NPA-sensitive auxin flux or auxin concentration are insufficient to explain PIN1 behaviour and attempt to identify a mechanism by which PIN1 senses and responds to auxin at a sub-cellular level. Following this, I demonstrate the requirement of the central region of the PIN1 hydrophilic loop to confer strigolactone sensitivity and characterise the effect of the loss of this response on plant phenotypes and bud growth dynamics. Finally, I demonstrate cross-species differences in PIN hormone responses.

As a whole, this work advances our understanding of hormonal control of auxin transport in the shoot and the way in which this affects shoot architecture.

Table of Contents

1 Introduction	1
1.1 Plant developmental plasticity	
1.1.1 The auxin transport canalisation theory of bud activation	3
1.1.2 The second messenger hypothesis	4
1.1.3 A combined theory for axillary meristem regulation	5
1.2 Auxin	
1.2.1 Transport	7
1.2.2 Regulation of auxin transport	10
1.2.3 Auxin homeostasis	10
1.2.4 Signalling	12
1.3 Cytokinin	
1.4 Strigolactone	
1.5 Control of meristem generation and maintenance	
1.6 Regulation of primordia initiation in the SAM	
1.7 Thesis outline	
2 Materials & Methods	19
2.1 Plant growth conditions and Media	
2.1.1 Plant lines	20
2.1.2 Growth conditions	20
2.1.3 Growth substrates	20
2.1.4 Seed sterilisation	20
2.1.5 Chemical treatments	20
2.2 Physiological assays	
2.2.1 Split-plate assays	21
2.2.2 Split-stem assays	22
2.2.3 Branch counts	22
2.2.4 Branch angle	23
2.2.5 Height	23
2.2.6 Stem width	23
2.2.7 Proportion of fertile fruits	24
2.2.8 Auxin transport assays	24
2.2.9 Internode length/cauline node number	24
2.2.10 2 – node assays	24

2.3 Molecular biology	
2.3.1 DNA extraction	25
2.3.2 PCR	25
2.3.3 Construct assembly	26
2.3.4 Transformation	26
2.3.5 Plant selection	27
2.4 Microscopy	
2.4.1 Confocal microscopy	27
2.4.2 Sample preparation for imaging	28
2.4.3 Signal intensity quantification	28
2.5 Bioinformatics	
2.5.1 Primer design	28
2.5.2 Statistics	28
2.5.3 Protein sequence alignment	28
2.5.3 Data visualisation	29
3 The role of auxin flux and developmental stage in modulating PIN polarisation behaviour	30
3.1 Introduction	
3.1.1 The role of PINs in canalisation	31
3.1.2 Aims	32
3.2 Results	
3.2.1 Assessing the behaviour of PIN3, PIN4 & PIN7	33
3.2.2 PIN1 behaviour differs in old and young tissue	35
3.3 Discussion	
3.3.1 PIN1 in young stems shows canalisation-like behaviours	44
3.3.2 PIN1 behaviours differ in young and old stems	45
3.3.3 Conclusions	46
4 The effect of intracellular:extracellular auxin ratios on PIN behaviour	47
4.1 Introduction	
4.1.1 Auxin and its synthetic analogues	48
4.1.2 Aims	49
4.2 Results	
4.2.1 NPA does not induce auxin retention in young stems	50

4.2.2 Synthetic auxins and transport inhibitors do not behave as predicted by cell culture studies	55
4.3 Discussion	
4.3.1 The effects of NPA on intracellular auxin accumulation differ with tissue age.	62
4.3.2 The synthetic auxin 2,4-D and influx inhibitor 2-NOA do not behave as predicted by single-cell models.	63
4.3.3 Natural auxins are less stable than synthetic auxins	64
4.3.4 Conclusions	65
5 The role of the central region of the PIN1 hydrophilic loop in regulating strigolactone sensitivity	66
5.1 Introduction	
5.1.1 Control of plasma membrane PIN localisation	67
5.1.2 Bud outgrowth is modulated by auxin and strigolactone	68
5.1.3 Aims	69
5.2 Results	
5.2.1 PIN1 strigolactone responsiveness is conferred by the central region of the hydrophilic loop	70
5.2.2 PIN1-PIN3 _{L2} -GFP exhibits increased membrane accumulation	73
5.2.3 PIN1-PIN3 _{L2} -GFP expression effectively rescues key <i>pin1</i> phenotypes	78
5.2.4 <i>PIN1-PIN3_{L2}-GFP</i> expression results in subtle branching phenotypes	82
5.2.5 PIN1 SL insensitivity phenocopies other <i>max</i> mutant phenotypes	91
5.2.6 PIN1 SL sensitivity is not required for SL to enhance bud-bud competition	94
5.3 Discussion	
5.3.1 The central portion of the PIN1 HL is responsible for SL sensitivity	99
5.3.2 Removing PIN1 SL sensitivity increases residence on the membrane.	101
5.3.3 PIN1 SL sensitivity is required for proper flower development and induction of senescence.	103
5.3.4 Shoot branching inhibition by strigolactone is only partially mediated through PIN1	104

5.3.5 Conclusions	106
5.3.6 Future directions	106

6 | Investigating evolutionary divergence in PIN behaviour 108

6.1 Introduction	
6.1.1 PIN diversity across plant species	109
6.1.2 Aims	110
6.2 Results	
6.2.1 The behaviour of diverse PINs in response to hormones. . .	111
6.2.2 Investigating the effects of strigolactone and cytokinin on SoPIN1 and PIN1b.	116
6.2.3 SoPIN1 expression alters shoot branching patterns.	118
6.3 Discussion	
6.3.1 BdSoPIN1 and BdPIN1b exhibit behaviours distinct from AtPIN1 120	
6.3.2 BdSoPIN1 expression alters shoot branching in Arabidopsis 122	
6.3.3 Conclusions	122

7 | Discussion, Conclusions and Future Directions 124

7.1 An experimental system for investigating auxin transport canalisation	
7.2 Towards a new-old model of auxin-dependent PIN1 allocation	
7.3 Demonstrating diversity in PIN responses	
7.4 New techniques for an old hypothesis	
7.5 Final remarks	

Appendix A - References	132
Appendix B - Experimental Methods	174

List of Figures

Figure 3.1	33
Figure 3.2	34
Figure 3.3	36
Figure 3.4	37
Figure 3.5	38
Figure 3.6	39
Figure 3.7	40
Figure 3.8	41
Figure 3.9	42
Figure 3.10	43
Figure 4.1	51
Figure 4.2	52
Figure 4.3	53
Figure 4.4	53
Figure 4.5	54
Figure 4.6	56
Figure 4.7	57
Figure 4.8	58
Figure 4.9	59
Figure 4.10	60
Figure 4.11	61
Figure 5.1	70
Figure 5.2	71
Figure 5.3	72
Figure 5.4	74
Figure 5.5	75
Figure 5.6	76
Figure 5.7	77
Figure 5.8	78
Figure 5.9	79
Figure 5.10	80
Figure 5.11	81
Figure 5.12	82
Figure 5.13	83
Figure 5.14	84
Figure 5.15	85
Figure 5.16	86
Figure 5.17	87

Figure 5.1888
Figure 5.1988
Figure 5.2089
Figure 5.2190
Figure 5.2291
Figure 5.2392
Figure 5.2493
Figure 5.2595
Figure 5.2696
Figure 5.2797
Figure 5.2898
Figure 5.29	100
Figure 6.1	112
Figure 6.2	113
Figure 6.3	114
Figure 6.4	115
Figure 6.5	116
Figure 6.6	117
Figure 6.7	118
Figure 6.8	119
Figure 6.9	119

List of Tables

Table 2.120
Table 2.221
Table 2.325
Table B.1	175
Table B.2	176

List of Diagrams

Diagram 1.1	6
Diagram 1.2	9
Diagram 1.3	11
Diagram 2.1	22
Diagram 2.2	23

Abbreviations

AAAP | AMINO ACID AUXIN PERMEASE

ABC | ATP BINDING CASSETTE

AFB | AUXIN SIGNALLING F-BOX

AM | Axillary Meristem

ARF | Auxin Response Factor

ARR | Arabidopsis Response Regulator

AUX1 | AUXIN RESISTANT 1

AuxRE | Auxin Responsive Element

BFA | Brefeldin A

BRC1 | BRANCHED 1

CAT | Connective Auxin Transport

CCD7 | CAROTENOID CLEAVAGE DIOXYGENASE 7

CCD8 | CAROTENOID CLEAVAGE DIOXYGENASE 8

CK | Cytokinin

CKX | Cytokinin Oxidase/Dehydrogenases

CLV1 | CLAVATA 1

CLV2 | CLAVATA 2

CLV3 | CLAVATA 3

CRF | CYTOKININ RESPONSE FACTOR

CRN | CORYNE

2,4-D | 2,4-Dichlorophenoxyacetic acid

D6PK | D6 PROTEIN KINASE

DAD1 | DECREASED APICAL DOMINANCE 1

DAD2 | DECREASED APICAL DOMINANCE 2

DAO | DIOXYGENASE OF AUXIN OXIDATION

DMSO | Dimethyl Sulphoxide

D10 | DWARF 10

D14 | DWARF 14

D27 | DWARF 27

D53 | DWARF 53

GH3 | GRETCHEN HAGEN 3

HK | Histidine kinase

HL | Hydrophilic loop

HP | Histidine phosphotransferases

IAOx | Indole-3-acetaldoxime

IAA | Indole-3-acetic acid

IAM | Indole-3-acetamide

IAMT1 | IAA CARBOXYLMETHYLTRANSFERASE

IBA | Indole-3-butyric acid

IPA | indole-3-pyruvate

IPyA | Indole-3-pyruvic acid

IPT | ISOPENTENYL TRANSFERASE

LAX | LIKE-AUXIN RESISTANT 1

LRR | Leucine rich repeat

MAX | MORE AXILLARY GROWTH

Me-CLA | Methyl carlactonoate

MES17 | METHYL ESTERASE 17

MGR | Maximum growth rate

MP | MONOPTEROS

MPK | MITOGEN-ACTIVATED PROTEIN KINASE

NAA | 1-Naphthaleneacetic Acid

NOA | 2-Naphthoxyacetic Acid

NPA | 1-N-Naphthylphthalamic Acid

PATS | Polar Auxin Transport Stream

PID | PINOID

PIN | PIN-FORMED

RAM | Root Apical Meristem

RR | Response Regulators

SAM | Shoot Apical Meristem

SCF | SKP1 CULLIN F-BOX

SL | Strigolactone

SMXL | SUPPRESSOR OF MAX2-LIKE

SoPIN1 | Sister of PIN1

STM | SHOOT MERISTEMLESS

TAA | TRYPTOPHN AMINOTRANSFERASES OF ARABIDOPSIS

TIR1 | TRANSPORT INHIBITOR RESPONSE 1
TPL | TOPLESS

WUS | WUSCHEL

1

Introduction

"Unless we remember, we cannot understand" - E.M. Forster

1.1 | Plant developmental plasticity

It is an oft stated fact that plants are sessile organisms, lacking the ability to migrate to new environments or to evade predation. In most contexts, this is something of a facile observation, however, when it comes to understanding why plants have developed such highly plastic developmental processes, it is deeply relevant. Plants are able to modulate a relatively simple set of developmental programmes according to variation in light availability, predation, temperature, nutrient availability and humidity to name but a few, producing ‘endless forms most beautiful’ (Darwin, C., 1859). Key to this is their ability to tightly regulate shoot branching according to their environment.

Plants shoots can be thought of as being composed of a series of repeating units each consisting of a leaf, node, internode and axillary meristem (AM) (Galinat, 1959; Irish and Sussex, 1992). Depending on the relative growth of each of these components, diverse morphologies can be realised. The AMs can remain inactive as a bud, resulting in a single unbranched shoot or be activated, resulting in a branchier plant. The primary shoot apical meristem (SAM) is able to influence the activity of the AMs, maintaining them in a dormant state in a phenomenon known as apical dominance, described by Snow (Snow, 1925) and mediated - at least in part - by the phytohormone auxin (Thimann and Skoog, 1933; Hall and Hillman, 1975; Tamas *et al.*, 1989). Removal of the SAM results in release of AMs below it, whilst supply of auxin to the decapitated stump prevents sustained bud activity (Snow, 1925; Thimann and Skoog, 1933). Furthermore, axillary meristems are able to influence each other’s growth in a similar way (Snow, 1929; Snow, 1931; R., 1937; Ongaro *et al.*, 2008). Since then, a large amount of work has been done to understand how auxin is transported from sites of synthesis in young expanding leaves (Ljung *et al.*, 2001) basipetally in the polar auxin transport stream (PATS), a highly polar, high conductance, high capacity transport path in the xylem parenchyma and vascular cambium (Goldsmith, 1977; Davies P.J., Lomax T.L., Munday G.K., 1995). This relies on the action of PIN-FORMED 1 (PIN1) auxin efflux carriers present on the basal plasma membrane of cells in PATS tissue and required for high PATS activity (Okada *et al.*, 1991; Gälweiler *et al.*, 1998; Goldsmith, 2003). The PATS has innumerable roles in regulating development: balancing root and shoot growth (Reed *et al.*, 1998; Bhalerao *et al.*, 2002); inducing cambial activity (Snow, 1935) and regulating shoot branching by influencing the activity of axillary shoot apical meristems (Thimann *et al.*, 1934). The PATS appears to tune root branching and cambial activity simply by delivery of auxin to relevant auxin-responsive tissues (Blilou *et al.*, 2005; Grieneisen *et al.*, 2007; Petersson *et al.*, 2009), whereas it seems to play a more indirect role in the regulation of shoot branching (Hall and Hillman, 1975; Morris, 1977; Brown *et al.*, 1979; Bennett *et al.*, 2006; Waldie and Leyser, 2018; Van Rongen *et al.*, 2019).

Whilst decapitation of the SAM can release apical dominance, so too can the application of the auxin efflux inhibitor naphthylphthalamic acid (NPA) (Katekar and Geissler, 1980; Tamas *et al.*, 1989), suggesting auxin transport is key to this phenomenon. However, a significant body of evidence suggests that auxin acts indirectly to suppress bud outgrowth. Experiments supplying auxin basally to stem sections or directly to buds demonstrate an inability to inhibit outgrowth, and auxin supplied apically is not transported into buds (Thimann *et al.*, 1934; Hall and Hillman, 1975). Taken together, these data suggest that auxin moving in the PATS acts indirectly to inhibit the activity of axillary meristems. There are two, non-exclusive hypotheses which aim to explain this.

1.1.1 | The auxin transport canalisation theory of bud activation

Darwin first proposed the existence of a downwardly mobile signal in plants, (Darwin and Darwin, 1880), later identified as a class of phytohormones known as auxins (Went, 1928). Through a series of elegant experiments, Tsvi Sachs demonstrated the role of auxin in regulating vascular regeneration in stems following wounding (Sachs, 1969). From this, he expounded the auxin transport canalisation hypothesis which holds that, an initial low flux of auxin from areas of high auxin concentration (source) to those of low auxin concentration (sink) upregulates and polarises auxin transport in the direction of flux, progressively generating narrow cell files with highly polar auxin transport, which then differentiate into vascular strands (Sachs, 1981).

There is evidence to suggest that axillary meristems must be able to export auxin into the main stem PATS in order to activate (Sachs and Thimann, 1967; Morris, 1977; Li and Bangerth, 1999; Balla *et al.*, 2011), requiring the establishment of a PATS connecting the bud apex to the stem. If this is indeed the case, it would explain why auxin moving in the main stem PATS is able to indirectly inhibit axillary meristem activity. The presence of large amounts of auxin in the stem would reduce its sink strength, resulting in lower initial flux of auxin from the bud to the stem, consequently reducing the ability of said bud to establish canalised flow of auxin out into the main stem PATS.

This model is able to account for diverse phenomena such as apical dominance itself and the basipetal activation sequence of AMs when the SAM is removed (Prusinkiewicz *et al.*, 2009). Upon decapitation, the main source of auxin is removed and auxin drains from the stem resulting in the top portion of the stem becoming a good sink, enabling the uppermost buds to establish auxin export and activate. In turn, the export of auxin from the upper buds make the stem a weaker sink for the lower buds, making it harder for them to activate. Furthermore, the model provides an explanation for observed bud-bud competition, with multiple AMs competing for access to the sink of the main stem PATS.

Despite this, the auxin transport canalisation model remains somewhat controversial because it is mechanistically obscure. A central element of the auxin transport canalisation hypothesis is that PIN localisation at the plasma membrane is correlated with auxin flux across it (Sachs, 1968; Sachs, 1981). A mechanism of this type can account for many phenomena in both vascular patterning and shoot branching control. There is also a significant body of evidence correlating PIN accumulation with likely auxin fluxes (Mitchison *et al.*, 1981; Prusinkiewicz *et al.*, 2009; Balla *et al.*, 2011). However, the mechanism by which PINs might polarise proportional to flux is unknown. Whilst there are several theoretical proposals for how this might occur, none of these are able to explain all observed phenomena (Mitchison *et al.*, 1981; Feugier *et al.*, 2005; Feugier and Iwasa, 2006; Fujita and Mochizuki, 2006a; Fujita and Mochizuki, 2006b; Jönsson *et al.*, 2006; Smith *et al.*, 2006; Merks *et al.*, 2007; Stoma *et al.*, 2008; Prusinkiewicz *et al.*, 2009; Crawford *et al.*, 2010; Krupinski and Jönsson, 2010; Balla *et al.*, 2011; Shinohara *et al.*, 2013; Bennett *et al.*, 2014; Cieslak *et al.*, 2015).

1.1.2 | The second messenger hypothesis

As described above, experiments tracing the movement of radiolabelled auxin demonstrate that it does not enter the bud from the stem and furthermore that direct application of auxin to buds does not inhibit their outgrowth (Hall and Hillman, 1975; Everat-Bourbouloux and Bonnemain, 1980; Booker, 2003). The second messenger hypothesis is a conceptually simpler explanation for the indirect action of auxin on the activity of axillary meristems. It involves concentration dependent action via second messengers that are modulated by auxin and act to transmit signals up, into the bud. There are two other hormones involved in branching which are proposed to act in this way, strigolactone (SL) & cytokinin (CK). It is known that auxin signalling, through the canonical Aux/IAA ARF transcriptional pathway (see Section 1.2.4) acts to regulate the transcription of genes necessary for the synthesis of SL and CK (Tanaka *et al.*, 2006; Zou *et al.*, 2006; Arite *et al.*, 2007; Ferguson and Beveridge, 2009; Hayward *et al.*, 2009; Shimizu-Sato *et al.*, 2009; Zhao *et al.*, 2010). Auxin down-regulates the expression of CK biosynthetic genes such that following decapitation, auxin depletion in the stem results in up-regulation of these genes and cytokinin synthesis (Tanaka *et al.*, 2006). Cytokinin can move acropetally in the transpiration stream and enter buds, directly promoting their activation, in part by downregulation of *BRC1*, a branch inhibiting transcription factor (Tanaka *et al.*, 2006; Minakuchi *et al.*, 2010; Dun *et al.*, 2011; Braun *et al.*, 2012). On the other hand, auxin up-regulates SL biosynthesis, which too can enter buds and upregulate *BRC1* expression (Brewer *et al.*, 2009; Hayward *et al.*, 2009; Zhao *et al.*, 2010; Braun *et al.*, 2012; Brewer *et al.*, 2015). This is supported by demonstrations that auxin upregulates *MAX3* and *MAX4* transcription (and orthologues in other species) which encode enzymes in the SL biosynthetic pathway (Sorefan *et al.*, 2003; Foo *et al.*, 2005; Johnson *et al.*, 2006; Arite *et al.*, 2007; Hayward *et al.*, 2009). SL

can inhibit bud growth when directly or basally supplied to buds in pea (Brewer *et al.*, 2009; Brewer *et al.*, 2015), although this is not the case in all species (Crawford *et al.*, 2010).

Both CK and SL are able to move acropetally in the xylem and thus are good candidates for relaying information regarding stem auxin levels into the buds, tuning their (in) activation and growth. However, there is a significant body of data which suggests that manipulation of SL & CK levels and resulting changes in *BRC1* expression are insufficient to explain auxin mediated bud control. Decapitation in CK biosynthetic mutants can still release buds from dormancy, whilst SL application can actually result in the activation of buds where auxin transport is compromised (Shinohara *et al.*, 2013; Müller *et al.*, 2015). In dicots, *max2 smx1678* buds have high *BRC1* expression but remain active (Seale *et al.*, 2017) and in monocots, there is little evidence to support SL-regulation of *BRC1* orthologues (Arite *et al.*, 2007; Guan *et al.*, 2012). Furthermore, in both monocots and dicots, mutations in *BRC1* and its orthologues do not always remove bud inhibition (Arite *et al.*, 2007; Braun *et al.*, 2012), indicating that this hypothesis cannot explain all observed phenomena.

1.1.3 | A combined theory for axillary meristem regulation

Perhaps a better approach to explaining bud behaviour is to integrate the above hypotheses, as together they can explain many of the observed phenomena. It has been demonstrated that SL and CK not only affect *BRC1* transcription but also modulate the levels of plasma membrane PIN auxin transporters through transcription-independent mechanisms, with SL inducing PIN depletion and CK inducing accumulation (Shinohara *et al.*, 2013; Waldie and Leyser, 2018; Zhang *et al.*, 2020). This is supported by data showing that auxin transport through the stem is increased in SL mutants and decreased in CK mutants (Bennett *et al.*, 2006; Waldie and Leyser, 2018). Furthermore, high *BRC1* expression does not always prevent buds activating nor are all buds active in *brc1brc2* mutants (Seale *et al.*, 2017).

Given this, it is possible to conceptualise a system whereby, in order to activate, buds must establish auxin export into the stem, which relies on establishing canalised files of auxin transporting cells connecting the bud to the stem. By dynamically affecting the accumulation of PIN auxin efflux transporters on the cell membrane, SL and CK are able to make this harder or easier, inhibiting or promoting bud activation respectively. In addition these hormones modulate *BRC1* expression, which while not necessary or sufficient for bud inhibition, appears to play a role in setting a threshold for bud activation – with high *BRC1* levels setting a high activation threshold such that activation only occurs in a scenario highly conducive to canalization (Seale *et al.*, 2017). These diverse pathways are summarised in Diagram 1.1.

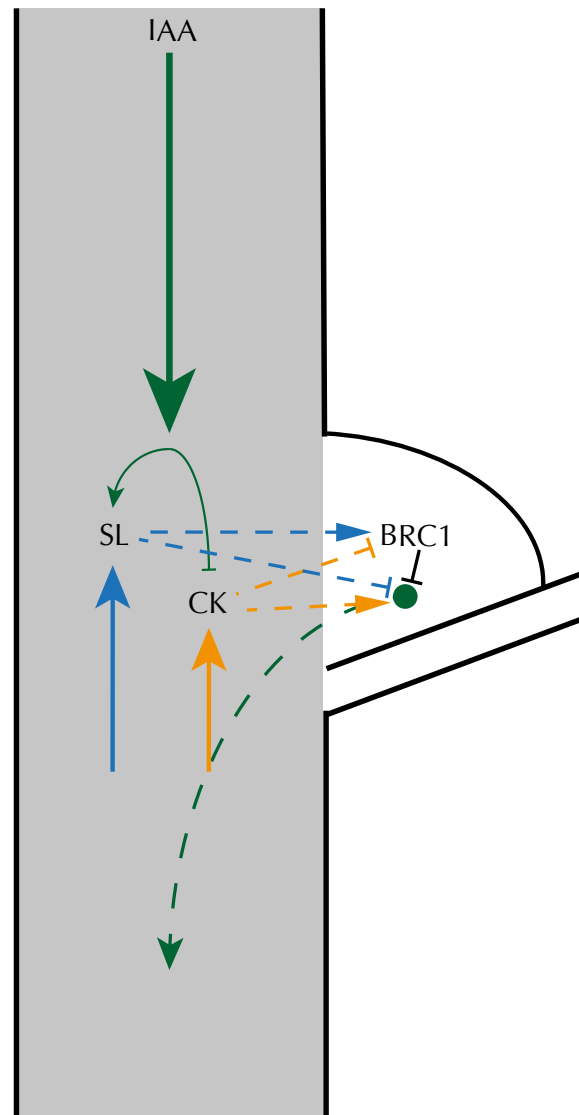


Diagram 1.1 | Cartoon depicting the signalling pathways involved in regulating bud dormancy/activation in a nodal *Arabidopsis* stem. Coloured arrows indicate auxin (green), strigolactone (blue) & cytokinin (orange) pathways.

This thresholding function of *BRC1* may relate to modulation of ABCB19, in turn affecting auxin loading in the bud and hence bud auxin source strength, supported by the ability of *abcb19* loss of function partially to suppress *brc1brc2* phenotypes (Van Rongen *et al.*, 2019).

This integrative hypothesis would allow for a highly tunable system, with multiple exogenous factors able to impact bud activity through a combination of modulating auxin, auxin transport, SL and CK synthesis and *BRC1* transcription.

1.2 | Auxin

The term auxin, literally ‘to grow’ from the Greek auxien, refers to any compound which elicits a certain set of responses in plants, including coleoptile curvature, induction of rooting in stem cuttings and promotion of cell division (Teale *et al.*, 2006).

1.2.1 | Transport

In planta, indole-3-acetic acid (IAA) is the predominant form of auxin. It is synthesised primarily in the young, expanding leaves of active shoot apices before export into the stem (Ljung *et al.*, 2001). As summarised in Diagram 1.2, auxin travels from this major source at the apex of the plant, basipetally towards the root. Some of this occurs through the vascular system, with the phloem acting as a mass flow system to carry auxin long distances from shoot to root (Morris and Thomas, 1978). Auxin in the phloem can subsequently enter the polar auxin transport (PAT) system (Cambridge and Morris, 1996) which, with its strict polarity of auxin transport, plays key roles in the regulation of plant development (Briggs, 1960; Leopold, 1964). This polar transport is widely accepted to be explained by the chemiosmotic hypothesis of auxin transport formulated in the 1970s (Rubery and Sheldrake, 1973; Rubery and Sheldrake, 1974; Raven, 1975; Goldsmith, 1977). IAA is a weak acid with a pKa of 4.85 and can exist in either a protonated or deprotonated state (Li *et al.*, 2017). The chemical properties of IAA mean it is partially protonated in the acidic (pH 5.5) apoplastic phase but deprotonated in the cytosol (pH 7) and as such is able to enter cells passively but relies on efflux carriers to leave the cell (Bibikova *et al.*, 1998; Hohm *et al.*, 2014). However, only ~ 17 % of IAA exists in a protonated state and is able to enter cells passively, the remaining 83% is ionised such that rapid auxin uptake requires a carrier protein (Hohm *et al.*, 2014).

The *AUX1/LAX* gene family encodes four proteins with a high degree of amino acid similarity which are AMINO ACID AUXIN PERMEASE (AAP) family members (Bennett *et al.*, 1996; Parry *et al.*, 2001; Swarup *et al.*, 2001; Péret *et al.*, 2012). These are responsible for the observed saturable component of auxin influx (Rubery and Sheldrake, 1974), which is reliant on proton motive force (Lomax *et al.*, 1985; Sabater and Rubery, 1987) and key for uptake of hydrophilic auxins but not lipophilic auxins (Delbarre *et al.*, 1996).

Once in the cytosol, IAA is deprotonated, forming a negatively charged ion which cannot passively cross the cell membrane and which must be actively exported from the cell by transporters (Rubery and Sheldrake, 1974; Goldsmith, 1977). The B subgroup of ABC transporters (ABCBs) consists of 21 members in *Arabidopsis thaliana*, of which only 8 appear to be related to auxin transport, namely ABCB1, 4, 6, 14, 15, 19, 20 & 21 (Geisler *et al.*, 2005; Santelia *et al.*, 2005; Terasaka *et al.*, 2005; Bouchard *et al.*, 2006; Geisler and Murphy, 2006; Bainbridge *et al.*, 2008; Santelia *et al.*, 2008; Kamimoto *et al.*, 2012; Zhang *et al.*, 2018). ABCBs are broadly plasma membrane localised, but in a non-polar fashion (Cho *et al.*, 2012) with mutation studies having demonstrated auxin transport-related phenotypes including root hair elongation and dwarfism when *ABCB1* & *ABCB19* function is lost (Noh, 2001). These appear to have a significant role in mediating auxin efflux, with mutation in *ABCB19* in some circumstances leading to a

greater reduction in basipetal auxin flux than observed in *pin1* (Blakeslee *et al.*, 2007). It is thought that this may be due to ABCB19 also playing a role in stabilisation of PIN1 on the membrane, as suggested by their co-localisation to detergent resistant membrane regions and reduced polar auxin transport when mislocalised in *twisted dwarf1* (*twd1*) mutants (Geisler *et al.*, 2003; Titapiwatanakun *et al.*, 2009). In the root, ABCB1 localises to the stele and appears to play a role in loading auxin for acropetal transport, along with ABCB4 (Geisler *et al.*, 2005; Lewis *et al.*, 2007). The latter is also involved in auxin distribution in the roots, while in the leaves ABCB21 regulates this, with both appearing to have dual function in enabling auxin import when intracellular auxin is low but switching to efflux activity when auxin levels are high (Yang and Murphy, 2009; Knöllner *et al.*, 2010; Kubeš *et al.*, 2012; Jenness *et al.*, 2019).

The PIN-FORMED family of auxin export carriers, named for the characteristic pin-like inflorescences of the *pin1* mutant, consists of 8 members in *Arabidopsis thaliana*. They are integral membrane proteins with two hydrophobic transmembrane domains of 5 alpha-helices each, linked by a hydrophilic loop composed of 4 regions (HC1-4) which are conserved between PINs and contain important glycosylation and phosphorylation sites (Zažímalová *et al.*, 2007; Bennett *et al.*, 2014a). The angiosperm PIN family is in turn subdivided into the 'long' PINs (1, 2, 3, 4, 7) and 'short' PINs (5, 6 & 8), with the latter having a shorter hydrophilic loop than that present in the former (Gälweiler *et al.*, 1998; Noh, 2001; Krecek *et al.*, 2009). The long PINs are typically polarly plasma membrane localised, being involved in directional auxin transport throughout the plant, whilst the short PINs localise to the endoplasmic reticulum with roles in regulating intracellular auxin levels (Okada *et al.*, 1991; Gälweiler *et al.*, 1998; Zažímalová *et al.*, 2007; Krecek *et al.*, 2009; Mravec *et al.*, 2009; Barbez and Kleine-Vehn, 2013; Adamowski and Friml, 2015). PIN1, PIN2, PIN3, PIN4 and PIN7 are able to localise in a polar manner and thus can create a directional flow of auxin, a feature vital to the auxin transport canalisation hypothesis (Wisniewska *et al.*, 2006).

The function of both PINs and ABCBs is known to be disrupted by the phytohormone, N-1-naphthylphthalamic acid (NPA). In the case of ABCBs, this occurs through what is thought to be a direct interaction, as ABCBs exhibit high affinity NPA binding and their export function is NPA sensitive (Okada *et al.*, 1991; Noh, 2001; Geisler *et al.*, 2005; Blakeslee *et al.*, 2007; Bailly *et al.*, 2008; Titapiwatanakun *et al.*, 2009). However, in the case of PINs, the mechanism by which NPA does this is obscure, but it has been hypothesised that it achieves its effect by binding to PIN auxin efflux carriers themselves or to a distinct regulatory protein (Rubery, 1979; Sussman and Goldsmith, 1981; Bailly *et al.*, 2008). This has been contradicted by demonstrations that NPA does not bind PINs with high affinity, indicating an indirect mechanism of action, perhaps through ABCBs (Blakeslee *et al.*, 2007; Titapiwatanakun *et al.*, 2009; Kim *et al.*, 2010). However, more recent work in protoplasts and heterologous transport assays has presented evi-

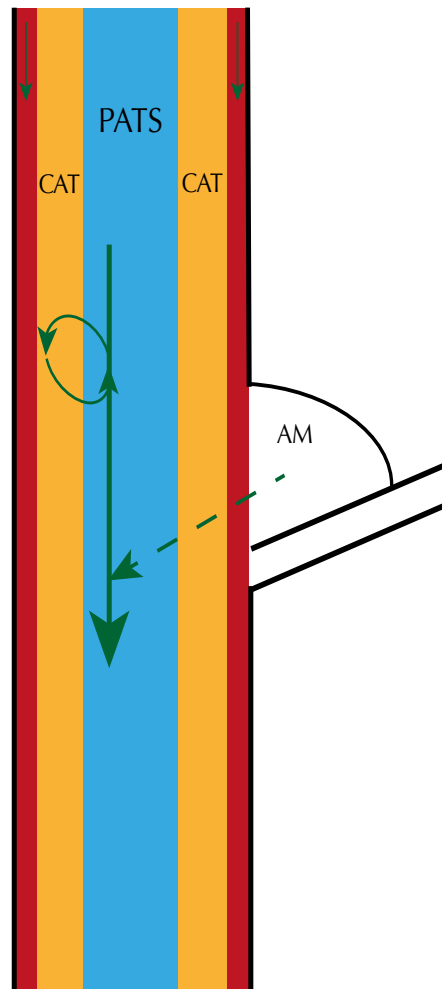


Diagram 1.2 | Cartoon depicting the transport of auxin in a nodal Arabidopsis stem segment. Green arrows represent the movement of auxin, blue represents the polar auxin transport Stream, orange the connective auxin transport & red phloem transport

dence of a direct interaction, independent of other NPA-binding proteins (Abas *et al.*, 2020; Teale *et al.*, 2021). Thus, it may be that NPA affects PINs through both direct and indirect interaction.

Stem auxin transport occurs chiefly in the PATS, but in addition to this there is a less polar, lower conductance auxin transport system that is more widely distributed across the stem - termed connective auxin transport (CAT), summarised in Diagram 1.2. This system appears to be key in enabling exchange of auxin between different stem tissues and chiefly involves PIN3, PIN4 & PIN7 (Bennett *et al.*, 2016). Data support a model in which auxin exchanges continually between the PATS & CAT as it moves down the stem, mediating communication between the PATS & peripheral tissues, including AMs (Bennett *et al.*, 2016). This role of PIN3, 4 & 7 correlates well with their observed broader expression domain and lower polarity, with expression generally being stronger in young inflorescence stems, coincident with the time of bud activation (Bennett *et al.*, 2016; Boot *et al.*, 2016; Van Rongen *et al.*, 2019).

1.2.2 | Regulation of auxin transport

PIN proteins have a hydrophilic, cytoplasmic loop (HL) which is a key target for phosphorylation, a process which has been demonstrated to control PIN polarity and transport activity (Barbosa and Schwechheimer, 2014). The AGCVIII subfamily of kinases are known to be important, plant-specific regulators of PIN proteins which are able to directly phosphorylate PINs in this HL. PINOID (PID) and WAGs are two examples of such kinases which, if lost, exhibit *pin1*-like phenotypes due to their role in mediating the apical-basal polarity switch of PIN1 & thus determining directionality of auxin flow (Nodzynski *et al.*, 2010; Benjamins *et al.*, 2001; Friml *et al.*, 2004; Dhonukshe *et al.*, 2010; Huang *et al.*, 2010). They phosphorylate PINs at highly conserved serine residues S1-S3 and appear to also be linked to PIN auxin transport activity (Zourelidou *et al.*, 2014). Observation of similar PIN behaviour in *pp2a* mutants led to the hypothesis that phosphorylation by PID/WAGS leads to apical localisation and dephosphorylation by PP2A leads to basal localisation (Michniewicz *et al.*, 2007). However, more recently it was noted that PIN1 could be phosphorylated by D6PK at the same residues as PID, but that this does not result in apical relocalisation of PIN1, suggesting a more complex picture (Weller *et al.*, 2017).

MITOGEN-ACTIVATED PROTEIN KINASEs (MPKs) have been characterised as controllers of PIN polarity in the stem, with MPK6 able to directly phosphorylate PIN1 at the S337 residue, controlling basal polarisation of PIN1, which in turn affects shoot branching. Replacing S337 with an asparagine phosphomimic led to apolar PIN1 in the xylem parenchyma and increased branching relative to wild type. Several MAPK target residues are conserved amongst the long PINs but S337 seems to be conserved only in PIN1 (Dai *et al.*, 2006; Jia *et al.*, 2016; Dory *et al.*, 2018). There are multiple MPKs and non-conserved phosphorylation sites in the central HL of PINs, providing a possible route by which MPKs could differentially regulate PIN localisation accounting for the different responses observed.

1.2.3 | Auxin homeostasis

IAA may exist in a free or conjugated state, with the former making up around a quarter of total IAA depending on tissue/species and the latter a storage form or path to degradation (Ludwig-Müller, 2011). Together with IAA precursors, this constitutes the cellular auxin pool, with precursors and conjugates able to contribute to the free IAA pool. Auxins are synthesised *de novo* via tryptophan-dependent & tryptophan-independent pathways, the former involving several routes via indole-3-acetaldoxime (IAOx), indole-3-acetamide (IAM) and indole-3-pyruvic acid (IPyA) (Normanly *et al.*, 1993; Sugawara *et al.*, 2009; Wang *et al.*, 2015a). The latter is the most prolific source of free IAA and involves the conversion of tryptophan to IPyA by TAA (TRYPTOPHAN

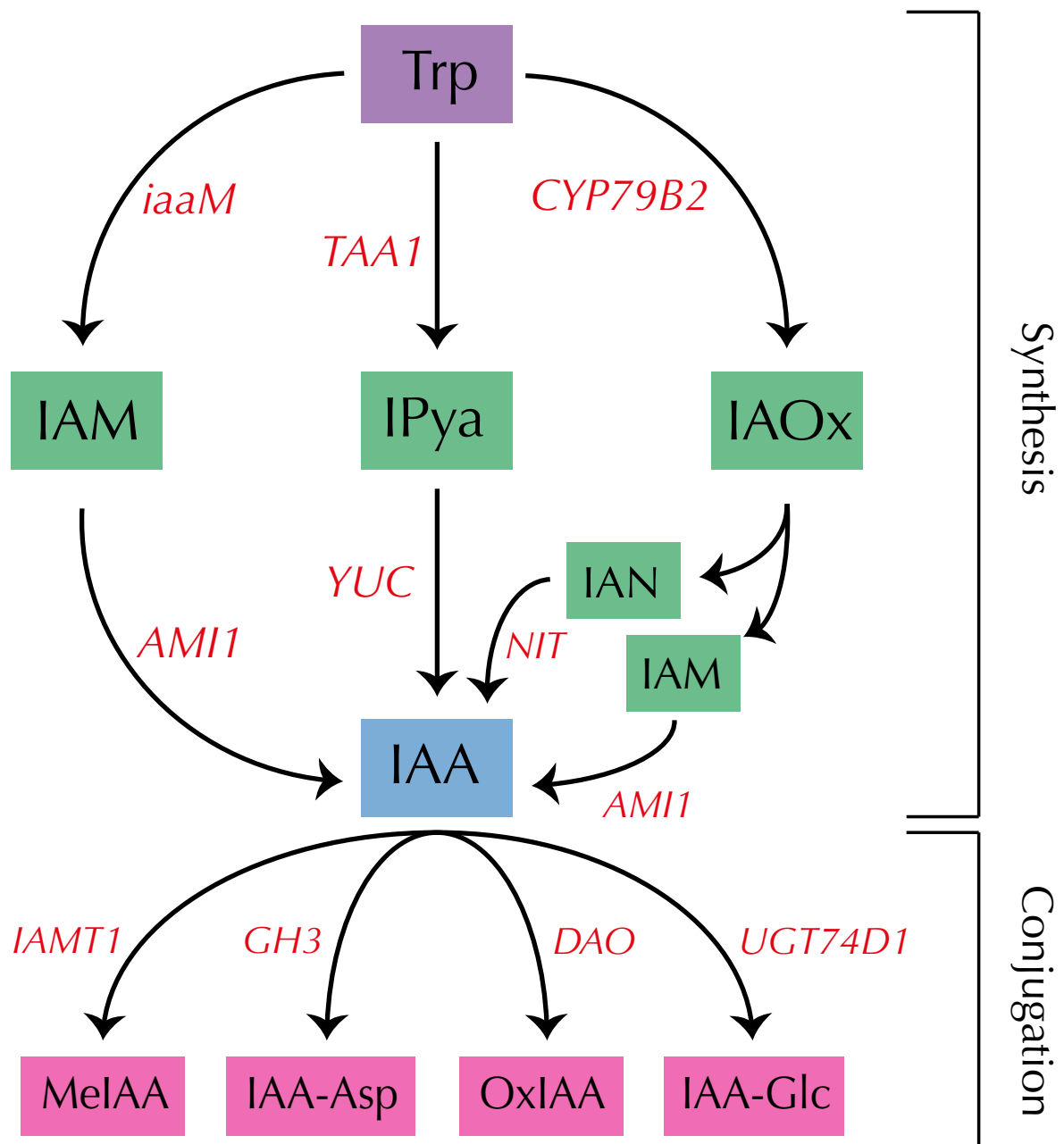


Diagram 1.3 | Cartoon depicting the homeostasis of indole-3-acetic acid. Black arrows represent pathways, red indicates enzymes, green boxes indicate synthesis intermediates and pink boxes conjugation products.

AMINOTRANSFERASES OF ARABIDOPSIS) and subsequently to IAA by YUCCA flavin monooxygenases (Zhao *et al.*, 2001; Stepanova *et al.*, 2008; Yamada *et al.*, 2009; Dai *et al.*, 2013). Mutation in *TAA1* or *YUCCAs* lead to reduced IAA accumulation, with higher order mutants displaying synergistic phenotypes, whilst overexpression results in auxin over-accumulation (Jeong *et al.*, 2007; Tao *et al.*, 2008; Mashiguchi *et al.*, 2011).

Once synthesised, auxins may be conjugated by ester linkage to sugars and amide linkage to amino acids or peptides (Szczeszen *et al.*, 1994; Barratt *et al.*, 1999; Tam *et al.*, 2000; Jackson *et al.*, 2001; Kowalczyk and Sandberg, 2001; Jackson *et al.*, 2002). These

lack auxin activity, acting as a storage mechanism from which auxin can be rapidly released to contribute to the free auxin pool (LeClere *et al.*, 2002; Rampey *et al.*, 2004; Jakubowska and Kowalczyk, 2005). UDP-glucosyl transferases attach IAA to glucose via ester linkages in a reversible manner, with ectopic expression of *UGT74D1* in *Arabidopsis* leading to considerable changes in auxin distribution and free IAA levels (Szerszen *et al.*, 1994; Ostrowski *et al.*, 2015; Jin *et al.*, 2021). The *GRETCHEN HAGEN3* (*GH3*) family of acyl amido synthetases is notable for its size and seeming importance in maintaining auxin homeostasis (Staswick *et al.*, 2005; Westfall *et al.*, 2010; Westfall *et al.*, 2016). Their expression is auxin inducible and loss of function leads to elevated free IAA as well as considerable developmental defects (Ludwig-Müller, 2011; Zheng *et al.*, 2016; Guo *et al.*, 2021). ILR1, IAE3 & ILL2 hydrolases in the endoplasmic reticulum are able to release IAA from amido conjugates, suggesting that the ER is an important component in auxin homeostasis (Bartel and Fink, 1995; LeClere *et al.*, 2002; Sanchez Carranza *et al.*, 2016). Furthermore, IAA can be converted to its methyl ester (MeIAA) and demethylated by IAA CARBOXYLMETHYLTRANSFERASE (*IAMT1*) & METHYL ESTERASE 17 (*MES17*) respectively (Zubieta *et al.*, 2003; Yang *et al.*, 2008; Takubo *et al.*, 2020). MeIAA itself lacks auxin activity but due to its less polar nature, is capable of transport independent of auxin carriers, perhaps having implications for PATS independent auxin transport. Overexpression of *IAMT1* leads to auxin-deficient/resistant-like phenotypes, with MeIAA application having the same effect as IAA application, suggesting physiological relevance of the methylated form (Qin *et al.*, 2005; Li *et al.*, 2008). However, reported levels of MeIAA in planta are low, placing a question mark over its contribution to auxin homeostasis (Qin *et al.*, 2005).

In addition to its role in storage, auxin conjugation can act as a route to deactivation, with particular conjugates such as IAA-Asp & IAA-Glu being poor substrates for hydrolases and as such are unlikely to return to the free IAA pool (Östin *et al.*, 1998; LeClere *et al.*, 2002). Additionally, IAA is catabolised, primarily by oxidation to oxIAA in an irreversible reaction catalysed by DIOXYGENASE OF AUXIN OXIDATION (DAO) dioxygenases, the loss of function of which leads to phenotypic aberrations in root hair length and cotyledon size (Porco *et al.*, 2016; Zhang *et al.*, 2016). Loss of IAA oxidation is partially compensated for by increased conjugation, particularly into IAA-Asp & IAA Glu (Porco *et al.*, 2016; Zhang *et al.*, 2016). Together, biosynthesis, conjugation & degradation pathways act to tightly regulate auxin homeostasis with redundant action, to provide resilience to the system.

1.2.4 | Signalling

Auxin-mediated regulation of transcription utilises a system of TRANSPORT INHIBITOR RESPONSE 1/AUXIN SIGNALLING F-BOX 1-5 (*TIR1/AFB*) proteins, Aux/IAA

transcriptional repressor proteins and auxin response factors (ARFs). In the absence of auxin, Aux/IAAs bind ARFs and recruit TOPLESS (TPL) resulting in repression of auxin-responsive genes by binding at auxin responsive elements (AuxREs) (Abel and Theologis, 1996; Ulmasov *et al.*, 1997b; Tiwari *et al.*, 2004; Guilfoyle and Hagen, 2007; Szemenyei *et al.*, 2008). The presence of auxin leads to a stabilisation of the interaction between TIR1/AFB & Aux/IAAs via the DII domain of the latter, resulting in poly-ubiquitination of the Aux/IAA by the SCF^{TIR1/AFB} E3-ubiquitin ligase complex and degradation via the 26S proteasome (Gray *et al.*, 1999; Gray *et al.*, 2001; Ramos *et al.*, 2001; Kepinski and Leyser, 2005; Tan *et al.*, 2007; Dos Santos Maraschin *et al.*, 2009). There are six TIR1/AFBs and 29 Aux/IAAs and which appear to act as co-receptors. Different pairings of AFBs and Aux/IAAs have been shown to have different auxin affinities, providing considerable potential for different responses mediated via different combinations (Calderón Villalobos *et al.*, 2012). Degradation of Aux/IAAs allows ARFs to recruit chromatin remodelling enzymes to AuxREs of auxin responsive genes, driving a transcriptional response (Ulmasov *et al.*, 1997a; Guilfoyle and Hagen, 2007; Wu *et al.*, 2015).

AuxREs consist of short sequence motifs initially identified in the soybean *GH3* promoter as TGTCTC, which were demonstrably able to confer auxin responsiveness to reporter genes (Liu *et al.*, 1994; Ulmasov *et al.*, 1995). Understanding of this system has enabled the design of synthetic promoters consisting of multiple tandem repeats of this motif, which, when placed in front of fluorophoric or enzymatic reporter genes, enable visualisation of auxin signalling in planta (Ulmasov *et al.*, 1997b). The exact sequence seems to differ slightly in terms of conferring responsiveness to different ARFs and TGTCGG has also been demonstrated to confer good responsiveness and even increased sensitivity to auxin (Franco-Zorrilla *et al.*, 2014; Liao *et al.*, 2015; O'Malley *et al.*, 2016).

1.3 | Cytokinin

Cytokinins are phytohormones known for their role as promoters of cell proliferation but also have significant links to positive regulation of shoot branching. They are synthesised by isopentenyl transferases (IPTs), catalysing the conversion of adenosine phosphate to trans-zeatin or isopentenyladenine depending on the substrate (Kudo *et al.*, 2010). Degradation on the other hand involves cytokinin oxidase dehydrogenases (CKXs) (Werner *et al.*, 2003).

CKs are perceived in a manner comparable to bacterial two-component systems, with ER-localised histidine kinase (HK) receptors perceiving CK and histidine phosphotransferases (HPs) propagating the signal from the cytosol to response regulators (RR) in the nucleus (Inoue *et al.*, 2001; Suzuki *et al.*, 2001; Schaller *et al.*, 2008). There are two classes of RR in *Arabidopsis*, Type-A & Type-B, distinguished by the presence or

absence of a DNA-binding domain. Type-Bs bind DNA and directly up-regulate transcription of CK responsive genes. Type-As typically have an inhibitory effect through a poorly understood mechanism. The transcription of genes encoding Type-As is directly activated by Type-Bs, creating a negative feedback loop (Hwang and Sheen, 2001; To *et al.*, 2004; Argyros *et al.*, 2008). Downstream of the RRs are cytokinin response factors (CRFs), transcription factors which bind to cytokinin regulatory elements upstream of secondary cytokinin responsive genes, which include PIN1 & PIN7 (Rashotte *et al.*, 2006; Šimášková *et al.*, 2015; Raines *et al.*, 2016). CRFs have been implicated in regulation of shoot branching through their ability to downregulate *BRC1* expression (Tanaka *et al.*, 2006; Minakuchi *et al.*, 2010; Dun *et al.*, 2011; Braun *et al.*, 2012) which, as described above, has been proposed as a thresholding mechanism determining how easily buds can activate (Seale *et al.*, 2017).

Cytokinins also exert non-transcriptional effects which contribute to shoot branching. For example, CK is able to increase the accumulation of PIN3 and PIN7 on the plasma membrane in stems, despite not altering transcription levels (Waldie and Leyser, 2018). This suggests that CK may be able to contribute to bud activation by increasing the competence of buds to establish a PATS from the bud to the stem.

1.4 | Strigolactone

Strigolactones are plant hormones involved in numerous aspects of plant biology from germination stimulants in parasitic weeds to establishing arbuscular mycorrhizal symbioses, stimulation of secondary stem growth and internode length, regulating leaf senescence and responding to nutrient availability (Cook *et al.*, 1972; Akiyama and Hayashi, 2006; Agusti *et al.*, 2011; de Saint Germain *et al.*, 2013; Yamada *et al.*, 2014). They are primarily produced in the roots where they may be exuded to the soil or move acropetally to the shoot, as supported by a number of grafting experiments (Beveridge *et al.*, 1994; Napoli, 1996; Foo *et al.*, 2001; Morris *et al.*, 2001; Turnbull *et al.*, 2002; Sorefan *et al.*, 2003).

Strigolactone synthesis in angiosperms occurs through a conserved pathway involving four enzymes. Initially, all-trans-beta-carotene is converted to 9-cis-beta-carotene by DWARF27 (D27) (Hao *et al.*, 2009; Waters *et al.*, 2012a). This is then cleaved by carotenoid cleavage dioxygenases encoded by *CCD7/MAX3* and *CCD8/MAX4* to yield carlactone (Booker *et al.*, 2004; Alder *et al.*, 2012). MAX1 cytochrome P450 enzymes then convert carlactone to carlactonoic acid (Abe *et al.*, 2014; Zhang *et al.*, 2014) Loss of function of any of these genes leads to a high branching phenotype which can be complemented by provision of strigolactone, for example the synthetic strigolactone GR24 (Gomez-Roldan *et al.*, 2008; Umehara *et al.*, 2008).

SL perception occurs via the DWAR14 (D14) receptor, loss of function of which leads to GR24 insensitive high branching phenotypes (Arite *et al.*, 2009; Hamiaux *et al.*, 2012; Waters *et al.*, 2012b; De Saint Germain *et al.*, 2016; Seto *et al.*, 2019). It is an alpha/beta-fold hydrolase with a serine/histidine/asparagine catalytic triad which is able to hydrolyse SLs, although hydrolysis may not be necessary for signalling (Hamiaux *et al.*, 2012; Seto *et al.*, 2019). DWARF53 (D53)/SUPPRESSOR OF MAX2-LIKE (SMXL6/7/8) are negative regulators of SL signalling which interact with D14 in the presence of SL, leading to degradation of D53 (Jiang *et al.*, 2013; Mach, 2015) via the 26S proteasome pathway and requires the F-box protein DWARF3 (D3)/MORE AXIL-LARY GROWTH2 (MAX2) (Zhou *et al.*, 2013; Wang *et al.*, 2015b). A negative feedback loop autoregulates SL signalling as SMXL6 binds to the promoters of SMXL 6/7/8, repressing their transcription and SMXL6 is degraded in the course of SL signalling (Wang *et al.*, 2020).

Once initiated, SL signalling has a number of transcriptional and non-transcriptional effects. SMXL6 acts as a repressor of *BRC1* such that the induction of SL signalling leads to increased *BRC1* levels, partially mediating SL-induced branching inhibition (Aguilar-Martinez *et al.*, 2007; Braun *et al.*, 2012; Seale *et al.*, 2017; Wang *et al.*, 2020). In addition, *max* mutants have increased PIN1 accumulation and SL has been shown to reduce PIN1 accumulation in the PATS (Bennett *et al.*, 2006; Crawford *et al.*, 2010), an effect that is dependent on SL signalling but independent of new protein synthesis and hence transcription (Shinohara *et al.*, 2013). Different PINs exhibit different SL sensitivities, with PIN1 and PIN7 being depleted from the plasma membrane upon SL treatment whilst PIN3 and PIN4 are not (Ticchiarelli, 2019). SLs have also been implicated in regulating vascular patterning (Ongaro *et al.*, 2008; Agusti *et al.*, 2011; Zhang *et al.*, 2020), a process which is thought to rely on auxin canalisation. Thus it is likely that SL regulates bud outgrowth in part by reducing the ability of buds to establish canalised auxin export into the main stem PATS through triggering PIN1 and PIN7 removal, while simultaneously inducing a high bud activation threshold through elevated *BRC1* expression (Seale *et al.*, 2017).

1.5 | Control of meristem generation and maintenance

Analysis of the role and mechanisms of action of auxin, auxin transport, SL and CK in shoot branching are complicated by their roles in regulating other aspects of shoot meristem biology. During embryonic development, the SAM and root apical meristem (RAM) are defined in the mature embryo. After fertilisation, the nascent zygote undergoes asymmetric division to generate an apical and basal daughter cell, each of which undergoes several rounds of division to form the proembryo and suspensor respectively (Chute and Maheshwari, 1951). At this point the apical and basal regions start to become distinguished by differential gene expression of *WOX* genes and *ML1*, and auxin

is transported from the basal to apical cell by PIN7 (Sessions *et al.*, 1999; Friml *et al.*, 2003; Haecker *et al.*, 2004). Of the eight cells in the proembryo, the upper four go on to give rise to the shoot apical meristem and cotyledons, whilst the lower four and the very uppermost region of the suspensor forms the precursor of the hypocotyl, root and root meristem (Jurgens and Mayer, 1994; Scheres *et al.*, 1994). Recognisable meristematic regions which generate new tissue are not present until the heart stage of embryogenesis and in the case of the SAM, consist of three zones with specific functions defined by differential gene expression (Barton and Poethig, 1993). The central zone consists of slowly dividing stem cells, the organising centre sits beneath this, acting to maintain stem cells, while the peripheral zone consists of rapidly dividing cells where the primordia are initiated (Laufs *et al.*, 1998; Mayer *et al.*, 1998; Fletcher, 1999; Trotschka *et al.*, 2000).

It is vital that the SAM be tightly regulated in order to maintain a pool of undifferentiated cells necessary for continued growth, while allowing some to undergo division to form organs. The SAM is maintained through a feedback loop in which CLAVATA 3 (CLV3), a small secreted peptide, is expressed in stem cells of the central zone and diffuses toward the organising centre where it binds CLAVATA 1 (CLV1) (Clark *et al.*, 1995; Ogawa *et al.*, 2008). CLV1 is a leucine rich repeat (LRR) receptor-like kinase which interacts with a complex of CLAVATA 2 and CORYNE (CRN) (Clark *et al.*, 1993; Jeong *et al.*, 1999; Müller *et al.*, 2008; Bleckmann *et al.*, 2010; Nimchuk *et al.*, 2011). This initiates a signal transduction cascade which leads to repression of *WUSCHEL* (*WUS*) in the organising centre (Van den Berg *et al.*, 1995; Mayer *et al.*, 1998; Brand *et al.*, 2000; Schoof *et al.*, 2000). *WUS* is a mobile protein which can move through the plasmodesmata and acts in a concentration-dependent manner, inhibiting CLV3 at high concentrations and activating it at low concentrations in the central zone where, in combination with HAIRY MERISTEM GRAS transcriptional factors, it regulates stem cell production and confines *CLV3* transcription to the outermost apex of the SAM (Zhou *et al.*, 2015; Perales *et al.*, 2016; Zhou *et al.*, 2018). Thus, clear boundaries of expression are defined in the SAM, acting to maintain the stem cell pool whilst also producing precursors to the differentiated tissues of the growing plant.

The axillary meristems (AMs) exhibit the same organisation as the SAM but are located in the axils of the leaf and initiated throughout the growth of the plant. The origin of these meristematic cells is not conclusively known, with one hypothesis suggesting that, during organogenesis of the leaf a population of stem cells “detaches” from the SAM and forms the AM (Garrison, 1955; Steeves and Sussex, 1989). Alternatively, it has been proposed that AMs are initiated *de novo* from differentiated cells in the axil (Snow and Snow, 1942; McConnell and Barton, 1998). Consistent with the detached meristem hypothesis, axillary meristems initiate from cells in the leaf axil that continuously

express the meristem marker *SHOOT MERISTEMLESS (STM)* (Burian *et al.*, 2016; Shi *et al.*, 2016).

AM formation is influenced by hormones, with an auxin minimum being necessary to initiate AMs and loss of auxin efflux or auxin overproduction leading to failure of AM formation (Wang *et al.*, 2014a; Wang *et al.*, 2014b). This appears to be partially mediated through *STM* expression, with auxin overproduction reducing its expression and stem cell differentiation (Shi *et al.*, 2016). Furthermore, elevated cytokinin levels are detectable during AM initiation, dependent on the presence of the auxin minimum (Wang *et al.*, 2014). It has since been demonstrated that CK activates *WUS* expression during AM initiation, mediated by Type-B ARRs directly binding the *WUS* promoter (Wang *et al.*, 2017). *WUS* in turn activates *STM* and binds *STM* proteins, activating *CLV3* expression (Su *et al.*, 2020).

Once formed, AMs are able to lie dormant or activate to generate a branch on the basis of multiple developmental and environmental inputs, a process primarily mediated through hormones as discussed above.

1.6 | Regulation of primordia initiation in the SAM

The SAM is responsible for generating the above ground structures of the plant, producing phytomers which consist of an organ, a stem section and an AM. The meristem can have different identities according to the organs it produces. The geometric arrangement of these around the central axis is known as phyllotaxis. There are two main categories, spiral and non-spiral phyllotaxis, although the latter is sub-divided into several categories. *Arabidopsis thaliana* exhibits a switch from the former to the latter after the first leaf pair (Church, 1920; Kawasaki and Bell, 1991; Bartholomew-Began and Jean, 1997). Phyllotaxis can be explained by the inhibitory field model, whereby new primordia initiation is inhibited by older primordia, and thus must form a minimum distance away where inhibition is lowest (Hofmeister, 1868; Snow and Snow, 1932).

Key to this patterning is auxin distribution, with defects in synthesis or transport leading to primordia patterning defects (Okada *et al.*, 1991; Gälweiler *et al.*, 1998; Reinhardt *et al.*, 2000; Gallavotti *et al.*, 2008; Phillips *et al.*, 2011). It appears that primordia initiation is linked to the creation of high auxin zones (Reinhardt *et al.*, 2000; Heisler *et al.*, 2005). These zones are generated by asymmetric distribution of PIN1, such that PIN1 is preferentially located to membranes adjacent to cells with the highest auxin concentration, moving auxin up the concentration gradient to produce auxin maxima and deplete surrounding cells of auxin (Vernoux *et al.*, 2000; Benková *et al.*, 2003; Heisler *et al.*, 2005; Vernoux *et al.*, 2011; O'Connor *et al.*, 2014). Thus, in this model, a lack of auxin is the inhibitory signal and prevents formation of primordia directly adja-

cent to one another (Reinhardt *et al.*, 2003; Reinhardt, 2005). The control of this PIN1 distribution is dependent on an ARF, *MONOPTEROS* (*MP*), with PIN1 polarity tracking MP activity, which is in turn determined by auxin distribution, suggesting a feedback loop in which high levels of auxin induce MP-mediated auxin signalling leading to increased transport of auxin towards those cells (Hardtke and Berleth, 1998; Bhatia *et al.*, 2016). Auxin efflux is not the only determining factor, with phyllotaxis demonstrably disturbed by the loss of *AUX1/LAX* influx carrier expression (Bainbridge *et al.*, 2008). It has been shown that auxin is able to affect the mechanical properties of the cell wall by promoting pectin demethylesterification, a process which influences lateral primordia initiation (Peaucelle *et al.*, 2008; Peaucelle *et al.*, 2011). Hormonal control of the meristem is not limited to auxin, cytokinin has a demonstrable role in controlling phyllotaxis. Mutants in cytokinin signalling such as *AHP6*, *ABPH1* and *DEC* lead to altered phyllotaxis and enlarged meristems (Giulini *et al.*, 2004; Itoh *et al.*, 2012; Besnard *et al.*, 2014).

1.7 | Thesis outline

In this thesis, with a view to understanding better the role and mechanism of action of hormonal control of PIN proteins in shoot branching, I aim to establish how auxin, strigolactone and cytokinin regulate PIN protein behaviour, the basis for this regulation at a protein domain level, whether it is conserved across different PIN clades, and how it contributes to shoot branching.

- ◇ **Chapter 2** will detail the experimental procedures performed in order to obtain the data presented here, as well as the analyses performed on said data.
- ◇ **Chapter 3** presents my investigation into the behaviour of *Arabidopsis* PIN proteins in response to auxin, strigolactone and cytokinin.
- ◇ **Chapter 4** will outline my attempts to quantify the effects of various auxins and auxin flux inhibitors on intracellular auxin levels and the way in which these relate to PIN polarity.
- ◇ **Chapter 5** establishes a basis for SL responsiveness in the HL using chimeric PIN proteins and investigates the phenotypic effects of PIN1 SL insensitivity.
- ◇ **Chapter 6** discusses the behaviour of *Brachypodium* PINs, SoPIN1 and PIN1b expressed in *Arabidopsis* with regard to hormone responses and branching patterns.
- ◇ **Chapter 7** draws together the previous chapters, contextualises them within the current research landscape and highlights the key takeaways from the body of research presented hence.

2

Materials & Methods

"Though this be madness, yet there is method in't" - W. Shakespeare

2.1 | Plant growth conditions and Media

2.1.1 | Plant lines

All lines of *Arabidopsis thaliana* referred to as wildtype (wt) in this thesis, were of ecotype Col-0. Further detail on specific transgenic lines can be found in Table B.1.

2.1.2 | Growth conditions

Before sowing, seeds were stratified at 4 °C on moist filter paper for 3-5 d in petri dishes sealed with parafilm. Seeds were sown on Levington F2 compost in PT24 (24 pots, 25 cm² per pot) or PT40 (40 pots, 16 cm² per pot) cellular trays and grown in Conviron MTPC (Multi-tiered) growth chambers under the conditions outlined in Table 2.1.

Condition	Period Light/ Dark (h)	Temperature day/night (°C)	Light Intensity ($\mu\text{mol m}^{-2} \text{s}^{-1}$)	Humidity (%)
Long day	16/8	21/17	170	65
Short day	8/16	21/17	170	65
Tissue culture	16/8	21/17	85	ambient

Table 2.1 | Plant growth conditions

2.1.3 | Growth substrates

For soil-based experiments, plants were grown in Levington F2 compost (Levington Horticulture, Ipswich, UK) pre-treated with Intercept at 0.02 g/l (ICL Specialty Fertilizers, Heerlen, The Netherlands) or Exemptor at 0.03 g/l (Bayer CropScience Limited, Cambridge, UK). For in vitro experiments, *Arabidopsis thaliana* Salts (ATS) medium (Composition: 70 mM H₃BO₃, 14 mM MnCl₂, 0.5 mM CuSO₄, 1 mM ZnSO₄, 0.2 mM NaMoO₄, 10 mM NaCl, 0.01 mM CoCl₂) (Wilson et al., 1990) was used, solidified with 0.8-1.0 % agar when required.

2.1.4 | Seed sterilisation

Surface sterilisation of seeds was performed by washing seeds with 70% ethanol (w/v) for 15 minutes. Seeds were then washed with 96% ethanol (w/v) and allowed to dry in a laminar flow hood. Sterile seeds were either plated dry using tweezers or suspended in sterile water and plated using a pipette.

2.1.5 | Chemical treatments

Solutions used in assays were produced and stored according to the conditions outlined in Table 2.2

Chemical	Source	Molecular weight (gmol ⁻¹)	Dissolved in	Storage conditions
Naphthaleneacetic acid (NAA)	Sigma-Aldrich	186.2	70 % EtOH	-20 °C
N-1-naphthylphthalamic acid (NPA)	Sigma-Aldrich	291.3	10 % DMSO + 70 % EtOH	-20 °C
Indole-3-acetic acid Free acid (IAA)	Sigma-Aldrich	175.2	70 % EtOH	-20 °C
2,4-Dichlorophenoxyacetic acid (2,4-D)	Sigma-Aldrich	221.0	70 % EtOH	-20 °C
Naphthoxyacetic acid Free acid (2-NOA)	Sigma-Aldrich	202.2	70 % EtOH	-20 °C
6-Benzylaminopurine (BA)	Sigma-Aldrich	225.3	DMSO	-20 °C
Racemic GR24	LeadGen Labs LLC	298.29	90 % Acetone	-80 °C
Brefeldin A	Sigma-Aldrich	280.36	90% DMSO	-20 °C

Table 2.2 | Chemical solutions

2.2 | Physiological assays

2.2.1 | Split-plate assays

Sterilin™ 100 mm Square Petri Dishes (Thermo Fisher Scientific, Massachusetts, US) were prepared by filling with 55 mL of agar-solidified *Arabidopsis thaliana* Salts (ATS) medium under sterile conditions in a laminar flow hood. Once solidified, a 1 cm wide trough was excised along the centre of the plate. Chemical solutions were applied as 25 µL of 1000x stocks by pipetting onto the upper or lower agar block and allowing to diffuse into the agar for 24 h in the dark at 4 °C before use. *Arabidopsis* plants were grown in PT40 trays under long-day conditions as described in Table 2.1, and bolting inflorescences excised when 5-10 cm tall. These were trimmed to 2 cm in length, with excess stem being removed from the apical end so as to leave the basal-most segment, and inserted into the treated plates such that the stem segments were held between the two agar blocks as shown in Diagram 2.1. Petri dishes were sealed with microporous tape and placed vertically in a controlled environment room (light intensity 170 µmoles m⁻² s⁻¹, day temperature 21 °C, night temperature 17 °C, humidity 65%) under long-day conditions (16 h light/8 h dark).

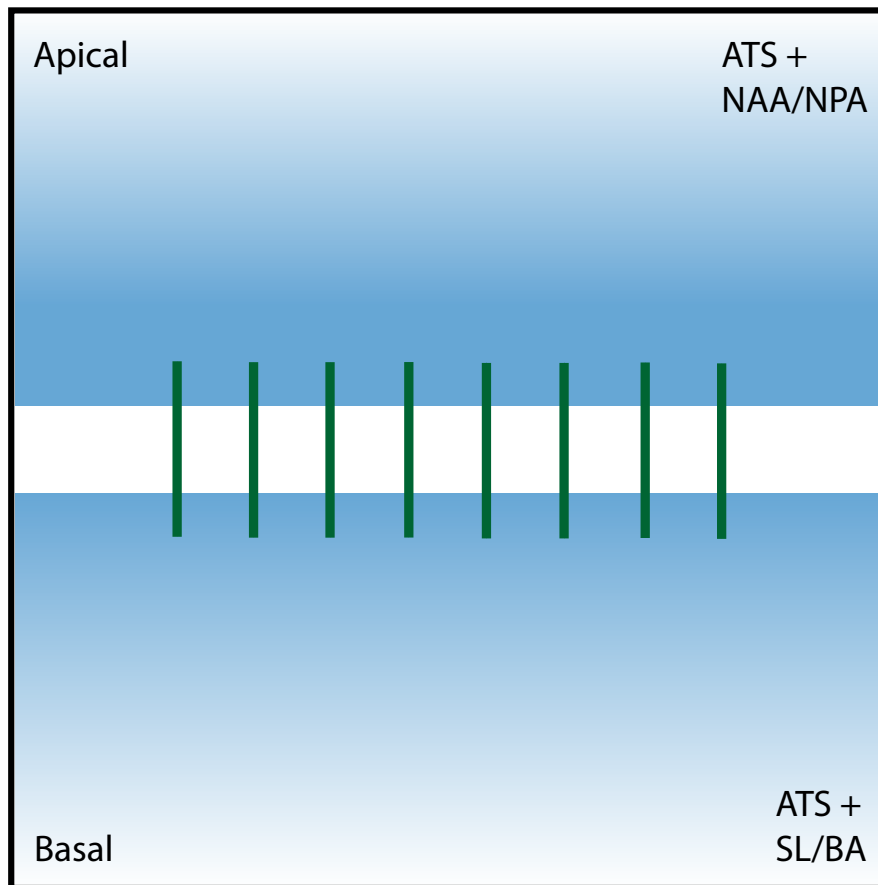


Diagram 2.1 | Cartoon depicting the set up of split-plate assays. Blue represents ATS set with agar, green represents *Arabidopsis* stem segments

2.2.2 | Split-stem assays

Arabidopsis plants were grown in PT40 trays under long-day conditions as described in Table 2.1, and bolting inflorescences excised when 5-10 cm tall. These were trimmed to 2 cm in length, with excess stem being removed from the apical end so as to leave the basal-most segment. These were sectioned longitudinally and placed in liquid ATS medium supplemented with chemical treatments in 2 mL Eppendorf tubes. Sections were incubated in tissue culture conditions (see Table 2.1) until imaging.

2.2.3 | Branch counts

Arabidopsis plants were grown in PT24 trays, either in long day conditions or initially under short day conditions and 28 d after germination were moved to long day growth conditions for the remainder of growth. As summarised in Diagram 2.2, rosette branches were defined as such if they originated from rosette nodes or as primary cauline if originating from cauline nodes on the primary inflorescence. Secondary cauline branches were defined as those emerging from the nodes on the primary cauline branch. Scoring was conducted at terminal flowering for intact plants, between 6 and 8 weeks after germination. For decapitation experiments, the bolting inflorescence was excised when 10 cm tall and plant scored 10 d after this (Greb et al., 2003).

2.2.4 | Branch angle

Arabidopsis plants were grown in PT24 trays, initially under short day conditions (see Table 2.1) and 28 d after germination were moved to long day growth conditions until terminal flowering. Branch angle was defined as the angle between the primary inflorescence and the adaxial side of the cauline branch. Images of branches were taken using a Nikon DSLR and the angle calculated using Image J software. This was done for the two cauline branches closest to the base and an average calculated for each plant.

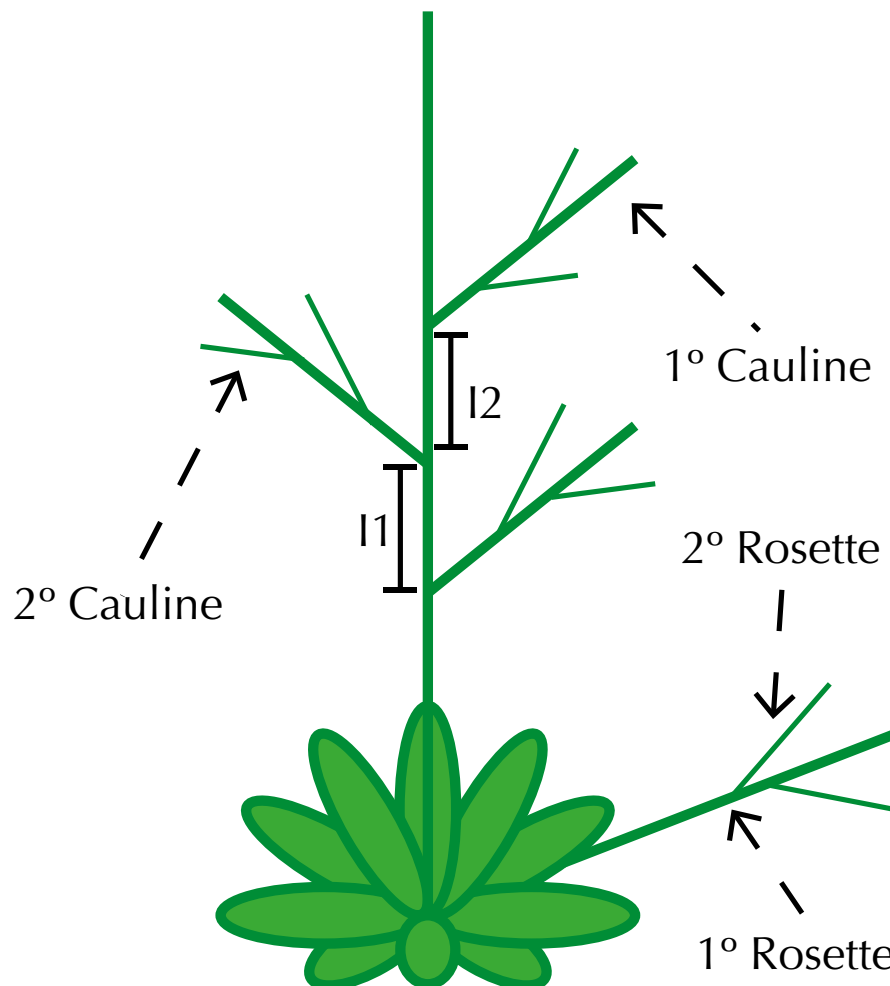


Diagram 2.2 | Cartoon depicting the branching nomenclature of *Arabidopsis*

2.2.5 | Height

Arabidopsis plants were grown in PT24 trays, either in long day conditions or initially under short day conditions and 28 d after germination were moved to long day growth conditions until terminal flowering, at which height was measured. A ruler was used to measure the distance from the base of the primary inflorescence to its tip.

2.2.6 | Stem width

Arabidopsis plants grown in long day conditions until terminal flowering were measured at the base of the primary inflorescence using a Digitronic caliper (Moore & Wright).

2.2.7 | Proportion of fertile fruits

The proportion of fertile fruits was estimated on long day grown plants at terminal flowering. Fruits were categorised as fertile if they consisted of an elongated, filled silique or sterile if they did not elongate/fill. The proportion of fertile fruits was calculated as a proportion of the total fruits observed as a proxy for fertility.

2.2.8 | Auxin transport assays

Standard “bulk” auxin transport assays were modified from those described in (Crawford et al., 2010). 15 mm stem segments were excised from the basal internodes of plants at terminal flowering, and the apical end submerged in 30 μ l ATS without sucrose (pH = 5.6), containing 1 μ M 14 C-IAA (American Radiolabeled Chemicals) in 96 well PCR plates. Stems were incubated for 18 h in tissue culture conditions (see Table 2.1), and the basal 5 mm of the segment was then excised, cut in half and placed in Isoplate™-96 plates containing 200 μ l scintillation liquid (MicroScint™ 20, PerkinElmer, Waltham, MA). These were shaken for 4 h at 450 RPM (MixMate microplate shaker, Eppendorf) prior to scintillation counting in an MB2 scintillation counter (PerkinElmer, Waltham, MA). Counts per minute (CPM) was used as a measure for the amount of auxin transported through the stem segment.

2.2.9 | Internode length/cauline node number

Plants were grown under long day conditions until terminal flowering and the distance between each cauline node measured using a ruler. Cauline node 1 was classified as the first emerging from the main stem in an acropetal direction. Internode 1 was classified as the distance between the 1st & 2nd cauline nodes as shown in Diagram 2.2.

2.2.10 | 2 – node assays

1.5 ml lidless Eppendorf tubes were filled with liquid ATS media, sealed using parafilm and a small hole was pierced in the parafilm using forceps. *Arabidopsis* plants were grown under long-day conditions in PT40 pots as described in section 2.1.2 and the bolting inflorescence excised when 1-2 cm tall with axillary meristems typically 0.5-2 mm in length. The apical meristem was excised using forceps to leave the two most basal axillary meristems and subtending leaves. This was then inserted through the hole in the parafilm such that the base of the stem was in contact with the ATS. Tubes were racked and placed in 40 cm x 20 cm plastic trays containing 1 cm depth of water to maintain humidity, covered with a clear plastic propagator lid and incubated in Conviron chambers under long-day conditions. Tubes were topped up with ATS daily and each bud was measured daily using a ruler for 10 days. For strigolactone treatment, 5 μ M GR24 was added to the ATS.

2.3 | Molecular biology

2.3.1 | DNA extraction

For genotyping, DNA was extracted using a method adapted from (Edwards et al., 1991). Plant tissue was collected in 96 well, racked microtubes (Qiagen Hilden, Germany), along with a 3 mm glass bead and frozen at -80 °C. Tissue was disrupted using a TissueLyser II (Qiagen, Hilden, Germany) and 400 µl of extraction buffer (200 mM Tris-HCl pH 7.5, 250 mM NaCl, 25 mM EDTA, 0.5% SDS) added. Plates were centrifuged in a Sigma 4-16 centrifuge (Sigma-Aldrich, Missouri, US) at 2500 rpm for 20 min at room temperature (RT). 300 µl supernatant was transferred to a Abgene™ 96 Well, 0.8 ml, Polypropylene Deepwell Storage Plate and 300 µl isopropanol (Sigma-Aldrich, Missouri, US) added to each. This was centrifuged for 35 min at 6000 rpm at RT, supernatant discarded and pellet allowed to air dry for 10 min before being resuspended in 50 µl of Tris-EDTA (TE) buffer.

Plasmid DNA was extracted from bacterial cells using the QIAprep Spin miniprep kit (Qiagen, Hilden, Germany) according to the manufacturer's instructions.

In all cases, quantity of DNA was assessed using a NanoDrop™ One Microvolume UV-Vis Spectrophotometer (Thermo Fisher Scientific, Massachusetts, US).

2.3.2 | PCR

Was performed using REExtract-N-Amp PCR ReadyMix (Sigma-Aldrich, Missouri, US) according to manufacturer's instructions and using the typical conditions outlined in Table 2.3 in a G-Storm GS4 Thermal Cycler.

	Reagent	Quantity
	REExtract-N-Amp PCR ReadyMix	10 µl
	Forward primer (10 mM)	1 µl
	Reverse primer (10 mM)	1 µl
	DNA	25-250 ng
	Sterile H ₂ O	To 20 µl
Phase	Temperature (°C)	Length (min)
Initial denaturation	94	3
Denaturation	94	0.5
Annealing	Primer T _m	0.5
Extension	72	1 min/kb
Final extension	72	10

Table 2.3 | PCR conditions

2.3.3 | Construct assembly

All constructs were made using Multi-site Gateway (Invitrogen, California, US) and DNA synthesis (GENEWIZ, Bishop's Stortford, UK). For complementation of the *pin1* mutant by a chimeric PIN protein, a Gateway vector (pDONR P4-P1r) carrying a 3.5 kb upstream *PIN1* promoter region previously reported to complement *pin1* when driving PIN1 expression (Heisler et al., 2005) was used. This was amplified from plasmid DNA (Primer ID 13-14, (O'Connor et al., 2017)) and inserted into pDONR P4-P1r via a BP recombination reaction between the *attB*-flanked PCR product and *attP* containing donor vector, according to the manufacturer's instructions, yielding an entry clone (BP reaction). The resulting plasmid was sanger sequenced to verify insertion and directionality (Primer ID 15-16). For chimeric PIN1-GFP constructs, the coding sequence (CDS) for the central region of the PIN3 hydrophilic loop was used to substitute the central region of the PIN1 hydrophilic loop CDS and the resulting chimeric sequence was synthesised (GENEWIZ, Bishop's Stortford, UK) with the *attL1* sequence and *attL2* sequence respectively as 5' and 3' flanking regions. This was delivered in a pUC57-Kan vector and sanger sequenced to verify its veracity (Primer ID 5-9). The P4-P1r carrying proAtPIN1 and the pUC57 carrying the *attL* tagged PIN chimeric regions were used as entry clones in an LR recombination reaction with the Gateway binary destination vector pH7m24GW (<https://gatewayvectors.vib.be/collection/ph7m24gw2>), conducted according to manufacturer's instructions (LR reaction). The resulting expression clone was verified by sanger sequencing (Primer ID 17-18) using Ape and CLC workbench. For detailed information about primer sequences, consult Table B.2 in appendix B.

2.3.4 | Transformation

Vectors were transformed into heat-shock competent DH5 alpha *Escherichia coli* by adding 1 µl of the BP or LR reaction described in section 2.3.3 to 50 µl competent cells which had been thawed on ice for 30 min. Cells were then incubated on ice for 30 min and heat shocked at 42 °C for 45 seconds before being returned to ice for 2 min. 950 µl of super optimal broth with catabolite repression (SOC) medium (Invitrogen, Waltham, US) was added and cells were incubated at 37 °C in a shaking incubator at 220 rpm for 1 h. This was then plated onto lysogeny broth (LB) (Merck, Darmstadt, Germany) (Bertani, 1951) solidified with 1.5 % Bacto™ Agar (Becton, Dickinson and Company, Sparks, US), supplemented with the relevant antibiotic and incubated at 37 °C overnight. Colonies were picked into 2 ml liquid LB and incubated at 37 °C in a shaking incubator at 220 rpm overnight. Selection was carried out on 50 µg/ml kanamycin for pDONR vectors and 50 µg/ml spectinomycin for pH7m24GW. Plasmid DNA was extracted from positive transformants using a QIAprep Spin Miniprep kit (QIAGEN, Hilden, Germany) according to the manufacturer's instructions.

Transformation of *Agrobacterium tumefaciens* was achieved by addition of 1 µl *E.coli*

miniprep plasmid DNA to 50 µl GV3101 electrocompetent cells and electroporated at 1500 V for 5 milliseconds. 950 µl of SOC medium was added and cells allowed to recover at 28 °C for in a shaking incubator at 220 rpm for 1 h. Cells were plated onto LB-agar and incubated at 28 °C for 48-72 h before selecting colonies into 2 ml of LB liquid supplemented with 100 µg/ml spectinomycin.

For plant transformation, the floral dip method was used (Clough and Bent, 1998). *Arabidopsis thaliana* was sown in 4x4 cm pots and grown until bolting inflorescences were ~10 cm tall. A 250 ml *Agrobacterium* culture was grown up overnight, spun down for 5 minutes at 5000 rpm and the pellet resuspended in a 250 ml sucrose (50 g/l) and silwet (200 µl/l) solution. *Arabidopsis* inflorescences were immersed in this solution for 30-60 s, agitated by swirling and placed under a transparent propagation lid for 24 h to maintain humidity. This was then removed and plants grown to seed set.

2.3.5 | Plant selection

Seeds of transformed plants (T1) were sterilised as outlined in section 2.1.4 and plated on 120 mm square plates containing ATS medium solidified with agar and supplemented with 25 µm/mL hygromycin. Seeds were stratified in darkness at 4 °C for 2 days before being exposed to light for 6 hours in tissue culture conditions outlined in table 2.1. Seeds were then wrapped in aluminium foil and placed in the dark at room temperature for 4 days. Resistant seedlings were then selected on the basis of elongated hypocotyls according to (Harrison et al., 2006). Plants were subsequently moved to tissue culture conditions outlined in table 2.1 for 3 days to promote photomorphogenesis, with resistant seedlings then transferred to soil. Seed was then harvested from these and segregation analysis performed in this T2 generation based on antibiotic resistance, and verified with expression of the fluorescent tag. 100 seeds from at least 50 T2 lines were assessed for a 3:1 ratio of resistant plants. 16 seedlings from at least 10 T2 lines exhibiting the correct ratio were then grown to maturity and T3 seed collected. 100 seeds from each T3 line were then assessed for homozygosity (i.e. all plants resistant) and 5 plants picked from each homozygous line to produce T4 seed.

2.4 | Microscopy

2.4.1 | Confocal microscopy

Confocal images were captured on a Zeiss LSM 700 or LSM 880 confocal microscopy equipped with a 20x immersion objective. Excitation was performed using 488 nm (3%–6% laser power) and 639 nm (2% laser power) lasers. Images were acquired using SP555 and LP640 emission filters for GFP and chloroplast autofluorescence. Transmitted light was used to confirm anatomy of tissue investigated. Pinhole size was set at one Airy unit for all acquired images.

If comparisons of signal intensity were to be made between genotypes, all acquisition parameters were kept constant between genotypes. Following acquisition, brightness and contrast were adjusted to optimise visualisation, again making the same adjustments to all images where comparisons were to be made. Image processing was conducted using ImageJ (<https://imagej.nih.gov/ij/>).

2.4.2 | Sample preparation for imaging

To image PIN protein localisation in stem segments, plants between 4-6 weeks old were used depending on the experiment. Following split plate treatments as described in 2.2.1, stems were hand-sectioned longitudinally through the vascular bundle using a razor blade, in order to expose xylem parenchyma for imaging. Cut stems were placed face up on a 90 mm round petri dish and secured at their midpoint using microporous tape. These were then immersed in water and imaged at the apical or basal end, or both.

For BFA & GR24 treatments, following the procedure described in 2.2.2, stems were prepared for imaging in the same way as above, with the difference that they were immersed in liquid ATS medium supplemented with the relevant treatment.

2.4.3 | Signal intensity quantification

The fluorescence signal intensity of nuclei or on the basal plasma membrane of xylem parenchyma cells was obtained using Zeiss Zen 2012 software. Plasma membranes or nuclei were manually traced round using the polygon tool and the arithmetic mean of the selected area recorded. This was done for at least 5 cells per sample and the average calculated.

2.5 | Bioinformatics

2.5.1 | Primer design

Primers used for sequencing and genotyping were designed using Primer3 web version 4.1.0. Chosen primers had length 18-23 base pairs, melting point of 55-62 °C and low secondary structure score.

2.5.2 | Statistics

Were conducted using RStudio version 1.3.959. Where two variables were being compared, a Student's t-test was used, where multiple variables were being compared a one-way ANOVA and a Tukey's HSD was performed, with significance values assigned using compact letter display with a threshold $p < 0.05$.

2.5.3 | Protein sequence alignment

Sequences were obtained from TAIR and aligned with T-Coffee Expresso (Notredame et al., 2000; O'Sullivan et al., 2004; Poirot et al., 2004; Armougom et al., 2006; Di

Tommaso et al., 2011) and processed to the format contained in this thesis using ESPript 3.0 (Robert and Gouet, 2014).

2.5.3 | Data visualisation

Graphs were produced using RStudio version 1.3.959 with the ggplot2 package installed. Figures were assembled in Microsoft PowerPoint & Adobe Photoshop. This thesis was written using Microsoft Word and formatted in Adobe InDesign.

3

The role of auxin flux and developmental stage in modulating PIN polarisation behaviour

"The tragedy of old age is not that one is old, but that one is young" - O. Wilde

3.1 | Introduction

Whilst plant development is plastic it is still the case that plants go through distinct growth stages, transitioning from embryogenesis to vegetative growth and subsequently entering the reproductive phase. During these transitions there is considerable morphological change and focus switches from resource acquisition to seed production (Huijser and Schmid, 2011). Plants must cope with both age-related changes in priorities as well as changing environmental conditions, as biotic and abiotic factors alter around them. To do so they exhibit dynamic responses during their development, over a diversity of timescales and a range of magnitudes. These changes can be phenotypically observed, for example, changes in the extent of branching depending on light availability and herbivory (Palmer *et al.*, 2013). This is dependent on the ability of plants to control the activity of axillary meristems which lie between the main stem and subtending leaves (Domagalska and Leyser, 2011). Significant phenotypic changes are often age-related and due to the continuous progression of plants to their final life stage, senescence (Bleecker and Patterson, 1997). Depending on developmental stage responses to the same environmental cues can be radically different, due to changes in plant competence to phase change (Bergonzi *et al.*, 2013; Poethig, 2013). Much of this plasticity can be related to auxin transport and signalling which acts as an integrator of diverse signals (Reviewed in Casal and Estevez, 2021).

Understanding how PIN behaviour changes during plant growth is pertinent to unravelling the way in which PIN polarity is regulated. In this chapter, I will first outline our current understanding of PIN behaviour and regulation, before discussing my novel results.

3.1.1 | The role of PINs in canalisation

The phenomenon of apical dominance is well characterised and involves release of buds from dormancy upon removal of the SAM in a process mediated by auxin, as has been discussed in detail previously (Section 1.1) (Sachs, 1975). Tsvi Sachs explained this occurrence through the auxin transport canalisation hypothesis, which proposes that auxin upregulates its own transport to generate narrow files of auxin transporting cells from an auxin source to an auxin sink (Sachs, 1969; Sachs, 1975; Sachs, 1981). Since then, a class of auxin efflux exporters (PINs) have been discovered which are able to localise in a polar manner in response to auxin, allowing directional auxin transport (Sauer *et al.*, 2006; Wisniewska *et al.*, 2006; Balla *et al.*, 2011; Prát *et al.*, 2018). This has been implicated in the formation of vasculature generally and during the establishment of bud outgrowth (Balla *et al.*, 2011; Mazur *et al.*, 2016; Mazur *et al.*, 2020b). Diverse mechanisms have been proposed for how PINs are able to sense auxin and alter their localisation in response. These range from sensing flux across the membrane

(Mitchison *et al.*, 1981), localising according to auxin concentration gradients (Jönsson *et al.*, 2006; Smith *et al.*, 2006), to mechanical stress (Jönsson *et al.*, 2010) and intra-cellular-extracellular receptor systems (Wabnik *et al.*, 2010). Whilst modelling based on these mechanisms is able to recapitulate features of canalisation, there is a notable absence of experimental evidence for how PINs sense these postulated signals.

In any case, establishment of polarity requires PIN allocation and removal from the plasma membrane on a dynamic basis. In roots there is some evidence to suggest there is rapid PIN cycling between the membrane and endosomal compartments (Teh and Moore, 2007; Kleine-Vehn *et al.*, 2008a; Naramoto *et al.*, 2010; Robert *et al.*, 2010; Kleine-Vehn *et al.*, 2011) but this does not appear relevant in stems (Shinohara *et al.*, 2013). However, the regulation of PIN membrane residency does appear to be an important mechanism by which cytokinin and strigolactone can feed into the establishment of canalisation in shoots, with regard to establishing vasculature and regulating bud outgrowth. Strigolactone has been demonstrated to induce PIN1 and PIN7 endocytosis in shoots (Shinohara *et al.*, 2013; Ticchiarelli, 2019) while cytokinin increases PIN3,4 & 7 allocation to the membrane (Waldie and Leyser, 2018). This behaviour correlates with observed effects of SL on inhibiting vasculature development and bud activation (Crawford *et al.*, 2010; Shinohara *et al.*, 2013; Zhang *et al.*, 2020) and of CK activating bud outgrowth (Wickson and Thimann, 1958; Chatfield *et al.*, 2000; Kalousek *et al.*, 2010).

Current data support the role of PIN polarisation in modulating shoot architecture, but our lack of understanding regarding the mechanistic basis by which PINs polarise in response to auxin represents a barrier to our comprehension of how it regulates phenotypic plasticity.

3.1.2 | Aims

In this chapter, I will detail investigations into whether developmental stage affects PIN polarity and accumulation in response to auxin flux, cytokinin and strigolactone. More specifically, I will address the following research questions:

- ◇ Do PIN3, PIN4 & PIN7 require auxin or auxin flux to maintain basal polarity?
- ◇ Does auxin concentration or flux drive PIN1 polarity?
- ◇ Is tissue age relevant to determining PIN1 response to cytokinin and strigolactone?
- ◇ How does PIN1 dynamism change with tissue age?

3.2 | Results

3.2.1 | Assessing the behaviour of PIN3, PIN4 & PIN7

Previous data suggests that PIN1 requires auxin, but not NPA-sensitive auxin flux to maintain its basal plasma membrane localisation in xylem parenchyma cells of excised inflorescence stem segments (Bennett *et al.*, 2016). To determine whether other shoot-expressed PIN proteins display auxin and/or flux-sensitive basal plasma membrane localisation, I assessed the behaviour of fluorescent protein tagged PIN3, PIN4 and PIN7, which we have previously shown to be widely expressed in the stem and to contribute to stem auxin transport and the establishment of active shoot branches (Bennett *et al.*, 2016; Van Rongen *et al.*, 2019).

As described in Chapter 2, basal inflorescence stem segments (~2 cm long) were excised from *pin3 PIN3:PIN3-GFP*, *pin4 PIN4:PIN4-GFP* and *pin7 PIN7:PIN7-GFP* expressing plants. We routinely use mature stem segments of ~6-week-old plants to analyse PIN1 polarisation but have previously found PIN3-GFP, PIN4-GFP and PIN7-GFP to be poorly expressed in these older tissues (Bennett *et al.*, 2016). Therefore, younger inflorescences from ~4 week old plants were used for my analyses. Stem segments were embedded between 2 agar blocks in Petri dishes, allowing pharmacological treatments

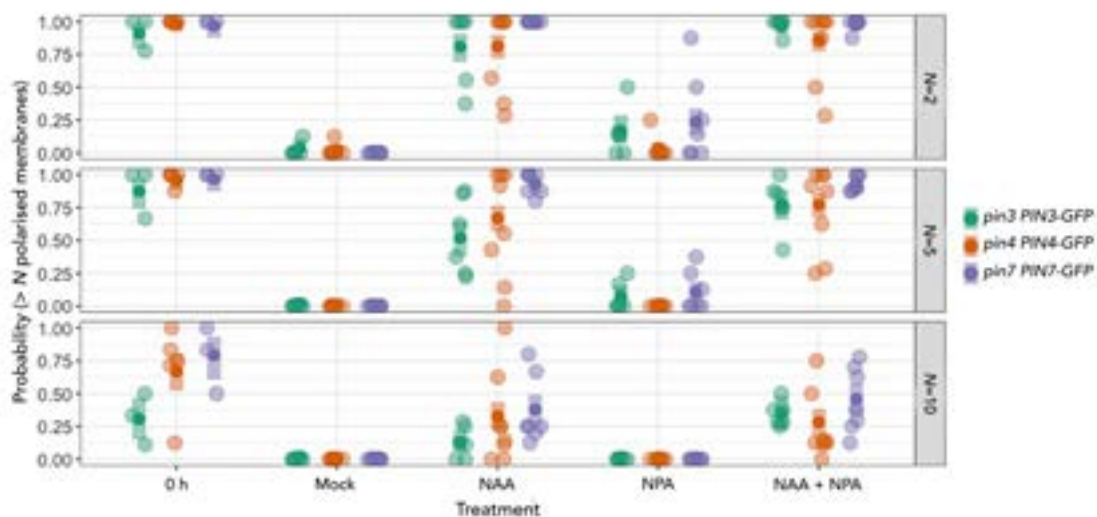


Figure 3.1 | Stem segments were harvested from ~4 week old plants treated, longitudinally sectioned & imaged apically. The number of membranes with visibly polar PIN-GFP were counted and the probability of the number of polarised cells in each repeat being greater than each than defined threshold (N=2, top panel; N=5, middle panel or N=10, bottom panel) calculated. For all treatments, each point represents a single repeat experiment in which at least 8 independent plants were analysed for PIN polarity, at least 6 repeats were conducted for all treatments for all PINs. For the 0 h control, each point represents a single experiment in which at least 5 independent plants were analysed for PIN polarity, at least 3 repeats were conducted. A logistic regression model was fitted to these data to estimate the 95% confidence interval, represented by the coloured bars. Green represents PIN3-GFP, orange PIN4-GFP and purple PIN7-GFP.

to be supplied apically or basally as desired by supplementing either the apical or basal agar block. Segments were treated apically with a mock solvent control, 1 μ M 1-Naphthaleneacetic acid (NAA, a synthetic auxin), 1 μ M NPA, or combined 1 μ M NAA and NPA. The presence of PINs at the basal plasma membrane of xylem parenchyma cells was assessed by longitudinally sectioning the stems and imaging the cut surface at the apical end of the stem segments using confocal microscopy. Two measures were used to quantify PIN behaviour. First, the number of cells per field with basal plasma membrane localised PINs was determined (Fig. 3.1). Second, fluorescence levels at the basal plasma membrane of cells with detectable PINs were assessed (Fig. 3.2).

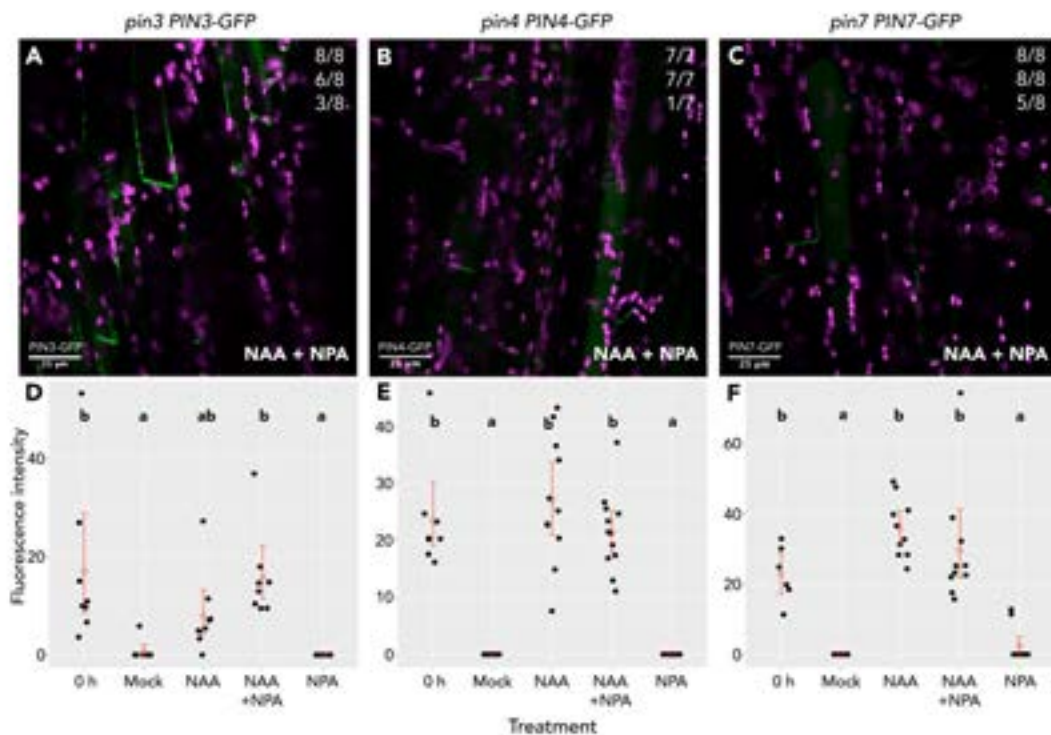


Figure 3.2 | (A-C) Representative confocal images demonstrating the localisation of PIN3-GFP (A), PIN4-GFP (B) and PIN7-GFP (C) in the xylem parenchyma and cells from \sim 2 cm stem segments treated for 3 d in vertical plates treated apically with both NAA & NPA. Stem segments were collected from \sim 4 week old plants, treated, sectioned longitudinally and imaged apically using a confocal microscope. Green represents GFP and magenta represents chloroplast autofluorescence. The number in the top right corner of each image represents the proportion of plants in which >2 (first line), >5 (second line) or >10 (third line) cells with basally polarised PIN-GFP were visible within a field of view across two separate images of each stem. (D-F) intensity measurements of PIN3-GFP (D), PIN4-GFP (E) & PIN7-GFP (F) present on the basal plasma membrane of xylem parenchyma cells quantified using at least 2 cells from 10 independent plants ($n=20$). Different letters indicate statistically significant differences following a one-way ANOVA and Tukey's HSD post-hoc testing.

Similar responses were observed for all three PINs. PINs were clearly detectable at the basal plasma membrane of xylem parenchyma cells immediately after stem segment excision (timepoint 0 h) (Fig. 3.1 & 3.2). After three days incubation in the absence of apical auxin all three PINs were depleted from the basal plasma membrane and very few cells with any detectable plasma membrane-localised PINs were observed (Fig. 3.1). Where PINs were detected, levels were very low relative to the 0 h control (Fig.

3.2). PIN3-GFP and PIN7-GFP were consistently retained at the plasma membrane in the presence of apical auxin, whilst the behaviour of PIN4-GFP was more erratic. In the presence of NPA all three PINs were strongly depleted from the plasma membrane but, in contrast, combined treatment with NAA and NPA resulted in substantial retention of plasma membrane PINs, similar to treatment with NAA alone.

These results show some similarities to, but also some major differences from those previously reported for PIN1 behaviour in stem segments from mature plants (Bennett *et al.*, 2016). In particular, while plasma membrane PIN1 was depleted in untreated stems and retained in auxin treated stems, it was also retained in stems treated with NPA alone. It has also been observed that following its depletion from the plasma membrane in untreated stems, resupply of apical auxin was unable to restore plasma membrane accumulation of PIN1, unless the auxin was added within the 1 to 3 day timeframe over which plasma membrane depletion occurred (Bennett *et al.*, 2016).

3.2.2 | PIN1 behaviour differs in old and young tissue

The behaviour of PIN3-GFP, PIN4-GFP & PIN7-GFP described above differs from observations of PIN1 behaviour in mature stems. NPA treatment led to the retention of PIN1-GFP on the plasma membrane, whereas PIN7-GFP, as well as PIN3-GFP and PIN4-GFP, are depleted. These differences between PIN1-GFP and PIN7-GFP could be due either to inherent differences in the proteins or to stem maturity, or both. To test these hypotheses, I investigated the behaviour of PIN1-GFP in young inflorescences.

To assess whether PIN1-GFP in young stem segments responds to inhibition of auxin transport, basal inflorescence stem segments were treated apically with either a mock solution, 1 μ M NAA, 1 μ M NPA or both for 6 d. Comparable to the data obtained for PIN3-GFP, PIN4-GFP and PIN7-GFP, apical NAA maintains basal plasma membrane PIN1-GFP at a similar level to the 0 h control in young stems (Fig. 3.3, B). Application of NPA alone resulted in significantly reduced PIN1-GFP levels on the basal plasma membrane (Fig. 3.3, B). However, simultaneous application of NAA and NPA maintained PIN1-GFP on the basal PM of cells of xylem parenchyma cells (Fig. 3.3, A, C).

I further tested the ability of PIN1-GFP to repolarise following depletion from the basal PM. Stem segments were treated apically with either a mock solution for 5 or 6 days, or mock solution for 5 days followed by 1 μ M NAA for 1 day. As expected, basally localised PIN1-GFP was strongly reduced in xylem parenchyma cells after 5 and 6 days of mock treatment (Fig. 3.4, A, B). Resupply of apical NAA for 1 day was sufficient to trigger re-accumulation of polar PIN1-GFP at the apical end in the majority of stem segments (Fig. 3.4, C). According to the auxin transport canalisation hypothesis, the passive flux of auxin between a source and a sink can upregulate and polarise PINs in the

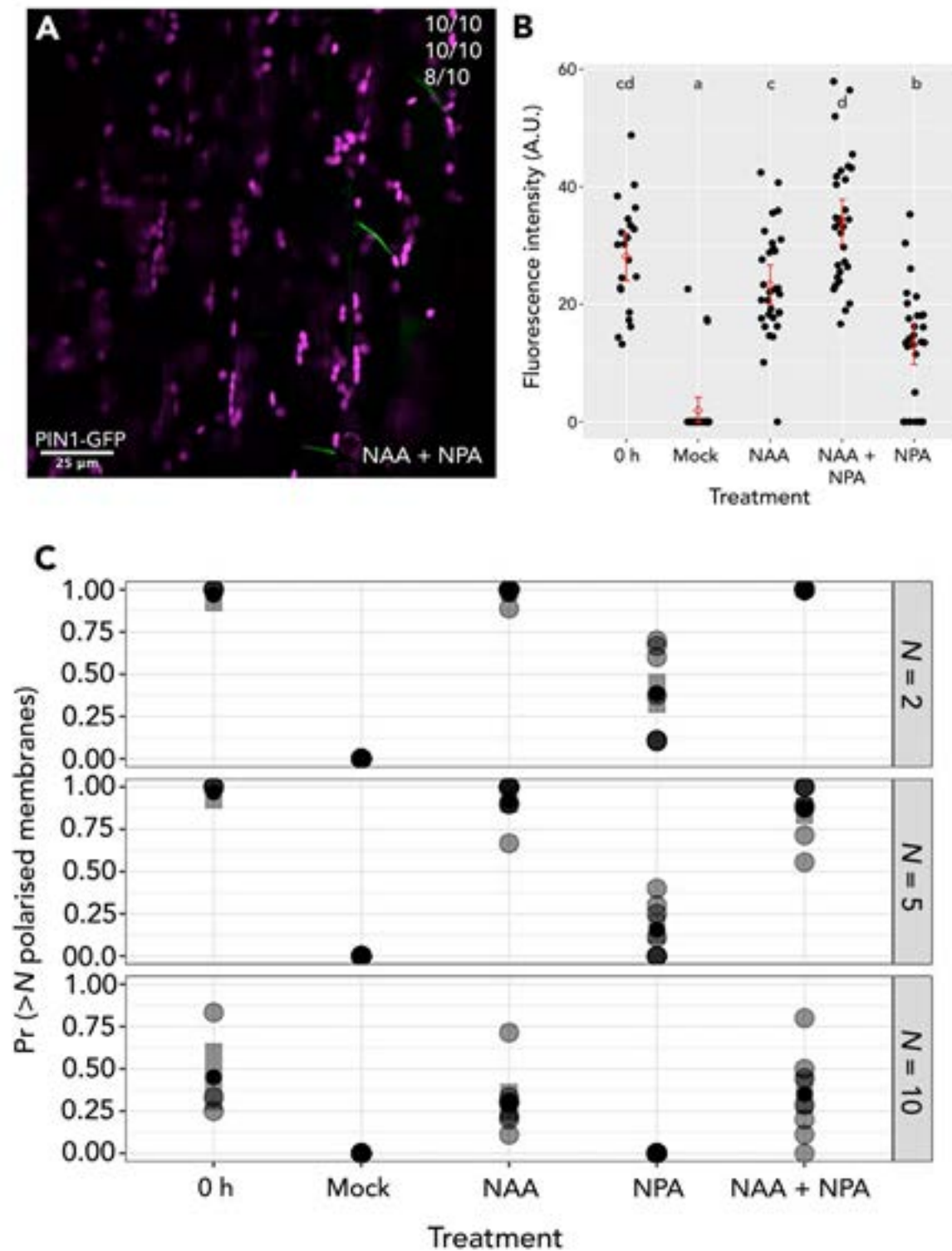


Figure 3.3 | (A) Representative confocal image demonstrating the localisation of PIN1-GFP in the xylem parenchyma and cambial cells of *pin1* PIN1-GFP stem segments treated for 6 d in vertical plates treated apically with both 1 μ M NAA and NPA. Stem segments were collected from ~4 week old plants, treated, sectioned longitudinally and imaged apically using a confocal microscope. Green represents GFP and magenta represents chloroplast autofluorescence. The number in the top right corner of each image represents the proportion of plants in which >2 (first line), >5 (second line) or >10 (third line) cells with basally polarised PIN1-GFP were visible within a field of view. (B) PIN1-GFP intensity present on the basal plasma membrane of xylem parenchyma & cells quantified using at least 5 cells from 10 independent plants and repeated thrice ($n > 150$). Different letters represent

significant differences after a one-way ANOVA followed by Tukey's honest significant difference post-hoc analysis. (C) The number of membranes with visibly polar PIN1-GFP were counted and the probability of the number of polarised cells in each repeat being greater than each arbitrary threshold calculated. For all treatments, each point represents a single repeat experiment in which at least 8 independent plants were analysed for PIN1 polarity, at least 6 repeats were conducted for all treatments ($n=48$). For the 0 h control, each point represents a single experiment in which at least 5 independent plants were analysed for PIN polarity, at least 3 repeats were conducted ($n=15$). We fitted a logistic regression model to these data to estimate the 95% confidence interval, represented by the grey bars.

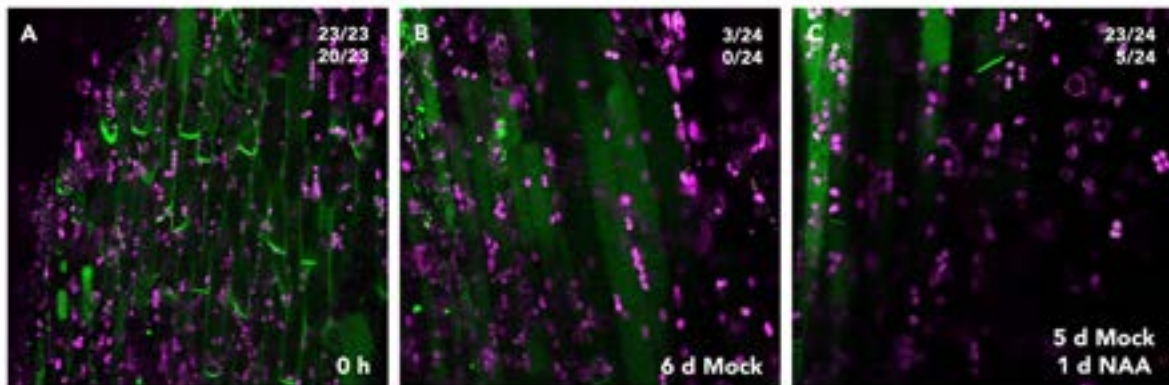


Figure 3.4 | Representative confocal image demonstrating the localisation of PIN1-GFP in the xylem parenchyma and cambial cells of 2 cm sections of bolting inflorescence stems of ~ 4 week old *pin1* PIN1-GFP expressing plants were treated apically with mock for 6d (B) or with mock for 5 d followed by 1 μ M NAA (C). Stem sections were sectioned longitudinally and imaged apically by confocal microscopy. Stems were also imaged immediately after harvesting (A). Green represents GFP and magenta represents chloroplast autofluorescence. The number in the top right corner of each image represents the proportion of plants in which >2 (first line), >5 (second line) cells with basally polarised PIN1-GFP were visible within a field of view, $n=23-24$.

direction of the sink (Mitchison *et al.*, 1981; Sachs, 1981). Data presented in figure 3.4 is consistent with this hypothesis, while the results presented in figure 3.3 suggest that PIN polarisation does not require NPA-sensitive auxin flux. However it does not rule out the possible role of auxin concentration.

As such, I tested how PIN1 behaves in the presence of a strong auxin source and whether PIN1 can reorient to generate a flow of auxin from a strong source towards a sink. Isolated stem segments were placed upright for 3 days between 2 untreated agar blocks in Petri dishes to allow PIN1-GFP to deplete from the membrane. Segments were then inverted and inserted between 2 agar blocks, with 1 μ M NAA or mock treatment in the upper block for 1 day, such that the original basal end of the stem was in contact with the treated agar. Stems were then sectioned and imaged at the apical and basal end ("apical" and "basal" ends here refer to the original shootward and rootward ends of the stem segment, respectively). If polar accumulation of PIN1 could be driven by auxin concentration alone, it would be expected that PIN1 would polarise following NAA treatment, either to the basal end of the cells if polarity is fixed or to the apical end of cells if polarity is determined by the applied auxin gradient. This was not the

case, those stems treated basally with NAA did not exhibit apically polarised PIN1-GFP, nor was there any change in the amount of PIN1-GFP on the basal plasma membrane relative to mock treated stem (Fig. 3.5). Unsurprisingly, there was more PIN1-GFP present on the basal PM at the basal end of the stem than at the apical end under both treatment regimes, as auxin drains from the apical to the basal end such that auxin depletion is slower in basal tissues. These data suggest that it is not possible to drive apical PIN1 polarisation by basal supply of auxin and beyond that, basal auxin supply is insufficient to drive any basal plasma membrane accumulation of PIN1-GFP, even locally where the basal end of the stem segment is inserted into agar containing 1 μ M NAA.

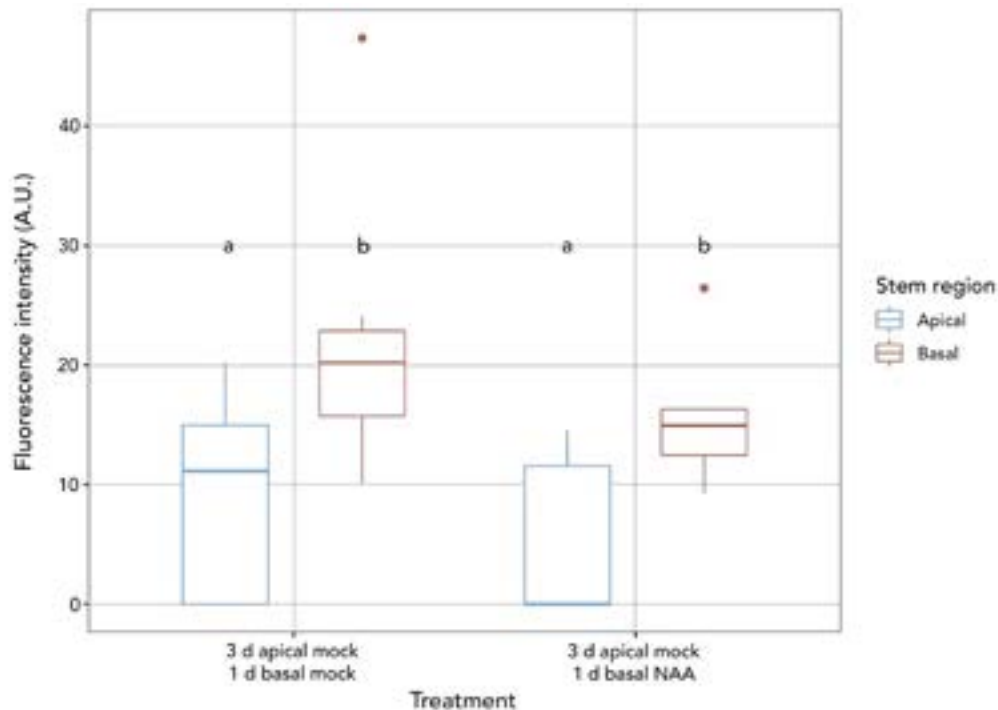


Figure 3.5 | 2 cm sections were excised from bolting inflorescences of ~ 4 week old plants expressing *pin1 PIN1-GFP* and placed in agar plates treated apically with mock. After 3 d, stems were inverted and placed into new plates treated apically with either mock or 1 μ M NAA for 1 d, such that the basal end was exposed to treatment. Stem segments were then longitudinally sectioned and cells of the xylem parenchyma at the apical (shootward) and basal (rootward) end of the stem imaged using confocal microscopy. Fluorescence data was extracted from these images using Zen Black (2012) software to trace round basal plasma membranes where PIN1-GFP was visible. No PIN1-GFP localised to the apical plasma membrane could be detected. This was done for at least 5 membranes per stem and at least 8 stems were analysed per treatment per experiment (n=40). The experiment was repeated three times. Membrane fluorescence values for each stem were averaged and plotted here as box and whisker plots. Different letters indicate statistically significant differences following a one-way ANOVA and Tukey's HSD post-hoc testing.

We have demonstrated previously that PIN7 retention on the plasma membrane correlates with intracellular auxin levels at the apical end of stem segments (Waldie, unpublished). However, it has also been shown that treating the basal end of stem segments with auxin does not support PIN1 (Fig 3.5) or PIN7 retention (Waldie, unpublished). In order to test whether basal auxin treatment was indeed driving high intracellular auxin levels, isolated stem segments from *DR5rev::GFP* expressing plants were

mock-treated for 3 days between 2 agar blocks in Petri dishes to allow auxin to drain from the stem. Segments were then inserted between 2 agar blocks either in an upright, or inverted orientation, with 1 μM NAA or mock treatment in the upper block for 1 day. Figure 3.6 shows that NAA application drives *DR5* expression when applied basally, indicating that basal auxin supply does increase intracellular auxin levels but that this does not straightforwardly correlate with PIN1 or PIN7 retention on the membrane.

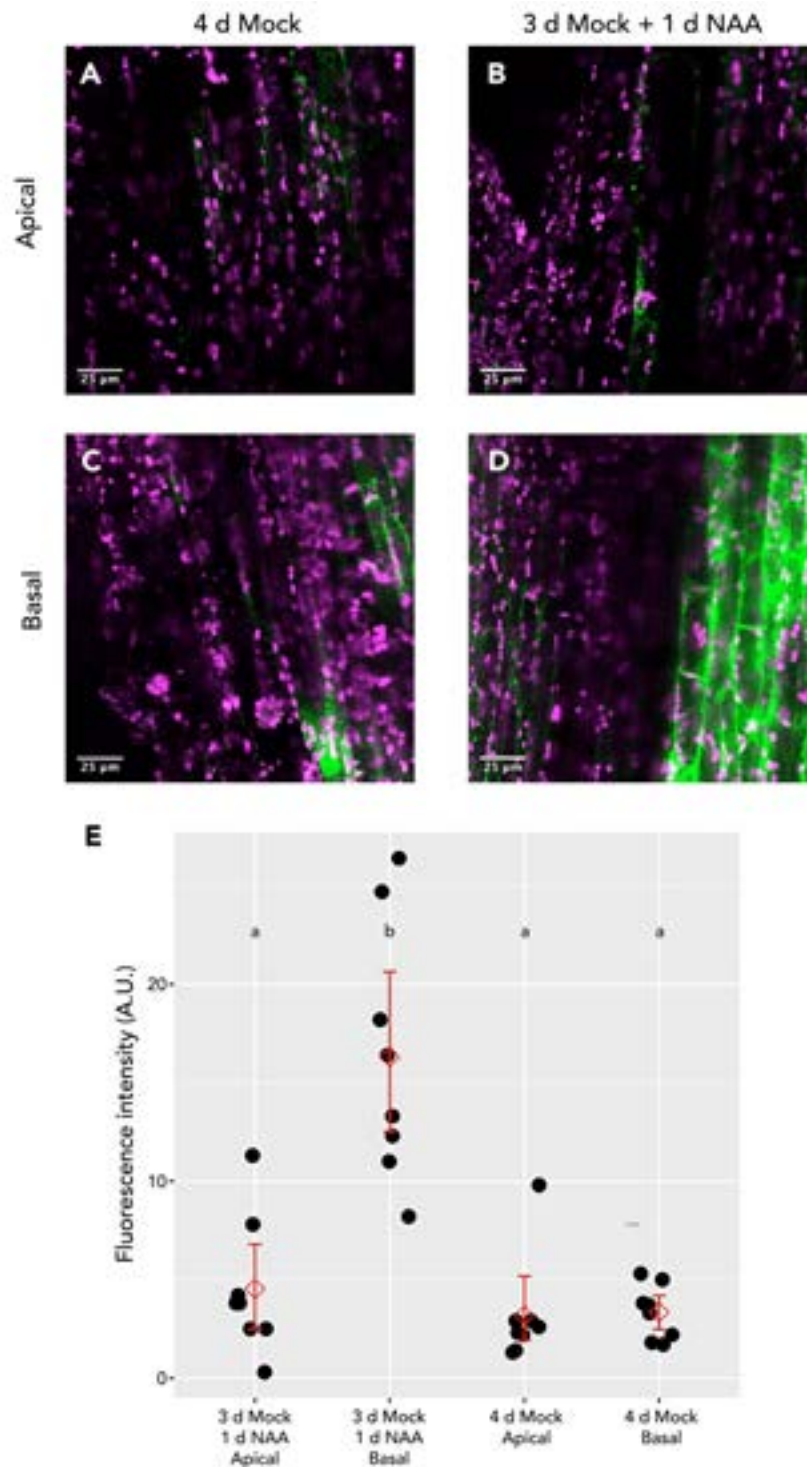


Figure 3.6 | (A-D) Representative confocal images showing *DR5rev::GFP* expression in xylem parenchyma and cambial cells from ~2 cm inflorescence stem segments treated for 4 d in vertically held plates supplemented apically (in the upper agar block) with mock (A & C), or mock for 3 d followed

by 1 μM NAA for 1 d (B & D). Stem segments were collected from the base of 5-15 cm inflorescences from 4-5 week old plants, placed in an upright orientation for 3 d and subsequently inverted for 1 d. As such, basal (rootward) stem ends shown were in contact with agar blocks supplemented with mock (A & C) or 1 μM NAA (B&D) for 1 day. Stem segments were sectioned longitudinally and imaged in apical (A & B) and basal (C & D) parts using confocal microscopy. Green shows *DR5rev::GFP* signal and magenta shows chloroplast autofluorescence. Each treatment was conducted using at least 8 independent plants. Fluorescence values were extracted for representative images of each stem and plotted here as black dots, red diamonds indicate the average value and the red line represents the 95% confidence interval. Each experiment was repeated at least three times. Different letters indicate statistically significant differences following a one-way ANOVA and Tukey's HSD post-hoc testing.

It has been shown previously that PIN1 in mature stem segments does not respond to CK treatment. This is in contrast to the increased accumulation of PIN3-GFP, PIN4-GFP and PIN7-GFP on the plasma membrane of xylem parenchyma cells in response to CK treatment of young stems (Waldie and Leyser, 2018). Since findings presented here demonstrate that PIN1 can dynamically respond to auxin in young inflorescence stems, I assessed whether CK treatment might also be able to affect PIN1 in younger tissues. Segments from 5 cm tall inflorescence stems expressing PIN1:GFP were treated for 4 hours with apical auxin (1 μM NAA) in the presence (1 μM BA) or absence (0.1% DMSO) of basal CK. In stems treated with basal CK the amount of PIN1-GFP present on the basal PM of xylem parenchyma was significantly higher compared to the mock controls (Fig. 3.7, A), but there was no effect on the number of cells with polar PIN1-GFP (Fig. 3.7, B).

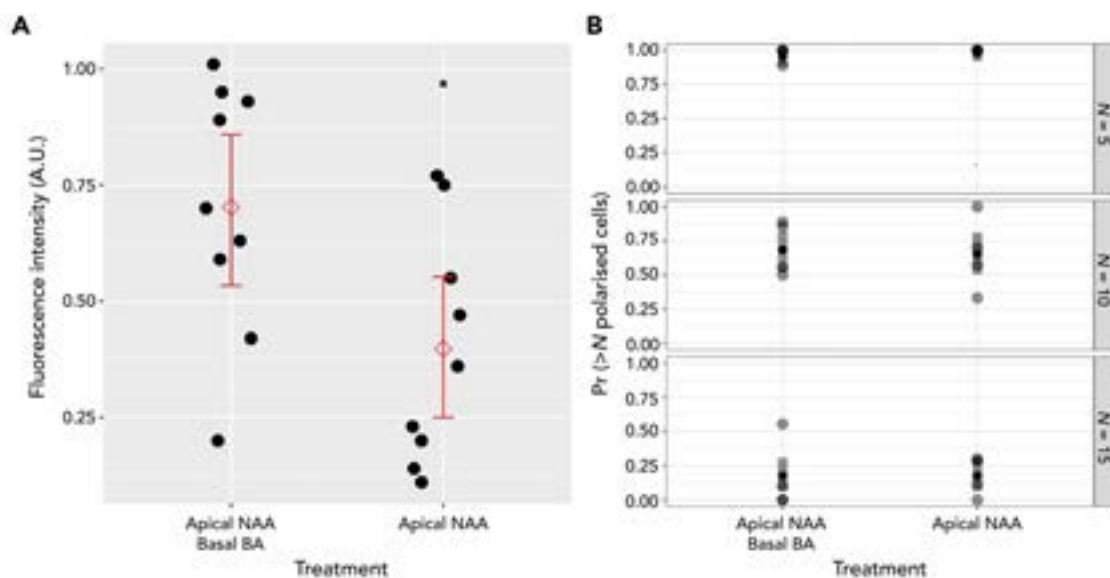


Figure 3.7 | 2 cm sections were excised from bolting inflorescences of ~ 4 week old plants expressing *pin1 PIN1-GFP* and placed in agar plates treated apically with 1 μM NAA and basally with either 1 μM BA or DMSO. After 4 hours, stems were longitudinally sectioned and the xylem parenchyma at the apical end imaged using confocal microscopy. (A) Fluorescence data was extracted from these images using Zen Black (2012) software to trace round basal plasma membranes where PIN1-GFP was visible. This was done for at least 5 membranes per stem and at least 8 stems were analysed per treatment per experiment (n=40). Membrane fluorescence values for each stem were averaged

and plotted here as black dots. The red diamond represents the average of these averages, the red line indicates the 95% confidence interval and the black asterisk indicates that the difference between the treatments was found to be significant by a two-sample Student's t-test ($p < 0.05$). (B) The number of membranes with visibly polar PIN1-GFP were counted and the probability of the number of polarised cells in each repeat being greater than each arbitrary threshold calculated.

Having established that cytokinin is able to increase the amount of PIN1-GFP when PIN1 is already present on the membrane, I tested whether it could also enhance the return of PIN1-GFP to the membrane. PIN1-GFP was allowed to deplete for 5 days before reapplying auxin apically either with or without basal cytokinin for 1 day. Data in figure 3.8 demonstrates that, whilst PIN1 is re-allocated to the basal PM when apical auxin is resupplied as previously shown in figure 3.4, provision of basal cytokinin does not significantly enhance either the amount of PIN1-GFP on membranes (Fig. 3.8 A) or the number of membranes with basally localised PIN1-GFP (Fig. 3.8 B).

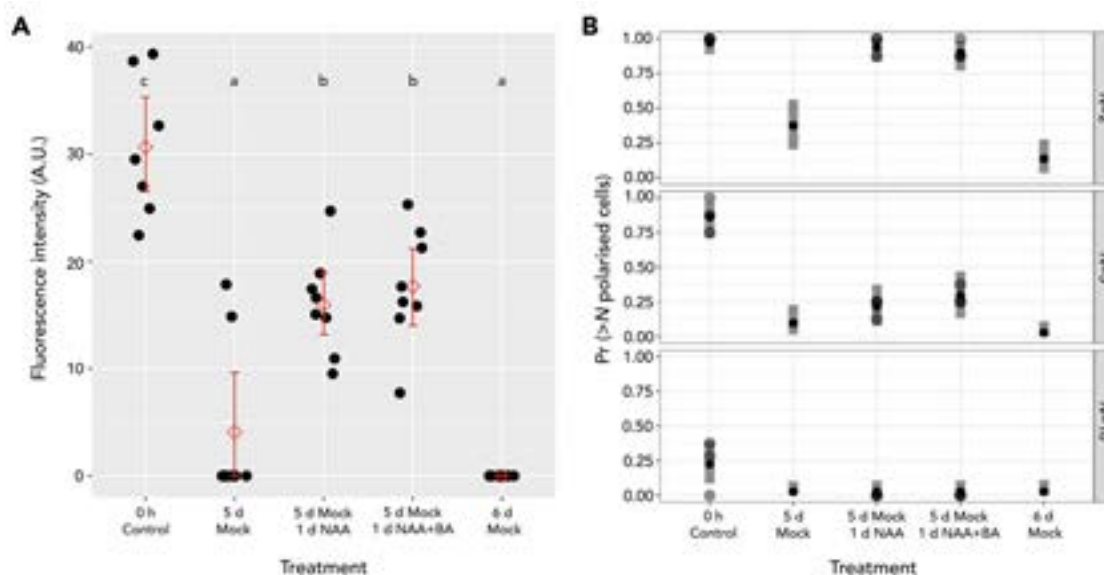


Figure 3.8 | 2 cm sections of bolting inflorescence stems of ~ 4 week old *pin1 PIN1-GFP Arabidopsis thaliana* were treated apically with mock for 5 d and 6d or with mock for 5 d followed by either 1 μM NAA + basal mock or 1 μM NAA + 1 μM basal BA. Stem sections were sectioned longitudinally and imaged apically by confocal microscopy. Stems were also imaged immediately after harvesting. (A) The amount of PIN1-GFP on the basal plasma membrane was assessed by manually tracing round the basal plasma membrane of cells using Zen Black (2012) software. This was done for at least 5 membranes in 8 independent plants for each treatment and the values averaged for each plant, plotted here as black dots. Three replicates were conducted. The red diamond represents the average of these averages and the red line the 95% confidence interval. Different letters indicate statistically significant differences following a one-way ANOVA and Tukey's HSD post-hoc testing. (B) The number of membranes with visibly polar PIN1-GFP were counted and the probability of the number of polarised cells in each repeat being greater than each arbitrary threshold calculated. For all treatments, each point represents a single repeat experiment in which at least 8 independent plants were analysed for PIN1 polarity, at least 6 repeats were conducted for all treatments ($n=48$).

From this, it can be concluded that PIN1 in young stem tissues can respond to CK with regard to enhanced accumulation, but not repolarisation. As for PIN1 sensitivity to changes in auxin supply and transport, the response appears to be age-sensitive and

does not occur in older inflorescence stems.

I further tested whether PIN1 in young stems exhibited strigolactone sensitivity and whether this was able to affect PIN1 membrane re-accumulation. PIN1 was allowed to deplete from the membrane for 3 days before re-supplying auxin apically with or without the presence of basal GR24 for 1 day. As expected, PIN1-GFP leaves the membrane over 4 days when mock-treated apically, while the presence of NAA is able to maintain PIN1-GFP on the basal PM (Fig. 3.9). In contrast to previous results, mock treatment for 3 d followed by re-supply of auxin for 1 d resulted in only a slight, non-significant increase in the amount of PIN1 present on the PM relative to stems treated with mock for 4 d. However, if auxin resupply was combined with the provision of basal GR24, PIN1-GFP levels on the membrane decreased below that of mock treated stems (Fig. 3.9). This suggests that SL sensitivity is retained in young stems.

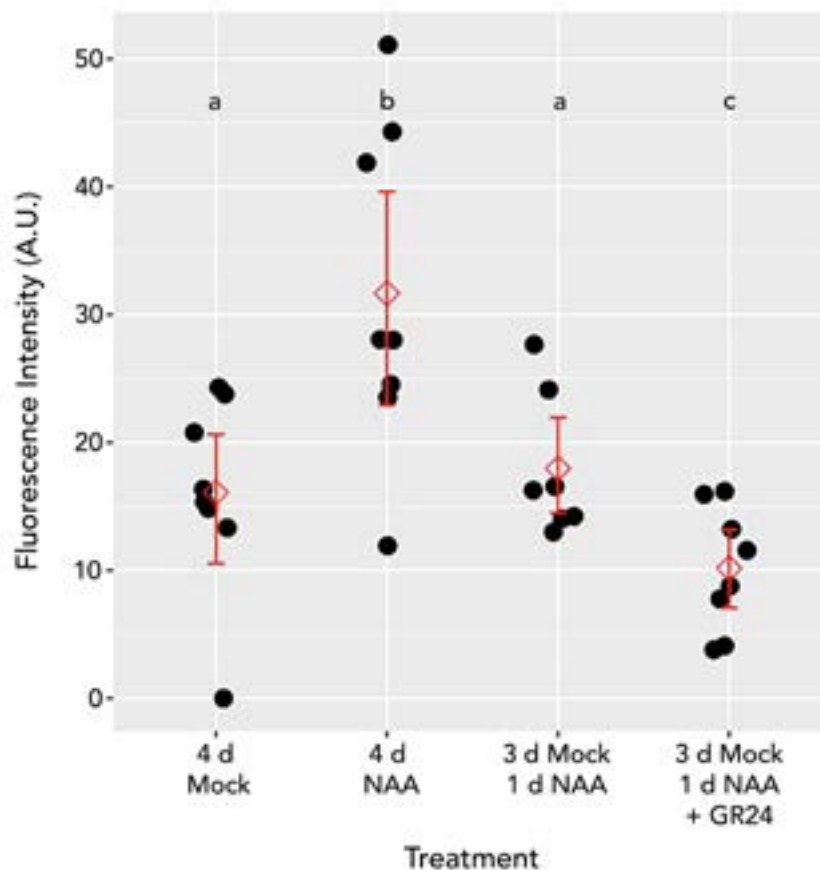


Figure 3.9 | 2 cm sections of bolting inflorescence stems of ~ 4 week old *pin1* PIN1-GFP *Arabidopsis thaliana* were treated apically with mock for 4 d or with mock for 3 d followed by either 1 μ M NAA + basal mock or 1 μ M NAA + 5 μ M basal GR24 for 1 d. Stem sections were sectioned longitudinally and imaged apically by confocal microscopy. The amount of PIN1-GFP on the basal plasma membrane was assessed by manually tracing round the basal plasma membrane of cells using Zen Black (2012) software. This was done for at least 5 membranes in 8 independent plants for each treatment and the values averaged for each plant, plotted here as black dots. Red diamonds represent the average of these averages and the red line the 95% confidence interval. Each experiment was repeated twice and the data shown representative. Different letters indicate statistically significant differences following a one-way ANOVA and Tukey's HSD post-hoc testing.

Together, these data suggest that PIN1 is in general less responsive to hormone treatments in mature vs young stems. I hypothesised that these differences might be attributable to increased PIN cycling in young stems relative to older tissue where very little cycling is seen (Shinohara *et al.*, 2013). In order to investigate this, stem sections were treated with 50 μM BFA for 6 h and the presence/absence of BFA bodies assessed. There were no BFA bodies observable in either mock or BFA-treated stems (Fig. 3.10 A, B) and BFA treatment did not reduce PIN1-GFP on the basal PM (Fig. 3.10 C), in line with data from mature tissue, suggesting that a change in PIN cycling is likely not the cause of the differences seen between young and old tissue.

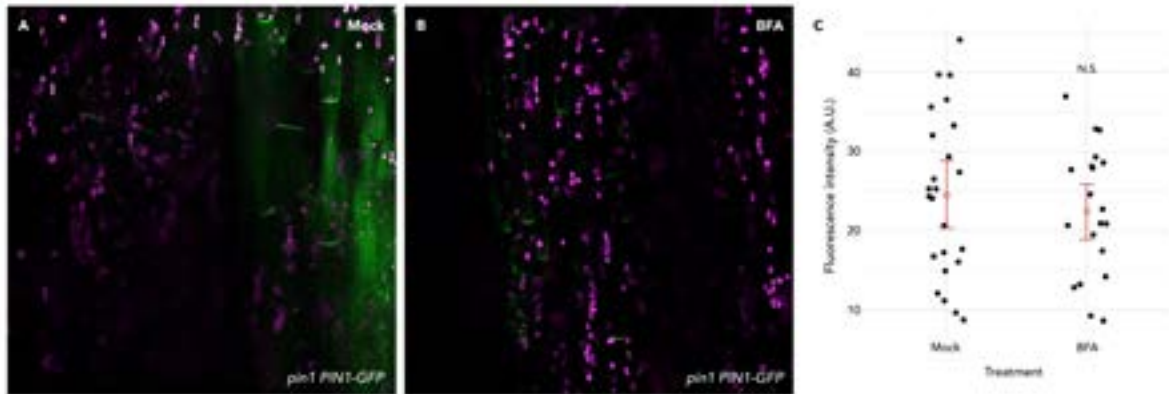


Figure 3.10 | (A, B) Representative confocal images demonstrating the localisation of PIN1-GFP in the xylem parenchyma and cambial cells from ~ 2 cm stem segments treated for 6 h with Mock (A) or 50 μM Brefeldin A (B). Stem segments were collected from ~ 4 week old *pin1 PIN1-GFP A.thaliana* plants, treated, sectioned longitudinally and imaged apically using a confocal microscope and the presence/absence of BFA bodies assessed, $n=21$. (C) The amount of PIN1-GFP on the basal plasma membrane was assessed by manually tracing round the basal plasma membrane of cells using Zen Black (2012) software. This was done for at least 5 membranes in 8 independent plants for each treatment and the values averaged for each plant, plotted here as black dots. Red diamonds represent the average of these averages and the red line the 95% confidence interval. Each experiment was repeated at least three times and compiled data presented here. A student's T-test was performed to assess the statistical significance between the mean fluorescence for each treatment and this was found to be non-significant ($P>0.05$).

3.3 | Discussion

A central tenet of the auxin transport canalisation hypothesis is that auxin both up-regulates and polarises its own transport through a mechanism in which auxin exporters are allocated to the cell membrane with the highest net efflux. In this way, a concentration-driven flux between the auxin source and the sink can be amplified to produce narrow files of cells with highly polar, high capacity auxin transport and, typically, high auxin concentration (Sachs, 1968; Sachs, 1969; Sachs, 1975; Mitchison *et al.*, 1981; Sachs, 1981). Recent work has demonstrated that the behaviours of members of the PIN family of auxin efflux carrier impressively match the behaviours predicted by Sachs, polarising in the direction of an auxin flux established by application of an exogenous auxin source to pea stems (Gocal *et al.*, 1991; Balla *et al.*, 2002; Balla *et al.*, 2011; Balla *et al.*, 2016; Zhang *et al.*, 2020). However, the mechanisms by which PINs

accumulate in the cell membrane with the highest net flux are unknown.

3.3.1 | PIN1 in young stems shows canalisation-like behaviours

Previous data suggest that, in mature stem segments, PIN1 lacks several key behaviours expected for auxin transport canalisation (Bennett *et al.*, 2016). Consistent with canalisation behaviours, continuous apical auxin supply maintained PIN1 at the membrane (Bennett *et al.*, 2016). However, apical supply of the auxin efflux inhibitor NPA also resulted in PIN1 retention, and following PIN1 depletion, resupply of auxin was unable to repolarise PIN1 (Bennett *et al.*, 2016).

The contrasting results, with more canalization-like behaviours reported for *Arabidopsis* by Mazur *et al* (Mazur *et al.*, 2016; Mazur *et al.*, 2020b; Mazur *et al.*, 2020a) and for PIN3, PIN4 and PIN7 (Fig 3.1 and Waldie, unpublished) led me to investigate PIN1 behaviour in young stems. The results presented here demonstrate that there are similarities, but also significant differences in both PIN1 behaviour and wider auxin transport properties in mature vs young stem segments. As with excised mature stem segments, in young stem segments, PIN1 depletes over time unless apical auxin is supplied. However, in contrast to mature stem segments, resupply of auxin is able to trigger re-accumulation of polar PIN1 at the plasma membrane of xylem parenchyma and vascular cambium cells.

Furthermore, the effects of NPA are significantly different in mature vs young segments. In mature segments, apical NPA treatment results in retention of auxin and PIN1 maintenance at the plasma membrane, whereas in young stem segments PIN1 appears to deplete despite NPA treatment. Treatment with both auxin and NPA results in PIN1 retention, suggesting that the presence of auxin, but not NPA-sensitive auxin transport, is necessary for PIN1 retention. However, it is also clear that a straightforward concentration-dependent mechanism cannot explain observed behaviours in stems, because when auxin is applied basally, PIN1 is not retained on the plasma membrane while *DR5* activity is driven. One possibility is that auxin gradients are important in driving PIN1 polarisation. The role of concentration would merit further investigation using other auxin reporters and even auxin sensors such as AuxSen in order to confirm this conclusion (Herud-Sikimic *et al.*, 2021).

These results are interesting in the context of the ongoing debate about the mechanism of flux-correlated accumulation of PIN1 polarisation at the plasma membrane. Recent results demonstrate the existence of intrinsic cell polarity in regenerating plant protoplasts that is marked by the BASL protein, but not PINs (Mansfield *et al.*, 2018; Chan *et al.*, 2020). This polarity is dynamic during isotropic cell growth, but becomes fixed and aligned with the growth axis in anisotropically growing cells. In leaves, ec-

topic *BASL* expression reveals a polarity field along the proximodistal axis of the leaf, for the most part running parallel to the midvein, but diverging at the leaf margins. PIN polarity aligns with this leaf field, suggesting that *BASL* and PINs respond to the same polarity cues (Mansfield *et al.*, 2018; Chan *et al.*, 2020). One hypothesis consistent with the current dataset is that the ability of PINs to accumulate in response to these polarity cues is dependent on an auxin gradient across the cell that aligns with the polarity cues (Jones *et al.*, 2002; Kramer 2009; Payne and Grierson 2009). An interesting feature of this hypothesis is that it would account for more robust polarity changes where a strong sink contributes to the establishment of such gradients. This feature is lacking when auxin is applied basally, but present when it is applied apically or at an exposed apical surface of a lateral wound site. This could account for PIN repolarisation to more lateral positions in the latter case, but not straightforwardly the more tortuous paths for vascular differentiation induce in some of the classical Sachs experiments.

3.3.2 | PIN1 behaviours differ in young and old stems

As described above, there are several significant differences in the auxin response behaviour of PIN1 in young vs old stems. Beyond this, I also observed differences in the behaviour of PIN1 with relation to CK, with PIN1 accumulation on the basal PM of young stems increased by CK treatment (Fig. 3.7) in a manner not observed in mature stems, but in common with that which has previously been described for PIN3, PIN4 and PIN7 (Waldie and Leyser, 2018). Whilst cytokinin can promote additional recruitment of PIN1 to the basal PM in young stems, it does not appear to affect re-allocation of PIN1 after it has been lost from the membrane (Fig. 3.8). Strigolactone response does not seem to be age-related, with SL treatment reducing PIN1 repolarisation in young stems (Fig. 3.9) in line with previous data that SL promotes PIN1 endocytosis in mature stems (Shinohara *et al.*, 2013).

These results suggest the possibility that PIN1 recycling might be generally more dynamic in young stems. In mature stems PIN1 patterns appear to be robustly maintained as long as auxin is present, with quantitative tuning by strigolactone, but otherwise limited dynamism (Crawford *et al.*, 2010; Shinohara *et al.*, 2013; Bennett *et al.*, 2016). In contrast, young stems have more dynamic PINs, including not only PIN1 but also PIN3, PIN4 and PIN7.

A substantial body of work in roots has led to the hypothesis that dynamic cycling of PINs between the plasma membrane and internal compartments is important, with auxin acting to retain PINs on the plasma membrane by inhibiting their endocytosis (Geldner *et al.*, 2001; Paciorek *et al.*, 2005; Dhonukshe *et al.*, 2007; Kleine-Vehn *et al.*, 2008a; Kleine-Vehn *et al.*, 2011; Mazur *et al.*, 2020a). This has been proposed as a mechanism to account for elements of canalisation-like behaviour. However, in stems

PINs appear to be more stable on the plasma membrane than in roots, with little evidence for the general rapid cycling observed in root tips. Consistent with significant root-shoot differences, cytokinin enhances auxin-mediated PIN accumulation in shoots, whereas in roots it correlates with PIN depletion from specific domains on the plasma membrane (Marhavý *et al.*, 2014).

I assessed whether increased stem PIN1 cycling could be observed in young stems by treating them with Brefeldin A and looking for evidence of intracellular accumulation of PIN1-GFP (Fig. 3.10). There was no indication that BFA treatment increased PIN1-GFP internalisation in young stems, in line with existing data from mature stems (Shinohara *et al.*, 2013) and in contrast to data from roots (Robert *et al.*, 2010). This suggests that cycling rates are slow in both young and mature stems and that this cannot account for the observed differences in PIN1 behaviour between young and mature stems.

While there is no evidence for a generally increased recycling in young stems, it is striking that PIN1 re-accumulation in response to auxin re-supply and PIN hyper-accumulation in response to CK are both stem-age sensitive, whereas PIN depletion triggered either by auxin depletion or strigolactone treatment are not (Bennett *et al.*, 2016; Waldie and Leyser, 2018; Ticchiarelli, 2019). One possibility consistent with these observations is that stem age affects PIN delivery to the plasma membrane in some way more strongly than PIN removal. It would be interesting to investigate whether similar behaviour is observed in other species as, while the hydrophilic loop is highly conserved across PIN1 homologues in model species such as *Z. mays*, *M. trunculata* & *O. sativa*, there are some residue differences and residues in the HL have been previously attributed to regulation of PIN1 localisation (O'Connor, 2014; Huang, 2010).

3.3.3 | Conclusions

- ◇ PIN1, PIN3, PIN4 and PIN7 membrane retention does not depend on NPA-sensitive auxin flux in young stems.
- ◇ PIN1 exhibits increased dynamism in young tissue.
- ◇ PIN1 cytokinin responsiveness depends on tissue age.
- ◇ Strigolactone sensitivity of PIN1 is not age-sensitive.
- ◇ PIN1 cycling speed is not increased in young stems.

4

The effect of intracellular:extracellular auxin ratios on PIN behaviour

"The truth is rarely pure and never simple" - O. Wilde

4.1 | Introduction

Results presented in chapter 3 demonstrate that NPA treatment does not result in PIN retention on the plasma membrane of xylem parenchyma cells of young stems, unlike mature stems. Nor did abolition of auxin flux result in PIN1 depletion in young stems. Previous data supported PIN1 allocation on the basis of auxin concentration as opposed to auxin flux in mature stems, but neither of these mechanisms are sufficient to explain the data reported in chapter 3. As such, I hypothesised that PINs may be able to respond to the ratio of intracellular to extracellular auxin and allocate accordingly. First, I will outline our understanding of the transport and accumulation of both natural and synthetic auxins, and the effects of transport inhibitors, before discussing my novel results.

4.1.1 | Auxin and its synthetic analogues

Since the characterisation of IAA as the major endogenous auxin in plants (Kögl *et al.*, 1934; Went F. W. 1903-1990. (Frits Warmolt), 1937), several other endogenous auxins such as Indole-3-butyric acid (IBA), phenylacetic acid (PAA) and chloroindole-3-acetic acid (4-Cl-IAA) have been identified (Zimmerman and Wilcoxon, 1935; Koepfli *et al.*, 1938; Porter and KV, 1965). Due to the relative instability of endogenous auxins such as IAA (Nissen and Sutter, 1990), much of the investigation into auxin transport has been conducted using synthetic auxins such as 2,4-dichlorophenoxyacetic acid (2,4-D) and 1-naphthaleneacetic acid (NAA) which are generally more stable.

The role of passive and active transport for IAA has been well characterised and is discussed extensively in the introduction (Section 1.2.1). However, due to their different structures, 2,4-D and NAA interact slightly differently with these transporters. Previous work in cell culture has identified 2,4-D to exhibit preferential affinity for auxin influx carriers relative to efflux carriers, relying on the former to enter cells but being able to exit passively (Depta and Rubery, 1984; Hertel, 1987; Sabater and Rubery, 1987; Delbarre *et al.*, 1996). NAA on the other hand primarily enter cells passively but relies on efflux carriers to leave (Delbarre *et al.*, 1996). It should be noted that IAA is able to compete with 2,4-D for influx carriers and with NAA for efflux carriers, with influx carriers having the highest affinity for IAA, followed by 2,4-D and NAA, whilst efflux carriers have the highest affinity for NAA (Rubery, 1977; Sussman and Goldsmith, 1981; Hertel *et al.*, 1983; Hertel, 1987; Simon *et al.*, 2013). Auxin drives multiple transcriptional responses, the activity of which can be measured through fusion of a reporter gene to a synthetic *DR5* promoter, composed of multiple AuxREs arranged in tandem (Ulmasov *et al.*, 1997). It has been demonstrated that different auxins drive the expression of these to different extents, with IAA being the most active in this context, and 2,4-D very similar, but NAA to a lesser degree (Simon *et al.*, 2013).

In addition to synthetic auxins, a number of synthetic transport inhibitors have been characterised which act to inhibit the function of auxin influx and efflux carriers. Most prominent amongst these is N-1-naphthylphthalamic acid (NPA). It is known to inhibit auxin efflux through direct interaction with ABCBs which exhibit high affinity NPA binding and NPA sensitive export (Noh, 2001; Bailly *et al.*, 2008; Titapiwatanakun *et al.*, 2009). PINs are also NPA sensitive, with NPA proposed to inhibit their function either indirectly (Blakeslee *et al.*, 2007; Titapiwatanakun *et al.*, 2009; Kim *et al.*, 2010). Or directly (Abas *et al.*, 2020; Teale *et al.*, 2021). NPA affects the transport of different auxins in different ways. In cell suspension it does not increase the accumulation of 2,4-D but does that of NAA & IAA, strengthening the idea that the latter rely on auxin efflux carriers to exit the cell, whilst the former does not (Delbarre *et al.*, 1996). 2-NOA on the other hand has been characterised as a specific inhibitor of auxin influx carriers, resulting in increased accumulation of 2,4-D but not NAA in tobacco cells (Lanková *et al.*, 2010).

These synthetic compounds represent useful tools to manipulate auxin transport and assess the effects this has on the components of the system such that we might gain greater understanding of it.

4.1.2 | Aims

In this chapter, I will discuss the effect of various auxins, both synthetic and natural, on gene expression from auxin responsive promoters and the effect they have on PIN1 localisation. I will further characterise the ability of select auxin transport inhibitors to inhibit auxin transport *in planta*. More specifically I will:

- ◇ Investigate whether NPA is effective at trapping auxin in cells of young stem tissue and more broadly at halting auxin transport.
- ◇ Determine whether and how auxin concentration relates to PIN localisation.
- ◇ Characterise the effects of a synthetic auxin, 2,4-Dichlorophenoxyacetic acid (2,4-D) on PIN localisation and auxin-responsive gene expression.
- ◇ Characterise the ability of 2-naphthoxyacetic acid (2-NOA) to inhibit auxin influx *in planta*.
- ◇ Use a combination of different treatments to manipulate intracellular:extracellular auxin ratios and determine the effect, if any, that this has on PIN localisation.

4.2 | Results

4.2.1 | NPA does not induce auxin retention in young stems

We had previously attributed the retention of PIN1 on the plasma membrane in NPA-treated mature stem segments to the retention of auxin in these cells, because NPA treatment blocks auxin efflux from the cell (Katekar and Geissler, 1980). Consistent with this idea, expression of GFP driven by the *DR5* auxin responsive promoter (Ulmasov *et al.*, 1997) remained high under NPA treatment but low under mock treatment, consistent with auxin draining away basally in these stems (Bennett *et al.*, 2016).

My results in chapter 3 using NPA in young stem segments differ from those observed in mature stem segments with regard to PIN1 behaviour. Indeed, in young stem segments, all the PINs tested are depleted from the plasma membrane in response to NPA treatment. This might suggest that NPA-sensitive auxin flux is important for maintaining PINs on the plasma membrane in young stem segments. However, for all the PINs we tested, dual treatment with NPA and auxin resulted in PIN retention on the plasma membrane, demonstrating that NPA-sensitive auxin flux is not required. As such I resolved to investigate the impact of NPA and dual NAA+NPA treatment on intracellular auxin signalling in young stems.

I utilised the same *DR5* reporter construct that we previously used for mature stems in an attempt to recapitulate these results in young tissue (Bennett *et al.*, 2016). When stems were mock-treated for 2 days, only weak GFP signal could be detected, whereas apical auxin treatment or combined auxin and NPA treatments all resulted in high *DR5rev::GFP* expression levels in the stems segments (Fig. 4.1). In contrast to previously reported results in mature stems, apical NPA treatment alone was ineffective at inducing auxin retention. To allow more accurate quantification of auxin signalling in these cells, a nuclear localised reporter, *DR5::NLS-VENUS*, was used.

DR5 driven, nuclear localised VENUS was detectable at time 0 in the xylem parenchyma cells, suggesting that, as would be expected, auxin is present (Fig. 4.2 A). After 6 days without auxin, fewer nuclei with detectable NLS-VENUS signal were observed and those that could be detected had significantly lower NLS-VENUS expression than at time 0 (Fig. 4.2 C, F). This is consistent with previous data that auxin drains away from the apex of stem segments after excision (Bennett *et al.*, 2016). NAA treatment is able to maintain and even significantly increase NLS-VENUS expression relative to levels at 0 time (Fig. 4.2 B, F). In NPA-treated stems *DR5::NLS-VENUS* expression is greatly reduced relative to time zero, resulting in levels comparable to mock treatments (Fig. 4.2 D, F).

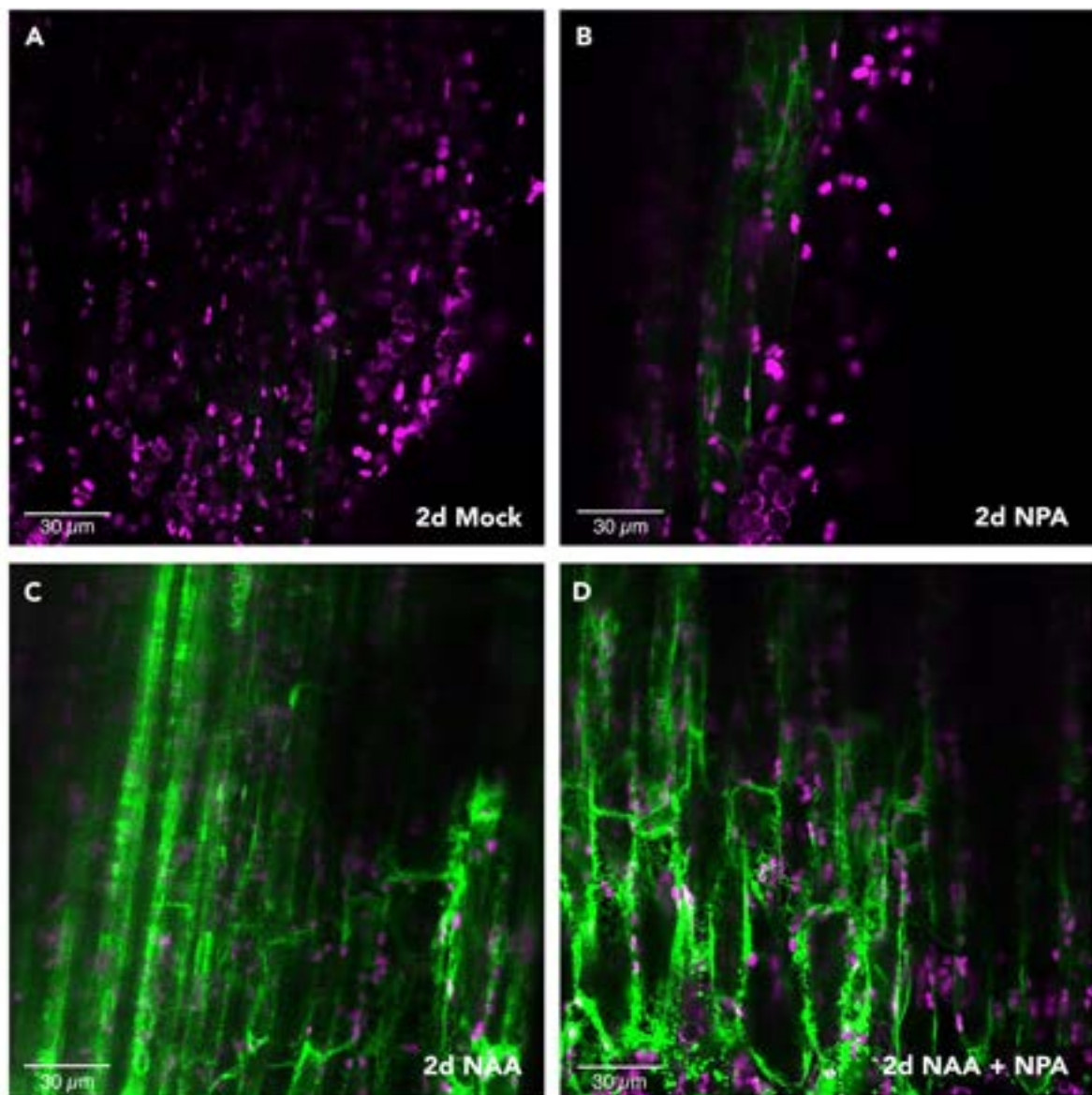


Figure 4.1 | Representative images demonstrating *DR5*-driven, ER-localised GFP expression under several treatment regimes. 2 cm inflorescence stem segments from ~4 week old plants were excised and placed into agar treated apically with Mock (A), NPA (B), NAA (C) or NAA + NPA (D). After 2 d stems were sectioned longitudinally and imaged at the apical end using confocal microscopy. Green represents GFP signal and magenta chlorophyll autofluorescence.

This result is somewhat surprising, since there is a substantial body of evidence that NPA inhibits auxin export from cells, trapping it and resulting in high intracellular auxin, something that is consistently observed in mature stems (Katekar and Geissler, 1980; Delbarre *et al.*, 1996; Bennett *et al.*, 2016). To assess whether nuclear VENUS detects auxin retention in response to NPA treatments at earlier time points, which might provide improved sensitivity, I quantified NLS-VENUS levels after 3 days of NAA treatment, instead of 6 days. The results were qualitatively indistinguishable from the 6-day treatments, with no significant difference between the untreated control and the NPA treated samples (Fig 4.2 G). There is therefore no evidence for NPA-induced auxin retention monitored using nuclear localised VENUS across the period when PIN depletion is occurring.

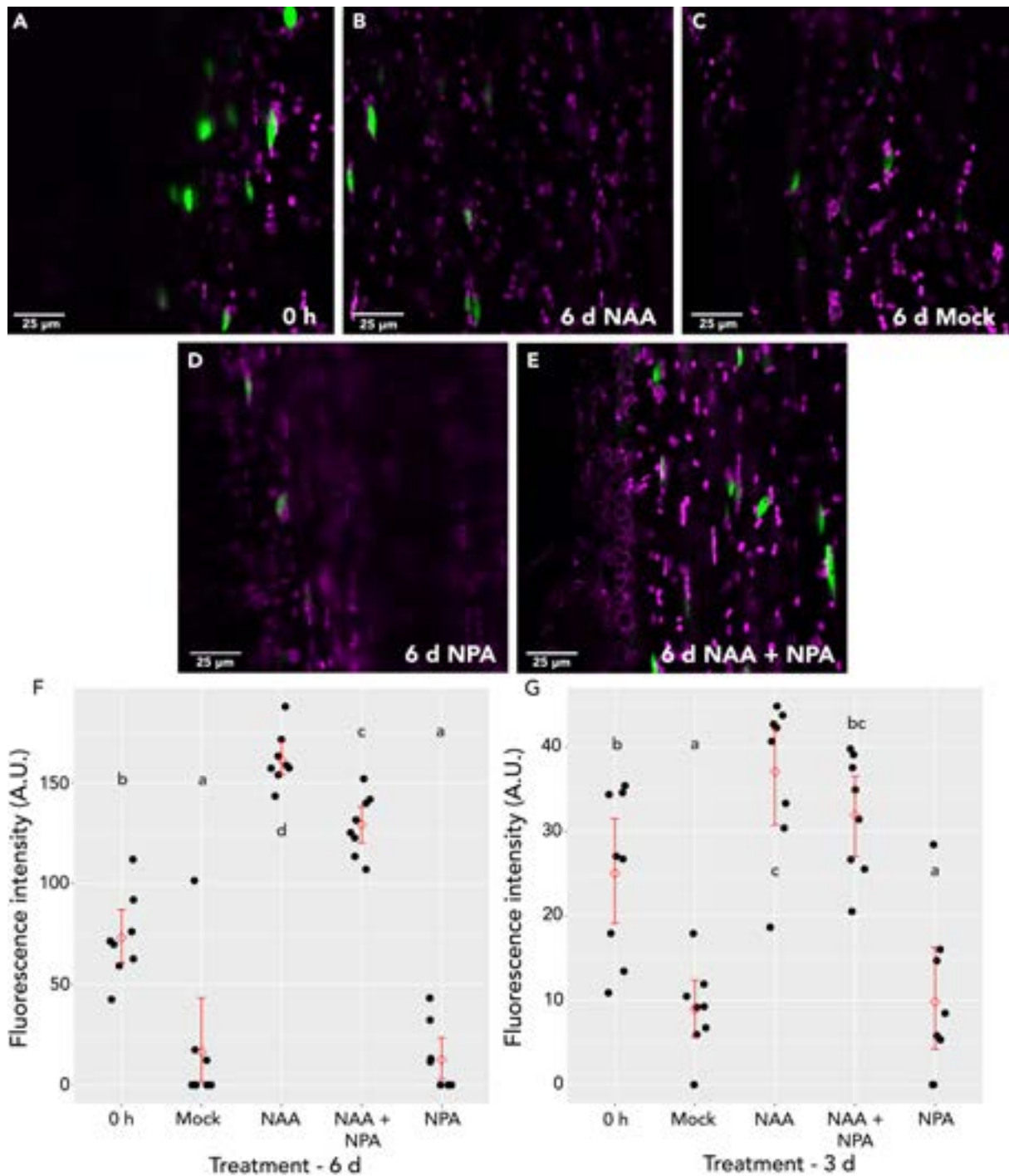


Figure 4.2 | (A-E) Representative confocal images of nuclei in cells of the xylem parenchyma in plants expressing *DR5::NLS-VENUS*. Images were taken from 2 cm stem segments imaged immediately after harvesting (A) or treated for 6 days in vertical plates supplemented with NAA (B), Mock (C), NPA (D) or NAA + NPA (E). Stem segments were harvested from ~ 4 week old plants treated, longitudinally sectioned & imaged apically. Magenta represents chloroplast autofluorescence whilst green represents VENUS. (F, G) Mean intensity of nuclei for each treatment after 6 d (F) or 3 d (G). ≥ 2 cells were measured in each biological repeat and each treatment was conducted using at least 8 independent plants ($n > 16$), plants where no or < 2 VENUS expressing nuclei were visible were assigned a 0 value. Fluorescence values were averaged for each stem and plotted here as black dots. Red diamonds indicate the average of these averages and the red line represents the 95% confidence interval. Each experiment was repeated at least three times. Different letters indicate statistically significant differences following a one-way ANOVA & Tukey's honest significant difference post-hoc test.

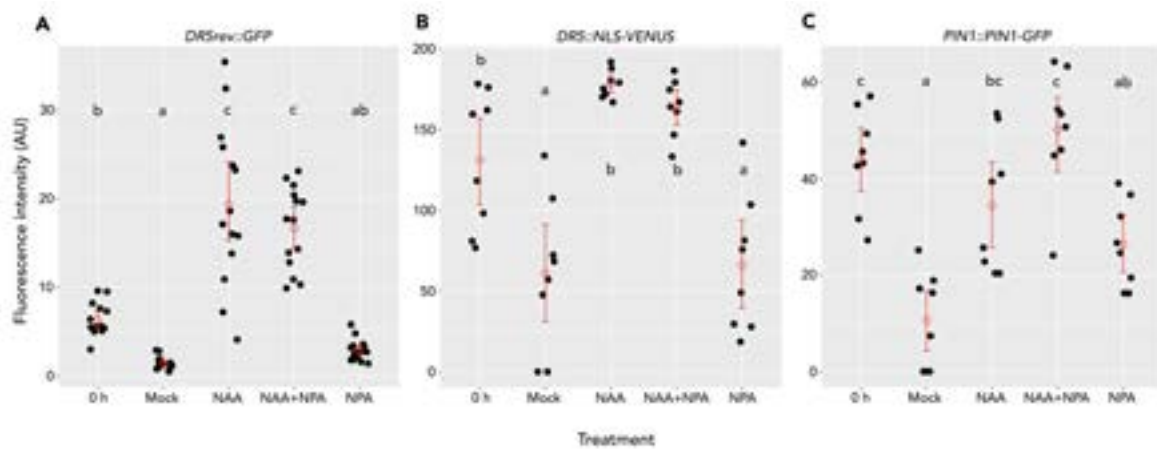


Figure 4.3 | Mean intensity of GFP/VENUS signal was measured in images taken from 2 cm stem segments immediately after harvesting or after being treated for 2 days in vertical plates supplemented with NAA, Mock, NAA or NAA + NPA. Stem segments were harvested from ~ 4 week old plants expressing *DR5rev::GFP* (A), *DR5::NLS-VENUS* (B) & *pin1 PIN1-GFP* (C), treated apically, longitudinally sectioned & imaged apically. ≥ 2 cells were measured in each biological repeat, each treatment was conducted using at least 8 independent plants ($n > 16$) and the experiment was repeated three times. Fluorescence values were averaged for each stem and plotted here as black dots. Red diamonds indicate the average of these averages and the red line represents the 95% confidence interval. Different letters indicate statistically significant differences following a one-way ANOVA & Tukey's honest significant difference post-hoc test.

These data confirmed that, even over a shorter timescale, both ER & nuclear localised *DR5* driven GFP, respond to NAA and combined treatment with NAA and NPA with elevated expression relative to fresh stems (Fig. 4.3 A, B). This is particularly the case for the *DR5rev::GFP* reporter (Fig 4.3 A). It is also clear that NPA treatment is unable to maintain expression of either the ER-localised or nuclear localised *DR5* driven reporter at the levels seen in fresh, NAA or NAA+NPA treated stems, with signal intensity comparable to mock treated stems (Fig 4.3 A, B). As was previously observed, NPA treatment does not result in PIN1-GFP retention on the membrane to the same extent as NAA+NPA treatment or NAA alone (Fig 3.3, Fig 4.2 A, B).

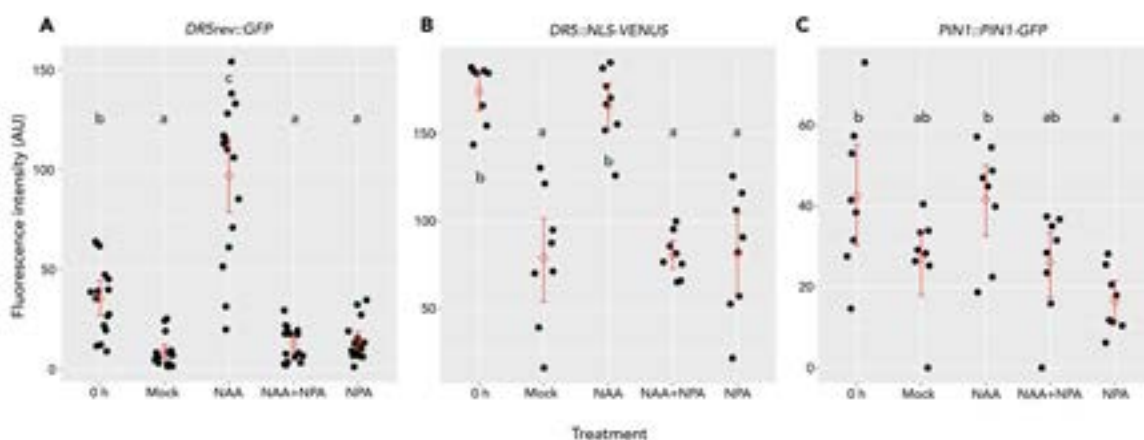


Figure 4.4 | Mean intensity of GFP/VENUS signal was measured in images taken from 2 cm stem segments immediately after harvesting or after being treated for 2 days in vertical plates supplemented with NAA, Mock, NAA or NAA + NPA. Stem segments were harvested from ~ 4 week old

plants expressing *DR5rev::GFP* (A), *DR5::NLS-VENUS* (B) & *pin1 PIN1-GFP* (C), treated apically, longitudinally sectioned & imaged basally. ≥ 2 cells were measured in each biological repeat, each treatment was conducted using at least 8 independent plants ($n=16$) and the experiment was repeated three times. Fluorescence values were averaged for each stem and plotted here as black dots. Red diamonds indicate the average of these averages and the red line represents the 95% confidence interval. Different letters indicate statistically significant differences following a one-way ANOVA & Tukey's honest significant difference post-hoc test.

Since this result was contrary to much previously reported data, I resolved to confirm the efficacy of our NPA stock in inhibiting auxin transport down the stem. To do this, the same experiment as described in figure 4.3 was performed but instead of imaging at the apical end where treatment was applied, stems were imaged basally to determine whether auxin had travelled down the stem from the treatment zone. These data suggest that NPA is indeed working to prevent auxin transport down the stem, as apical treatment with both NPA and NAA results in reduced *DR5*-driven reporter expression relative to treatment with NAA alone in both reporter lines (Fig 4.4 A, B). Interestingly, whilst NPA alone results in PIN1 depletion from the membrane, so too does combined treatment with NAA, a stark contrast to observations at the apical end of the stem (Fig 4.3 C, 4.4 C).

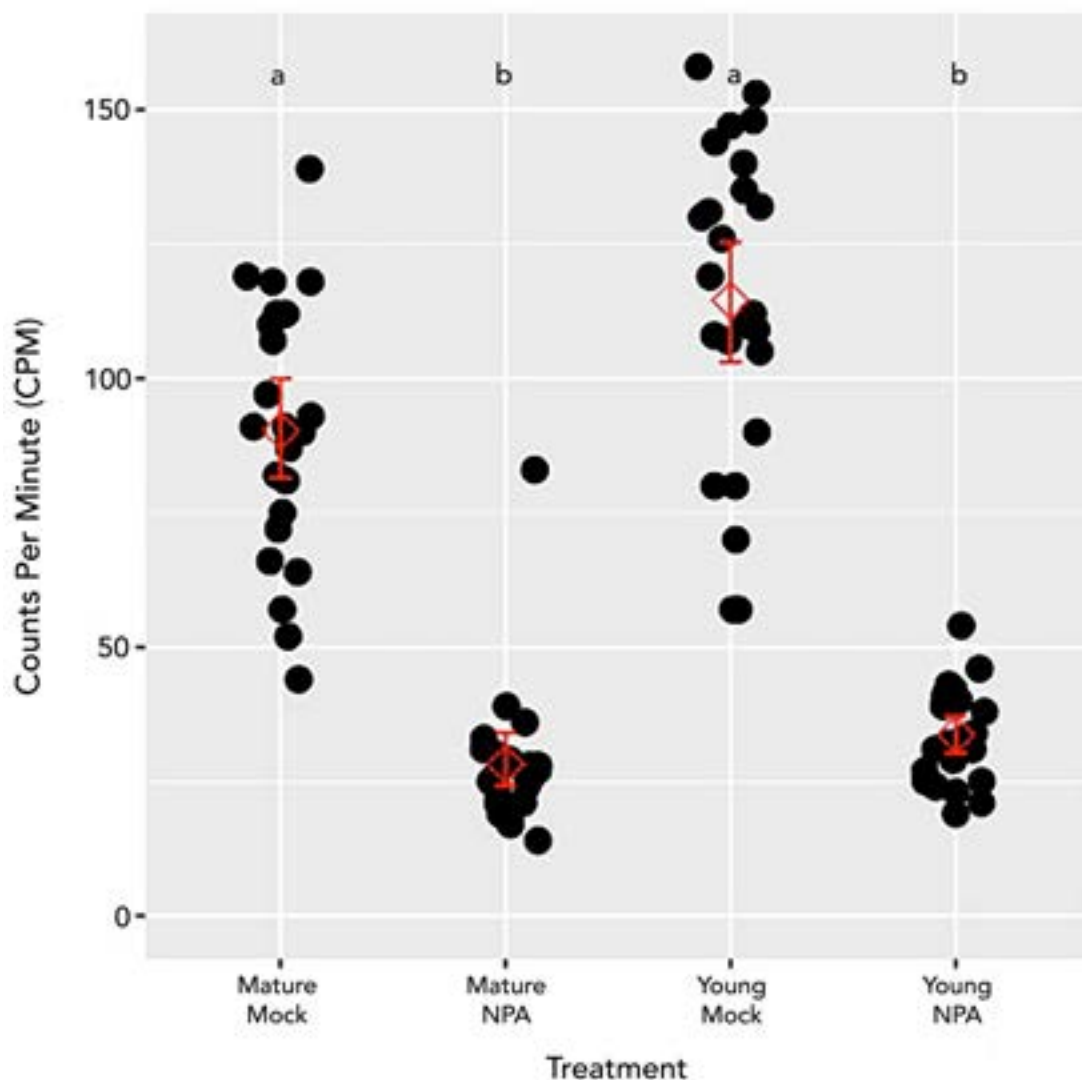


Figure 4.5 | 15 mm segments of plants expressing *pin1 PIN1-GFP* were taken from the base of the primary inflorescence of long day grown plants at terminal flowering (old) or at 4 weeks (young) and used in bulk transport assays over 18 h in the presence or absence of NPA. 24 stems were used per treatment (n=24). Each point represents an individual plant. Red diamonds indicate the mean CPM and horizontal lines indicate the 95% confidence interval. Different letters indicate statistically significant differences following a one-way ANOVA and Tukey's HSD post-hoc testing.

I also tested the ability of NPA to inhibit auxin transport in the stem and whether this differs between young and old tissue, by performing a bulk auxin transport assay. Stem segments from the basal internodes of *PIN1-GFP* expressing plants were treated apically with 1 μM ^{14}C -IAA for 18 h in the presence or absence of NPA, and the amount of radiolabel present in the basal 5 mm measured. NPA treatment clearly decreases the amount of auxin reaching the base of stem segments relative to mock (Fig. 4.5), supporting data from figure 4.4 that NPA is effective at inhibiting auxin transport. Furthermore, this effect is not age-dependent, as the degree to which auxin transport is inhibited in NPA-treated stems does not differ between young and old tissue (Fig. 4.5).

4.2.2 | Synthetic auxins and transport inhibitors do not behave as predicted by cell culture studies

It has previously been proposed that *PIN1* may be allocated to the membrane by a concentration-based mechanism or according to auxin flux across the membrane (Bennett *et al.*, 2014; Bennett *et al.*, 2016). In chapter 3, I established that neither auxin concentration nor NPA-sensitive auxin flux across the membrane seem to be straightforwardly linked to plasma membrane localisation of *PIN1*. Basal application of auxin was unable to increase *PIN1* plasma membrane localisation despite increasing intracellular auxin levels (Figure 3.6 & 3.7). Furthermore, supply of NPA in combination with NAA did not result in *PIN1* depletion but in fact resulted in hyperaccumulation in many cases (Fig. 3.3). As such, it was considered possible that the ratio of extracellular to intracellular auxin may play a role. For example, perhaps the combined treatment of NAA & NPA generates a high intracellular and high extracellular auxin level that leads to elevated levels of *PIN1* on the membrane. There being no way of determining extracellular auxin levels, I elected to use auxins and auxin transport inhibitors with different transporter affinities and membrane permeabilities in order to manipulate this ratio artificially and consequently determine the resulting effect on *PIN1* polarity.

Previous studies have identified 2,4-dichlorophenoxyacetic acid (2,4-D) as a synthetic auxin which has a higher affinity for influx carriers than efflux carriers and which relies on influx carriers to enter cells but is able to exit diffusively (Depta and Rubery, 1984; Hertel, 1987; Sabater and Rubery, 1987; Delbarre *et al.*, 1996). 2-Naphthoxyacetic acid (2-NOA, henceforth referred to as NOA) is known to inhibit auxin influx into the cell and specifically affects 2,4-D import in tobacco BY-2 cells, yet seems not to impact auxin efflux, unlike 1-NOA (Lanková *et al.*, 2010). As such, these two compounds,

along with previously deployed NAA & NPA, were deemed suitable candidates to manipulate intracellular:extracellular auxin ratio *in planta*.

I first investigated whether 2,4-D and NOA had the expected effect on PIN1 polarity *in planta*. It is clear from figure 4.6 that 2,4-D is as effective as NAA at maintaining PIN1 on the basal plasma membrane, suggesting that 2,4-D is entering cells. Furthermore, 2-NOA is comparable to NPA in that it does not result in PIN1 retention on the basal PM to the same degree as mock treatment.

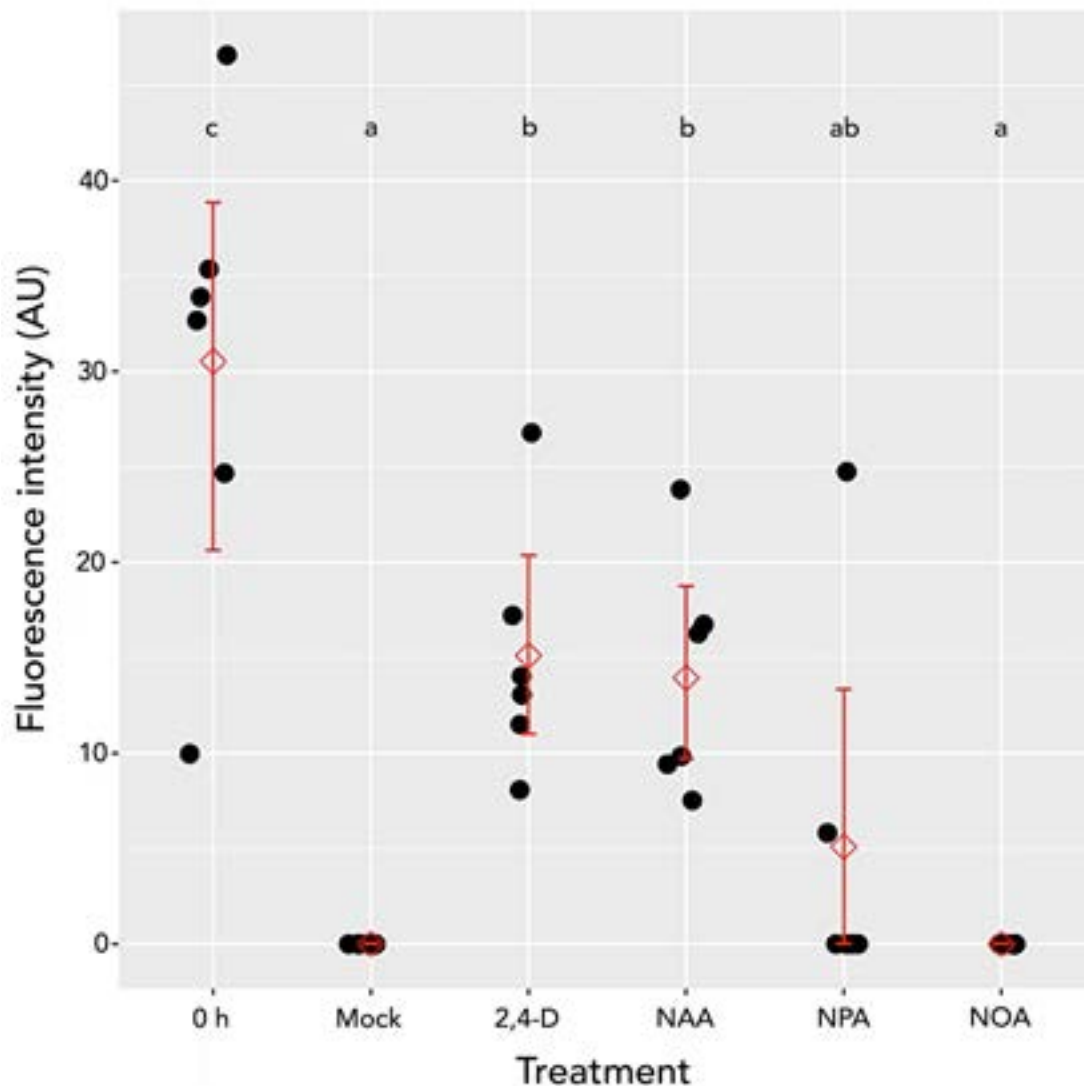


Figure 4.6 | Membrane fluorescence values were extracted from images of 2 cm stem segments excised from bolting inflorescences of 4-week old plants expressing *pin1 PIN1-GFP* and either imaged immediately after harvesting or treated for 6 days in vertical plates supplemented apically with mock, 1 μ M 2,4-D, 1 μ M NAA, 1 μ M NPA or 1 μ M NOA. Stem segments were longitudinally sectioned and the xylem parenchyma at the apical end imaged using confocal microscopy. Fluorescence data was extracted from these images using Zen Black (2012) software to trace round basal plasma membranes where PIN1-GFP was visible. This was done for at least 5 membranes per stem and at least 6 stems were analysed per treatment per experiment (n=30). The experiment was repeated three times, the figure is representative of all of these. Membrane fluorescence values for each stem were averaged and plotted here as black dots. Red diamonds represent the average of

these averages, the red line indicates the 95% confidence interval. Different letters indicate statistically significant differences following a one-way ANOVA and Tukey's HSD post-hoc testing.

Having confirmed that 2,4-D and NOA were not yielding unanticipated effects on PIN1 polarity, combined treatments were used and their impact on PIN1 polarity investigated. I hypothesised that 2,4-D + NOA would lead to high extracellular auxin and low intracellular auxin since 2,4-D requires auxin influx transporters to enter cells and NOA inhibits these. 2,4-D + NPA treatment was predicted to have no effect relative to 2,4-D alone as 2,4-D is reported to diffuse out of cells passively and does not significantly rely on auxin efflux carriers (Delbarre *et al.*, 1996). NAA+NOA was included as an additional control as NAA entry into cells should not be greatly impacted by inhibition of influx carriers as NAA enters primarily by diffusion. Figure 4.7A demonstrates that combined treatment with 2,4-D and NOA has no effect on PIN1 polarity relative to 2,4-D or NAA alone. Furthermore, 2,4-D+NPA & NAA+NOA slightly increased the level of PIN1 on the membrane relative to 2,4-D or NAA, albeit not significantly. A similar trend was seen in the number of membranes observed to have polarly localised PIN1 (Figure 4.7, B).

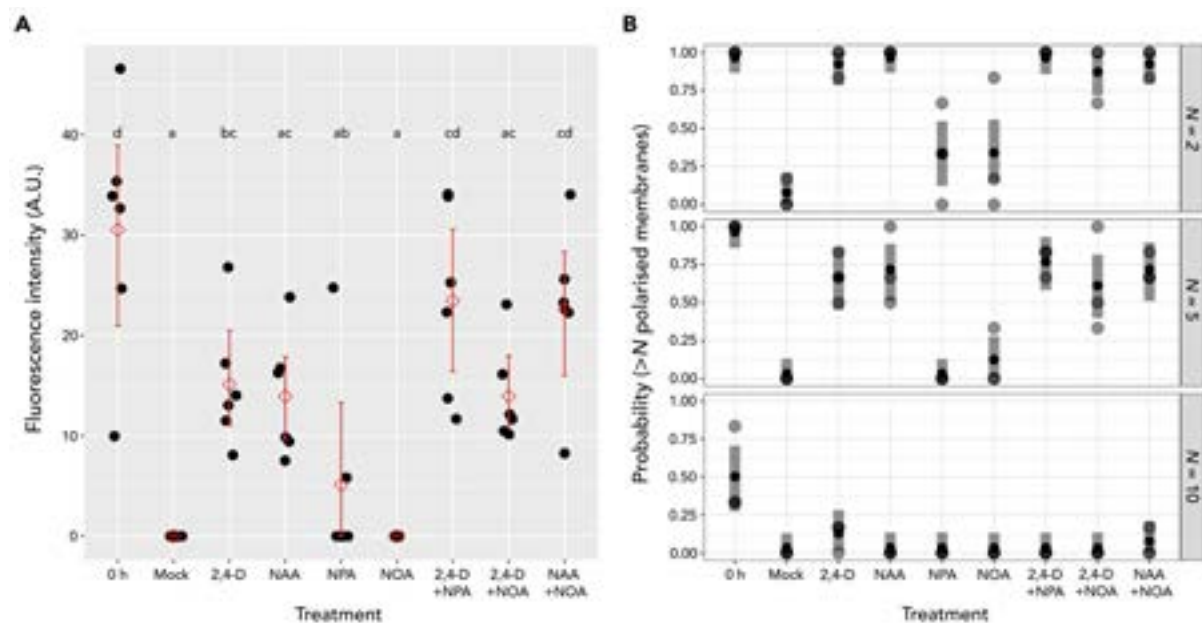


Figure 4.7 | (A) PIN1-GFP intensity present on the basal plasma membrane of xylem parenchyma & cells quantified using at least 5 cells from 6 independent *pin1* PIN1-GFP plants ($n=30$). Different letters indicate statistically significant differences following a one-way ANOVA and Tukey's HSD post-hoc testing. (B), the number of membranes with visibly polar PIN1-GFP were counted and the probability of the number of polarised cells in each repeat being greater than each arbitrary threshold calculated. For all treatments, each point represents a single repeat experiment in which at least 6 independent plants were analysed for PIN1 polarity, at least 3 repeats were conducted for all treatments, at least 3 repeats were conducted ($n=18$). A logistic regression model was fitted to these data to estimate the 95% confidence interval, represented by the grey bars.

These data suggest that, intracellular:extracellular auxin ratio is not a controlling factor in determining PIN1 polarity. However, in order to determine whether auxin levels were changing with treatments in the predicted manner, lines expressing *DR5::NLS-VE-NUS* were deployed to investigate the effects of these treatments on intracellular auxin levels. Figure 4.8 shows that the amount of auxin in cells decreases significantly after 6 d mock treatment whilst both NAA & 2,4-D are able to maintain and even increase NLS-VENUS expression above 0 h levels. Both NPA and NOA were effective at reducing NLS-VENUS expression to mock levels. Thus, individually, treatments behaved in line with previous results and predictions. Combined 2,4-D and NPA did not lead to a significant change in intracellular auxin, with levels of NLS-VENUS in fact slightly lower than 2,4-D alone. On the other hand, combined treatment with 2,4-D and NOA had no effect on intracellular auxin relative to 2,4-D alone when it was expected that a significant reduction would be observed. Thus it seems that the treatments were ineffective at manipulating the intracellular:extracellular auxin ratio in the anticipated manner and did not result in any change in PIN1 polarity relative to auxins alone.

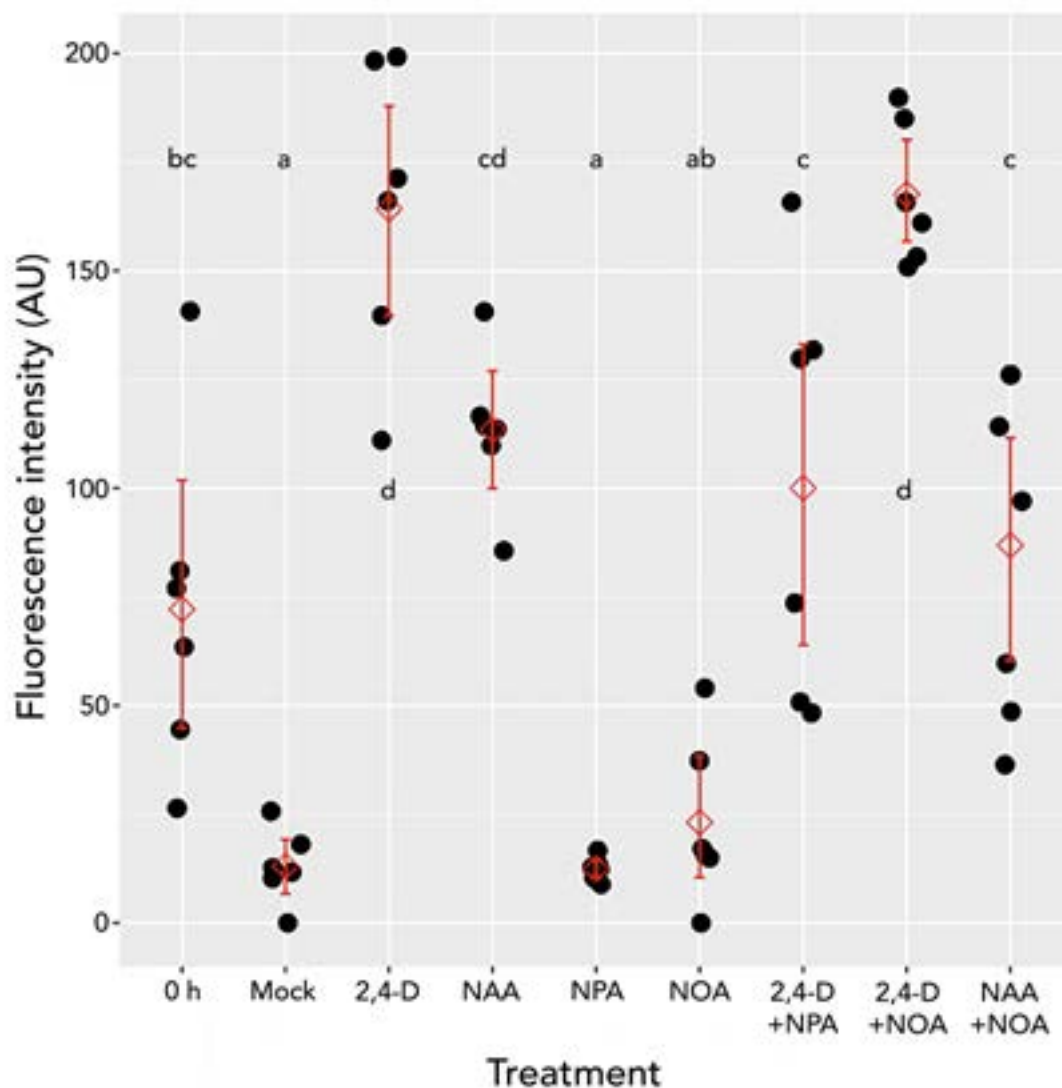


Figure 4.8 | Nuclear localised VENUS signal was quantified from images of 2 cm segments harvested from 4 week old plants expressing *DR5::NLS-VENUS* and either imaged immediately after har-

vesting or treated for 6 days in vertical plates supplemented apically with Mock, 2,4-D, NAA, NPA, NOA, 2,4-D+NPA, 2,4-D+NOA, NAA+NOA. Stem segments were then longitudinally sectioned and the xylem parenchyma at the apical end imaged using confocal microscopy. Fluorescence data was extracted from these images using Zen Black (2012) software to trace round nuclei where NLS-VENUS was visible. This was done for at least 5 membranes per stem and at least 6 stems were analysed per treatment per experiment (n=30). The experiment was repeated three times, the figure is representative of all of these. Membrane fluorescence values for each stem were averaged and plotted here as black dots, red diamonds represent the average of these averages, the red line indicates the 95% confidence interval. Different letters indicate statistically significant differences following a one-way ANOVA and Tukey's HSD post-hoc testing.

Since 2,4-D did not appear to be behaving as expected from existing data on its membrane permeability, I opted to test indole-3-acetic acid (IAA) which is a naturally occurring auxin. It is reported to rely on both diffusion and carrier mediated transport to enter and exit cells, with the latter playing a more significant role (Delbarre *et al.*, 1996). Thus, I repeated the previous experiment using using IAA instead of 2,4-D or NAA.

These data seem to suggest that IAA treatment is ineffective at retaining PIN1 on the membrane (Fig. 4.9 A) or at driving *DR5* promoter activity (Fig. 4.9 B). As such it is difficult to determine whether IAA+NOA treatments or NOA alone were having any effect. This data is surprising as IAA is a natural auxin and therefore should be efficacious in activating *DR5* promoters and maintaining PIN1 on the basal PM. This may have been due to the relatively long treatment time (6 d), as IAA is known to be relatively unstable, particularly in response to light in solid media (Yamakawa *et al.*, 1979; Nissen and Sutter, 1990). Thus, it was considered that a shorter treatment time and/or higher starting

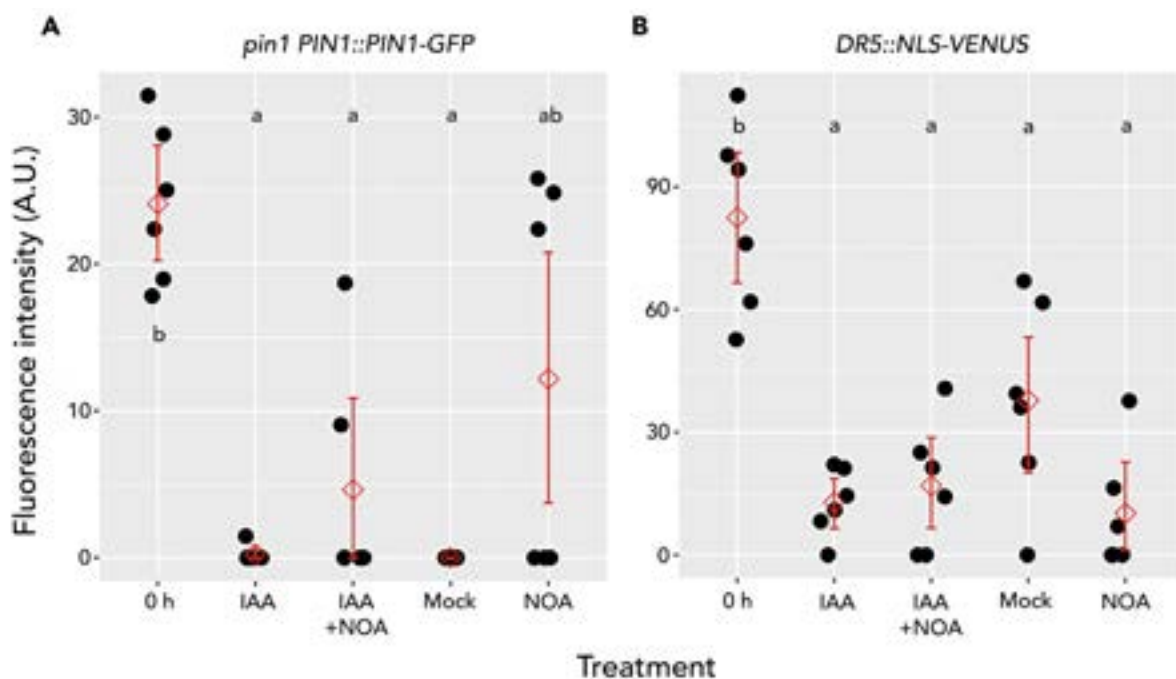


Figure 4.9 | Fluorescence intensity values were extracted from images of 2 cm segments were harvested from 4 week old plants expressing *pin1 PIN1::PIN1-GFP* (A) or *DR5::NLS-VENUS* (B) and

either imaged immediately after harvesting or treated for 6 days in vertical plates supplemented apically with IAA, IAA+NOA, Mock or NOA. Stem segments were then longitudinally sectioned and the xylem parenchyma at the apical end and imaged using confocal microscopy. Fluorescence data was extracted from these images using Zen Black (2012) software to trace round membranes or nuclei where PIN1-GFP or NLS-VENUS respectively was visible. This was done for at least 6 membranes/nuclei per stem and at least 6 stems were analysed per treatment per experiment ($n=36$). The experiment was repeated twice. Fluorescence values for each stem were averaged and plotted here as black dots. Red diamonds represent the average of these averages, the red line indicates the 95% confidence interval. Different letters indicate statistically significant differences following a one-way ANOVA and Tukey's HSD post-hoc testing.

concentration might be more effective.

The experiment was repeated over a 2 d timescale and with 5 μM IAA and NOA as opposed to 1 μM . Figure 4.10 shows that, under these conditions, IAA is able to drive *DR5* activity and maintain PIN1 polarity at a level similar to that seen at 0 h and after NAA treatment. This indicates that IAA does degrade over time and thus is only useful in experiments over a relatively short timescale. Plants treated with 5 μM IAA over a 5 d timescale showed similarly low expression of both NLS-VENUS and PIN1-GFP (data

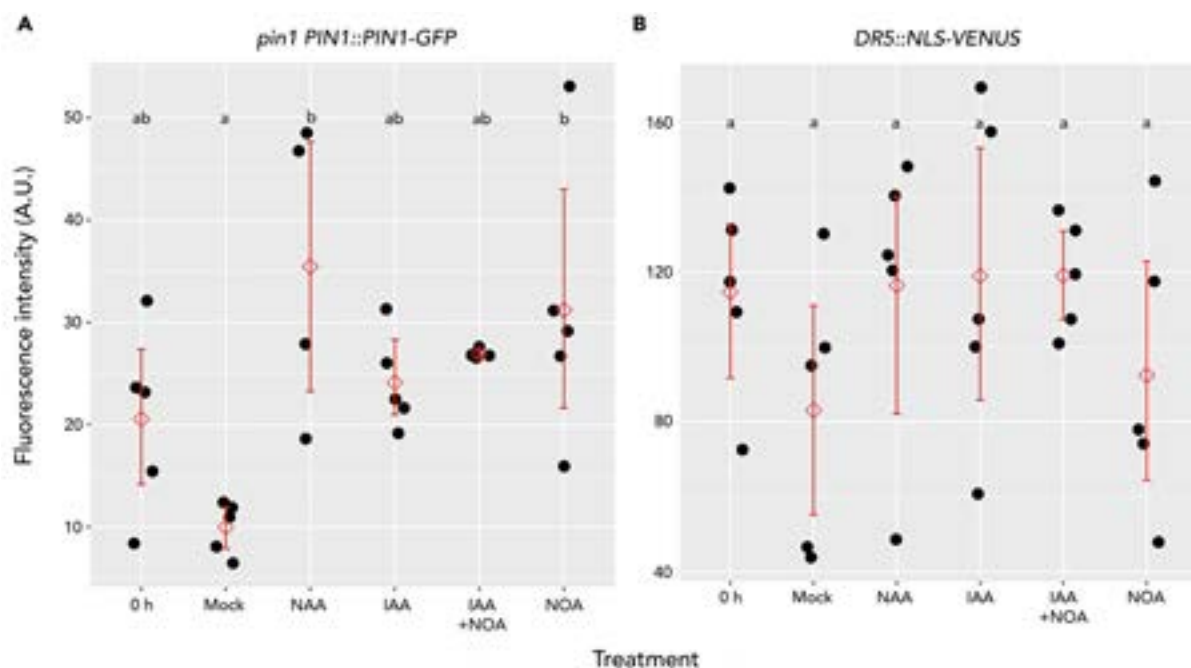


Figure 4.10 | Fluorescence values were extracted from images of 2 cm segments were harvested from 4 week old plants expressing *pin1 PIN1-GFP* (A) or *DR5::NLS-VENUS* (B) and either imaged immediately after harvesting or treated for 2 days in vertical plates supplemented apically with Mock, 1 μM NAA, 5 μM IAA, 5 μM IAA+NOA, or 5 μM NOA. Stem segments were then longitudinally sectioned and the xylem parenchyma at the apical end and imaged using confocal microscopy. Fluorescence data was extracted from these images using Zen Black (2012) software to trace round membranes or nuclei where PIN1-GFP or NLS-VENUS respectively was visible. This was done for at least 6 membranes/nuclei per stem and at least 5 stems were analysed per treatment per experiment ($n=30$). The experiment was repeated twice. Fluorescence values for each stem were averaged and plotted here as black dots. Red diamonds represent the average of these averages, the red line indicates the 95% confidence interval. Different letters indicate statistically significant differences following a one-way ANOVA and Tukey's HSD post-hoc testing.

not shown) as those treated with 1 μM IAA, suggesting that it is length of treatment as opposed to initial concentration that determines IAA efficacy. Treatment with NOA in combination with IAA had no effect on either *DR5* activity or PIN1 polarisation in any of the three repeats conducted (Fig. 4.10).

2-NOA is reported to be an inhibitor of auxin influx carriers and has been demonstrated to reduce auxin uptake by cells, something which our above data does not corroborate. 2-NOA does not completely inhibit auxin influx in cell culture so it is possible that, in previous experiments, the desired effect was not achieved due to compensation through increased influx carrier expression or compensation by carriers which are not targeted by NOA. An *aux1-21* mutant expressing GFP tagged PIN1 was used in order to try and reduce auxin influx further by inhibiting auxin influx carriers using 2-NOA in a context where one such transporter was non-functional. Figure 4.11 demonstrates that, in this background, 2-NOA alone or in combination with IAA does not have any impact on PIN1-GFP localisation relative to IAA alone or 0 h (Fig. 4.11 A). Furthermore, PIN1-GFP localisation at the base of stems is not affected by NOA treatment, suggesting that it was not effective at preventing auxin transport down the stem (Fig. 4.11 B).

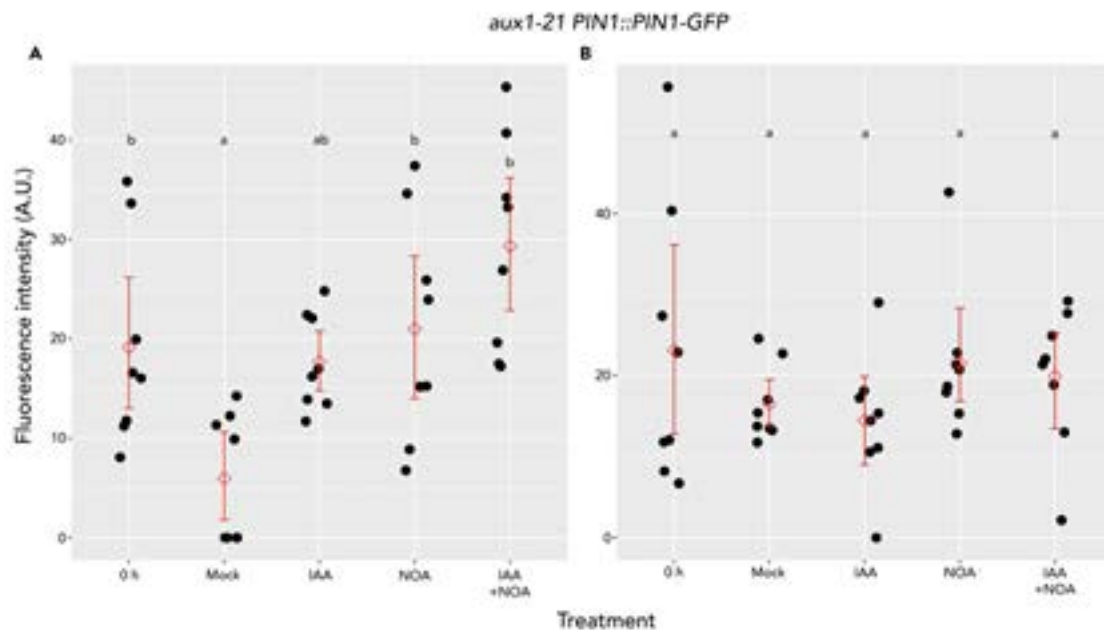


Figure 4.11 | 2 cm segments were harvested from 4 week old *aux1-21* mutants expressing PIN1-GFP and either imaged immediately after harvesting or treated for 2 days in vertical plates supplemented apically with Mock, 1 μM IAA, 1 μM IAA+NOA, or 1 μM NOA. Stem segments were then longitudinally sectioned and the xylem parenchyma at the apical (A) and basal (B) end and imaged using confocal microscopy. Fluorescence data was extracted from these images using Zen Black (2012) software to trace round membranes where PIN1-GFP was visible. This was done for at least 6 membranes/nuclei per stem and at least 8 stems were analysed per treatment per experiment (n=48). The experiment was repeated five times. Fluorescence values for each stem were averaged and plotted here as black dots. Red diamonds represent the average of these averages, the red line indicates the 95% confidence interval. Statistical testing was performed using a one-way ANOVA followed by Tukey's honest significant difference post-hoc analysis and the significance indicated by compact letter display.

4.3 | Discussion

In the past 50 years of auxin research a range of synthetic compounds have been used to investigate the auxin transport system. For many of these, it is unknown precisely how they act in a biochemical context and much of the research that has been done is in artificial single-cell systems. Here, I will discuss the implications of the data presented here for the use of these compounds in investigating auxin transport.

4.3.1 | The effects of NPA on intracellular auxin accumulation differ with tissue age

Here I have demonstrated that, in young, bolting inflorescences, NPA is ineffectual at causing auxin accumulation in the cells of the xylem parenchyma in contrast to its previously reported effects in mature tissue at terminal flowering (Fig. 4.1 B) (Bennett *et al.*, 2016). The effects of NPA are significantly different in mature vs young stem segments. In mature segments, apical NPA treatment results in retention of auxin and PIN1 whereas, in young stem segments auxin appears to deplete despite NPA treatment, and this is associated with PIN1 depletion (See chapter 3). Treatment with both auxin and NPA results in PIN1 retention and a considerable degree of auxin accumulation, suggesting that the presence of auxin, but not NPA-sensitive auxin transport is necessary for PIN1 retention. However, I have also demonstrated that high auxin concentration alone is not sufficient to promote PIN1 polarisation (Figs. 3.5, 3.6). This is in contrast to published data which demonstrated that combined treatment of an auxin and NPA did not lead to PIN1 hyper accumulation nor *DR5* activation (Mazur *et al.*, 2020). However, the aforementioned experiment used IAA instead of NAA or 2,4-D, which I have here demonstrated to lose efficacy over the 4-6 d timescale used in these experiments (Figure 4.9), raising the possibility that the observed lack of PIN1-GFP or *DR5* activation may be an artefact of degrading IAA.

The observation that NPA fails to trigger intracellular auxin accumulation in young stems is unexpected. NPA is highly effective at inhibiting long range polar auxin transport in diverse tissues and cell systems (Morgan, 1964; Petrášek *et al.*, 2002; Van Noorden *et al.*, 2006; Brewer *et al.*, 2015). NPA is known to bind and inhibit the activity of ABCB and PIN auxin transporters, typically reducing cellular auxin efflux and trapping auxin in cells (Delbarre *et al.*, 1996; Petrášek *et al.*, 2002; Petrášek *et al.*, 2003; Blakeslee *et al.*, 2007; Teale and Palme, 2018; Abas *et al.*, 2020; Teale *et al.*, 2021). In contrast, not only does NPA fail to prevent loss of *DR5* activity in the cells of excised young stem segments, my results consistently show that dual treatment with auxin and NPA results in slightly less activity from the *DR5* promoter than treatment with NAA alone, suggesting an active effect of NPA in reducing intracellular and/or nuclear auxin. There are several possible non-exclusive explanations for this. For example, there may be an NPA-promoted mechanism for auxin efflux in these cells that is lost as stems

mature, For example, It is known that some ABCBs (ABCB4 & ABCB21) switch from acting as auxin importers to auxin exporters when intracellular auxin is high (Geisler *et al.*, 2005; Lewis *et al.*, 2007; Yang and Murphy, 2009; Knöllner *et al.*, 2010; Kubeš *et al.*, 2012; Jenness *et al.*, 2019). If NPA has a differential effect on ABCB-mediated auxin import vs export, NPA-treatment might trigger net auxin export. NPA is known to be hydrolysed to naphthylamine and phthalic acid by aminopeptidases so it might be that NPA became degraded over the course of the treatment and became ineffective (Murphy and Taiz, 1999). The latter is unlikely as NPA has been shown to be active over several days and the observed phenomena were apparent even over 2 & 3 d treatments (Figure 4.2, 4.3). Furthermore, it was demonstrated that NPA reduced transport of NAA from the apical region, with *DR5* activity and PIN polarity being reduced at the basal ends of stem segments (Figure 4.4). It could be the case that actual auxin levels are high in this context but that there are feedback mechanisms in play. For example, *AUX/IAA* genes, which encode negative regulators of auxin-induced gene expression, are themselves auxin up-regulated. Very high auxin levels achieved through combined auxin and NPA treatment might lead to a strong repression of the *DR5* transcriptional auxin response (Jain *et al.*, 2006; Shi *et al.*, 2020). However, there is evidence to demonstrate that auxin induced gene expression exhibits a plateauing dose-response curve, which would argue against this (Gray *et al.*, 2001; Shimizu-Mitao and Kakimoto, 2014). Additionally, NPA could trigger auxin conjugation or a reduction in nuclear accumulation of auxin, preventing it from interacting with the predominantly nuclear receptor machinery involved in *DR5* promoter activation (Reviewed in Wang and Estelle, 2014).

These data suggest that, while NPA is consistently able to stop bulk auxin transport from the point of its application to regions below, the effect this has on PIN1 localisation and auxin accumulation in cells at the point of application differs considerably between young and old tissue.

4.3.2 | The synthetic auxin 2,4-D and influx inhibitor 2-NOA do not behave as predicted by single-cell models.

Given the above data suggesting that neither NPA-sensitive auxin flux nor straightforward auxin concentration are able to explain PIN behaviour, attempts were made to use 2,4-D & 2-NOA to manipulate the ratio of intracellular to extracellular auxin. On the basis of data indicating a reliance of 2,4-D on influx carriers for import and the ability of 2-NOA to inhibit said carriers, I predicted that a combined treatment of 2,4-D & 2-NOA ought to lead to low intracellular auxin and high extracellular auxin (Delbarre *et al.*, 1996; Lanková *et al.*, 2010).

Contrary to these predictions and to existing data (Simon *et al.*, 2013), 2,4-D + 2-NOA did not lead to the expected response, with PIN1 polarity remaining high (Fig.

4.7) and not significantly different from 2,4-D alone. However, since there was also no change in *DR5* driven NLS-VENUS signal (Fig. 4.8), a role of auxin ratios cannot be ruled out. This might suggest that, *in planta*, 2,4-D and 2-NOA do not behave as has been previously demonstrated using isolated tobacco BY-2 cells (Delbarre *et al.*, 1996; Lanková *et al.*, 2010; Hošek *et al.*, 2012). This could be due to the high concentrations used in these previous experiments which are not necessarily physiologically relevant. Alternatively, it may be that, over the relatively longer time-course of these experiments, intracellular and extracellular auxin equilibrated due to incomplete inhibition of active auxin influx and/or a small amount of diffusive influx of 2,4-D through the plasma membrane, combined with poor efflux of 2,4-D from the cell. The latter is unlikely as 2,4-D has been demonstrated to be poorly transported in *planta* (Ito and Gray, 2006) although some modelling suggests that passive diffusion may play an important role (Hošek *et al.*, 2012). In addition, since *DR5* activation data is not giving a direct report of the amount of auxin in the cell, merely a proxy in the form of the amount of auxin signalling, it is possible that 2,4-D is a 'stronger' activator of *DR5*. This could result in a scenario where treatment had effectively reduced the amount of auxin in the cell but the little that remained induced a high *DR5* activity such that signal is saturated under both 2,4-D and 2,4-D+NOA treatment even if there was less intracellular auxin in the latter. This notion is supported by that observation of higher VENUS signal in stems treated with 2,4-D relative to NAA (figure 4.8) and previous reports that 2,4-D drives higher *DR5rev::GFP* expression than NAA in roots (Simon *et al.*, 2013). However, it has also been demonstrated that 2,4-D binds auxin signalling components more weakly (Kepinski and Leyser, 2005), such that any greater activation by 2,4-D is usually attributed to its greater intracellular accumulation and stability.

It is interesting to note that combined treatment with 2,4-D and NPA led to a decrease in the amount of *DR5* activity but an increase in plasma membrane PIN1 relative to 2,4-D alone (Figure 4.7, 4.8). This is the opposite of what would be anticipated based on data that 2,4-D is a poor substrate for auxin efflux carriers generally and NPA inhibits efflux carriers (Titapiwatanakun *et al.*, 2009). It also draws interesting parallels with previous data that combined NAA+NPA treatment leads to a slight decrease in *DR5* activity but an increase in plasma membrane PIN1, it is unclear why this may be the case. Much of the data on auxin accumulation kinetics is based on experiments using radiolabelled auxins (Delbarre *et al.*, 1996; Lanková *et al.*, 2010). However, when these are metabolised the metabolites remain inside the cell, giving a false impression of how much free, active auxin is actually present intracellularly (Hošek *et al.*, 2012). This may provide some explanation for the disparity between these data and that presented here.

4.3.3 | Natural auxins are less stable than synthetic auxins

Unlike NAA and 2,4-D, IAA was unable to maintain PIN1 on the plasma membrane,

nor induce *DR5* activity at a level greater than mock over a 6 d treatment (Fig. 4.9). This can likely be explained by the reported instability of IAA, particularly when exposed to light in a solid medium as was the case here, or perhaps by a greater sensitivity to degradation/conjugation (Yamakawa *et al.*, 1979; Dunlap and Robacker, 1988; Nissen and Sutter, 1990). This is supported by the demonstration that, over a 2 d treatment, IAA was as effective at maintaining PIN1 on the membrane and inducing *DR5* activity as NAA (Figure 4.10). Once again, NOA treatment had no observable effect on IAA accumulation in the cell, nor on PIN1 accumulation on the membrane, even in a mutant *aux1* transporter background (Fig 4.10, 4.11). Whilst it was anticipated that the latter at least should have a marginal effect, the result does not necessarily conflict with previous data that IAA relies on both diffusion and active transport to enter cells such that the impact of a reduction in active transport is conceivably marginal over a 2 d treatment (Delbarre *et al.*, 1996). However, roots of mutants in the *aux1* influx carrier have been shown to be highly resistant to 2,4-D and IAA (Marchant *et al.*, 1999) and *aux1* quadruple mutants exhibit reduced overall auxin transports and different transport profiles (Boot *et al.*, 2016), suggesting that there is significant dependence on these uptake carriers *in planta*. Interestingly, NOA had no observable impact on *DR5* activity in the basal region of apically treated stems (Fig 4.11, B), suggesting that it has very little impact on IAA transport down the stem relative to NPA. It must be noted, that no positive control was included for the activity of 2-NOA, so a definitive conclusion cannot be drawn.

4.3.4 | Conclusions

The data presented in this chapter, whilst inconclusive, is nevertheless interesting insofar as it raises further questions. This data appears to rule out the role of NPA-sensitive flux or simple auxin concentration in determining the allocation of PIN1 protein, but it does not provide convincing evidence for an alternative mechanism. The notion of an auxin gradient sensing system, whilst intriguing, has proved challenging to test and could not be achieved here. However, in attempting to do so I note that many of the chemical tools the field relies on do not necessarily behave as predicted by single-cell models when used in a multicellular system. In order to satisfactorily test the original hypothesis, a method of directly measuring auxin levels will be required as opposed to the proxy methods which were available and utilised in this thesis. Fortunately, such tools are now becoming reality with the recent advent of auxin biosensors such as AuxSen (Herud-Sikimic *et al.*, 2021), although this still does not enable measurement of apoplastic auxin levels.

- ◇ NPA is ineffective at trapping auxin in the cells of young stems of *Arabidopsis* nor does it induce PIN1 retention on the basal PM
- ◇ NPA remains effective at reducing bulk auxin flow in young stems
- ◇ 2-NOA may not halt IAA transport down the stem

5

The role of the central region of the PIN1 hydrophilic loop in regulating strigolactone sensitivity

"One can only believe entirely, perhaps, in what one cannot see" - V. Woolfe

5.1 | Introduction

The regulation of shoot architecture is strongly dependent on the ability of auxin to exert control over axillary meristems through apical dominance. The auxin transport canalisation hypothesis states that, buds must establish auxin export into the main stem in order to activate and that this in turn depends on the activity and localisation of auxin transporters, particularly PINs (Sachs, 1968a, 1975, 1981). Whilst it has been well established here and previously that different PIN proteins exhibit considerable differences with regard to their localisation in response to auxin, strigolactone and cytokinin, there is still little understanding of the mechanistic basis for these distinct behaviours at the protein level (Bennett, Hines, *et al.*, 2016; Waldie and Leyser, 2018; Ticchiarelli, 2019; Van Rongen *et al.*, 2019). In order to unravel the complex control of shoot branching it is important that we understand the way in which hormones can control PIN localisation, which in turn will open up avenues to manipulate PINs in a targeted manner. In chapter 3 and 4 I detailed investigations into the role of auxin and the way PINs respond to it. In this chapter I will present my investigations into the domain basis for strigolactone sensitivity of PINs and the effect of PIN1 SL insensitivity on aerial architecture.

Firstly, I will first outline our current understanding of PIN behaviour in response to SL and its effect on bud activity before presenting my novel results.

5.1.1 | Control of plasma membrane PIN localisation

PIN1 and PIN7 have been shown to exhibit sensitivity to strigolactone by depleting from the plasma membrane, while PIN3 and PIN4 are insensitive (Shinohara, Taylor and Leyser, 2013; Ticchiarelli, 2019; Van Rongen *et al.*, 2019). I have previously shown that PIN1 behaviour in response to auxin, NPA and cytokinin varies with age (Chapter 3) whilst it has been reported that PIN3, PIN4 and PIN7 exhibit very little polarity in mature tissue (Bennett, Hines, *et al.*, 2016; Ticchiarelli, 2019). Long PINs consist of 10 transmembrane helices and a 320-360 amino acid hydrophilic loop. One possible explanation for diverse behaviours of different PINs might relate to the presence of different amino acid residues in the hydrophilic loop. The HL is well characterised as being the target of different classes of kinases, resulting in different patterns of phosphorylation which can alter PIN localisation and transport capacity (Barbosa, Hammes and Schwechheimer, 2018). There are four classes of kinase which have been demonstrated to phosphorylate residues in the PIN HL: AGC kinases act on serine residues to alter PIN phosphorylation and polarity (Michniewicz *et al.*, 2007; Dhonukshe *et al.*, 2010; Zourelidou *et al.*, 2014; Grones *et al.*, 2018); MAP kinases target both threonine and serine residues (Jia *et al.*, 2016; Dory *et al.*, 2018); CALCIUM-DEPENDENT PROTEIN KINASE (CPKs) and CPK-related kinases (CRKs) have targets in the HLs of several

PINs and have been linked to PIN polarity (Rigó *et al.*, 2013; Baba *et al.*, 2019; Lee *et al.*, 2021); CAMEL (Canalization-related Auxin-regulated Malectin-type RLK) is able to phosphorylate several residues in the HL of PINs (Hajný *et al.*, 2020). Whilst much of this activity has been characterised in the root, it is becoming increasingly apparent that some of these kinases also exhibit control in the shoot (Jia *et al.*, 2016). Whilst there are several phosphorylatable residues which are non-conserved across the PINs, none have been shown to be individually responsible for differing PIN behaviour. It is likely that many of these kinases share targets and that particular patterns of phosphorylation lead to particular PIN behaviours (Barbosa, Hammes and Schwechheimer, 2018).

SL biosynthesis and perception mutants exhibit increased PIN1 accumulation and SL has been shown to reduce PIN1 accumulation in the PATS (Bennett *et al.*, 2006; Crawford *et al.*, 2010) and this is dependent on SL signalling (Shinohara, Taylor and Leyser, 2013). More recently, it has been shown that different PINs exhibit different SL sensitivities, with PIN1 and PIN7 being endocytosed upon SL treatment whilst PIN3 and PIN4 are not (Ticchiarelli, 2019). It has also been demonstrated that the middle region of the PIN1 HL is able to confer SL sensitivity to PIN3 (Ticchiarelli, 2019). Thus, it seems likely that regions in the HL are responsible at least in part for determining PIN SL sensitivity.

5.1.2 | Bud outgrowth is modulated by auxin and strigolactone

It's well established that auxin moving in the PATS is able to inhibit the activity of axillary meristems and that, by stopping this flow either by decapitation or application of NPA, bud dormancy is released (Snow, 1925; Thimann and Skoog, 1933). It is also clear that auxin is not able to move acropetally into the buds and likely acts indirectly (Thimann, Kerckhoff and Skoog, 1934; Hall and Hillman, 1975; Prasad, Hosokawa and Cline, 1989; Booker, 2003).

Strigolactone has been identified as a regulator of branching in several model organisms (Gomez-Roldan *et al.*, 2008; Umehara *et al.*, 2008). Mutations in the biosynthetic or perception pathway lead to altered shoot branching levels, with loss of function of *MAX1*, *MAX3*, *MAX4* or *D27* in the synthesis pathway, and *D14* or *MAX2* in the perception pathway, increasing activation of dormant buds (Stirnberg, van de Sande and Leyser, 2002; Sorefan *et al.*, 2003; Booker *et al.*, 2004; Arite *et al.*, 2009; Waters *et al.*, 2012). This and data demonstrating the insensitivity of SL mutant buds to apical auxin implicate SL in the inhibition of bud outgrowth (Beveridge, Symons and Turnbull, 2000; Sorefan *et al.*, 2003; Bennett *et al.*, 2006). Two routes by which this might occur have been proposed. According to the second messenger theory, auxin in the stem acts to upregulate SL synthesis and SL moves into the bud repressing bud growth (Brewer *et al.*, 2009). Auxin is able to upregulate transcription of elements of the SL biosynthetic pathway (Sorefan *et al.*, 2003; Foo *et al.*, 2005; Johnson *et al.*, 2006; Arite *et al.*, 2007;

Hayward *et al.*, 2009) and SL has been shown to inhibit bud growth through direct or basal supply to buds (Brewer *et al.*, 2009, 2015), although this requires a competing auxin source (Crawford *et al.*, 2010). Under this hypothesis, in a state where the SAM is present, high auxin levels in the PATS would induce SL synthesis which would move into buds and maintain dormancy on a local level, possibly via modulating *BRC1* transcription (Aguilar-Martinez, Poza-Carrion and Cubas, 2007).

Under the predictions of the auxin transport canalisation hypothesis, bud activation requires establishing of auxin export into the stem, moving from a strong source to a strong sink (Sachs, 1968b, 1969, 1981). Thus SL might act by regulating auxin transport itself, with SL mutants displaying decreased auxin transport and GR24 application able to do the same in wild type plants (Bennett *et al.*, 2006; Prusinkiewicz *et al.*, 2009; Crawford *et al.*, 2010). Furthermore, as discussed in section 5.1.2, membrane residency of PIN1 and PIN7 is SL sensitive. In this regard, SL-induced depletion of PIN1 and PIN7 from the basal PM would reduce the ability of buds to export auxin into the PATS whilst also reducing the sink strength of the stem, making it more difficult for buds to establish canalisation and thus reducing activation. Plants expressing SL sensitive PIN3-PIN1 chimeras under PIN1 promoter activity exhibited greater ability to complement auxin transport and branching phenotypes of *pin1* mutants than SL insensitive chimeras, suggesting that SL-regulation of PINs is an important component in the control of shoot branching (Ticchiarelli, 2019). It is therefore likely that both SL regulation of the ability of buds to activate and of their ability to export auxin contribute to its ability to inhibit bud outgrowth as suggested by (Seale, Bennett and Leyser, 2017).

5.1.3 | Aims

Given the previous implication of the central region of PIN1 HL in conferring SL sensitivity, I decided to investigate whether the reverse was also true and, if so, the implication this has for shoot branching. With the aim of answering the following questions

- ◇ Can the central region of the PIN3 HL confer SL insensitivity to PIN1?
- ◇ Does SL insensitivity affect other features of the behaviour of PIN1?
- ◇ Is an SL insensitive PIN1 able to effectively rescue *pin1* phenotypes?
- ◇ What effect does PIN1 SL insensitivity have on morphology of plants when expressed in place of PIN1?
- ◇ Is the ability of PIN1 to respond to SL related to its ability to transport auxin?
- ◇ Does expression of an SL insensitive PIN1 impact shoot branching?
- ◇ How do bud growth dynamics and interbud competition change if PIN1 is SL insensitive?

5.2 | Results

5.2.1 | PIN1 strigolactone responsiveness is conferred by the central region of the hydrophilic loop

The long PIN proteins consist of 3 main regions, two regions of transmembrane domains each consisting of 5 highly conserved helices separated by a hydrophilic loop (HL) which is exposed to the cytosol. The HL exhibits a considerable degree of variability between PINs and acts as a site at which post-translational modifications including ubiquitination and phosphorylation can occur, regulating PIN polarity and activity. Through a series of domain swap experiments, a previous member of the lab identified the central region of the hydrophilic loop as a key regulator of strigolactone responsiveness and by swapping this region from PIN1 into PIN3, was able to generate a chimeric PIN3-PIN1_{L2}-GFP protein which was responsive to SL (Ticchiarelli, 2019). This opened up the possibility of creating a version of PIN1 which is not sensitive to SL. To do this, I identified the 3 loop regions used previously and chose to focus on the central one due to its ability to confer SL sensitivity to PIN3. I generated chimeric DNA sequence consisting of the PIN1 transmembrane domains and first and third region of the HL, with the second region of the HL replaced with corresponding sequence from PIN3. GFP coding sequence was placed in the middle of the third loop region as terminal tagging impairs protein function. The entire sequence was synthesised (Genewiz, South Plainfield, US) and placed under control of the *PIN1* promoter (Heisler and Jönsson, 2006) using multisite gateway cloning, as summarised in figure 5.1.

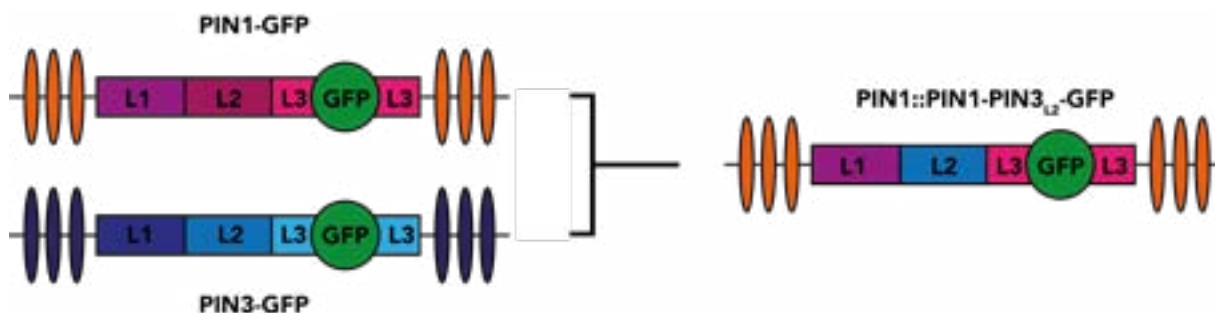


Figure 5.1 | Cartoon structure of the chimeric PIN1 construct generated and used in this thesis. PIN1 is coloured in magenta hues, PIN3 is represented by blue and GFP by green. Rectangles represent the hydrophilic loop while ovals represent the transmembrane domains.

Multiple independent transgenic lines were made in a *pin1-613* mutant background and taken to homozygosity of both the *pin1-613* allele and the construct. The *pin1-613* allele is a null T-DNA insertion allele which exhibits severe organ initiation defects in the inflorescence (Bennett *et al.*, 2006; Smith *et al.*, 2006; Zourelidou *et al.*, 2014) and will henceforth be referred to as *pin1*. All lines were able to complement obvious *pin1* phenotypes, 5 independent insertions were assessed for expression of the construct in comparison to an existing PIN1-GFP line and one line was selected for further detailed analysis on the basis of this.

I first assessed the responsiveness of PIN1-PIN3_{L2}-GFP to strigolactone. In order to test this, the basal 2 cm of primary inflorescences from 4 week old plants were sectioned longitudinally by hand and incubated with 5 μ M GR24 or mock for 6 h before imaging. *PIN1::PIN1-GFP*, *PIN3::PIN3-GFP* in a *pin1* and *pin3* background respectively and *PIN1::PIN3-PIN1_{L2}-GFP* in a Col-0 background were included for comparison. It is clear that, as reported in (Fig. 3.9 and Ticchiarelli, 2019, Shinohara *et al*, 2013), PIN1 is depleted from the membrane in response to strigolactone treatment (Fig. 5.2, A), whilst PIN3 is not (Fig. 5.2, B). As demonstrated by (Ticchiarelli, 2019), replacing the central

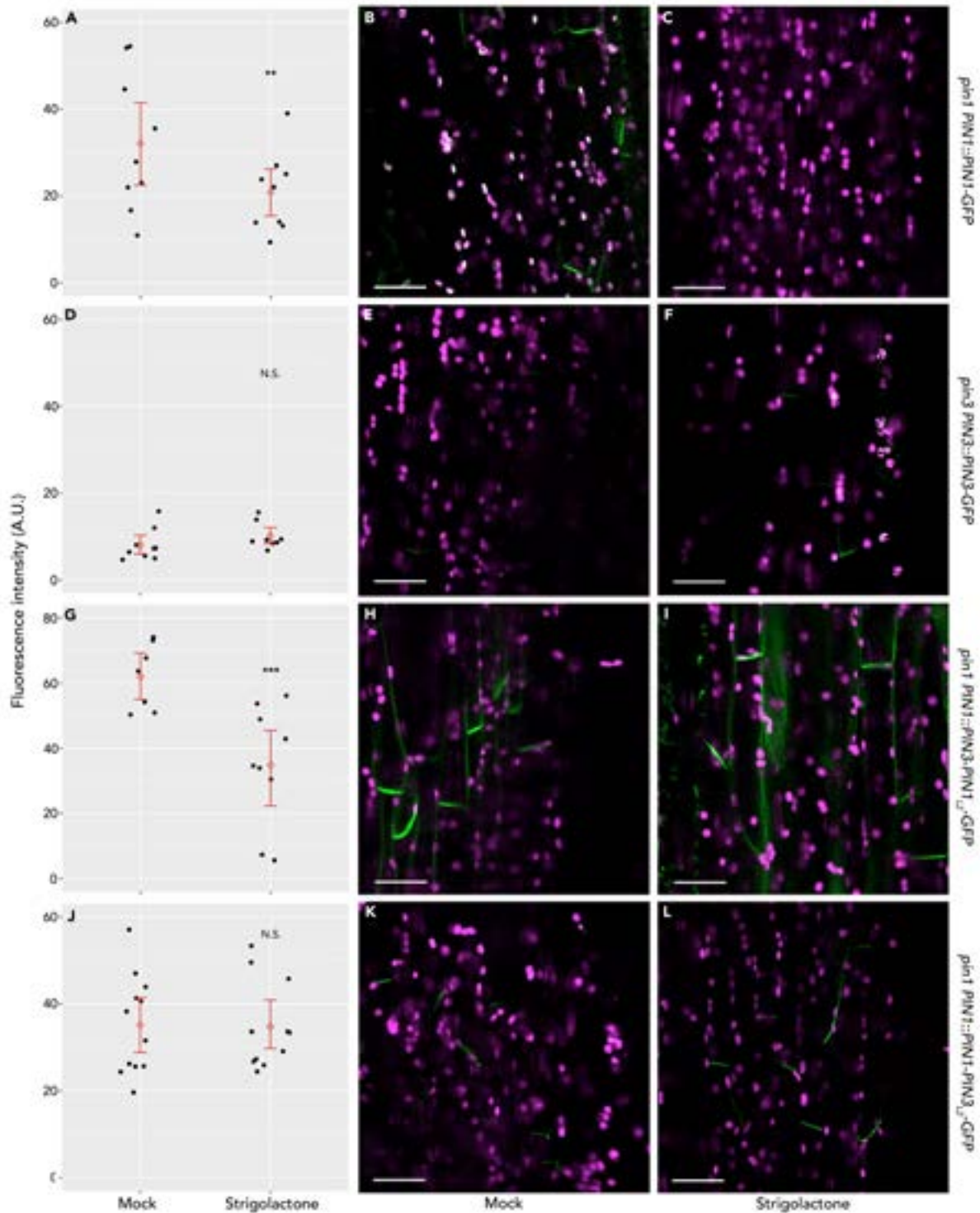


Figure 5.2 | 2 cm stem segments from the base of the primary inflorescence of ~4 week old plants expressing *pin1* PIN1-GFP (A, B, C), *pin3* PIN3-GFP (D, E, F), *pin1* PIN3-PIN1_{L2}-GFP (G, H, I) or *pin1* PIN1-PIN3_{L2}-GFP (J, K, L) were sectioned longitudinally and treated with either a mock treatment or strigolactone for 6 h. Segments were then imaged using a Zeiss LSM700 confocal microscope and representative examples shown (B, C, E, F, H, I, K, L). GFP fluorescence intensity of basal plasma membranes was extracted from these images using ZEN software. This was done for at least ten membranes per stem and at least eight stems were used for each treatment and each genotype. The experiment was repeated three times, and the results presented are typical. (A, D, G, J) the average membrane fluorescence for each stem was calculated and is represented here as black dots. Red diamonds indicate the average of averages and red bars indicate the 95% confidence interval. Statistics were performed using a Student's t-test with significance being indicated as non-significant (N.S.), $p < 0.05$ (*), $p < 0.01$ (**) or $p < 0.001$ (***). Scale bars represent 25 μ M.

part of the hydrophilic loop of PIN3 with that of PIN1 confers PIN3 with SL sensitivity, something which is reproducible here (Fig. 5.2, C). Furthermore, performing the opposite swap as I have done, replacing the central region of the hydrophilic loop of PIN1 with that of PIN3, effectively eliminates PIN1 SL sensitivity, with no detectable depletion from the membrane in response to SL (Fig. 5.2, D). As demonstrated previously for PIN1 (Fig. 3.9) and PIN7 (Waldie, unpublished), SL supply reduces the re-accumulation of PINs to the plasma membrane after depletion. Here I show that, PIN1-PIN3_{L2}-GFP does not exhibit this behaviour, with apical resupply of NAA in combination with basal GR24 resulting in re-accumulation to the same level as treatment with NAA alone. In both cases the amount of PIN on the basal PM is restored to levels similar to that of stems treated with NAA for 4 d and is significantly higher than that of mock treated stems. (Fig. 5.3). This is further evidence that strigolactone sensitivity is absent in this

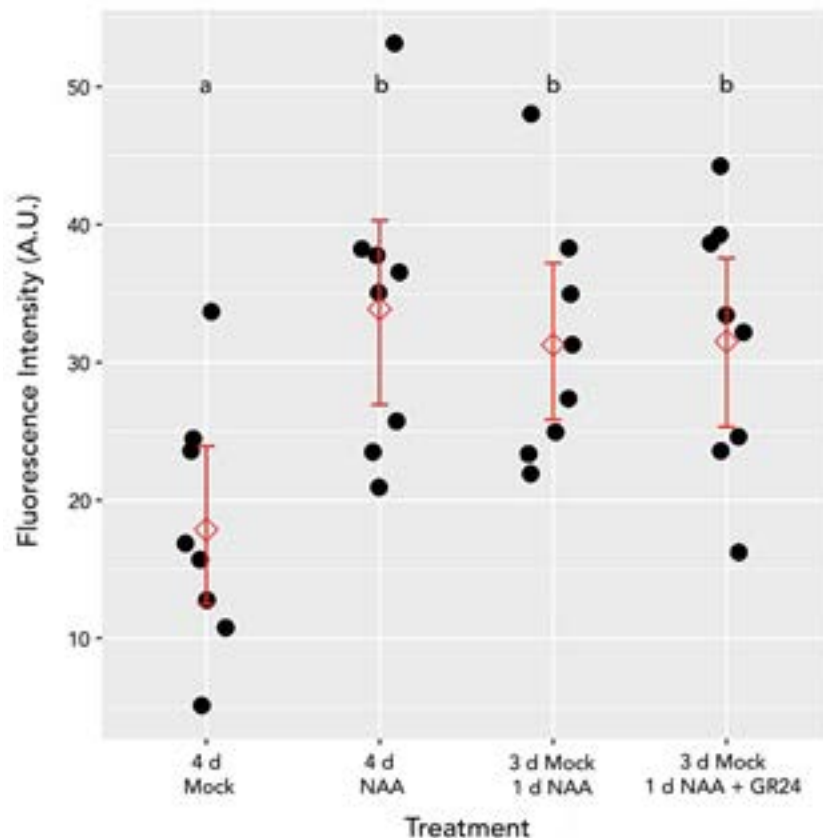


Figure 5.3 | 2 cm stem segments from the base of the primary inflorescence of ~4 week old plants expressing *pin1 PIN1-PIN3_{L2}-GFP* were treated apically with mock treatment for 4 d, NAA for 4 d, mock for 3 d followed by NAA or mock for 3 d followed by NAA and basal GR24. Segments were sectioned longitudinally by hand and imaged using a Zeiss LSM700 confocal microscope. GFP fluorescence intensity of basal plasma membranes was extracted from these images using ZEN software. This was done for at least five membranes per stem and at least eight stems were used for each treatment (n=40). The experiment was repeated three times, and the results presented are typical. The average membrane fluorescence for each stem was calculated and is represented here as black dots, with red diamonds indicating the average of averages and red bars indicating the 95% confidence interval. Different letters indicate statistical significance following a one-way ANOVA followed by Tukey's HSD post-hoc test.

line.

5.2.2 | PIN1-PIN3_{L2}-GFP exhibits increased membrane accumulation

Given the lack of responsiveness to SL exhibited by PIN1-PIN3_{L2}-GFP and the increased PIN1 membrane accumulation seen in SL biosynthesis/perception mutants, I assessed whether this was also the case when the PIN itself was insensitive to SL (Bennett *et al.*, 2006; Crawford *et al.*, 2010; Jiang *et al.*, 2013). The basal 2 cm of the primary inflorescences of 4 week old plants were hand sectioned, mounted on a Petri dish with micropore tape and imaged immediately. From these data it is clear that, as reported previously, PIN1-GFP localisation to the membrane is increased in the *d14* SL signalling mutant relative to a wild type background (Fig. 5.4 A, C). The same phenomenon is seen for PIN1-PIN3_{L2}-GFP, which exhibits increased localisation to the basal plasma membrane relative to PIN1-GFP and PIN3-GFP (Fig. 5.4 A, B, D). Extraction of the fluorescence intensity on the basal PM demonstrated that this visual difference is quantifiable, with PIN1-PIN3_{L2}-GFP exhibiting similar membrane fluorescence to PIN1-GFP in a *d14* background, with both of these significantly higher than *pin1 PIN1-GFP* or *pin3 PIN3-GFP* (Figure 5.4, E). There is also evidence to suggest that there is increased lateral localisation of PIN1-PIN3_{L2}-GFP, with fluorescence appearing to be brighter and more prevalent than PIN1-GFP (Fig. 5.5 A, C). This is also apparent for PIN1-GFP in a *d14* background (Fig. 5.5, B) and is quantifiable (Fig. 5.5, D). It is possible that this is a function of PIN1-PIN3_{L2}-GFP exhibiting higher membrane localisation generally as shown in figure 5.4. To distinguish whether there is in fact increased relative lateral allocation, I calculated the ratio of mean lateral to mean basal membrane fluorescence of each stem for *pin1 PIN1-GFP* in and *d14 PIN1-GFP* backgrounds and for *pin1 PIN1-PIN3_{L2}-GFP* (Fig. 5.5, E). While there is a slight suggestion that proportional lateral localisation of PIN1-PIN3_{L2}-GFP is increased relative to PIN1-GFP, this difference is not significant.

I investigated whether a lack of SL sensitivity affected the retention of PIN1-PIN3_{L2}-GFP on the membrane in response to auxin depletion. To investigate this, 2 cm segments from the basal internodes of 4 week old plants were excised and either imaged immediately or placed in agar plates without apical auxin supply for 4 and 6 days

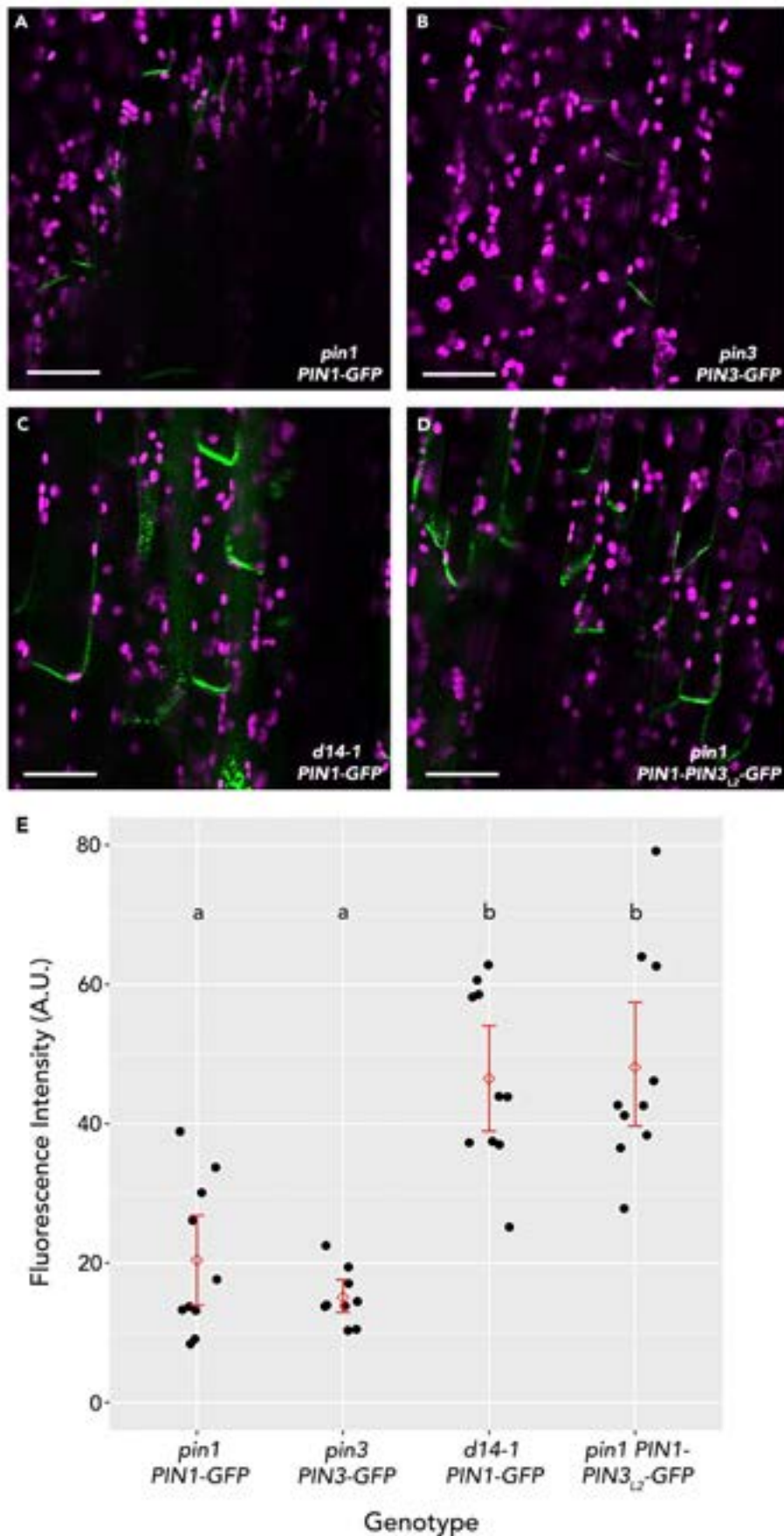


Figure 5.4 | Representative images showing the expression of *pin1 PIN1-GFP* (A), *pin3 PIN3-GFP* (B), *d14-1 PIN1-GFP* (C) and *pin1 PIN1-PIN3_{L2}-GFP* (D) in the xylem parenchyma of 4 week old stems. 2 cm stem segments were taken from the base of the primary inflorescence and immediately hand sectioned longitudinally before imaging the xylem parenchyma with confocal microscopy. (E)

GFP fluorescence intensity of basal plasma membranes was extracted from these images using ZEN software. This was done for at least ten membranes per stem and at least 8 stems per genotype (n=80). The average membrane fluorescence for each stem was calculated and is represented here as black dots, with red diamonds indicating the average of averages and red bars indicating the 95% confidence interval. Different letters indicate statistically significant differences following a one-way ANOVA and Tukey's HSD post-hoc test. Scale bars represent 25 μ M.

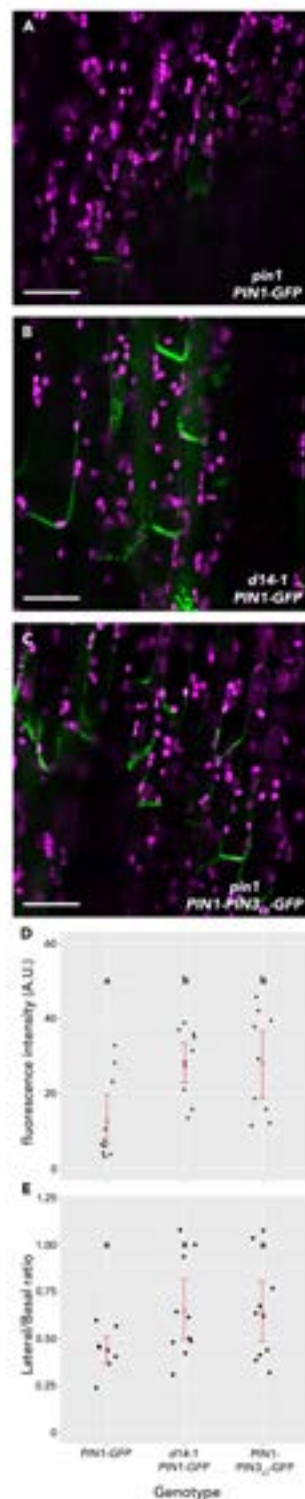


Figure 5.5 | Representative images showing the membrane localisation of *pin1* PIN1-GFP (A), *d14-1* PIN1-GFP (B) and *pin1* PIN1-PIN3_{L2}-GFP (C) in the xylem parenchyma of 4 week old stems. 2 cm stem segments were taken from the base of the primary inflorescence and immediately hand sectioned longitudinally before imaging the xylem parenchyma with confocal microscopy. (D) GFP fluorescence intensity of lateral plasma membranes was extracted from these images using ZEN software. This was done for at least 5 membranes per stem and at least 8 stems per genotype (n=40). The average membrane fluorescence for each stem was calculated and is represented here as black dots, with red diamonds indicating the average of averages and red bars indicating the 95% confidence interval. (E) Mean lateral membrane intensity was divided by mean basal membrane intensity for each stem to give a ratio. Black dots represent the ratio value for each stem, with the red triangle representing the mean of means and the red bars the 95% CI. Different letters indicate statistically significant differences following a one-way ANOVA and Tukey's HSD post-hoc test. Scale bars represent 25 μ M.

before sectioning and imaging. In fresh stems, PIN1-PIN3_{L2}-GFP membrane localisation and PIN1-GFP localisation in a *d14* background is significantly higher than PIN1-GFP in a *pin1* background as reported previously (Fig. 5.4, 5.6). After 6 days, PIN1-GFP is effectively depleted from the basal plasma membrane and this is also the case in the *d14* mutant background (figure 5.6). The PIN1-PIN3_{L2}-GFP construct on the other hand exhibits only a slight decrease in membrane localisation over 6 days. No significant difference between the three lines was observed after 4 d of mock treatment, although PIN1-PIN3_{L2}-GFP exhibited slightly higher membrane accumulation

I next investigated whether the construct remained sensitive to auxin in older stems. 2 cm stem segments from the base of the primary inflorescence of young (4 week old) and old (6 week old) *pin1* PIN1-PIN3_{L2}-GFP plants were placed into agar plates treated apically with mock, NAA, NPA, or NAA+NPA for 6 days before sectioning and imaging. In young tissue, PIN1-PIN3_{L2}-GFP depletes from the membrane significantly when treated with mock or NPA relative to 0 h, NAA and NAA+NPA (Fig. 5.7 A). This change is

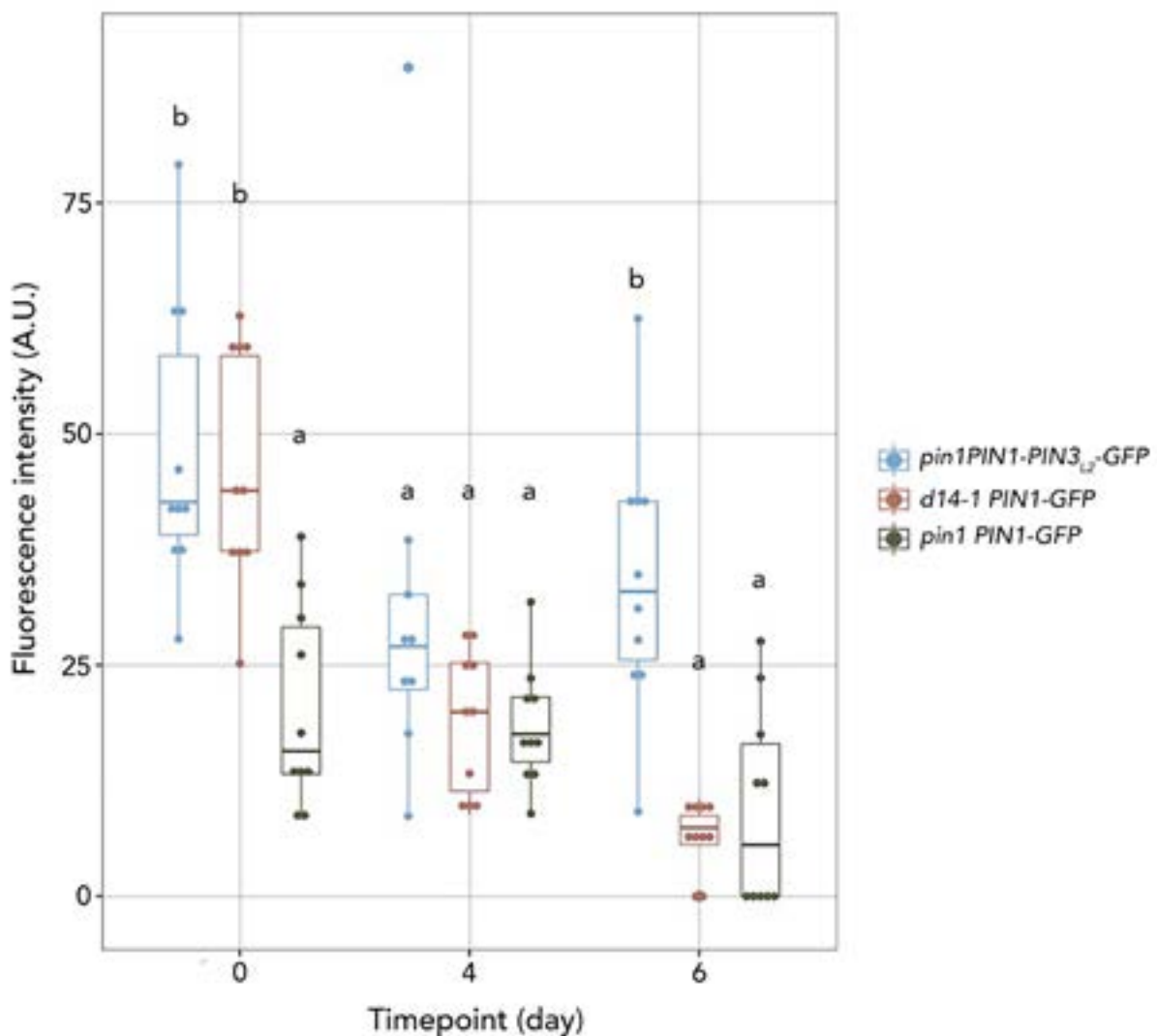


Figure 5.6 | 2 cm sections from the base of primary inflorescences of 4 week old plants expressing PIN1-PIN3_{L2}-GFP in a *pin1* background (blue), PIN1-GFP in a *d14* mutant (red) or PIN1-GFP in a *pin1*

background (green) and either imaged immediately or after 4 and 6 days in untreated agar plates such that no apical auxin was supplied. Stems were then hand sectioned longitudinally and imaged apically. ZEN software was used to extract the fluorescence values of the basal plasma membrane, this was done for 10 membranes per stem and 8 stems per genotype per timepoint (n=80). The ggplot2 package was used to plot these values as dotplots with box and whisker plots overlaid, such that each dot represents the average fluorescence for one stem. Within each timepoint, different letters indicate statistical difference after a one-way ANOVA followed by post-hoc Tukey's test.

less dramatic relative to that previously observed for PIN1-GFP (Fig. 3.3 A), which can likely be attributed to the decreased membrane removal of PIN1-PIN3_{L2}-GFP reported in figure 5.6 and increased membrane localisation seen more generally (Fig. 5.4). PIN1-PIN3_{L2}-GFP remains on the membrane to a higher degree when treated with NAA and hyper-accumulates relative to NAA when treated with both NAA+NPA, as reported previously for PIN1-GFP (Fig 3.3 & Fig 5.7 A). Furthermore, slight but significant membrane depletion is seen under mock treatment in mature stems but PIN1-PIN3_{L2}-GFP remains on the membrane with all other treatments as reported previously (Bennett, Hines, *et al.*, 2016) (Fig. 5.7 B). In both cases, decrease in membrane allocation under mock and NPA treatment is lower than that previously observed for PIN1 (Fig. 3.3) and, unlike PIN3-GFP, PIN1-PIN3_{L2}-GFP is still visible in mature stems. These results sug-

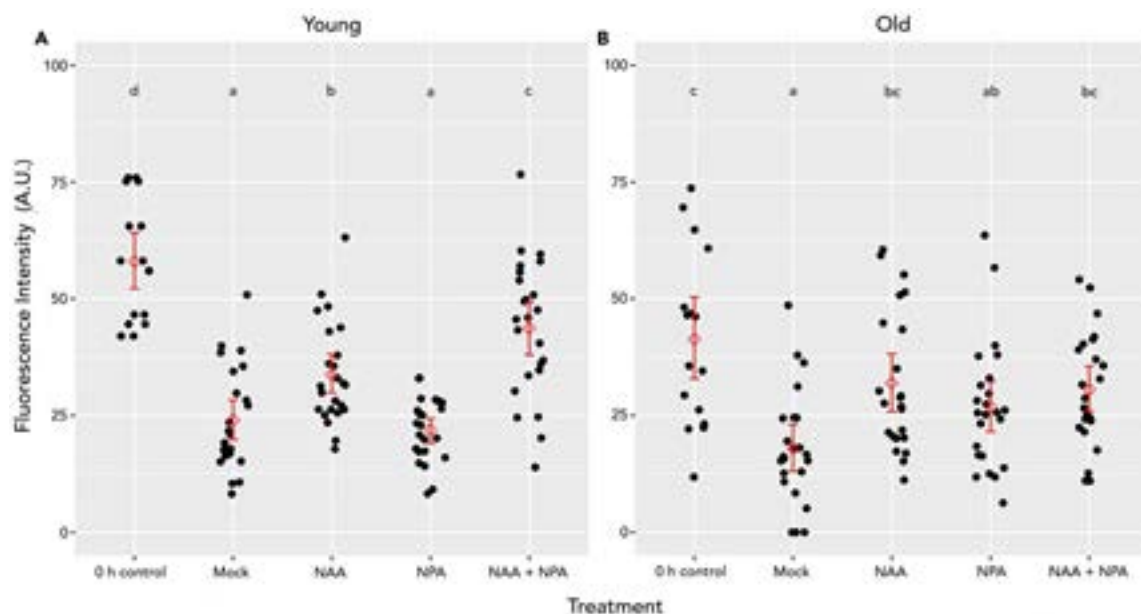


Figure 5.7 | 2 cm stem segments from the base of the primary inflorescence of young (A) or old (B) plants expressing PIN1-PIN3_{L2}-GFP in a *pin1* background, were either imaged immediately or treated apically with mock, NAA, NPA or NAA+NPA for 6 d. Stem segments were sectioned longitudinally by hand, imaged apically using a Zeiss LSM700 confocal microscope and GFP fluorescence intensity on basal plasma membranes was extracted from these images using ZEN software. This was done for at least ten membranes per stem and at least eight stems were used for each treatment and the experiment was repeated three times with compiled data from all repeats shown here. The average membrane fluorescence for each stem was calculated and is represented here as black dots, with red diamonds indicating the average of averages and red bars indicating the 95% confidence interval. Different letters indicate statistical significance following a one-way ANOVA followed by Tukey's HSD post-hoc test.

gest that exchanging the central loop region does not alter PIN1 behaviour with regard to NAA or NPA relative to PIN1-GFP, nor does it alter age-based behavioural changes reported previously in chapter 3.

Taken together, this suggests that the PIN1-PIN3_{L2}-GFP chimera exhibits increased plasma membrane localisation relative to PIN1-GFP and that it is less prone to decreases in membrane accumulation. This could be attributable to increased auxin mediated allocation or increased ability of auxin to prevent removal. However, responses to NPA and age-dependent changes in this responsiveness appears to be unchanged, suggesting the most significant effect of the central region of the HL is with regard to SL sensitivity.

5.2.3 | PIN1-PIN3_{L2}-GFP expression effectively rescues key *pin1* phenotypes

Having established that PIN1-PIN3_{L2}-GFP is not sensitive to SL-induced plasma membrane depletion, I wanted to study the effects of replacing PIN1 with SL insensitive chimeric PIN1 on shoot development. The *pin1-613* null mutant has severe developmental defects. Plants are able to generate a rosette and form new leaves, although these are usually abnormally shaped. The inflorescence elongates vertically, is usually foreshortened and develops few nodes, with those that do develop generally lacking axillary meristems such that branches are rare. Flowering occurs only occasionally and any flowers that do form are deformed, having variable numbers of organs and often lacking stamens such that these plants are sterile (Okada *et al.*, 1991). *PIN1::PIN1-PIN3_{L2}-GFP* was expressed in a homozygous *pin1* background in order to investigate what, if any,



Figure 5.8 | Visual comparison of plants at terminal flowering. Plants were grown under long day conditions and representative examples photographed 49 days after germination.

phenotypical changes resulted from this domain swap.

Firstly, plants were grown under long day conditions and visually inspected at the end of life, with cursory investigation suggesting that this construct certainly rescues the major morphological defects of *pin1* such as forming inflorescences and generating filled siliques (Fig. 5.8).

In order to determine the extent to which *PIN1-PIN3_{L2}-GFP* is able to rescue *pin1*, I quantified the proportion of siliques which had not properly formed at terminal flowering. This was defined as being < 3 mm in length and/or not containing any seed. It is apparent that *pin1 PIN1-PIN3_{L2}-GFP* does form siliques which contain seed and is fertile (Fig. 5.9) but that this rescue is not complete. The proportion of fertile fruits produced by *pin1 PIN1-PIN3_{L2}-GFP* remains slightly, but significantly, lower than either wild type or *pin1 PIN1-GFP*.

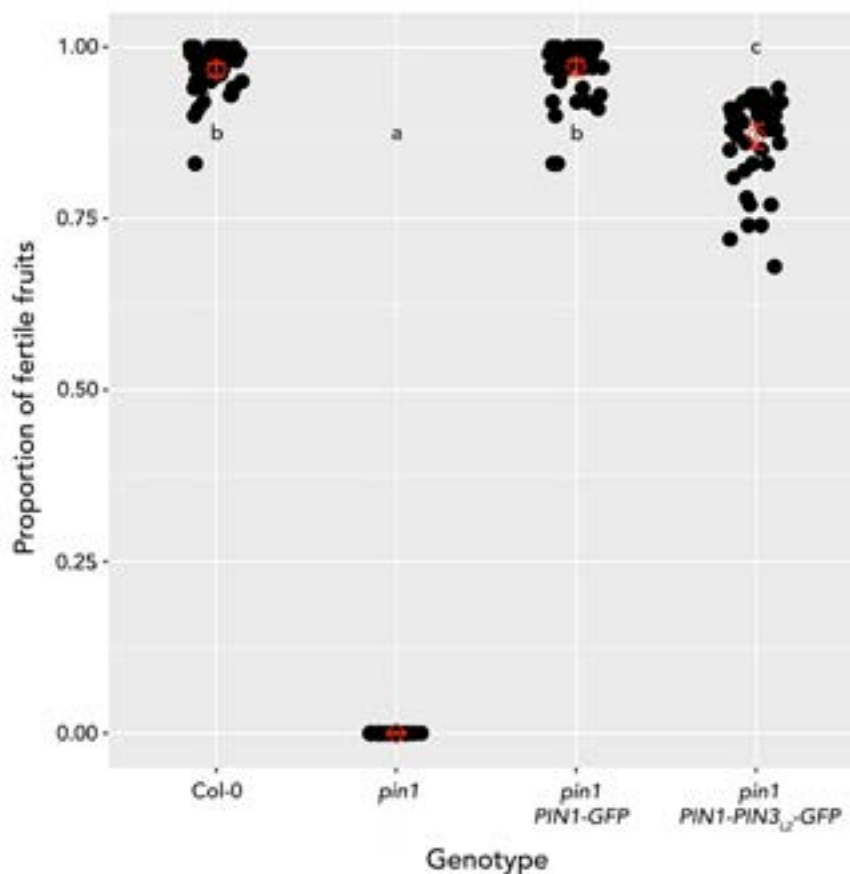


Figure 5.9 | Col-0, *pin1*, *pin1 PIN1-GFP* and *pin1 PIN1-PIN3_{L2}-GFP* plants were grown under long day conditions until terminal flowering. ~100 siliques were observed and the number which were not properly developed recorded and presented as a proportion of the total number counted. This was done for 15 plants per replicate and three independent replicates were conducted, with the compiled data plotted here (n>45). Each point represents data from an individual plant. Red diamonds represent the average for all plants and the red line indicates the 95% confidence interval. Statistical testing was performed using a one-way ANOVA followed by Tukey's honest significant difference post-hoc analysis, with significance difference displayed using compact letter display whereby a difference in letter indicates a significant difference. *pin1* does not produce siliques and was thus given value zero.

The results displayed in Fig 5.9 raised the question of whether there were any defects in floral development. Upon observation of the flowers it is apparent that this is indeed the case. As can be seen from figure 5.10 C, in some instances the pistil of *pin1 PIN1-PIN3_{L2}-GFP* flowers is elongated and protrudes from the flower before it opens, which is not observed in wild-type or *pin1 PIN1-GFP* (Fig 5.10 A, B) plants and may explain the decrease in fecundity seen in Fig. 5.9.

Mutants in *pin1* are deficient in auxin transport (Okada *et al.*, 1991). To determine whether *PIN1-PIN3_{L2}-GFP* is able to restore this and whether PIN1 SL insensitivity would impact auxin transport capacity, I conducted auxin transport assays using radiolabelled auxin. The most basal 15 mm of the primary inflorescence was excised and supplied apically with ¹⁴C-IAA for 18 hours before obtaining scintillation counts for the most basal 5 mm of stem. As displayed in figure 5.11, *pin1* transports less auxin down the stem during the experiment than wild type, with observed levels of radiolabel in

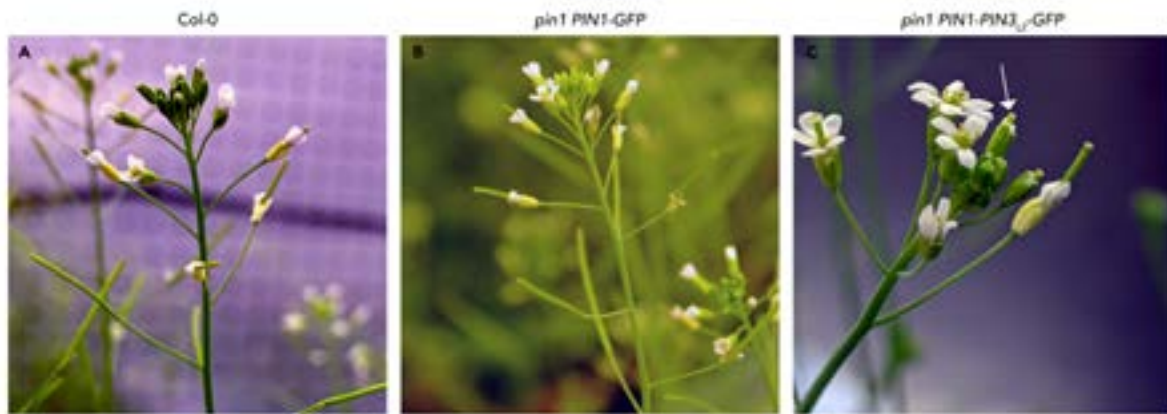


Figure 5.10 | Representative images of Col-0 (A), *pin1 PIN1-GFP* (B) and *pin1 PIN1-PIN3_{L2}-GFP* (C) flowers from ~5 weeks old, long day grown plants in various stages of opening. The white arrow indicates the protruding stigma.

the scintillant being not significantly different from background level. *PIN1-PIN3_{L2}-GFP* expression was able to completely restore auxin transport back to wild type levels. Suggesting that the ability of *PIN1-PIN3_{L2}-GFP* to export auxin from cells is equal to that of native PIN1 and that lack of PIN1 SL responsiveness does not impact bulk auxin transport. This is in contrast to strigolactone insensitive mutants which have been shown to have bulk auxin transport levels well above wild-type levels (Bennett *et al.*, 2006; Bennett, Hines, *et al.*, 2016; Van Rongen *et al.*, 2019).

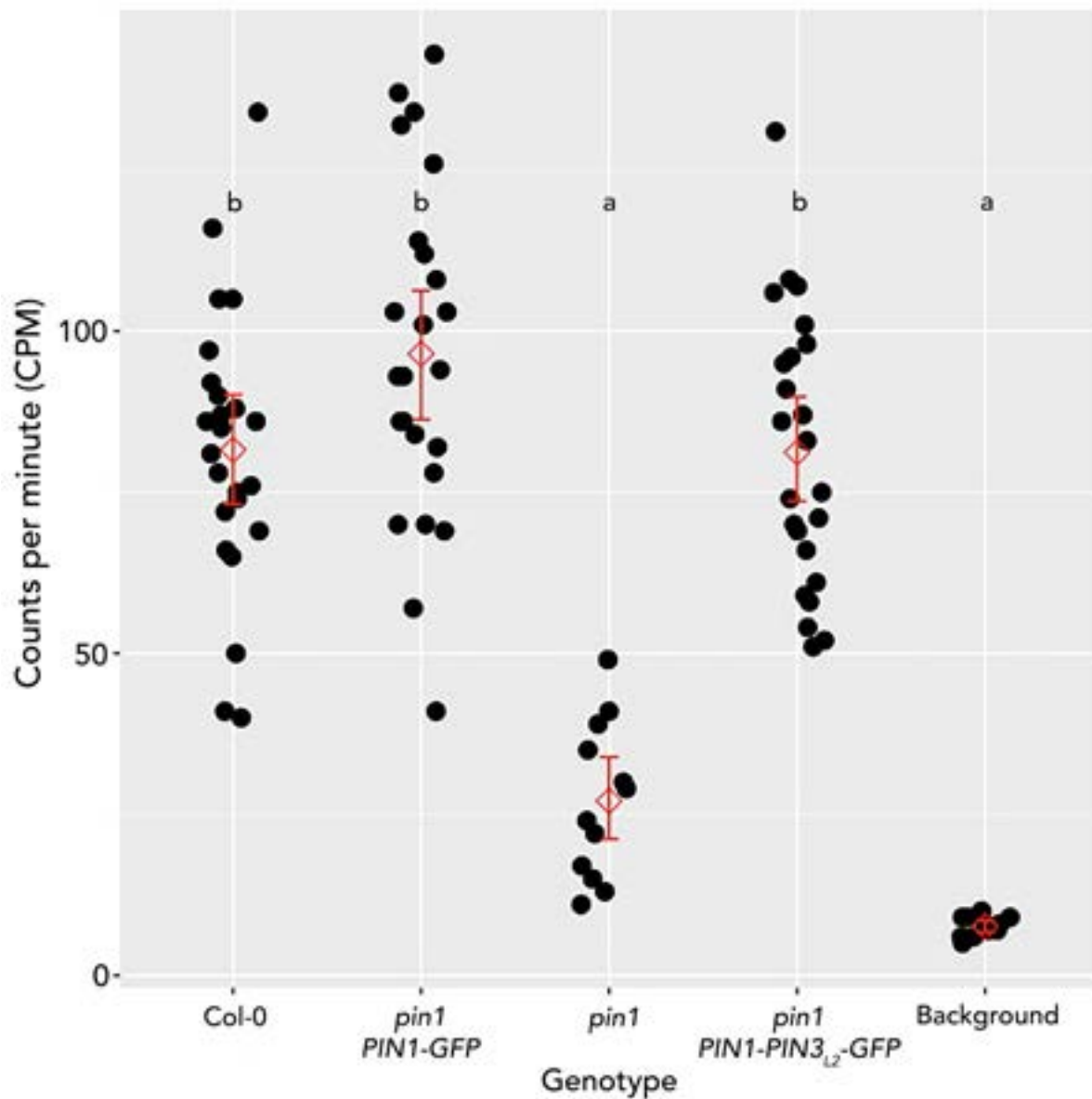


Figure 5.11 | 15 mm basal stem sections were taken from mature Col-0, *pin1* PIN1-GFP, *pin1*, *pin1* PIN1-PIN3_{L2}-GFP plants and placed with their apical ends in 1 μm ¹⁴C-IAA for 18 h. The basal 5 mm was then harvested in two 2.5 mm sections and shaken in scintillant for 4 h before being placed in a scintillation counter. This was done for 24 plants per genotype per replicate and three independent replicates conducted (n=72), with the exception of *pin1* where n=36. The data presented is representative. Each point represents data from an individual plant, red diamonds represent the average for all plants and the red line indicates the 95% confidence interval. Statistical testing was performed using a one-way ANOVA followed by Tukey's honest significant difference post-hoc analysis, with significance difference displayed using compact letter display whereby a difference in letter indicates a significant difference.

5.2.4 | *PIN1-PIN3_{L2}-GFP* expression results in subtle branching phenotypes

Visual observation of *pin1 PIN1-PIN3_{L2}-GFP* expressing plants, as shown in figure 5.8, suggested that, while the construct rescues *pin1* there are several ways in which the rescued differ from wild type, particularly with regard to height, branchiness and branch angle.

Height differences were borne out in quantitative measurements, which show that the *pin1 PIN1-PIN3_{L2}-GFP* line is consistently and significantly taller than either wild type or *pin1 PIN1-GFP* controls under long day conditions by >20 % (Fig. 5.12 A). This can also be seen under short day-long day transfer conditions, albeit not significantly (Fig. 5.12 B). This is the opposite of the reduced stature typically observed in strigolactone deficient/insensitive mutants (Bennett *et al.*, 2006; Arite *et al.*, 2009; Van Rongen *et al.*, 2019).

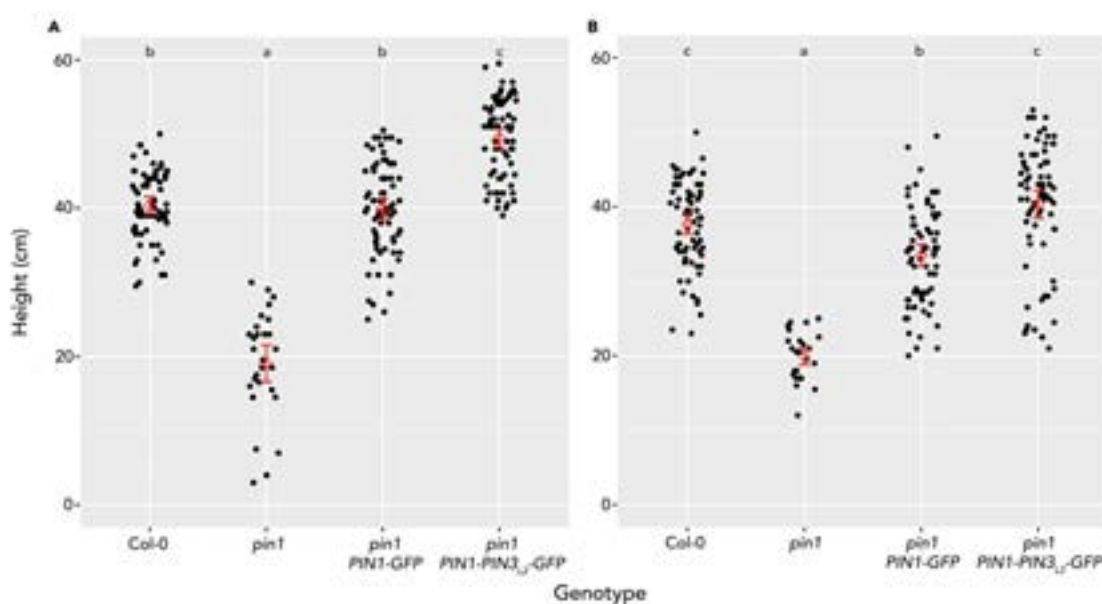


Figure 5.12 | Col-0, *pin1*, *pin1 PIN1-GFP* and *pin1 PIN1-PIN3_{L2}-GFP* plants grown under long day conditions (A) or under short day conditions for 4 weeks before transfer to long day (B) were measured at terminal flowering using a ruler. Each experiment was conducted with 24 plants per genotype and repeated three times, results from the three experiments were compiled and plotted ($n > 70$). With the exception of *pin1* where $n > 24$. Each point represents an individual plant, red diamonds represent the average height for all plants and the red line indicates the 95% confidence interval. Statistical testing was performed using a one-way ANOVA followed by Tukey's honest significant difference post-hoc analysis, with significance difference displayed using compact letter display whereby a difference in letter indicates a significant difference.

I wondered whether the increase in height observed in *pin1 PIN1-PIN3_{L2}-GFP* might be due to an increase in the number of cauline nodes produced or a change in the distance between nodes. To assess this, I measured the number of cauline nodes and the internode length of wt, *pin1 PIN1-PIN3_{L2}-GFP* and *pin1 PIN1-GFP* expressing plants at 7 weeks of age. From this, it is clear that *pin1 PIN1-PIN3_{L2}-GFP* exhibits a decreased number of cauline nodes relative to either wt or *pin1 PIN1-GFP* (Fig. 5.13, A). The distance between node 1 and node 2 (I1) was unchanged between all genotypes but I2

was significantly longer for *pin1 PIN1-PIN3_{L2}-GFP*, as was the distance between the uppermost node and the third silique (Fig. 5.13 B). This suggests that the increased height of *pin1 PIN1-PIN3_{L2}-GFP* observed in figure 5.12 is attributable to increased internode elongation as opposed to increased production of cauline nodes. *pin1 PIN1-PIN3_{L2}-GFP* also displayed a much higher likelihood of still being flowering at the time of measuring (Fig. 5.13 C), which may indicate a delay in senescence for this genotype.

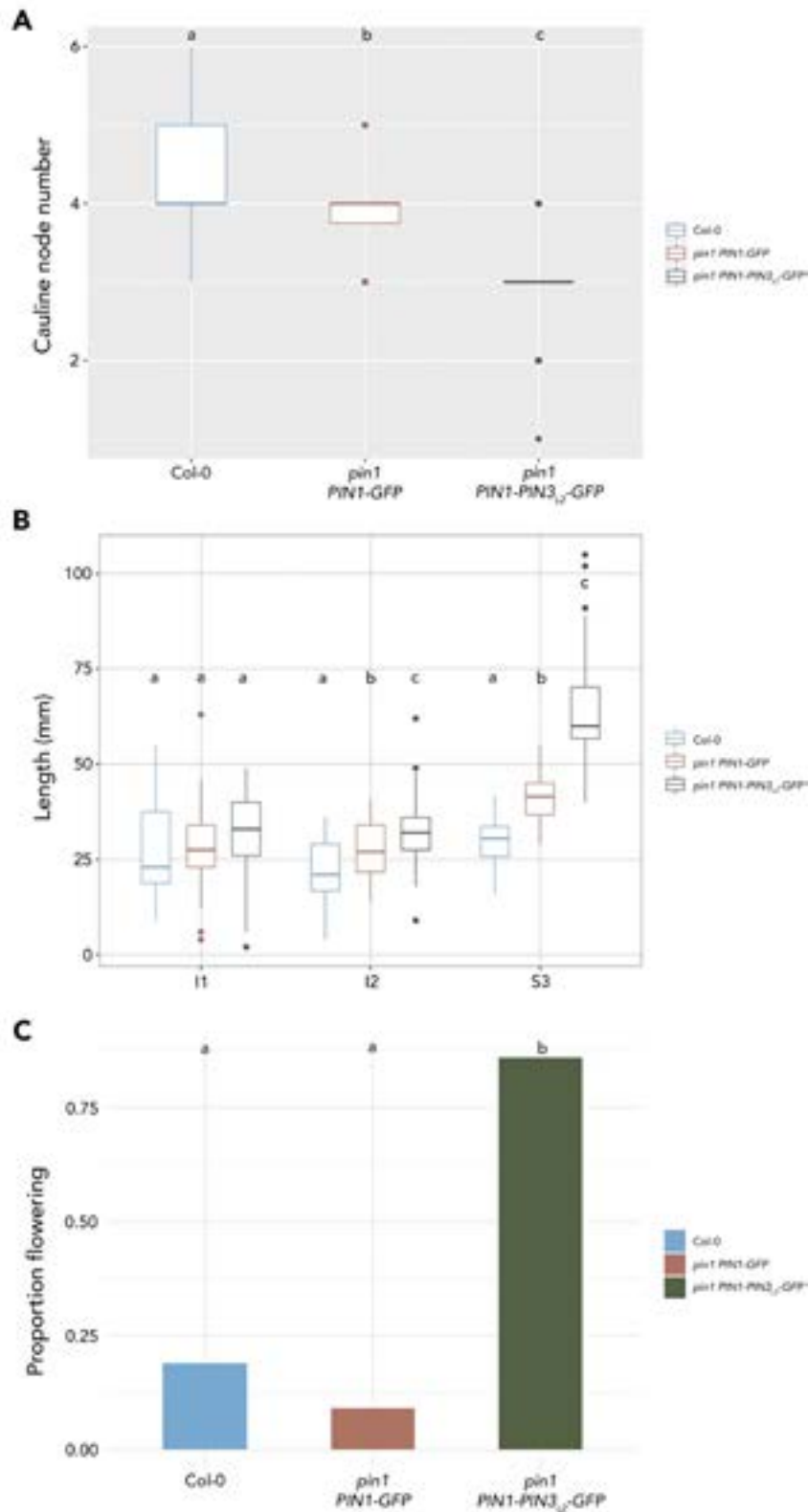


Figure 5.13 | The number of cauline nodes (A), the internode length (B) and the proportion of plants still producing flowers (C) was recorded for Col-0 (blue), *pin1 PIN1-GFP* (red) and *pin1 PIN1-PIN3_{L2}-GFP* (green) grown under long day conditions for 7 weeks. (A) Cauline nodes were defined as any points on the main stem where a leaf and/or branch emerged. (B) Distance between cauline nodes (internode length) was measured using a ruler, with I1 representing the distance between the 1st and second node, I2 the distance between the 2nd and 3rd node and S3 the distance from the top-most node to the 3rd silique, as described in Diagram 2.2. (C) Each plant was visually inspected to determine whether new flowers were being produced at the apex and expressed as a proportion of the total number of plants. 12 plants were assessed per replicate and 3 replicates conducted (n=36) Different letters represent statistically significant differences following a one-way Anova and Tukey's HSD post-hoc test.

Furthermore, measurements of branch angle demonstrate that *pin1 PIN1-PIN3_{L2}-GFP* plants have a more acute angle between the primary inflorescence and the cauline branches than wild type or *pin1 PIN1-GFP* by approximately 5° & 7° respectively (Fig. 5.14), that is to say, the branches are more upright. This phenotype is typical of SL deficient and insensitive mutants, as reported previously for *max2* & *d14*, although the difference was much greater for these mutants (Bennett, Liang, *et al.*, 2016; Van Rongen

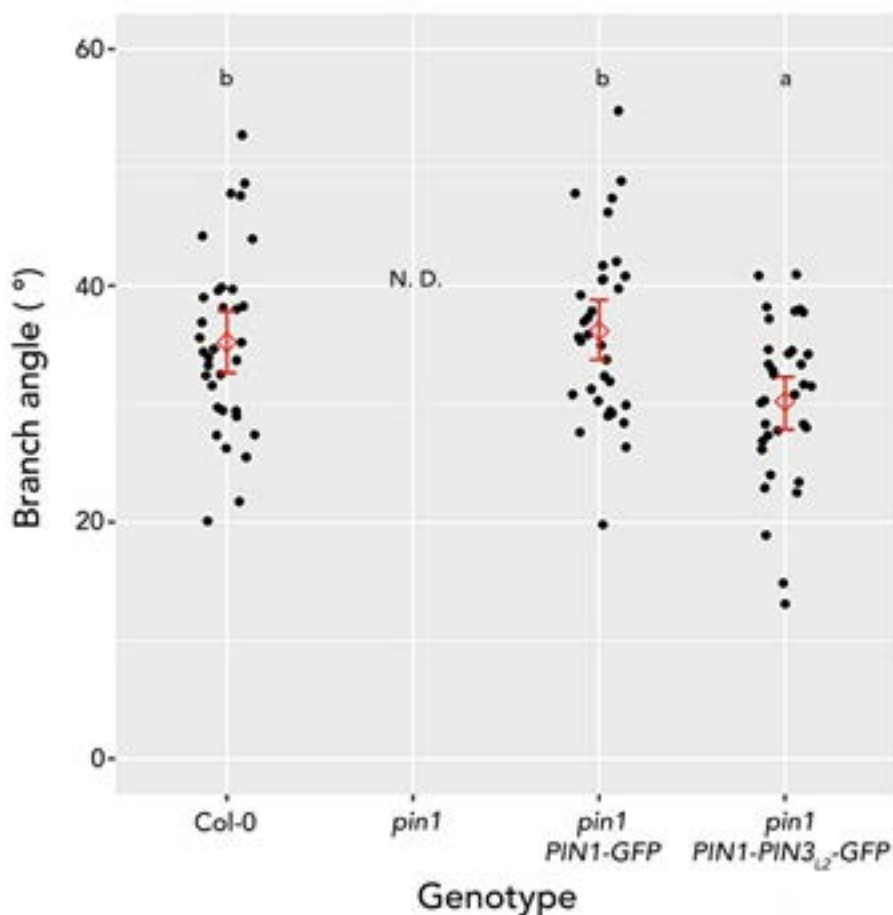


Figure 5.14 | The branch angle of Col-0, *pin1*, *pin1 PIN1-GFP* and *pin1 PIN1-PIN3_{L2}-GFP* was calculated from images taken of the junction between the most basal two cauline branches and the primary inflorescence of long day grown plants. Using ImageJ software's angle measuring tool, the average angle of these two branches was calculated for each plant and this was done for 10 plants per replicate with three replicates being performed. The compiled data from all replicates is dis-

played here ($n > 30$). Each point represents an individual plant, red diamonds represent the average height for all plants and the red line indicates the 95% confidence interval. Statistical testing was performed using a one-way ANOVA followed by Tukey's honest significant difference post-hoc analysis, with significance difference displayed using compact letter display whereby a difference in letter indicates a significant difference. No data was gathered for *pin1* as it did not reliably produce cauline branches.

et al., 2019).

I also investigated whether there was any measurable difference in the number of branches produced by *pin1 PIN1-PIN3_{L2}-GFP* expressing plants, quantifying the number of primary cauline, rosette and secondary cauline branches produced at terminal flowering in long day grown plants. Cauline branches were defined as those emerging from the axils of cauline leaves on the main inflorescence and longer than 1 cm, whilst ro-

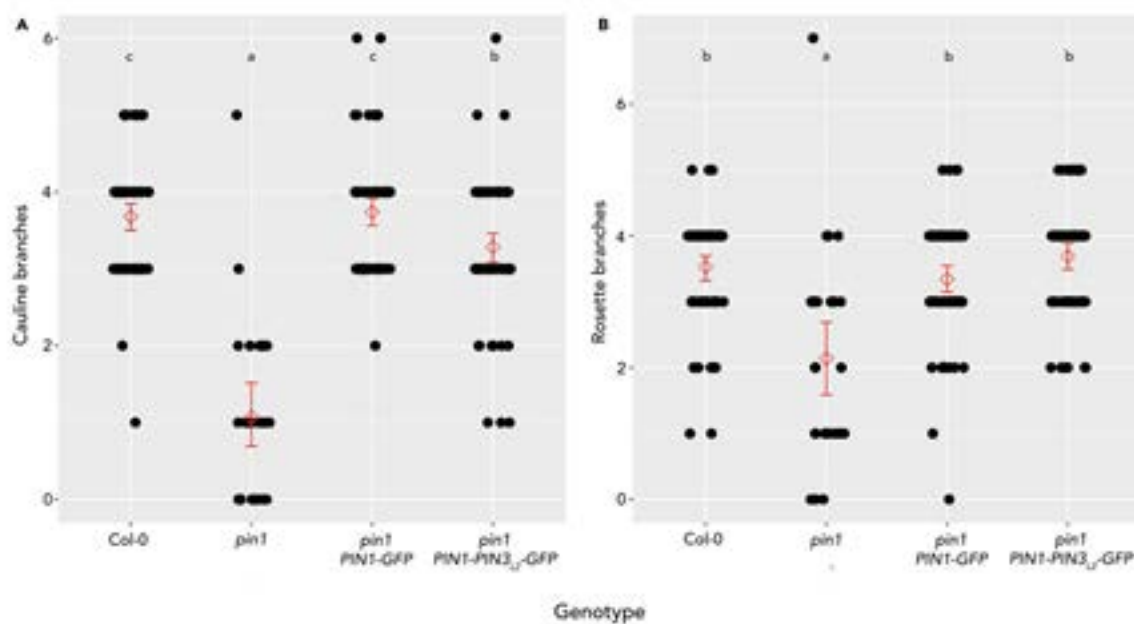


Figure 5.15 | Col-0, *pin1*, *pin1 PIN1-GFP* and *pin1 PIN1-PIN3_{L2}-GFP* plants were grown to terminal flowering (6-8 weeks) under long day conditions and the number of primary cauline branches (A) and rosette branches (B) counted. Each experiment was conducted with 24 plants per genotype and repeated three times ($n > 70$), results from the three experiments were compiled and plotted. With the exception of *pin1* where $n > 29$. Each point represents an individual plant, the red diamond represents the average height for all plants and the red line indicates the 95% confidence interval. Statistical testing was performed using a one-way ANOVA followed by Tukey's honest significant difference post-hoc analysis, with significance difference displayed using compact letter display whereby a difference in letter indicates a significant difference.

sette branches were defined as those emerging from the rosette nodes longer than 1 cm.

This data suggests that there are significantly fewer primary cauline branches (Fig. 5.15 A) and slightly more rosette branches (Fig. 5.15 B) produced by *pin1 PIN1-PIN3_{L2}-GFP* compared to wild type or *pin1 PIN1-GFP*. However, it is clear that *PIN1-PIN3_{L2}-GFP* expression effectively rescues the branching phenotype of *pin1*. In order to assess whether there was any difference in the overall degree of branching and to ameliorate

any potential mischaracterisation of cauline and rosette branches, I also plotted the total number of branches counted (Fig. 5.16). These data indicate that there is no significant difference in the degree of total branching exhibited by *pin1 PIN1-PIN3_{L2}-GFP* relative to wild type or *pin1 PIN1-GFP* but that *pin1* is effectively rescued.

The number of secondary cauline branches, defined here as those emerging from the primary cauline branches, exhibits a slight but significant increase in plants expressing *pin1 PIN1-PIN3_{L2}-GFP* relative to the wt but not *pin1 PIN1-GFP* (Fig. 5.17). This indicates that the branching phenotype of this line is subtle and may require a more sensitive assays to detect.

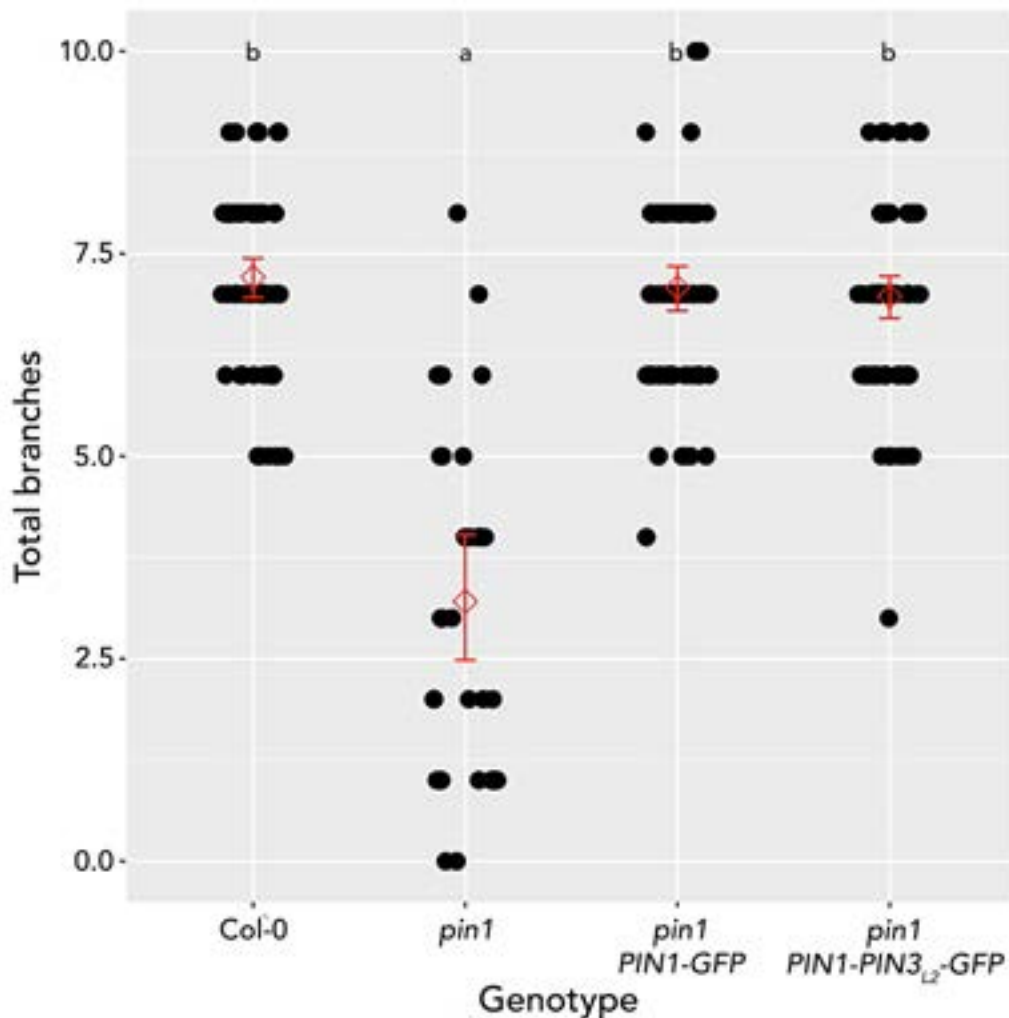


Figure 5.16 | Col-0, *pin1*, *pin1 PIN1-GFP* and *pin1 PIN1-PIN3_{L2}-GFP* plants were grown to terminal flowering (6-8 weeks) under long day conditions and the number of branches counted including those emerging directly from the primary inflorescence (cauline) and those emerging from the base (rosette). Each experiment was conducted with 24 plants per genotype and repeated three times ($n > 70$), results from the three experiments were compiled and plotted. With the exception of *pin1* where $n > 29$. Each point represents an individual plant, red diamonds represent the average for all plants and the red line indicates the 95% confidence interval. Statistical testing was performed using a one-way ANOVA followed by Tukey's honest significant difference post-hoc analysis, with significance difference displayed using compact letter display whereby a difference in letter indicates a significant difference.

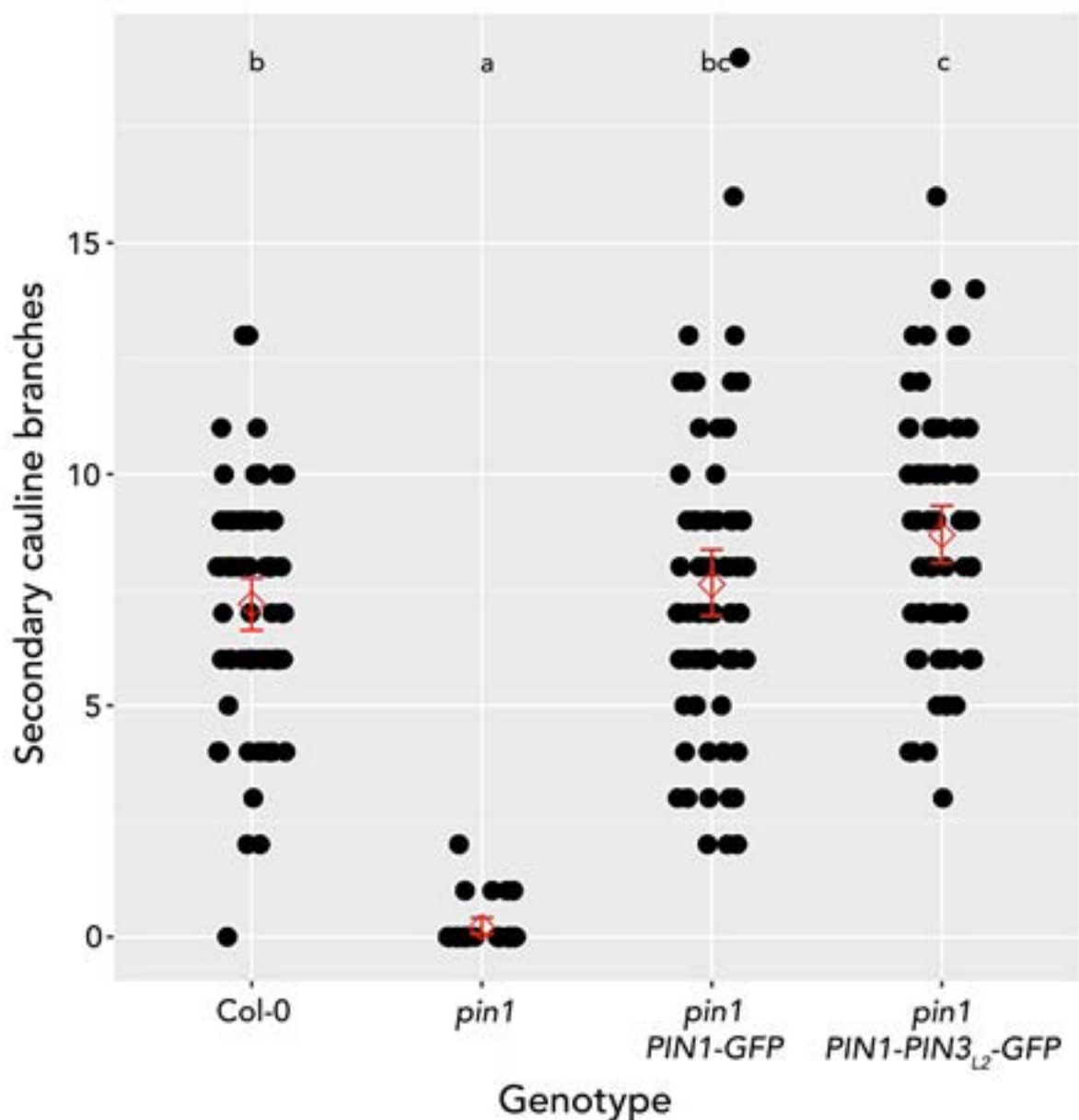


Figure 5.17 | Col-0, *pin1*, *pin1 PIN1-GFP* and *pin1 PIN1-PIN3_{L2}-GFP* plants were grown to terminal flowering (6-8 weeks) under long day conditions and the number of branches emerging from the primary cauline branches counted. Each experiment was conducted with 24 plants per genotype and repeated three times ($n > 70$), results from the three experiments were compiled and plotted. With the exception of *pin1* where $n > 29$. Each point represents an individual plant, red diamonds represent the average for all plants and the red line indicates the 95% confidence interval. Statistical testing was performed using a one-way ANOVA followed by Tukey's honest significant difference post-hoc analysis, with significance difference displayed using compact letter display whereby a difference in letter indicates a significant difference.

By growing plants initially under short day conditions before transfer to long day conditions, floral transition is delayed. The number of cauline & rosette leaves, and hence the number of cauline & rosette nodes increases considerably, allowing more subtle branching phenotypes to be detected. Using this method, the number of primary cauline branches (Fig. 5.18 A) and rosette branches (Fig. 5.18 B) in *pin1 PIN1-PIN3_{L2}-GFP* is significantly increased relative to wild type and *pin1 PIN1-GFP*. Unsurprisingly,

this difference is even clearer when total branches are plotted (Fig. 5.19), which could suggest that SL insensitivity of PIN1 results in increased axillary meristem activation relative to wild type. Furthermore, the increased secondary cauline branching of *pin1 PIN1-PIN3_{L2}-GFP* seen under long day conditions (Fig 5.17) is also observed under these conditions and is even clearer here (Fig. 5.20). Although this may be a factor of the presence of more cauline branches in *pin1 PIN1-PIN3_{L2}-GFP*.

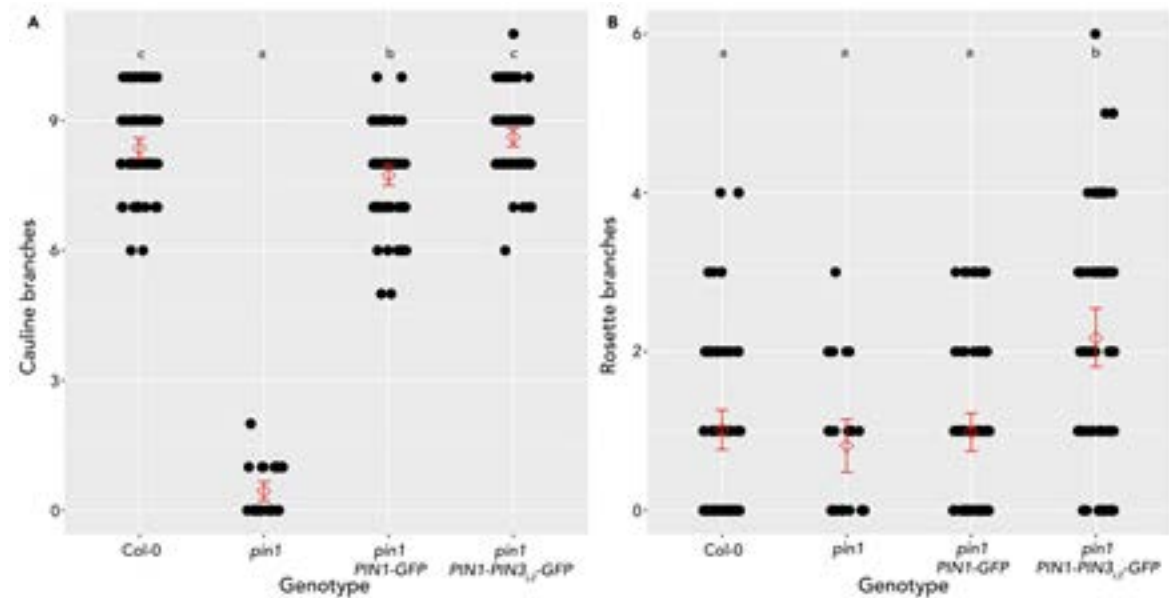


Figure 5.18 | Col-0, *pin1*, *pin1 PIN1-GFP* and *pin1 PIN1-PIN3_{L2}-GFP* plants were grown under short day conditions for 4 weeks before transfer to long day conditions until terminal flowering when primary cauline branches (A) and rosette branches (B) were counted. Each experiment was conducted with 24 plants per genotype and repeated three times ($n > 70$), results from the three experiments were compiled and plotted. With the exception of *pin1* where $n > 29$. Each point represents data from an individual plant, red diamonds represent the average for all plants and the red line indicates the 95% confidence interval. Statistical testing was performed using a one-way ANOVA followed by Tukey's honest significant difference post-hoc analysis, with significance difference displayed using compact letter display whereby a difference in letter indicates a significant difference.

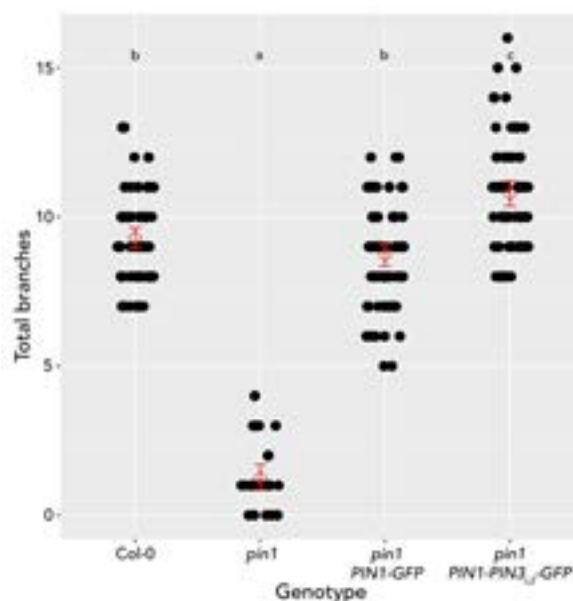


Figure 5.19 | *Col-0*, *pin1*, *pin1 PIN1-GFP* and *pin1 PIN1-PIN3_{L2}-GFP* plants were grown under short day conditions for 4 weeks before transfer to long day conditions until terminal flowering and the total number of primary cauline and rosette branches counted. Each experiment was conducted with 24 plants per genotype and repeated three times ($n > 70$), results from the three experiments were compiled and plotted. With the exception of *pin1* where $n > 29$. Each point represents data from an individual plant, the red diamonds represent the average for all plants and the red line indicates the 95% confidence interval. Statistical testing was performed using a one-way ANOVA followed by Tukey's honest significant difference post-hoc analysis, with significance difference displayed using compact letter display whereby a difference in letter indicates a significant difference.

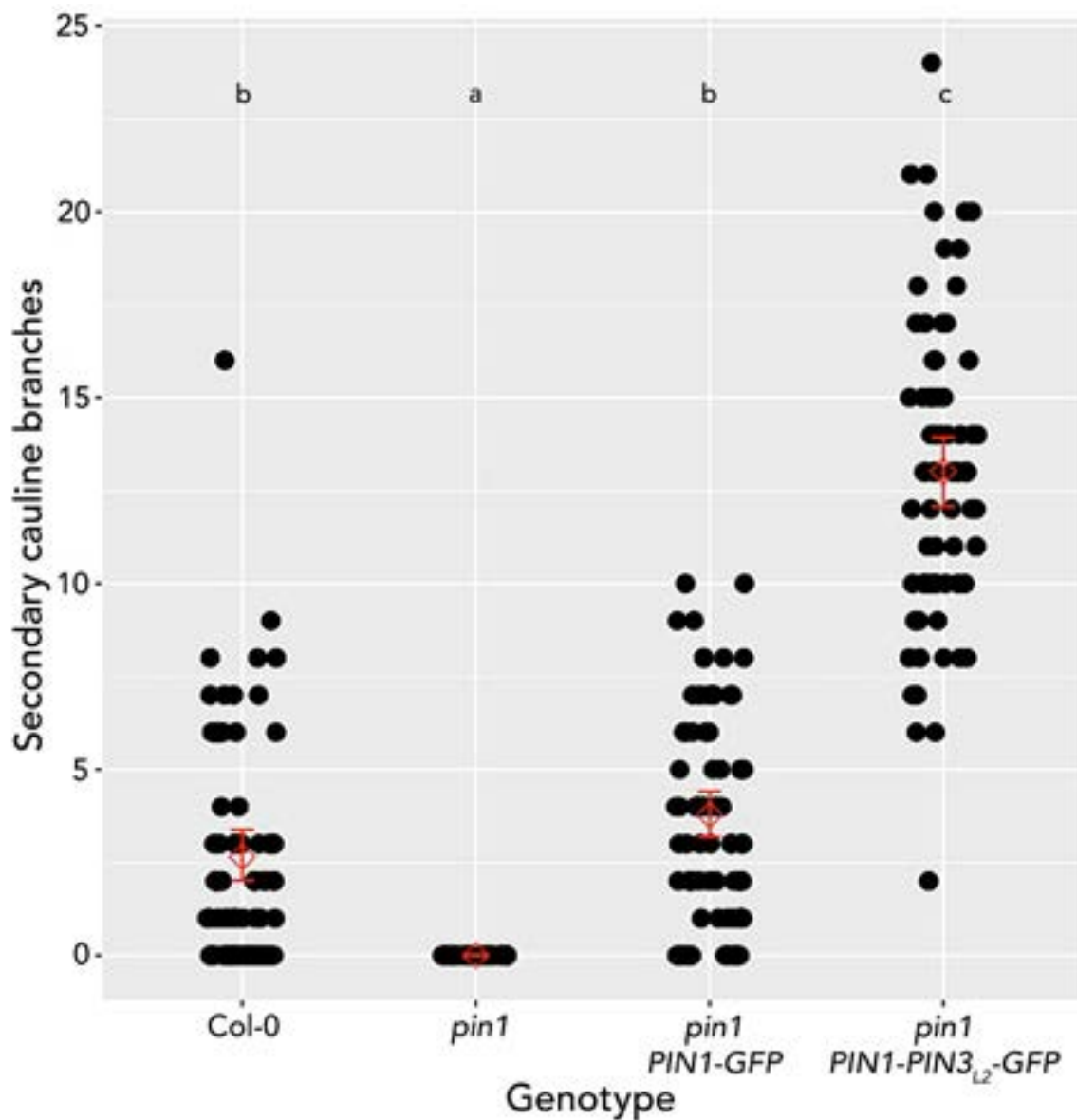


Figure 5.20 | *Col-0*, *pin1*, *pin1 PIN1-GFP* and *pin1 PIN1-PIN3_{L2}-GFP* plants were grown under short day conditions for 4 weeks before transfer to long day conditions until terminal flowering and the total number of secondary cauline branches counted. Each experiment was conducted with 24 plants per genotype and repeated three times ($n > 70$), results from the three experiments were compiled and plotted. With the exception of *pin1* where $n > 29$. Each point represents data from an individual plant, the red diamond represents the average for all plants and the red line indicates the 95% confidence interval. Statistical testing was performed using a one-way ANOVA followed by Tukey's honest significant difference post-hoc analysis, with significance difference displayed using compact letter display whereby a difference in letter indicates a significant difference.

Growth under the same short day-long day transfer conditions combined with removal of the primary inflorescence at 10 cm tall results in increased rosette bud activation for all lines assayed (Fig. 5.21). There is a clear increase in rosette branching of *pin1 PIN1-PIN3_{L2}-GFP* relative to wild type and *pin1 PIN1-GFP* under these conditions (Fig. 5.21).

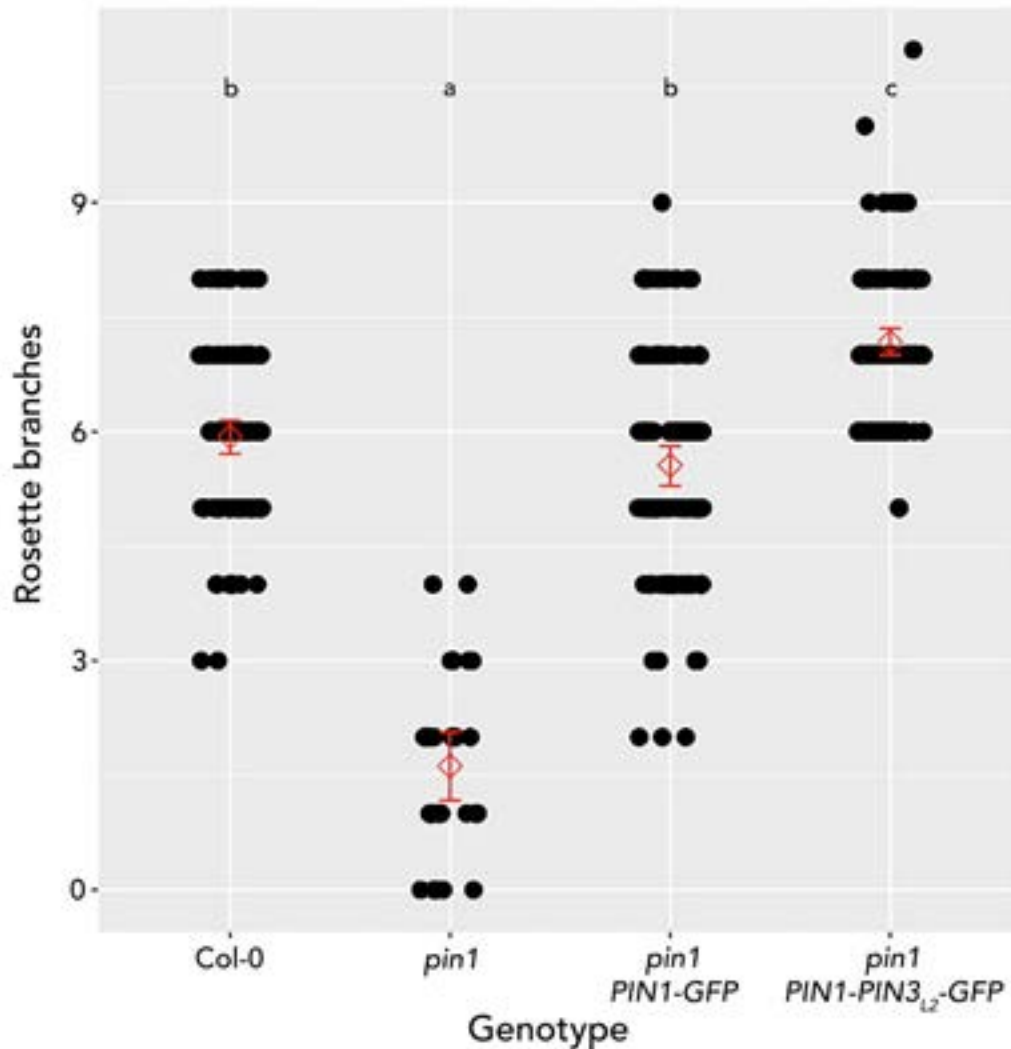


Figure 5.21 | *Col-0*, *pin1*, *pin1 PIN1-GFP* and *pin1 PIN1-PIN3_{L2}-GFP* plants were grown under short day conditions for 4 weeks before transfer to long day conditions and decapitation at 10 cm. The total number of rosette branches was counted 10 days after decapitation. Each experiment was conducted with 24 plants per genotype and repeated three times ($n > 70$), results from the three experiments were compiled and plotted. With the exception of *pin1* where $n > 24$. Each point represents data from an individual plant, the red diamonds represent the average for all plants and the red line indicates the 95% confidence interval. Statistical testing was performed using a one way ANOVA followed by Tukey's honest significant difference post-hoc analysis, with significance difference displayed using compact letter display whereby a difference in letter indicates a significant difference.

Taken together, these data demonstrate that expression of *PIN1-PIN3_{L2}-GFP* results in significant but slight changes in the overall shoot system architecture of *Arabidopsis*, growing taller, producing more branches and orienting these branches closer to the main stem.

5.2.5 | PIN1 SL insensitivity phenocopies other *max* mutant phenotypes

The phenotypes described in section 5.2.4 bear resemblance to those previously observed in *max* mutants with regard to branching and branch angle (Stirnberg, van de Sande and Leyser, 2002; Sorefan *et al.*, 2003; Booker *et al.*, 2004, 2005; Bennett *et al.*, 2006). Given the demonstrated SL insensitivity of *PIN1-PIN3_{L2}-GFP*, I investigated whether PIN1 SL insensitivity results in similar phenotypes to those observed in SL perception and synthesis mutants.

Firstly, I investigated leaf shape. In SL mutants, leaves are shorter but not wider than wild type leaves. In line with this, there was no clear difference between the leaf width of *pin1 PIN1-PIN3_{L2}-GFP* and *pin1 PIN1-GFP* although both were increased relative to wt (Fig. 5.22 A). There is some suggestion that leaf length is slightly reduced relative to wild type and *pin1 PIN1-GFP*, analogous to SL mutants, but this difference is not significant from wt (Fig. 5.22 B). When the ratio of width to length is calculated for each individual leaf and this value plotted in figure 5.22 C, *pin1 PIN1-PIN3_{L2}-GFP* exhibits a higher value than the very consistent values of wild type and *pin1 PIN1-GFP*, in line with data reported for example, for *max1* and *max2* leaves (Stirnberg, van de Sande and Leyser, 2002). This indicates that, while there are limited changes in width or length, on an individual plant basis, *PIN1-PIN3_{L2}-GFP* expression results in a subtle *max*-like leaf shape phenotype.

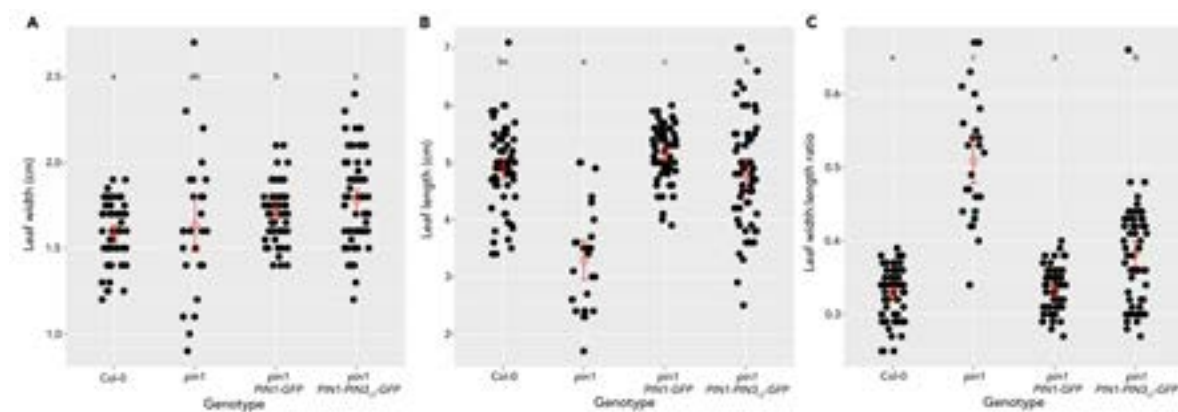


Figure 5.22 | *Col-0*, *pin1*, *pin1 PIN1-GFP* and *pin1 PIN1-PIN3_{L2}-GFP* plants were grown under long day conditions and leaf width and length measured after 35 days. The leaf width (A) was measured at its' widest point and length (B) at its longest point. For each plant, width was divided by length to give a ratio (C). Each experiment was conducted with 20 plants per genotype and repeated three times (n=60), results from the three experiments were compiled and plotted. With the exception of *pin1* where n>24. Each point represents data from an individual plant, red diamonds represent the average for all plants and the red line indicates the 95% confidence interval. Statistical testing was performed using a one way ANOVA followed by Tukey's honest significant difference post-hoc analysis, with significance difference displayed using compact letter display whereby a difference in letter indicates a significant difference.

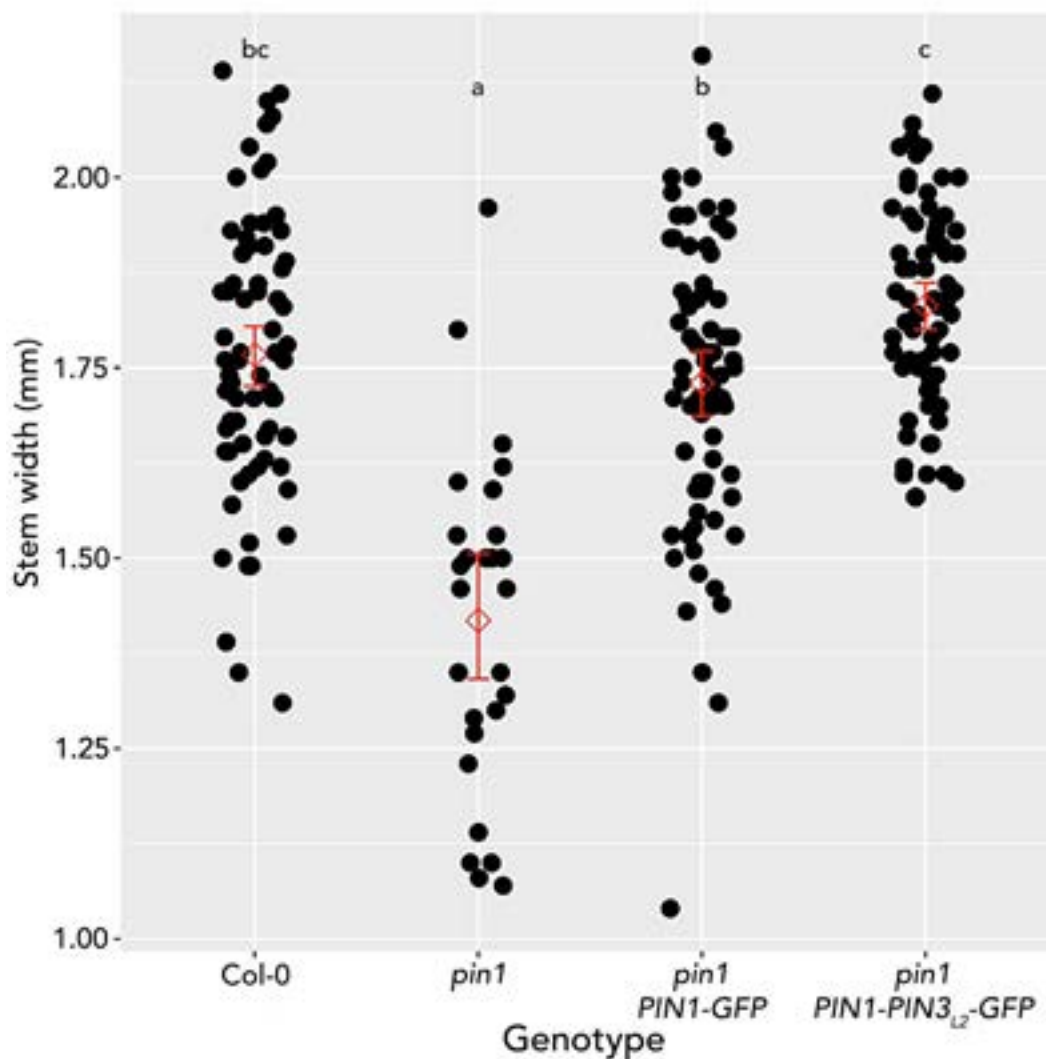


Figure 5.23 | Col-0, *pin1*, *pin1 PIN1-GFP* and *pin1 PIN1-PIN3_{L2}-GFP* plants were grown under long day conditions and stem width measured at the base of the primary inflorescence at terminal flowering. Each experiment was conducted with 10 plants per genotype and repeated three times (n=34), results from the three experiments were compiled and plotted. Each point represents data from an individual plant, red diamonds represent the average for all plants and the red line indicates the 95% confidence interval. Statistical analysis was performed using a one-way ANOVA followed by Tukey's honest significant difference post-hoc analysis, with significance difference displayed using compact letter display whereby a difference in letter indicates a significant difference.

Stem width is also affected, with *PIN1-PIN3_{L2}-GFP* expression able to rescue the reduced stem width observed in *pin1* mutants and even increase stem width relative to *pin1 PIN1-GFP* and wt, albeit not significantly in the latter case (Fig. 5.23). This is the opposite of what is observed in *max2* and *d14* mutants, where stem thickness is reduced (Bennett *et al.*, 2006; Van Rongen *et al.*, 2019). In order to investigate whether PIN1 SL insensitivity had any impact on tissue organisation, I sectioned stems transversely and stained with toluidine blue. Interfascicular cambium derived tissue is typically reduced in *max* mutants due to reduced cambium activity (Agusti *et al.*, 2011), which appears evident here (Fig. 5.24, B). There was no observable difference between Col-0 and *pin1 PIN1-PIN3_{L2}-GFP*, with vascular bundle number, structure, and spacing appearing unchanged (Fig. 5.24).

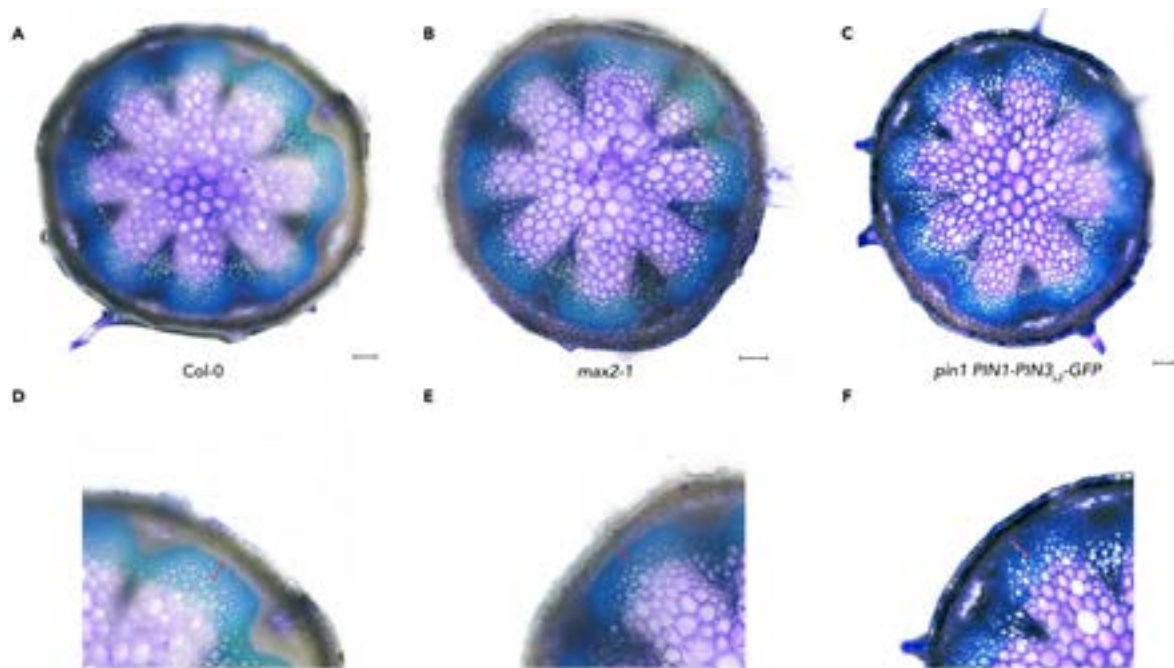


Figure 5.24 | Representative images of mature Col-0 (A, D), *max2-1* (B,E) and *pin1 PIN1-PIN3_{L2}-GFP* (C,F) stems were sectioned by hand and stained with toluidine blue before imaged on a Keyence 7000 light microscope system. 5 stems were analysed per genotype. Scale bar represents 100 μ m and red bars in panels D,E, F indicate the interfascicular cambium derived tissue.

From these data it can be concluded that, replacing the central region of PIN1 HL with that of PIN3 has a number of morphological impacts, many of which are analogous to those observed in SL biosynthesis or response mutants, such as branch number, branch angle and leaf shape. However, there are a number of ways in which *pin1 PIN1-PIN3_{L2}-GFP* differs, and indeed has the opposite phenotype to *max* mutants, such as increased height and stem width. This is correlated with chimera SL insensitivity, although it is possible that the domain swap conducted had other effects which were not detected here.

5.2.6 | PIN1 SL sensitivity is not required for SL to enhance bud-bud competition

One of the effects of strigolactone is to enhance the competition between buds (Crawford *et al.*, 2010; Van Rongen *et al.*, 2019). This can be assessed using an assay in which stem segments carrying 2 cauline nodes are excised, and the growth of their associated buds tracked over time. While typically both buds begin to elongate, in wild-type plants, it is often the case that only one bud establishes rapid growth, with the other re-entering dormancy. In SL mutants, both buds almost always activate fully. Basal supply of strigolactone typically increases the proportion of explants with only 1 active bud in wild-type and SL deficient plants, whereas SL response mutants are resistant to this effect. I reasoned that, since PIN1-PIN3_{L2}-GFP is unresponsive to SL, bud-bud competition and its response to SL to enhance it could be reduced or eliminated. To test this, I conducted 2-node assays on decapitated explants over 10 days, with or without basal GR24 supply and assessed the growth dynamics of wt and *pin1 PIN1-PIN3_{L2}-GFP* buds.

These data are displayed as bud growth traces in figure 5.25, with the length of both top and bottom bud plotted over the course of 10 days. I also calculated the relative growth rate (RGI) by dividing the length of the longest bud by the combined length of both buds for each explant (Fig. 5.26). If the RGI is closer to 0.5 that indicates both buds grow and if it's closer to 1, that one bud wins. From these it can be concluded that, in wild-type explants, there are a mixture of behaviours, with both buds growing out in some instances or one bud winning (Fig. 5.25 A, B), reinforced by the intermediate RGI of 0.73 (Fig. 5.26). In this case, GR24 treatment results in less overall growth for the winning bud relative to mock treatment and has little effect on RGI (Fig. 5.25 E, F & 5.26). For *pin1 PIN1-PIN3_{L2}-GFP* plants, bud-bud competition was less strong in mock-treated explants (Fig. 5.25 C, D), as reflected by the significantly lower RGI relative to wt (Fig. 5.26). Figure 5.25 G & H shows that SL treatment resulted in similar behaviour of *pin1 PIN1-PIN3_{L2}-GFP* to wild-type, with the top bud tending to win. However, *pin1 PIN1-PIN3_{L2}-GFP* treatment with SL results in significantly increased RGI, back to levels observed in wt (Fig 5.26) and the winning bud tends to grow more than seen in the wild-type controls (Fig. 5.25 G, H).

There is some indication of a shift in bud activation time, from day 5-6 in Col-0 plants to day 4-5 in *pin1 PIN1-PIN3_{L2}-GFP* expressing plants under mock treatment (Fig 5.25 A, B, C, D). Whilst fewer buds activate and those that do activate do so later in both Col-0 and *pin1 PIN1-PIN3_{L2}-GFP* lines treated with GR24 relative to mock (Fig. 5.25 E, F, G, H), *pin1 PIN1-PIN3_{L2}-GFP* buds still seem to activate slightly earlier. There also appears to be an increase in the total number of buds activating across all repeats for *pin1 PIN1-PIN3_{L2}-GFP*.

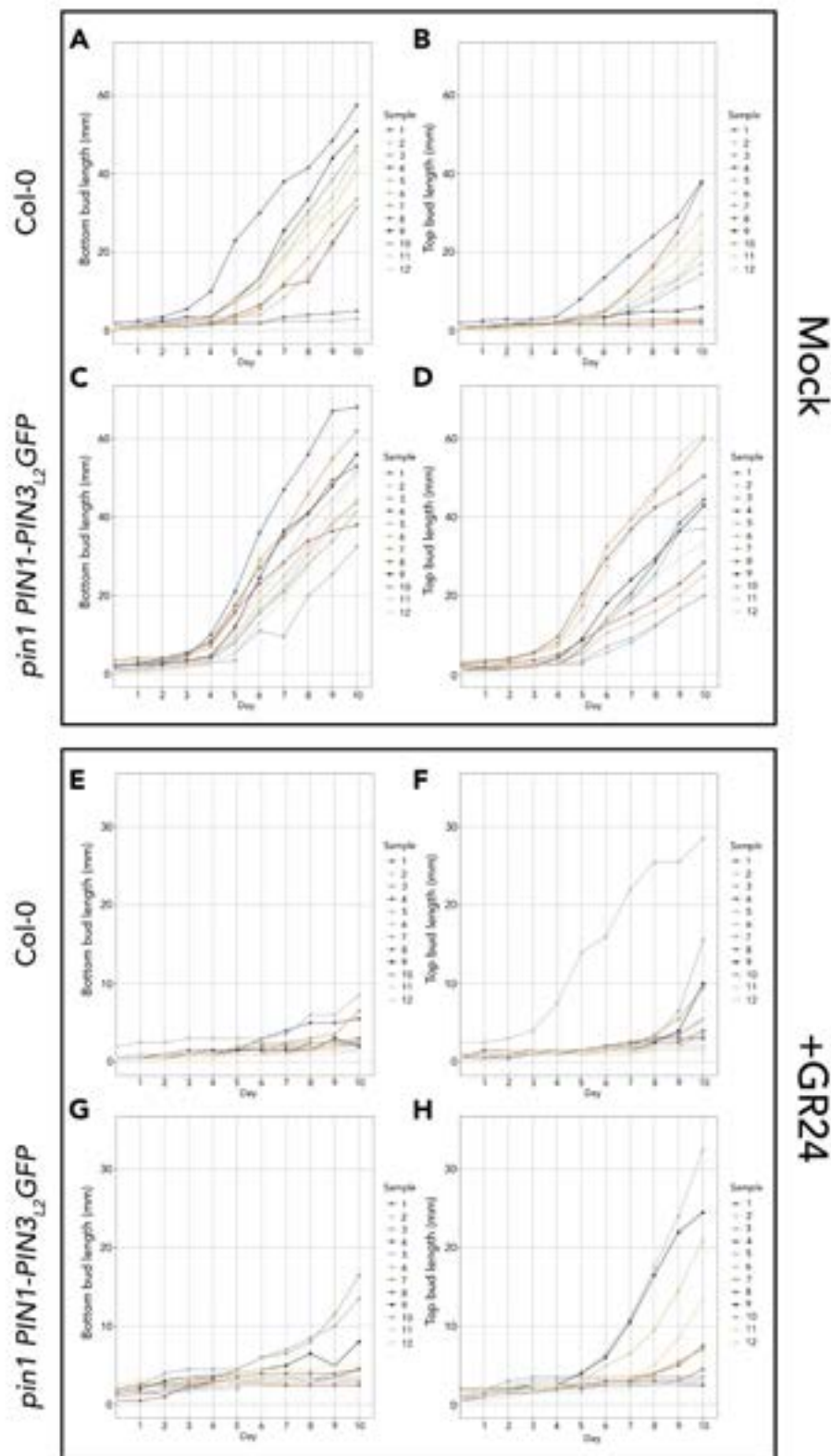


Figure 5.25 | Growth dynamics of bottom (A, C, E, G) and top (B, D, F, H) buds in a 2-node set-up, treated basally without (A, B, C, D) and with GR24 (E, F, G, H). Primary inflorescences of Col-0 and *pin1 PIN1-PIN3_{L2}-GFP* were excised at 2-5 mm tall and the apical meristem removed to leave a stem bearing two buds. These were placed in 1.5 ml Eppendorf tubes filled with liquid ATS media supplemented with 5 μ M GR24 or mock, the length of each bud was measured daily for 10 days using a ruler. Length of each bud is plotted over time, with each sample being represented by a different colour. Twelve buds were used per treatment per genotype and the experiment repeated twice (n=24).

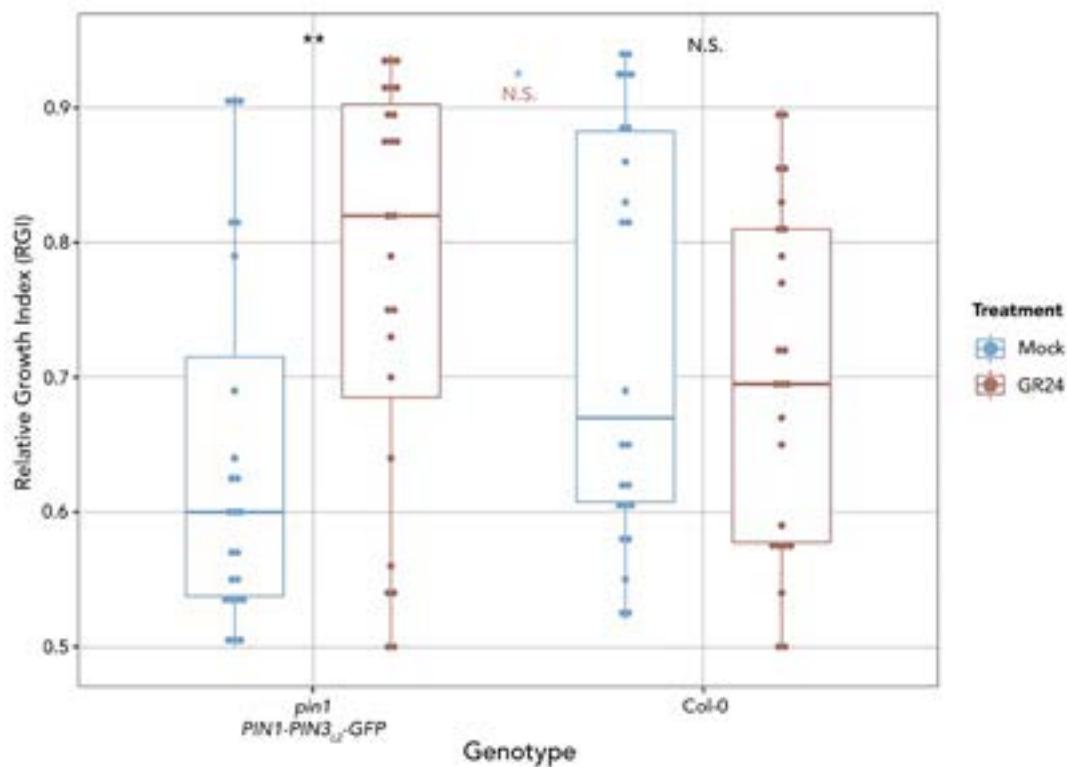


Figure 5.26 | Relative growth index (RGI) was calculated for explants of Col-0 and *pin1 PIN1-PIN3_{L2}-GFP* expressing explants grown in a 2-node setup treated basally with mock (blue) or 5 μ M GR24 (red). Primary inflorescences were excised at 2-5 mm tall and the SAM removed to leave an explant bearing two buds. These were placed in 1.5 mL Eppendorf tubes filled with liquid ATS supplemented with mock or GR24. The length of each bud was measured every 24 h over 10 days and the length on day 10 used to calculate the RGI by dividing the length of the longest bud by the combined length of both buds. 12 buds were assessed per replicate and 2 replicates conducted, with compiled data shown here. A Shapiro test was used to determine normality of distribution of data. A Student's t-test was conducted where data was found to be normally distributed & a Mann-Whitney-Wilcoxon test where distribution was non-normal in order to analyse statistical differences between treatments within each genotype and between genotypes for each treatment and indicated by symbols ** ($p < 0.01$), * ($p < 0.05$), N.S. (non-significant). Black symbols indicate tests within genotypes, blue indicates a test between genotypes treated with mock and red a test between genotypes treated with GR24.

In order to quantify these changes, I fitted a logistic model to bud growth traces and used this to extract the maximum growth rate (MGR) (mm/day) and the days taken to reach this value. Data were filtered to exclude any buds which did not reach at least 15 mm by day 10 or where the MGR had not been reached by day 10 as these were considered to have not grown. Buds were classified as winning or losing based on whether they elongated more or less than their counterpart respectively. Figure 5.27A shows that, whilst the maximum growth rate is unchanged in all cases, the number of days taken to reach MGR was decreased for *pin1 PIN1-PIN3_{L2}-GFP* under mock treatment. GR24 treatment increases the days to MGR for *pin1 PIN1-PIN3_{L2}-GFP*. Thus, it seems that the bud growth dynamics of *pin1 PIN1-PIN3_{L2}-GFP* are not changed but the activation time is brought forward. In order to investigate this further, I calculated the break-point day, i.e. the day when buds switch from slow growth to fast growth, and plotted

this in figure 5.28. From these data it is clear that *pin1 PIN1-PIN3_{L2}-GFP* both activates earlier than *col-0* under both GR24 and mock treatment and, in both genotypes, GR24 had the effect of delaying activation (Fig. 5.28 A). In general, more buds are active (defined as reaching 10 mm by day 10) for *pin1 PIN1-PIN3_{L2}-GFP* than *col-0* and this is also the case when GR24 treated (Fig 5.28 B). Since many *Col-0* buds did not grow at all when GR24 treated, this makes the data harder to interpret and indicates that a lower GR24 concentration should be used in future experiments.

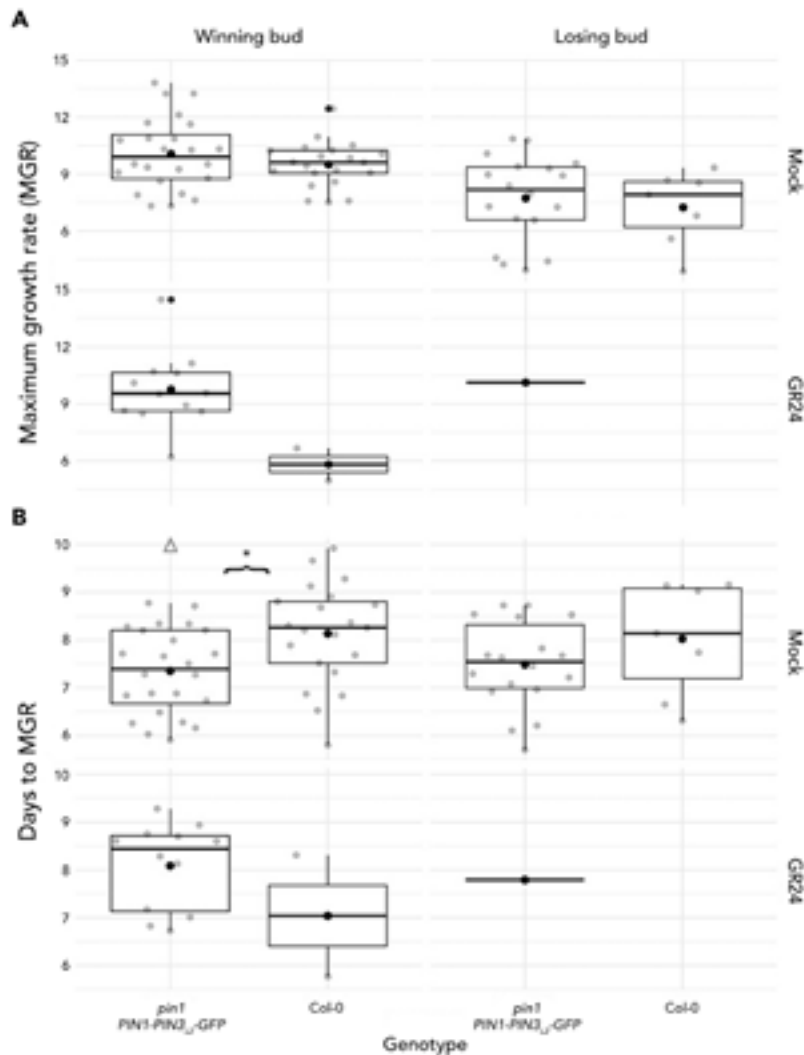


Figure 5.27 | Maximum growth rate (MGR) (A) and days taken to reach maximum growth rate (B) was calculated for winning and losing buds of both *Col-0* and *pin1 PIN1-PIN3_{L2}-GFP* plants treated with or without GR24. Explants bearing two buds were excised when 2-5 mm tall, the apex removed and were placed in 1.5 mL Eppendorf tubes filled with liquid ATS supplemented with mock or GR24. The buds were measured every 24 h for 10 days and this experiment repeated twice with twelve buds analysed per genotype per treatment per repeat (n=24). A logistic model was fitted to the bud data and from this metrics were plotted were extracted, these data were filtered to exclude any buds which did not reach at least 15 mm by day 10 or where the MGR had not been reached by day 10 and plotted as box and whisker plots. Grey dots indicate individual data points and black dots the mean. Winning and losing bud refers to which of the two buds per explant grew the most. Statistical testing was performed using a Student's t-test with statistical significance between genotypes within treatments indicated by * (p<0.05) and within genotypes but between treatments indicated by a grey triangle (p<0.05).

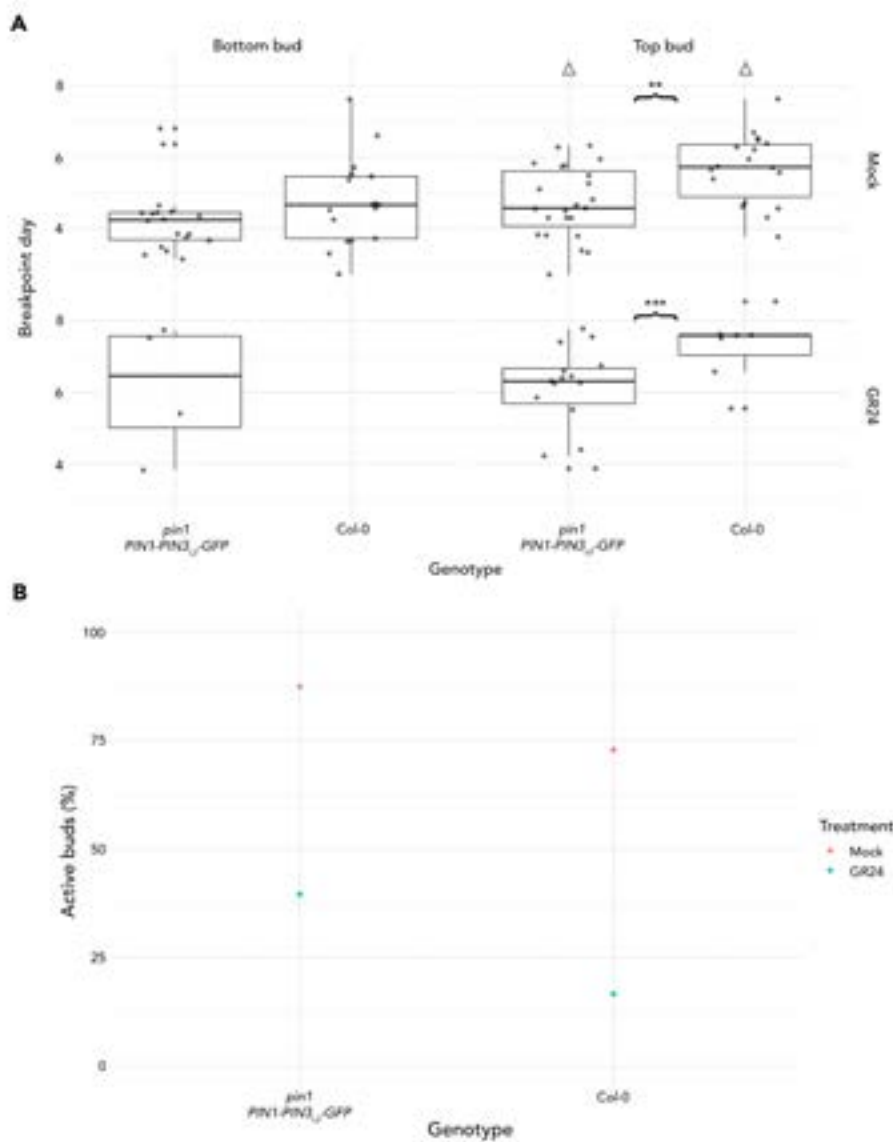


Figure 5.28 | The breakpoint day (A) and the percentage of active buds (B) was calculated for top and bottom buds of both Col-0 and *pin1 PIN1-PIN3_{L2}-GFP* plants treated with or without GR24. Explants bearing two buds were excised when 2-5 mm tall, the apex removed and were placed in 1.5 mL Eppendorf tubes filled with liquid ATS supplemented with mock or GR24. The buds were measured every 24 h for 10 days and this experiment repeated twice with twelve buds analysed per genotype per treatment per repeat (n=24). (A) Two linear regressions were fitted to individual bud traces and the intersection of these used to define the breakpoint, that is, when the bud began to grow. These data were filtered to exclude any buds which did not reach at least 10 mm by day 10 and plotted as box and whisker graphs overlaying the individual data points, represented by grey dots. Statistical testing was performed between genotypes and treatments using a Student's t-test with statistical significance between genotypes indicated by ** (p<0.01) and *** (p<0.001) while differences between treatments within genotypes are indicated by a grey triangle (p<0.001). (B) bud traces were thresholded such that they were defined as inactive if they did not exceed 10 mm by day 10, the percentage of total buds that did activate was calculated and plotted here.

Together, these data suggest that abolition of PIN1 SL responsiveness does not abolish the ability of SL to increase bud-bud competition in a 2-node system. It also reveals that SL insensitivity of PIN1 is correlated with buds activating more readily, even when SL is present.

5.3 | Discussion

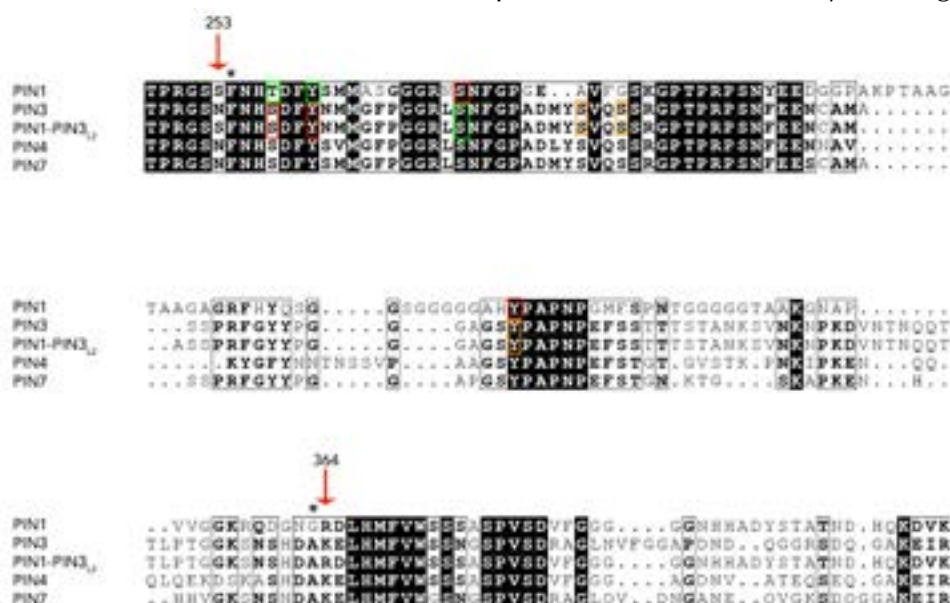
5.3.1 | The central portion of the PIN1 HL is responsible for SL sensitivity

It has been shown previously and repeated here, that PIN1 responds to strigolactone by depletion from the plasma membrane, whilst PIN3 does not (Ticchiarelli, 2019). It has also been demonstrated through swapping sections of the hydrophilic loop that, by replacing the central portion of the hydrophilic loop of PIN3 with that of PIN1 (PIN3-PIN1_{L2}-GFP), it was possible to confer SL responsiveness to PIN3 (Ticchiarelli, 2019). In order to confirm this and with the idea of producing plants where PIN1 is SL insensitive for further investigation, I elected to conduct the inverse swap. The central region of PIN1 HL was replaced with that of PIN3, tagged with GFP and placed under the control of the *PIN1* promoter (PIN1-PIN3_{L2}-GFP), as described in figure 5.1.

Following this, I assessed the ability of the chimeric protein to respond to SL and was able to demonstrate that PIN1-PIN3_{L2}-GFP does not deplete from the basal plasma membrane of cells in the xylem parenchyma in response to SL, in a manner analogous to native PIN3 (Fig. 5.2 J, K, L). In this setup, PIN1-GFP and PIN3-PIN1_{L2}-GFP were both SL responsive as reported previously (Shinohara, Taylor and Leyser, 2013; Ticchiarelli, 2019). Not only was SL unable to induce removal of PIN1-PIN3_{L2}-GFP from the membrane, it also did not affect re-allocation to the membrane after leaving triggered by auxin depletion (Figure 5.3). Furthermore, I was able to demonstrate that PIN1-PIN3_{L2}-GFP over-accumulates on both the basal and lateral membranes compared to PIN1-GFP (Fig. 5.4 & 5.5, D). PIN3 has been demonstrated to accumulate to a greater extent on the lateral membranes (Ticchiarelli, 2019), suggesting that this region may also play a role in regulating PIN3 polarity. However, when lateral membrane fluorescence intensity was expressed relative to the corresponding basal intensity, it was clear that relative lateral polarity of PIN1-PIN3_{L2}-GFP was not significantly higher than that of PIN1-GFP (Fig. 5.5 E).

As discussed in section 5.1.4, phosphosites have been characterised as regulators of PIN polarity in the stem, raising the possibility that the ability of this central loop to confer SL (in)sensitivity is due to the presence/absence of residues which are known sites of phosphorylation or ubiquitination such as serine (S), Lysine (K) or Threonine (T) (Leitner *et al.*, 2012; Barbosa and Schwechheimer, 2014; Zourelidou *et al.*, 2014). Previously the threonine at position 350 which is conserved in SL sensitive PIN1 and PIN7 but not SL insensitive PIN3 has been suggested as a potential candidate (Ticchiarelli, 2019). It is substituted by non-phosphorylatable valine in PIN4 but by serine in PIN3. The latter should still be a target for kinases, arguing against a role in conferring response to SL (Barbosa, Hammes and Schwechheimer, 2018; Ticchiarelli, 2019). However, the positional context of residues relative to their position in the peptide has been demon-

strated to affect the action of some kinases, with the ability of PID kinase to phosphorylate certain phosphosites dependent on phosphorylation of sites elsewhere in the sequence (Grones *et al.*, 2018). There is also data to suggest that the mutation of targets for one class of kinase does not impact the ability of other kinases to phosphorylate the hydrophilic loop, that is, different kinases have distinct profiles of phosphorylation patterns (Lee *et al.*, 2021). Interestingly, a new kinase has recently been characterised. Calcium-dependent protein kinase 29 (CPK29) is a PM-localised, Ca^{2+} activated kinase which is able to directly phosphorylate the PIN HL (Lee *et al.*, 2021). This kinase has multiple targets in the swapped region, some of which have been shown to modulate PIN localisation and which are non-conserved between PIN1 and PIN3. Thus, these could be candidates for the differential SL responsiveness conferred by this region.



1

Figure 5.29 | Multisequence alignment of PIN1, PIN1-PIN3_{L2}, PIN3, PIN4 and PIN7 amino acid residues across the central region of the HL where domain swap was conducted. Red arrows indicate the amino acid position, asterisks refer to the start and end of the swapped region. Green boxes indicate identified phosphosites of CPK29 while red boxes refer to residues which are not phosphorylated despite having the same amino acid in that position. Orange boxes indicate where a residue was phosphorylated only when the phosphorylation state of CPK29 was altered. Phosphosites identified from (Lee *et al.*, 2021).

To investigate whether any of the sites identified by (Lee *et al.*, 2021) might be candidates for conferring SL (in)sensitivity, I aligned the protein sequences of PIN1, PIN3, PIN1-PIN3_{L2}, PIN4 and PIN7 across the region where I conducted the domain swap between PIN1 and PIN3 (Fig. 5.29). I noted several amino acids in this region which (Lee *et al.*, 2021) identified as differentially phosphorylated between PIN1 and PIN3, these are highlighted in (Fig. 5.29). It is worth noting that several of the sites exhibited differential phosphorylation between PIN1 and PIN3, despite the amino acid residues being the same (Lee *et al.*, 2021). Raising the possibility that particular patterns of phosphorylation give rise to PIN SL responsiveness and suggesting a role for peptide context in determining phosphorylation of certain residues.

The data presented in this chapter supports previous data that elements within the hydrophilic loop, between residues 253 and 364, are key in determining PIN sensitivity to SL, but does not confirm precisely what these are. Previous suggestions of the relevance of patterns of phosphorylation as opposed to individual residues in conferring different PIN behaviours and responsiveness are likely, but remain difficult to investigate (Barbosa, Hammes and Schwechheimer, 2018; Ticchiarelli, 2019; Lee *et al.*, 2021).

5.3.2 | Removing PIN1 SL sensitivity increases residence on the membrane

There is a considerable body of evidence showing that, in mutants where SL signalling or perception is defective, the amount of PIN1 on the basal PM is increased (Bennett *et al.*, 2006; Crawford *et al.*, 2010; Bennett, Liang, *et al.*, 2016; Liang *et al.*, 2016). Here I show that PIN1-PIN3_{L2}-GFP exhibits increased levels on both the basal and lateral membranes of xylem parenchyma cells relative to PIN1-GFP in a *pin1* background, in a manner similar to native PIN1 in a *d14* background (Fig.5.4, Fig 5.5). This could be due to two things, increased insertion to the membrane or decreased removal of existing PIN1 from the membrane. Given previous reports highlighting the role of SL in inducing PIN1 removal from the membrane, likely via clathrin-mediated endocytosis, the latter seems the most likely explanation (Shinohara, Taylor and Leyser, 2013; Ticchiarelli, 2019) but this was not tested here.

I measured the amount of PIN1-PIN3_{L2}-GFP on the basal PM over 6 days without apical auxin supply. After 6 days, PIN1-PIN3_{L2}-GFP remains at significantly higher levels on the basal PM than native PIN1-GFP, which is almost completely depleted in both a *pin1* and *d14* background (Fig. 5.6). This could be explained by a lack of SL sensitivity, resulting in either increased accumulation on the plasma membrane and a slower rate of depletion or a combination of the two. I have previously shown that PIN1 re-accumulation is sensitive to SL, with basal provision in combination with apical auxin resulting in less PIN1 returning to the membrane after depletion (Fig. 3.9). When SL sensitivity is abolished in PIN1-PIN3_{L2}-GFP, this response is abolished (Fig 5.3), which could suggest that reduced PIN1 insertion to the membrane in response to SL is relevant to this response. Yet the presence of auxin has been shown to inhibit PIN endocytosis and SL is thought to act by interfering with this (Paciorek *et al.*, 2005; Wabnik *et al.*, 2010; Zhang *et al.*, 2020), so this result could be attributable to reduced PIN removal.

That PIN1-GFP membrane retention was not seen in *d14* mutants after 6 days while PIN1-PIN3_{L2}-GFP in a *pin1* background is interesting (Fig. 5.6), as it hints that loss of SL signalling via the canonical D14 pathway has an effect distinct from that when PIN1 alone is non-receptive to SL signalling. There are a number of speculative ways by which this observation could be explained. It may be that there is a pathway other than

via D14 by which SL induces endocytosis and which remains active in *d14* mutants, such that SL-induced PIN1 endocytosis is reduced, but not eliminated entirely. Alternatively, SL could be affecting PIN localisation via two signalling pathways, one which induces PIN endocytosis via D14 and another which reduces PIN allocation to the membrane. There is a paralogous receptor to D14 which is karrikin (KAR)-sensitive, KAI2. KAR and SL having very similar structures and the KAR signalling pathway bearing close resemblance to that of SL, even sharing a common element in the form of MAX2 (Nelson *et al.*, 2011). However, these signals appear not to be interchangeable (Nelson *et al.*, 2011; Scaffidi *et al.*, 2013, 2014) suggesting that KAI2 is unlikely to be involved in this context but raising the possibility of an as-yet uncharacterised SL receptor which is responsible for a small subset of responses.

It has been shown that ABCB19 stabilises PIN1 on the membrane but that that ABCB19 accumulation is reduced in the *d14* background (Titapiwatanakun *et al.*, 2009; Van Rongen *et al.*, 2019). It is conceivable that SL affects ABCB19 levels on the membrane and thus affects PIN1 stability, although there is no direct evidence to support this. In this scenario, loss of SL perception in *d14* would result in elevated PIN1 as SL cannot induce endocytosis and PIN1 would continue to be allocated/not removed from the membrane in response to auxin. However, when auxin supply is removed, PIN1 depletes from the membrane and the lack of ABCB19 would further destabilise PIN1 on the membrane. Whilst for PIN1-PIN3_{L2}-GFP, SL perception is not compromised, so stabilising ABCB19 would remain on the membrane, but PIN1 could not be removed by SL-induced endocytosis, which could account for why PIN1-PIN3_{L2}-GFP localisation is elevated and remains high even once apical auxin is removed.

Auxin transport in PIN1-PIN3_{L2}-GFP whilst rescued relative to *pin1*, was no higher than in wt. This is surprising given the elevated levels of PIN1-PIN3_{L2}-GFP on the basal PM and previous observations from *max2* & *d14* mutants whereby increased PIN1 membrane allocation correlates with increased auxin transport relative to wt (Bennett *et al.*, 2006; Crawford *et al.*, 2010; Shinohara, Taylor and Leyser, 2013; Bennett, Liang, *et al.*, 2016; Van Rongen *et al.*, 2019). Perhaps ABCB19 normally plays some role in limiting the amount of auxin transported by PIN1 and this capacity is lost in *d14*. However, this is unlikely as *abcb19* mutants exhibit reduced auxin transport whilst *d14* has reduced ABCB19 expression but increased auxin transport (Van Rongen *et al.*, 2019). Alternatively, domains in the swapped region of PIN1-PIN3_{L2}-GFP might also be affecting PIN capacity to transport auxin. Loss of PIN347 results in only a small reduction in auxin transport, which could suggest PIN3 is not responsible for much auxin transport. Thus, it may be the case that PIN1-PIN3_{L2}-GFP has reduced auxin efflux capacity relative to PIN1, but due to the greater accumulation on the membrane, bulk auxin transport is not affected overall. However, data gathered from PIN3-PIN1 chimeras indicate

that it may be the transmembrane region of PINs that are most important for regulating auxin transport capacity (Ticchiarelli, 2019). It is worth noting that PIN3 accumulation is not affected in *max2* (Van Rongen *et al.*, 2019), suggesting that the increased accumulation of PIN1-PIN3_{L2}-GFP is not due to the presence of PIN3 domains. There is some evidence that PINs exist in non-mobile clusters and that this increases polar retention (Kleine-Vehn *et al.*, 2011; Li *et al.*, 2021). It's possible that manipulation of the hydrophilic loop has affected these properties and that this accounts for the behaviour presented here.

The observed phenomena are difficult to explain but here I postulate several hypothetical mechanisms which would correlate with existing data and that contained in this chapter. It seems likely that, by exchanging regions of the HL, phosphorylation patterns are changed such that strigolactone sensitivity, membrane residency and auxin transport capacity are simultaneously affected in a complex manner. In order to assess this further, it would be worthwhile to investigate the behaviour of this chimera in a SL perception mutant. In addition, it would be valuable to perform experiments similar to those done by (Zhang *et al.*, 2020) to determine how vascular regeneration is impacted by the presence of an SL insensitive PIN1 chimera.

5.3.3 | PIN1 SL sensitivity is required for proper flower development and induction of senescence

Genetic techniques were used to assess whether the central region of the PIN3 HL is important for SL non-responsiveness. This was confirmed to be the case at a subcellular level. PIN1-PIN3_{L2}-GFP in a *pin1* background was able to rescue *pin1* phenotypes and in some cases resulted in decreased axillary meristem inhibition. Floral meristem initiation is severely compromised in *pin1*, resulting in infertility, a phenotype which is mostly rescued by PIN1-PIN3_{L2}-GFP expression. However, there is still a small decline in fertility relative to wild type plants, which I postulate to be due to occasionally observed floral defects whereby the pistil protrudes from the unopened flower (Fig. 5.10, 5.11). This is also observed in mutants of *pax1-1*, a positive regulator of *AXR3* (Tanimoto *et al.*, 2007) amongst many other auxin-related mutants (Tashiro *et al.*, 2009; Zhang *et al.*, 2016). This is perhaps unsurprising since auxin fluxes/gradients have been implicated in many aspects of floral development, including pollen maturation and FM determinacy (Cecchetti *et al.*, 2015, 2017; Yamaguchi *et al.*, 2017). Furthermore, auxin maxima generated via polar transport appear to be important in specifying identity of tissues in the gynoecium, relying on fine control of PIN localisation (Larsson, Franks and Sundberg, 2013; Larsson *et al.*, 2014; Moubayidin and Østergaard, 2014; Kuhn *et al.*, 2019; Xu *et al.*, 2021). It's conceivable that loss of PIN1 SL sensitivity is able to disrupt the latter process resulting in aberrations during gynoecium formation and result in the phenotype observed here. SL has also been linked to floral development through the

results of *in silico* analyses of transcriptional regulation (Marzec *et al.*, 2020) although SL perception/biosynthetic mutants do not have noticeable floral defects.

Expression of PIN1-PIN3_{L2}-GFP also results in consistently increased height relative to wt, associated with fewer cauline nodes and increased internode length (Fig. 5.12, 5.13). This could be a result of delayed senescence, as suggested by the significant increase in how many *pin1 PIN1-PIN3_{L2}-GFP* plants continued to flower (Fig. 5.13 C). Strigolactone mutants have previously been demonstrated to exhibit delayed senescence phenotypes of leaves and sepals but are also dwarfed relative to wt (Snowden *et al.*, 2005; Yan *et al.*, 2007; Yamada *et al.*, 2014; Ueda and Kusaba, 2015), indicating that this relationship between height and senescence is not straightforward. The observed height increase presented here may suggest that SL affects senescence by influencing PIN localisation and thus auxin flux. However, in order to draw this conclusion firmly, better measures of senescence such as leaf chlorophyll content would be required.

Loss of PIN1 SL sensitivity did not appear to have any effect on vascular development with respect to interfascicular cambium activity in the experiments conducted but did cause a slight increase in stem width, suggesting further investigation may be worthwhile.

5.3.4 | Shoot branching inhibition by strigolactone is only partially mediated through PIN1

I analysed the degree of branching observed in the PIN1-PIN3 chimera which revealed that presence of a SL insensitive version of PIN1 led to a slight but consistent increase in the total number of active primary branches by 1-2 on average under SD-LD conditions (Fig. 5.19). Significantly increased rosette branching was seen when plants were decapitated under the latter conditions (Fig. 5.21). I also observed a large increase in the number of secondary cauline branches of ~10 (fig 5.20), which may be attributable to the increased number of cauline branches in these conditions. High branching phenotypes are observed in *max2*, *d14* and *brc1/2* mutants (Bennett *et al.*, 2006; Aguilar-Martinez, Poza-Carrion and Cubas, 2007; Chevalier *et al.*, 2014) although the increases observed in these backgrounds are much greater and the effect on secondary branching small. In the context of the canalisation hypothesis, the latter is explained in the context that compromised SL signalling leads to reduced removal of PIN from the membrane, making it easier for buds to establish auxin export into the main stem and thus activate, resulting in observed high branching (Prusinkiewicz *et al.*, 2009; Crawford *et al.*, 2010; Shinohara, Taylor and Leyser, 2013). The fact that branching levels intermediate between that of wt and SL mutants are observed when PIN1 cannot be removed from the membrane by SL suggests that other factors are also at play, such as the

continued presence of SL sensitive PIN7. The second messenger hypothesis relies on the idea that auxin acts to upregulate SL biosynthesis (Sorefan *et al.*, 2003; Foo *et al.*, 2005; Brewer *et al.*, 2009; Hayward *et al.*, 2009) which in turn enters buds and maintains dormancy locally by upregulating *BRC1/2*. *BRC1* is highly expressed in dormant buds, down-regulated when buds activate and mutation causes a high branching phenotype (Doebley, Stec and Hubbard, 1997; Aguilar-Martinez, Poza-Carrion and Cubas, 2007; Seale, Bennett and Leyser, 2017). It has been shown recently that high *BRC1* expression does not suppress bud outgrowth but instead is suggested to act as a thresholding system in buds determining how activation-prone they are (Seale, Bennett and Leyser, 2017).

The data I present here supports the notion that there are two systems in place to regulate bud dormancy. On the one hand, SL insensitivity of PIN1-PIN3_{L2}-GFP creates an environment in which it is easier for buds to export auxin into the main stem, but on the other hand SL signalling remains in place, allowing apical auxin to upregulate *BRC1* and thus increasing the activation threshold. This is supported by the observation that, in a 2-node setup, I observe increased and earlier activation for *pin1 PIN1-PIN3_{L2}-GFP* than *col-0* in the absence of apical auxin or basal SL (Fig. 5.27, 5.28). With basal SL provision resulting in fewer buds activating for both genotypes but to a greater extent for wt (Fig. 5.28). GR24 remains able to enhance bud-bud competition in *pin1 PIN1-PIN3_{L2}-GFP* plants as reported previously (Fig. 5.26) (Crawford *et al.*, 2010). That this is not the case for *col-0* is unusual and may indicate that a lower GR24 concentration should have been used. These data align with proposals that SL may be enhancing competition by controlling the speed at which buds are able to generate canalised files of cells expressing polar PIN1 in order to export auxin into the main PATS upon removal of apical dominance. In the context of PIN1-PIN3_{L2}-GFP, when basal GR24 is supplied, inducing high *BRC1* expression and setting a high activation threshold, PIN1-PIN3_{L2}-GFP can canalise more rapidly, establish auxin export into the stem sink and resulting in faster bud activation. This would also be in line with observations that SL mutants exhibit increased vascular regeneration (Zhang *et al.*, 2020). This could explain why strigolactone remains able to enhance bud-bud competition in the way previously reported (Crawford *et al.*, 2010) even when PIN1 is SL insensitive. SL is still able to upregulate *BRC1* and set a high activation threshold but PIN1 is able to canalise more easily such that, when auxin drains basipetally, buds can rapidly establish auxin export into the strengthened stem sink and overcome the threshold set by *BRC1* (Seale, Bennett and Leyser, 2017). It would be worthwhile to test this hypothesis by analysing the *BRC1* expression in buds of *pin1 PIN1-PIN3_{L2}-GFP* to determine whether it is changed relative to wt. Further to this, assessment of bud-bud competition in a *pin1brc1brc2 PIN1-PIN3_{L2}-GFP* background would be valuable to determine whether GR24 continues to be effective at increasing competition. Further to this, the presence of an SL sensitive

PIN in the form of PIN7 may be partially compensating for the loss of SL sensitive PIN1 and confounding some of the effects on bud dynamics. Assessment of bud dynamics in a *pin1pin7 PIN1-PIN3_{L2}-GFP* line will be critical to resolve this.

Branch angle was more acute than wt, but again this was to a lesser degree than observed in SL mutants. PIN7 is known to be involved in setting the gravitropic set point angle (GSA) in roots and is SL responsive so it may be that it is also playing this role in shoots, accounting for the observed intermediate branch angle observed in PIN1-PIN3_{L2}-GFP (Rosquete, Waidmann and Kleine-Vehn, 2018; Roychoudhry *et al.*, 2019; Van Rongen *et al.*, 2019). In this and all assays conducted, the confounding variable of the presence of SL sensitive PIN7 must be considered due to its being implicated in strigolactone-mediated branching and bud-bud competition (Van Rongen *et al.*, 2019). As such, it would be worth crossing existing *pin1 PIN1-PIN3_{L2}-GFP* lines with *pin7* in order to determine how significant an effect this has. Even more convincing would be a SL-insensitive PIN7 created through a similar chimeric approach and expressed in a *pin1pin7* background along with the chimera characterised here.

5.3.5 | Conclusions

- ◇ Domains in the central hydrophilic loop of PIN3 is sufficient to confer strigolactone insensitivity.
- ◇ SL insensitive PIN1 exhibits increased basal and lateral membrane localisation and is more stable on the membrane.
- ◇ Expression of *PIN1-PIN3_{L2}-GFP* is able to complement major *pin1* phenotypes.
- ◇ *PIN1-PIN3_{L2}-GFP* expression results in minor phenotypic aberrations relative to wt, some of which resemble SL biosynthesis/perception mutants.
- ◇ PIN1 SL sensitivity may be required for proper floral development.
- ◇ PIN1 SL insensitivity is associated with increased branch activation but to a lower degree than SL biosynthetic/perception mutants.
- ◇ PIN1 SL sensitivity is not required for SL induced bud-bud competition.

5.3.6 | Future directions

- ◇ Cross the existing *PIN1-PIN3_{L2}-GFP pin1* line with a *pin1pin7* mutant and perform similar assessments to those conducted in this chapter to determine the effects of having no SL sensitive PINs.
- ◇ Create a PIN7-PIN3 chimera such that the other functions of PIN7 could be retained but its SL sensitivity eliminated.
- ◇ Assess the *BRC1* transcription levels of buds.

- ◇ Assessment of branching in a *brc1brc2pin1* mutant expressing *PIN1-PIN3_{L2}-GFP*.
- ◇ Investigate whether *PIN1-PIN3_{L2}-GFP* expression in an SL mutant background reveals any additive phenotypes.
- ◇ Investigate the auxin efflux capacity of *PIN1-PIN3_{L2}-GFP* relative to *PIN1* in cell culture.

6

Investigating evolutionary divergence in PIN behaviour

"Conformity is the last refuge of the unimaginative" - O. Wilde

6.1 | Introduction

6.1.1 | PIN diversity across plant species

Arabidopsis thaliana is used extensively as a model plant to conduct fundamental research, including that on shoot branching and has been used exclusively in the research conducted in this thesis. There are four canonical long PIN clades amongst the angiosperms: PIN1, PIN2, PIN3/4/7 and SoPIN1 (Bennett *et al.*, 2014; O'Connor *et al.*, 2014). *Arabidopsis* possesses three of these clades and these are well-known to exhibit different behaviours, localisations and perform a variety of functions which have been described previously. However, *Arabidopsis* and all Brassicaceae are unique amongst the angiosperms in lacking a clade of PINs, previously described as sister of PIN (SoPIN1) (Peng and Chen, 2011; O'Connor *et al.*, 2014; Martinez *et al.*, 2016). Relatively little investigation has been conducted to characterise the behaviour and function of these and other PINs outside of *Arabidopsis*. In *Brachypodium*, SoPIN1 has been demonstrated to play a role in generating auxin maxima for organ initiation in the shoot apical meristem tunica, with loss of function leading to similar phenotypes to those displayed by *Arabidopsis pin1* mutants (Okada *et al.*, 1991; O'Connor *et al.*, 2014, 2017). SoPIN1 appears to play an analogous role in tomato and loss of function can be complemented by expression of *AtPIN1* (Martinez *et al.*, 2016). Yet, while *AtPIN1* seems able to complement SoPIN1 loss of function in tomato, *BdSoPIN1* is unable to fully complement the *pin1* phenotype of *Arabidopsis* even when under control of an *AtPIN1* promoter, exhibiting floral defects and sterility, which suggests important functional differences (Martinez *et al.*, 2016; O'Connor *et al.*, 2017).

In addition to the presence of *SoPIN1*, *Brachypodium* and other species have undergone a duplication of *PIN1* to yield *PIN1a* and *PIN1b* (Carraro *et al.*, 2006; Forestan, Farinati and Varotto, 2012; O'Connor *et al.*, 2014). In *Brachypodium*, *PIN1a* and *PIN1b* appear to play a role in stem growth, with mutants exhibiting fairly minimal morphological defects besides internode elongation (O'Connor *et al.*, 2017). *PIN1b* is unable to rescue *Atpin1* auxin transport or organ initiation phenotypes when expressed in *Arabidopsis* under an *AtPIN1* promoter.

SoPIN1 and *PIN1b* have distinct expression patterns and polarisation behaviours in *Brachypodium*, the former being expressed in the epidermis and polarising toward auxin maxima whilst the latter are primarily localised to sub-epidermal tissues and orient away from auxin maxima (O'Connor *et al.*, 2014). The behaviour exhibited by SoPIN1 is consistent with up-the gradient (UTG) models of PIN localisation which have been used to explain observed convergent polarisation to form auxin maxima during organ initiation (Jönsson *et al.*, 2006; Smith *et al.*, 2006; Bilsborough *et al.*, 2011; van

Mourik *et al.*, 2012). PIN1b on the other hand seems to polarise with-the-flux (WTF), a mechanism which, in models, can recapitulate vascular patterning (Mitchison, 1980; Mitchison, Hanke and Sheldrake, 1981; Feugier, Mochizuki and Iwasa, 2005; Rolland-Lagan and Prusinkiewicz, 2005; Stoma *et al.*, 2008). Independently, these models have been unable to explain both organ initiation and vascular development data but models in which SoPIN1 and PIN1b follow UTG and WTF behaviour respectively are able to explain experimentally observed behaviours (O'Connor *et al.*, 2014).

The different abilities of *SoPIN1* and *PIN1b* expression to rescue *Atpin1* has been attributed to their different tissue localisation, transport activity and polarisation patterns, exhibited even when under control of the *AtPIN1* promoter (O'Connor *et al.*, 2017). Thus, it seems likely that there are inherent aspects of the proteins that regulate these factors through post-translational modification, determining their function. In *Arabidopsis* and presumably the wider Brassicaceae, it seems the PIN1 has acquired the functions fulfilled by three PINs in *Brachypodium*.

Whilst the role of *AtPIN1* and *Arabidopsis* PINs more widely in mediating shoot branching has been extensively studied, little has been done in this regard with relation to *SoPIN1* and *PIN1* in other species. Similarly, *AtPIN1* regulation by auxin, strigolactone and cytokinin has been well characterised, as discussed in previous chapters and has recently been investigated in pea, but is relatively unexplored in PINs from other species (J. Zhang *et al.*, 2020).

6.1.2 | Aims

- ◇ Characterise the behaviour of *BdSoPIN1* and *BdPIN1b* expressed in *Arabidopsis* in response to auxin, strigolactone and cytokinin
- ◇ Determine the capability of *SoPIN1* to influence shoot branching in *Arabidopsis*

6.2 | Results

In order to investigate the behaviour of these PINs, I used existing lines from (O'Connor *et al.*, 2017) consisting of citrine tagged *Brachypodium distachyon* sister of PIN1 (BdSoPIN1) and *Brachypodium distachyon* (BdPIN1b) under control of the *Arabidopsis PIN1* promoter (Heisler *et al.*, 2005) and expressed in either an *Arabidopsis* Col-0 or *pin1-613* background. In this chapter, these shall henceforth be referred to as SoPIN1 and PIN1b while native *Arabidopsis* PIN1 shall be referred to as simply PIN1.

6.2.1 | The behaviour of diverse PINs in response to hormones

Since PIN1b and SoPIN1 are evolutionarily diverged from AtPIN1, I first investigated whether they responded in the same manner as PIN1 to auxin, strigolactones and cytokinin.

To assess their response to auxin, I repeated the setup used to investigate PIN1 in chapter 3. I excised 2 cm stem segments from the inflorescences of young (4 week old) and mature (6 week old) plants expressing PIN1b and SoPIN1 in a Col-0 background. These stems were either sectioned immediately or treated apically with mock, NAA, NPA or NAA+NPA for 6 d before sectioning and imaging. Representative images from young stems are shown in figure 6.1, from which several initial impressions can be drawn. PIN1b exhibits lower accumulation overall relative to SoPIN1, including in fresh stems (Fig. 6.1 A, B). Mock and NPA treatment appears to result in PIN1b depletion from the plasma membrane (Fig. 6.1 C, G), whilst it appears to be retained with NAA or NAA+NPA (Fig. 6.1 E, I & Fig. 6.2). SoPIN1 on the other hand is present robustly on the basal PM across all treatments (Fig. 6.1 D, F, H, J). From this initial assessment it was also clear that levels of PIN1b are extremely low in mature stems and as such further investigation in mature stems was not carried out.

I then undertook quantitative assessments of both the amount of SoPIN1 & PIN1b on basal membranes and the number of membranes displaying polarised PIN. Figure 6.2 shows that, for PIN1b, membrane localisation is typically low in fresh stems but is maintained by NAA and NAA+NPA, while mock and NPA treatment results in depolarisation (Fig. 6.2 A). These trends are also reflected in the number of membranes displaying polar PIN1b (Fig. 6.2 B). Thus, it appears that PIN1b responds to auxin flux in much the same way as PIN1 in young stems (Fig. 3.3) but that the baseline levels of PIN1b are lower. An exception is that PIN1b does not hyper-accumulate at the membrane when treated with both NAA and NPA.

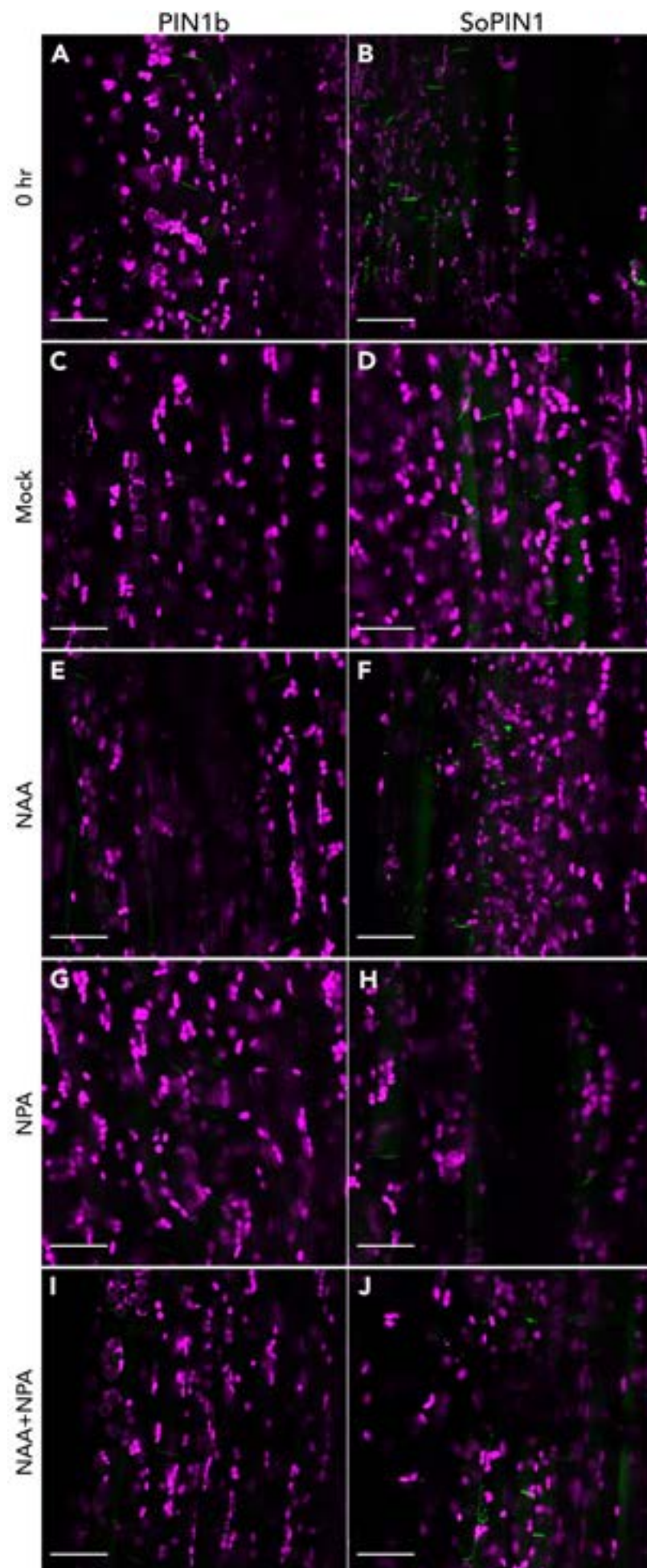


Figure 6.1 | Representative images of cells in the xylem parenchyma of wt plants expressing *PIN1b-citrine* (A, C, E, G, I) and *SoPIN1-citrine* (B, D, F, H, J). The basal 2cm of bolting inflorescences from 4 week old plants were either imaged immediately (A, B) or treated apically with mock (C, D), NAA (E, F), NPA (G, H), NAA+NPA (I, J) for 6 d. Stem segments were hand-sectioned longitudinally and imaged confocally. 8 stems per genotype per treatment were investigated and this was repeated thrice. Green represents citrine fluorescence whilst magenta indicates chlorophyll autofluorescence. Scale bars represent 25 μ M. White arrows indicate polar PIN.

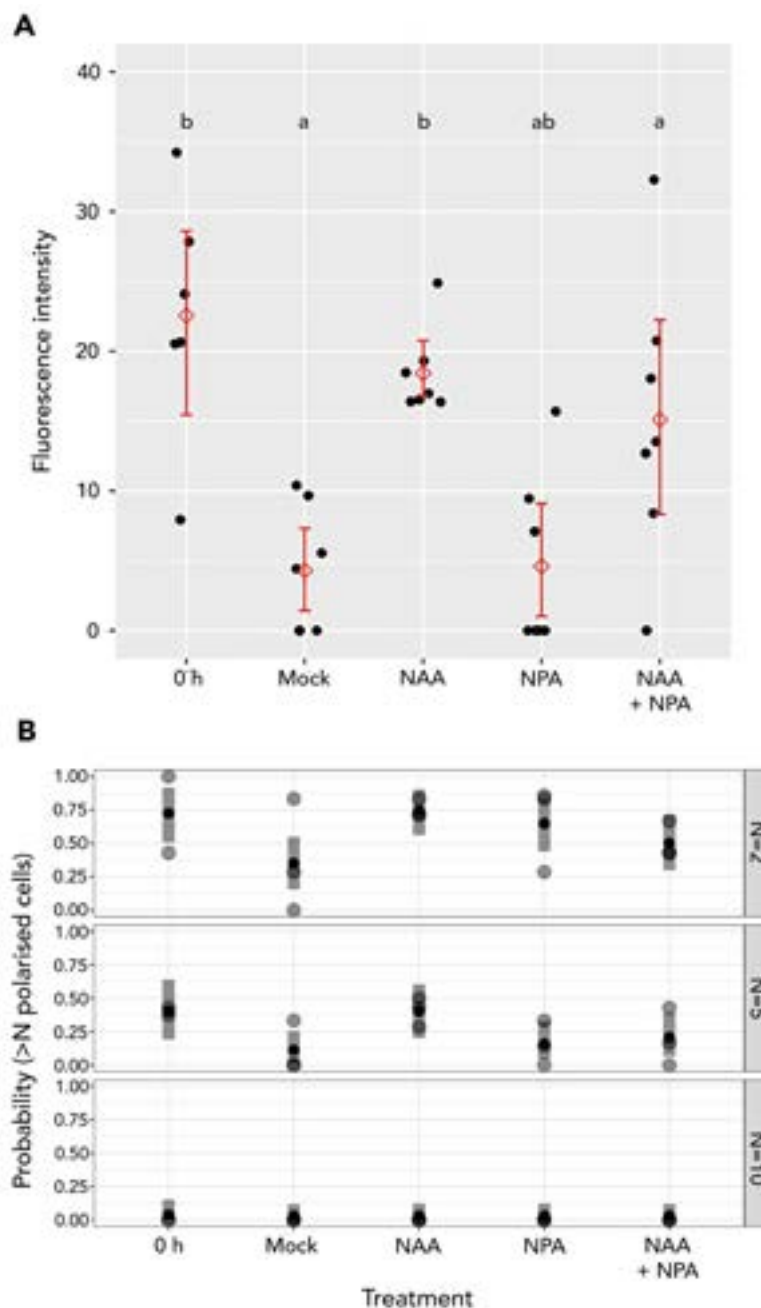


Figure 6.2 | Quantification of *PIN1b-citrine* polarisation in young stems. 2 cm stem segments were excised from the basal internode of bolting plants expressing *PIN1b-citrine*, hand sectioned longitudinally and imaged confocally immediately upon harvesting (0 h) or after being treated apically with mock, NAA, NPA or NAA+NPA for 6 d. (A) The amount of citrine fluorescence on the basal plasma membrane of cells in the xylem parenchyma was quantified using Zeiss Zen Blue software and is plotted here. At least 6 stems were assessed per treatment and at least 2 membranes per stem quantified. The experiment was repeated thrice, and the results displayed here are representative of all repeats. Black dots represent the mean fluorescence for a single stem, red diamonds represent the mean of means, red lines represent the 95% CI. (B) The number of membranes with visibly polar *PIN1b-citrine* were counted and the probability of the number of polarised cells in each repeat being greater than each defined threshold (N=2, top panel; N=5, middle panel, or N=10, bottom panel) calculated. For all treatments, each point represents a single repeat experiment in which at least 6 independent plants were analysed for PIN polarity, at least 4 repeats were conducted for all treatments. A logistic regression model was fitted to these data to estimate the 95% confidence interval, represented by grey bars.

I conducted the same analysis for *SoPIN1-citrine* expressing lines in both young and mature stems, which demonstrated quite a different response. In young stems, the amount of SoPIN1 on membranes and the number of membranes with polar SoPIN1 was similar to that of PIN1 (Fig. 3.3) and higher than that seen for PIN1b (Fig. 6.3 A, C). However, in young stems SoPIN1 remains on the membrane over the course of the experiment under all treatments tested, in contrast to both PIN1 (Fig.3.3) and PIN1b (Fig. 6.2). In mature stems, there does not appear to be a change in the amount of polar SoPIN1 relative to young stems and responses to treatments are the same, with the exception of evidence of depolarisation under mock treatment (Fig. 6.3 B, D). This behaviour is similar to PIN1 in mature stems, although depletion is stronger for PIN1 (Bennett *et al.*, 2016).

I also assessed the ability of SoPIN1 to repolarise after depletion by first treating stem segments apically with mock for 5 d followed by provision of apical auxin or mock for 1 d. Unlike PIN1 (Fig. 3.4), provision of apical NAA did not result in significant repolarisation of SoPIN1 in either young (Fig 6.4 A) or mature (Fig. 6.4 B) stems. There is some apparent repolarisation in the latter case but this is not significant. This analysis was not conducted for PIN1b as so few polarised membranes were visible after either treatment that a meaningful result could not be obtained.

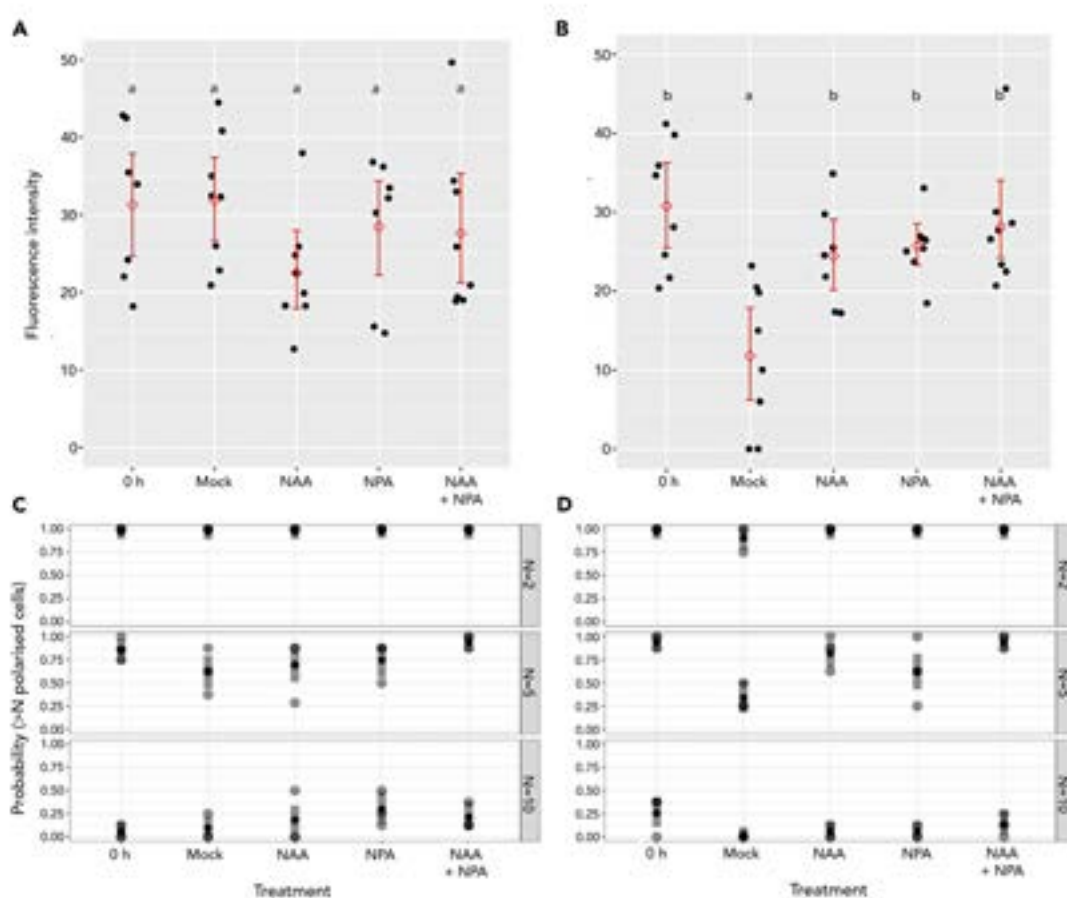


Figure 6.3 | Quantification of SoPIN1 polarity was investigated in young and mature tissue. 2 cm stem segments of 4 week (A, C) and 6 week (B, D) old plants expressing *pin1SoPIN1-citrine* were

hand sectioned longitudinally and imaged confocally immediately upon harvesting (0 h) or after being treated apically with mock, NAA, NPA or NAA+NPA for 6 d. (A, B), the amount of citrine fluorescence on the basal plasma membrane of cells in the xylem parenchyma was quantified using Zeiss Zen Blue software and is plotted here. At least 6 stems were assessed per treatment and at least 2 membranes per stem quantified. The experiment was repeated thrice (n=36). Black dots represent the mean fluorescence for a single stem, red diamonds represent the mean of means, red lines represent the 95% CI. (B) The number of membranes with visibly polar SoPIN1-citrine were counted and the probability of the number of polarised cells in each repeat being greater than each defined threshold (N=2, top panel; N=5, middle panel, or N=10, bottom panel) calculated. For all treatments, each point represents a single repeat experiment in which at least 6 independent plants were analysed for PIN polarity, at least 3 repeats were conducted for all treatments. A logistic regression model was fitted to these data to estimate the 95% confidence interval, represented by grey bars.

Taken together, these data hint at an interesting divergence in the response of PINs to auxin. That of PIN1 has been well characterised in chapter 3, with PIN1b seeming to demonstrate similar responses. SoPIN1 on the other hand exhibits notable differences. It seems to be extremely stable on the membrane whether auxin or NPA-sensitive auxin flux is present or not. Furthermore, while PIN1 becomes more stable in mature stems, SoPIN1 seems to do the opposite.

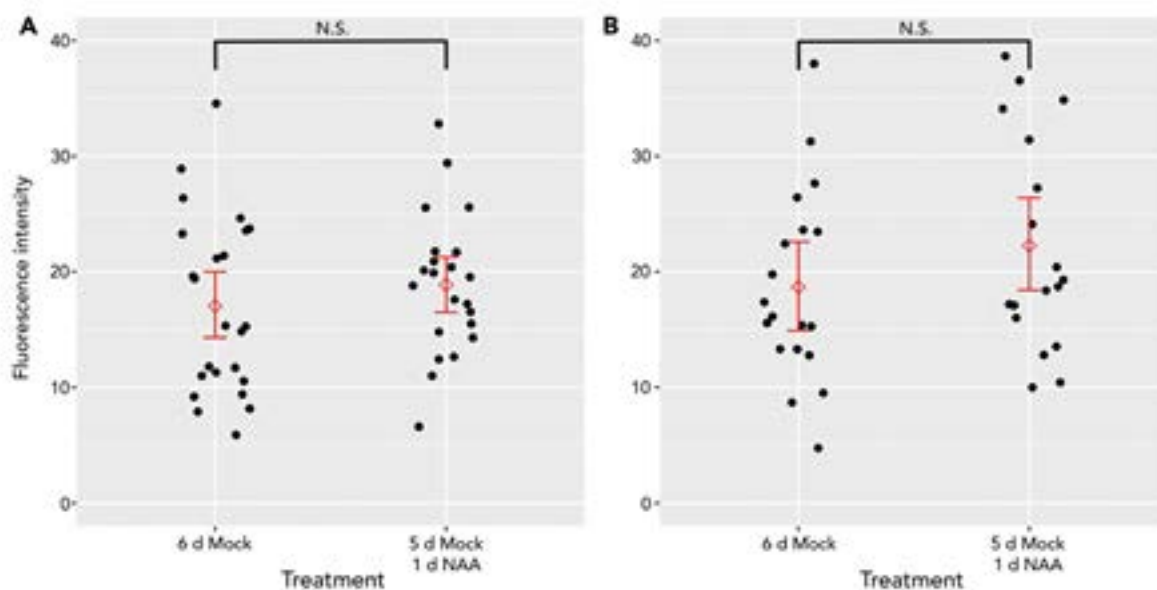


Figure 6.4 | The ability of SoPIN1 to repolarise was investigated using 2 cm stem segments of 4 week (A) and 6 week (B) old plants expressing *pin1 SoPIN1-citrine* which were excised and treated apically with mock for 6 days or mock for 5 days followed by NAA for 1 d. The amount of citrine fluorescence on the basal plasma membrane of cells in the xylem parenchyma was quantified using Zeiss Zen Blue software and is plotted here. At least 6 stems were assessed per treatment and at least 2 membranes per stem quantified. The experiment was repeated thrice (n=36). Black dots represent the mean fluorescence for a single stem, red diamonds represent the mean of means, red lines represent the 95% CI. A student's T-test was conducted and differences between treatment groups found to be non-significant (N.S), $p > 0.05$.

6.2.2 | Investigating the effects of strigolactone and cytokinin on SoPIN1 and PIN1b.

Having established that SoPIN1 exhibits different responses to auxin relative to PIN1, I assessed whether this was also the case for strigolactone and cytokinin. To do this, I utilised the same experimental setups as used previously for PIN1 (Fig 3.6-3.8), with strigolactone treatment conducted on longitudinally sectioned stems for 6 h and cytokinin treatment in agar plates treated apically with auxin and basally with BA for 4 h. The data demonstrate that SoPIN1b is sensitive to strigolactone in young stems, with treatment resulting in significant depletion from the plasma membrane after 6 h relative to mock (Fig. 6.5 A). However, it is also clear that this sensitivity disappears in mature stems (Fig. 6.5 B), a phenomenon which is not observed for PIN1 (Crawford *et al.*, 2010; Shinohara, Taylor and Leyser, 2013; Ticchiarelli, 2019). SoPIN1 does not exhibit cytokinin sensitivity in either young (Fig. 6.5 C) or mature (Fig 6.5 D) stems.

This is unlike PIN1 which I have previously demonstrated to be CK sensitive in young stems (Fig. 3.6). I also assessed these responses in PIN1b and found it to be unresponsive to both SL and CK (Fig. 6.6 A, B). Thus, it is clear that SoPIN1 and PIN1b proteins exhibit distinct and divergent behaviours with regard to hormones that are known to be key in regulating shoot branching in *Arabidopsis*.

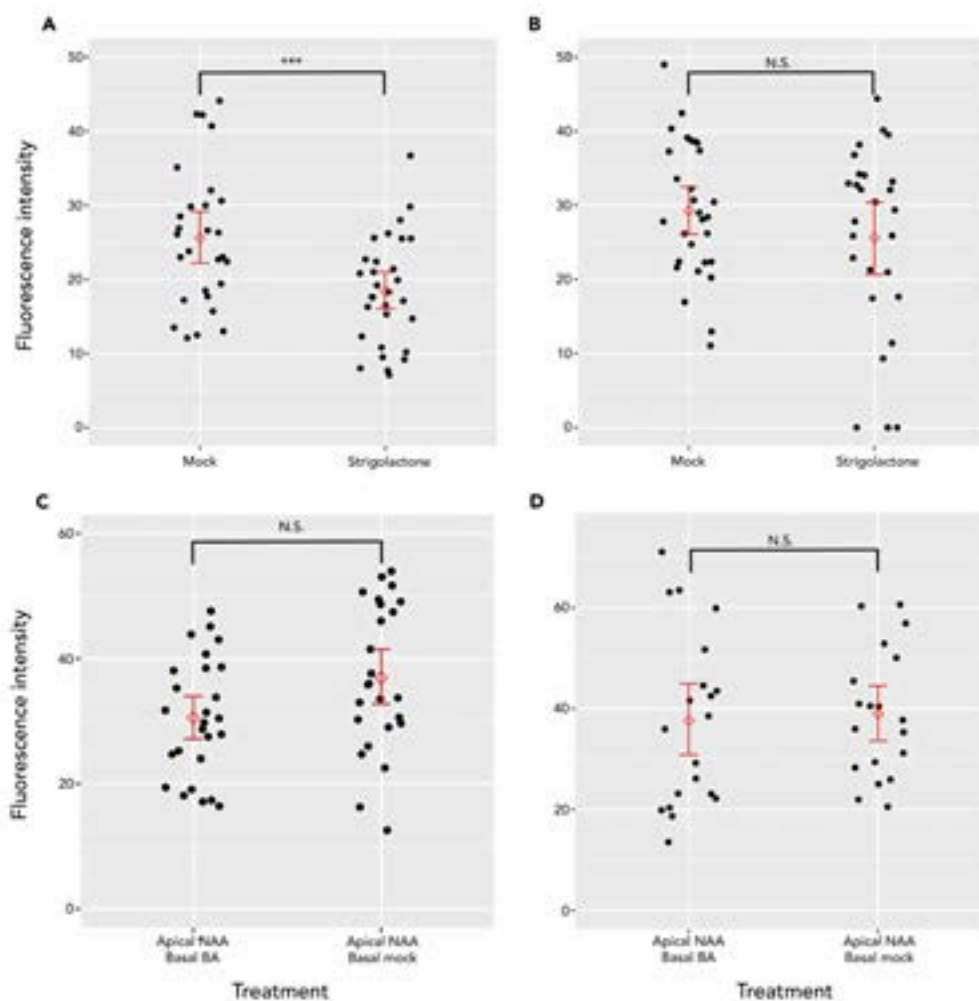


Figure 6.5 | Effect of strigolactone and cytokinin on SoPIN1 polarity. 2 cm segments from young (A, C) and mature (B, D) plants expressing *SoPIN1-citrine* were hand sectioned and treated with mock or GR24 for 6 h in ATS liquid (A-B) or with apical NAA +/- basal BA in split plates before sectioning (C-D). Sections were imaged confocally using a Zeiss LSM700 system and the amount of SoPIN1-citrine on the basal PM of xylem parenchyma cells quantified using Zeiss Zen software. This was done for at least 2 membranes per stem, at least 10 stems per treatment and repeated three times ($n > 60$). Black points represent the mean membrane fluorescence for cells of a single stem, red diamonds the mean of means and red lines the 95% CI. Statistical testing was performed using a Student's T-test, N.S. represents a non-significant difference between treatments while *** indicates $p < 0.001$.

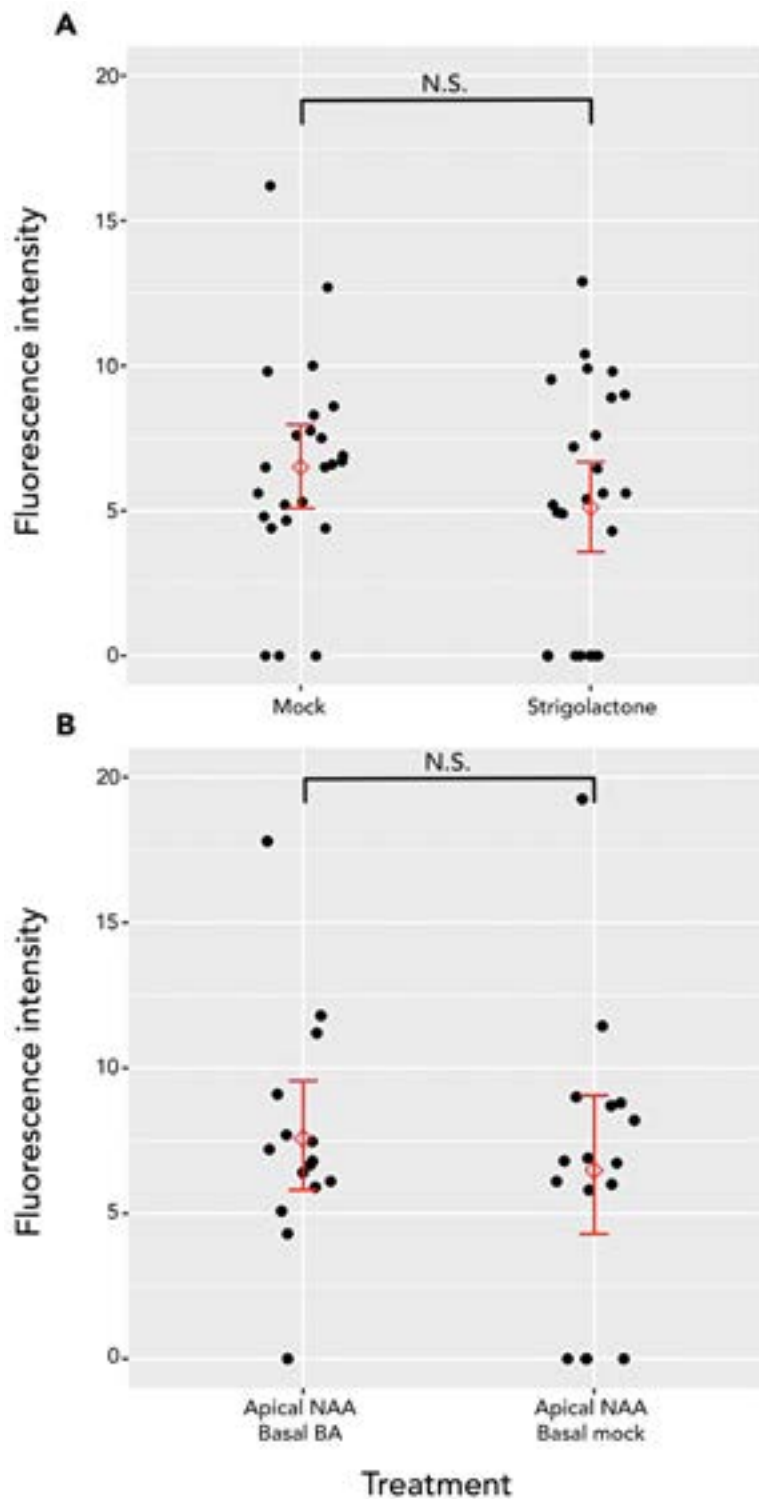


Figure 6.6 | PIN1b polarity in response to strigolactone and cytokinin 2 cm segments from young plants expressing *PIN1b-citrine* were hand sectioned and treated with mock or GR24 for 6 h in ATS liquid (A) or with apical NAA +/- basal BA in split plates before sectioning (B). Sections were imaged confocally using a Zeiss LSM700 system and the amount of PIN1b-citrine on the basal PM of xylem parenchyma cells quantified using Zeiss Zen software. This was done for at least 2 membranes per stem, 5-10 stems per treatment and repeated three times ($n = 30-60$). Black points represent the mean membrane fluorescence for cells of a single stem, red diamonds the mean of means and red lines the 95% CI. Statistical testing was performed using a student's T-test, N.S. represents a non-significant difference between treatments.

6.2.3 | SoPIN1 expression alters shoot branching patterns

Given the different behaviour of SoPIN1 relative to PIN1 in relation to SL and CK, I undertook to investigate whether this had any impact on branching levels. SoPIN1-citrine expressed in an *Arabidopsis pin1* background on rescues *pin1* phenotypes well with regard to organ initiation, however similar analysis could not be conducted with PIN1b as it rescues the *pin1* phenotype poorly with regard to organ initiation and auxin transport as mentioned in section 6.1.1 (O'Connor *et al.*, 2017). Figure 6.7 shows that *SoPIN1* expression results in small but significant increases in secondary rosette branching and decreases in cauline and total primary branching relative to either Col-0 or SoPIN1 expressed in a Col-0 background. Given that any changes in branching in SoPIN1 complemented lines were likely to be small, I conducted more sensitive assays for branching by growing plants in short day conditions for 4 weeks before transfer to long day. Plants were either grown to terminal flowering (Fig. 6.8) or decapitated when the bolting inflorescence reached 10 cm (Fig. 6.9). These assays demonstrated a large increase in the degree of rosette branching in SoPIN1 *pin1* plants (Fig. 6.8 & 6.9). The previously observed decrease in cauline branching (Fig. 6.7) was also noted here (Fig. 6.8). The latter is likely not due to differences in branching but due to the presence of fewer cauline nodes, however this was not quantified.

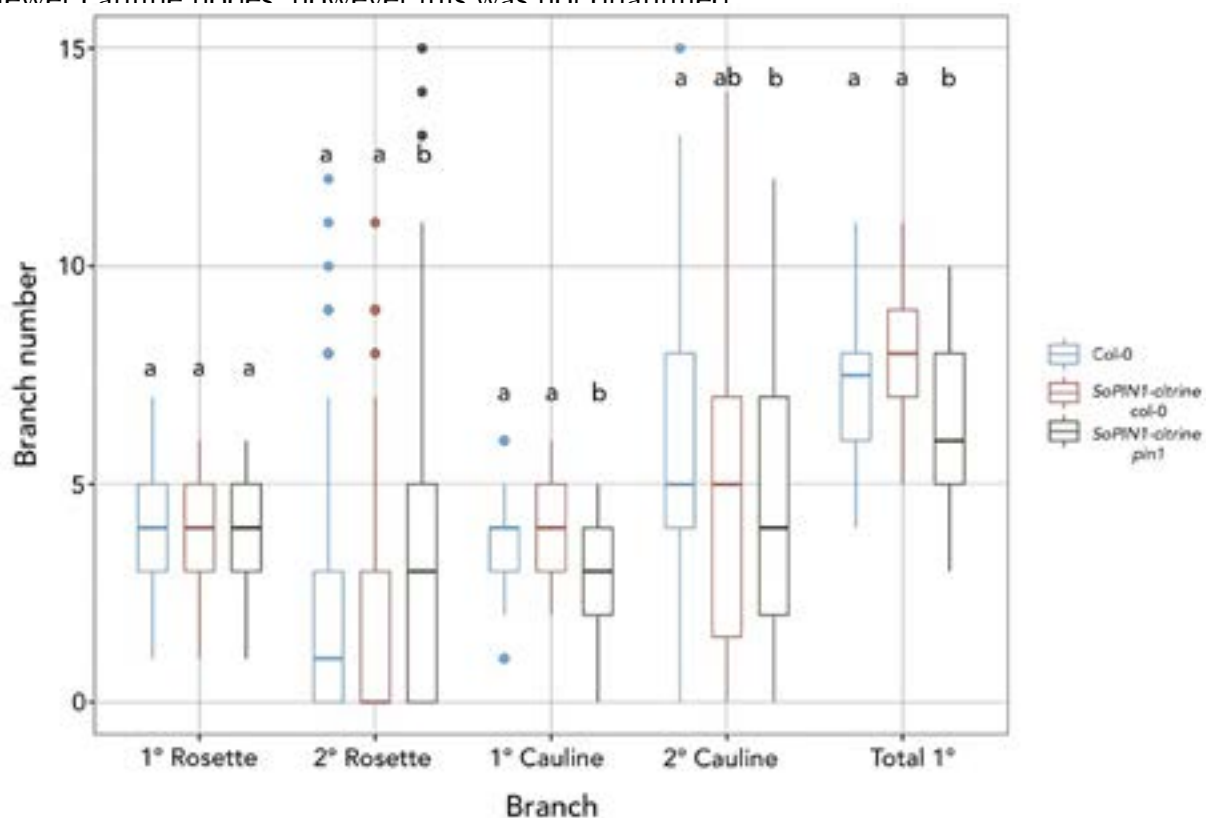


Figure 6.7 | Branching behaviour of Col-0 (blue), *SoPIN1-citrine* in a Col-0 background (red) and *SoPIN1-citrine* in a *pin1* background (green). Plants were grown to terminal flowering under long day conditions and the number of 1° and 2° rosette and cauline branches counted. Branches were counted if they were more than 1 cm long. Three repeats were conducted and the results compiled and plotted here as boxplots, n=70-158. A one-way ANOVA was conducted followed by Tukey's HSD post-hoc testing, with significance values represented as compact letter display.

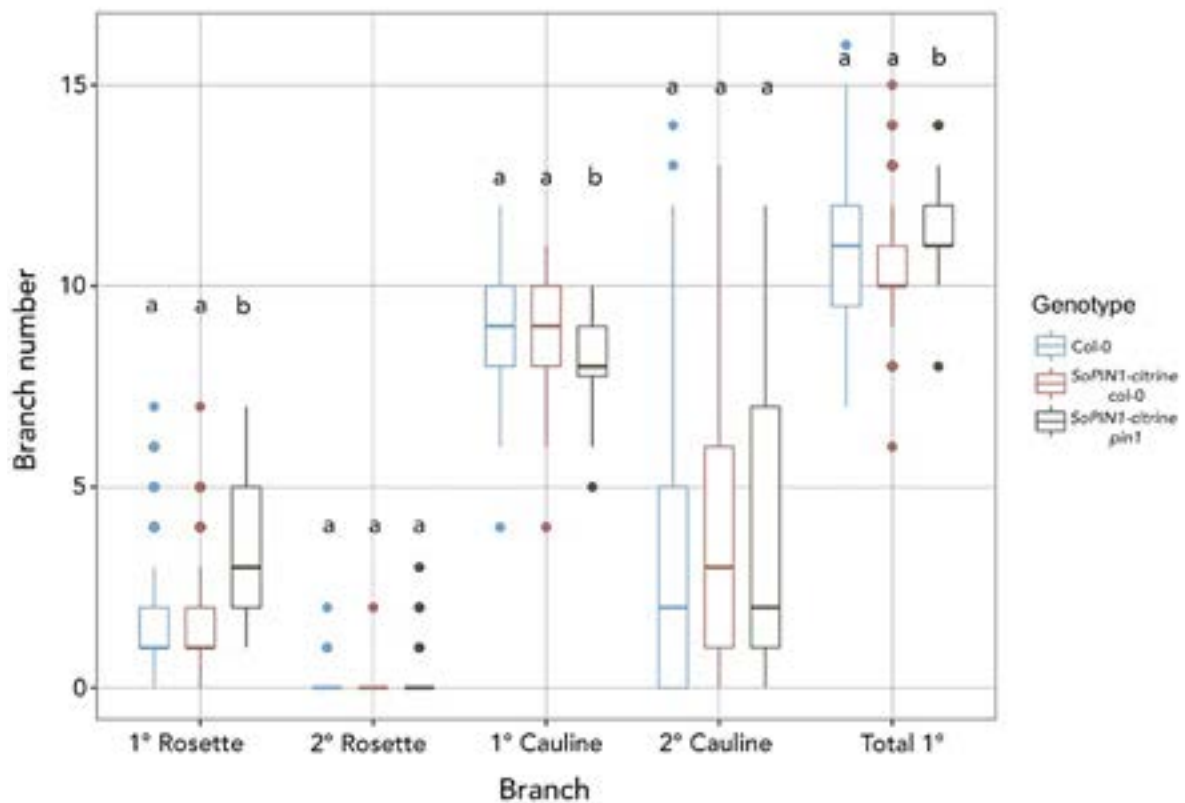


Figure 6.8 | Branching behaviour of Col-0 (blue), *SoPIN1-citrine* in a Col-0 background (red) and *SoPIN1-citrine* in a *pin1* background (green). Plants were grown under short day conditions for 4 weeks before transfer to long day conditions until terminal flowering, and the number of 1° and 2° rosette and cauline branches counted. Branches were counted if they were more than 1 cm long. Three repeats were conducted and the results compiled and plotted here as boxplots, n=44-260. A one-way Anova was conducted followed by Tukey's HSD post-hoc testing, with significance values displayed as compact letter display.

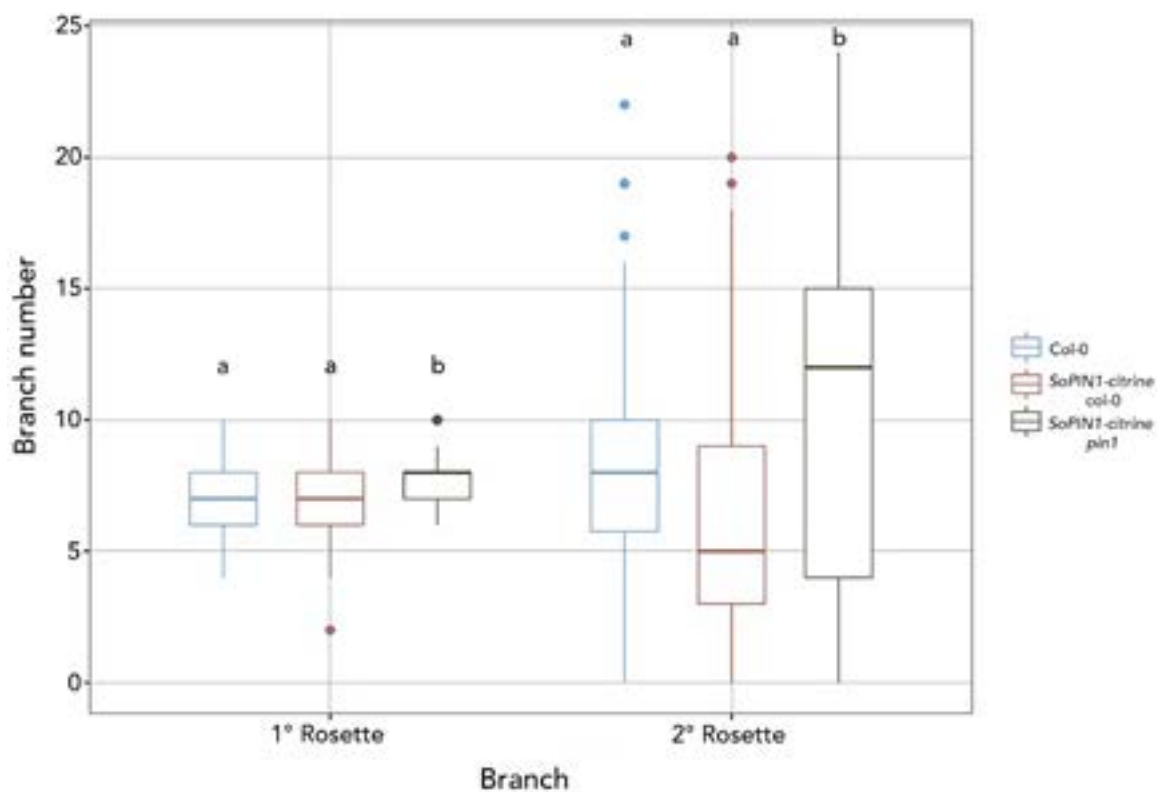


Figure 6.9 | Branching behaviour of Col-0 (blue), *SoPIN1-citrine* in a Col-0 background (red) and *SoPIN1-citrine* in a *pin1* background (green). Plants were grown under short day conditions for 4 weeks before transfer to long day conditions and decapitated when bolting inflorescences were 10 cm tall. The number of 1° and 2° rosette were counted. Branches were counted if they were more than 1 cm long. Three repeats were conducted and the results compiled and plotted here as box-plots, n=45-247. A one-way Anova was conducted followed by Tukey's HSD post-hoc testing, with significance values displayed as compact letter display.

Taken together, the data presented here suggest that, during their evolutionary divergence, as assessed in *Arabidopsis*, AtPIN1, BdSoPIN1 and BdPIN1b have acquired different behaviours with regard to auxin, strigolactone and cytokinin and that *SoPIN1* expression in place of *PIN1* expression alters branching patterns.

6.3 | Discussion

6.3.1 | BdSoPIN1 and BdPIN1b exhibit behaviours distinct from AtPIN1

In section 3.3.2, I characterised the responsiveness of AtPIN1 to the presence of auxin and NPA. Here I have demonstrated that BdSoPIN1 exhibits distinct behaviour in this regard. As reported previously (O'Connor *et al.*, 2017), BdSoPIN1 showed expression and polar localisation in fresh tissue (Fig. 6.3 A), with levels similar to those observed for PIN1 (Fig. 3.3). However, while in young stems PIN1 demonstrates depolarisation in response to lack of apical auxin or NPA treatment (Fig. 3.3), SoPIN1 does not, remaining on the membrane under all treatments (Fig. 6.3 A, B). In mature tissue, SoPIN1 depolarises only when apical auxin is removed, behaviour more analogous to PIN1 in mature tissue (Fig. 6.3 C, D) (Bennett *et al.*, 2016). This indicates three things: firstly, SoPIN1 is not dynamically allocated to the membrane in response to auxin flux in young tissue or NPA-sensitive auxin flux in mature tissue; secondly, SoPIN1 is more stable on the membrane than PIN1; thirdly, age-dependent behavioural changes are not a phenomenon restricted to *Arabidopsis* PIN1. Previously it has been posited that SoPIN1 is allocated according to an 'up-the-gradient' model whereby it orients towards the cell with the highest auxin concentration (O'Connor *et al.*, 2014), as opposed to a with-the-flux allocation. The behaviour of SoPIN1 in young stems presented here demonstrates that changes in auxin and auxin flux appear to have no impact on SoPIN1 membrane allocation, arguing against a simple with-the-flux model. However, there is also little evidence of up-the-gradient allocation, since SoPIN1 remains basally oriented with apical auxin supply and remains on the membrane when there is no apical auxin supply and auxin has drained from the stem. It may be the case that, since *Arabidopsis* has lost this clade of PINs, it has also lost mechanisms to regulate SoPIN1 allocation. Similarly, it could be that SoPIN1 lacks the necessary domains to be targeted by *Arabidopsis* relevant endocytosis and exocytosis mechanisms, resulting in consistent SoPIN1 levels on the membrane across the treatments examined. This could be due to reported differences in the motifs present in the hydrophilic loop (Bennett *et al.*, 2014; Y. Zhang

et al., 2020). SoPIN1 lacks two domains which are present & highly conserved in PIN1, PIN1a & PIN1b across species. In addition SoPIN1 exhibits highly conserved sequence across species in a region toward the end of the HL. All of these regions contain multiple serine & threonine residues which are known targets of phosphorylation-regulated control as discussed previously (O'Connor, 2014) (Section 1.2.2). The idea that cycling of SoPIN1 in *Arabidopsis* differs from AtPIN1 is consistent with reports that AtPIN1 accumulates in the stem pith cells early in development but that it is cleared as development progresses, whilst SoPIN1 expressed in *Arabidopsis* stems is not cleared in this way (O'Connor *et al.*, 2017). In this context it is interesting to note that SLs can trigger depletion of SoPIN1 from the plasma membrane in young *Arabidopsis* stems.

PIN1b on the other hand, exhibits behaviour more analogous to PIN1 in young tissue, depolarising under both mock and NPA treatments (Figure 6.2). This is in line with modelling, which was able to recapitulate PIN1b behaviour in *Brachypodium* by assigning it a 'with the flux' polarisation behaviour, such that it is allocated in accordance with net flux across the membrane, as has been proposed to be the case in the auxin canalisation hypothesis, and for PIN1 (Mitchison, Hanke and Sheldrake, 1981; Sachs, 1981; O'Connor *et al.*, 2014). However, the retention of PIN1b on the membrane when treated with both NAA & NPA, suggests that if PIN1b is flux-sensitive, this is non-NPA sensitive flux, in common with PIN1. That PIN1b can be regulated in a similar way to PIN1 is in line with reports that PIN orthologues from diverse land plants respond to trafficking inhibitors in the same way as AtPIN1 and appeared to be targeted by native phosphorylation mechanisms in *Arabidopsis* (Y. Zhang *et al.*, 2020).

The sterility of lines expressing *PIN1b* & *SoPIN1* in a *pin1-613* background meant that in order to have sufficient numbers of plants at the correct stage for analysis, the number of plants that would have to be sown and PCR genotyped would have been impractical. As such, these behaviours were assessed in a Col-0 background. This may have confounded results since it has been reported previously that SoPIN1 and PIN1b accumulation is increased in a *pin1-613* background, suggesting that AtPIN1 can compete with PIN1b and SoPIN1 for membrane residency (O'Connor *et al.*, 2017). This may explain why polar PIN1b is low in young stems and virtually undetectable in mature stems.

These results look at *Brachypodium* PINs in an *Arabidopsis* background and thus are inherently hard to interpret. It is well known that there are differences in the regulation of shoot branching between species, for example, SL upregulates *BRC1* in *Arabidopsis* and pea but does not in rice (Aguilar-Martinez, Poza-Carrion and Cubas, 2007; Minakuchi *et al.*, 2010; Dun *et al.*, 2011; Drummond *et al.*, 2015). Given this, and possible other confounding effects of incomplete rescue by *SoPIN1*, linking hormonal

responses to branching with any confidence is not possible from these data. However, these data do provide insight into how the regulation of PIN localisation may have diverged between the Brassicaceae and other angiosperms, and could have interesting implications for unpicking the role of SL/CK in controlling shoot branching across species.

6.3.2 | BdSoPIN1 expression alters shoot branching in *Arabidopsis*

It has been previously demonstrated that the expression of BdSoPIN1 under control of the *AtPIN1* promoter is able to complement many of the *Atpin1* phenotypes, including bulk auxin transport and organ initiation (O'Connor *et al.*, 2017). However, no investigation has been conducted into the effect on branching patterns. Given the different behaviours of SoPIN1 observed in response to hormones in section 6.3.1 and the previously discussed relevance of SL and CK to shoot branching (Section 1.3, 1.4), I elected to investigate the effect of the functional replacement of *AtPIN1* with SoPIN1 in *Arabidopsis*. This was achieved using existing lines where SoPIN1-citrine is expressed under control of the *AtPIN1* promoter in an *Arabidopsis pin1-613* background (O'Connor *et al.*, 2017). Three different assays were conducted in which plants were either grown under long day (LD) conditions until terminal flowering, under short day (SD) conditions for 4 weeks before transfer to LD conditions until terminal flowering or under SD conditions for 4 weeks before transfer to LD followed by excision of the main stem at 10 cm. Together these assays demonstrated that *SoPIN1-citrine* expression resulted in increased rosette branching and decreased cauline branching relative to wild type. The latter may be attributable to a decrease in cauline nodes as opposed to fewer activating as it is uncommon to see cauline nodes with inactive buds, however this was not measured. The increase in rosette branches seen after decapitation (Fig. 6.9) is perhaps most pertinent as this is independent of cauline branch number and may be less impacted by sterility issues. It may be that, since SoPIN1 seems to lose SL sensitivity in mature stems, buds which inherently activate later in development are unable to be inhibited by SL. Since buds activate in a basipetal sequence after floral transition (Hempel and Feldman, 1994), this might explain the observed increase in rosette branching. Insensitivity of SoPIN1 to depolarisation may also have had an effect here.

Taken together, these data show that BdPIN1b and BdSoPIN1 exhibit distinct hormonal responses to *AtPIN1*. This is likely due, at least partially, to changes in their protein sequence as has been speculated previously (Bennett *et al.*, 2014; O'Connor *et al.*, 2017; Y. Zhang *et al.*, 2020). In turn, expression of BdSoPIN1 in *Arabidopsis* results in rosette branching phenotypes which, whilst interesting, are difficult to explain.

6.3.3 | Conclusions

- ◇ BdPIN1b behaves similarly to *AtPIN1* with regard to auxin.

- ◇ BdSoPIN1 is insensitive to auxin in young tissue but gains auxin sensitivity in mature tissue.
- ◇ Neither BdPIN1b nor BdSoPIN1 exhibit cytokinin-sensitive membrane localisation.
- ◇ BdPIN1b is SL insensitive whilst BdSoPIN1 loses sensitivity with age.
- ◇ BdSoPIN1 expression in an *Arabidopsis pin1* background results in increased rosette branching.

7

Discussion, Conclusions and Future Directions

"Everything is going to be fine in the end. If it's not fine it's not the end." - O. Wilde

This thesis presents a detailed investigation into the hormonal response of PIN proteins at the cell level, with the aim of investigating the role of the auxin transport network in the control of shoot branching. This research represents a step towards developing a system in which the behaviour of PINs in response to individual hormones can be understood and manipulated to determine their contribution to shoot branching. A particular focus was to enhance our understanding of auxin transport canalisation and its role in controlling the aerial architecture of plants.

7.1 | An experimental system for investigating auxin transport canalisation

The auxin transport canalisation hypothesis aims to provide an explanation for diverse behaviours such as apical dominance, venation and vascular generation. An important aspect of this hypothesis is that PIN allocation is positively correlated with auxin flux across the plasma membrane (Sachs, 1975, 1981; Mitchison, Hanke and Sheldrake, 1981; Sauer *et al.*, 2006). Whilst there is a significant body of work supporting flux-correlated membrane allocation of PIN, which in turn is able to explain many of the observed phenomena such as auxin dependent PIN polarity changes and vascular regeneration after wounding (Sauer *et al.*, 2006; Scarpella *et al.*, 2006; Nodzynski *et al.*, 2010; Balla *et al.*, 2011; Mazur, Benková and Friml, 2016), we lack an understanding of the mechanism (s) by which PINs might be allocated proportional to flux. Many plausible implementations have been proposed, primarily on the basis of theoretical modelling. Those range from the existence of tally molecules in the form of dedicated molecules, auxin transporters themselves or protons, to the presence of extracellular auxin concentration sensors, with ROP proteins being a possible candidate for the latter (Coen *et al.*, 2004; Feugier, Mochizuki and Iwasa, 2005; Feugier and Iwasa, 2006; Fujita and Mochizuki, 2006; Stoma *et al.*, 2008; Kramer, 2009; Cieslak, Runions and Prusinkiewicz, 2015).

In parallel to this, there is a considerable amount of evidence for PIN membrane allocation on the basis of auxin concentration of neighbouring cells in an up-the-gradient manner. Modelling based on this second option is able to recapitulate some real-world observations, including the generation of auxin maxima (Reinhardt *et al.*, 2003; Heisler *et al.*, 2005; Jönsson *et al.*, 2006; Smith *et al.*, 2006; Merks *et al.*, 2007; Bennett *et al.*, 2016). However, the relationship between gradient-based and flux-based allocation processes is still a matter of considerable debate, despite several attempts having been made to unify these hypotheses into a coherent model able to explain all behaviours described (Bayer *et al.*, 2009; Cieslak, Runions and Prusinkiewicz, 2015). Progress in unravelling this has been hampered by the absence of a simple experimental system to study PIN allocation in *Arabidopsis*. Whilst (Mazur, Kulik, *et al.*, 2020) has made some strides in developing such a system, it remains a highly intricate set up.

Here, I build on the work of previous lab members using isolated stem segments (Bennett *et al.*, 2016; Waldie and Leyser, 2018). Using this system, I investigated the effect of auxin and auxin flux on *Arabidopsis* PIN1, PIN3, PIN4 and PIN7.

In contrast to existing data showing that NPA treatment induced PIN1 retention on the plasma membrane, which suggested that PIN1 localisation is regulated by auxin concentration as opposed to flux, I have demonstrated that this is not the case in young tissue. In this instance, PIN1 was depleted from the membrane in the presence of NPA but hyper-accumulated when simultaneously treated with NAA, demonstrating that NPA-sensitive auxin flux is not regulating PIN1 localisation but that the presence of auxin is clearly important. However, results from *DR5* reporter lines did not indicate a straightforward relationship between auxin signalling/concentration and PIN1 polarity, with basal supply of auxin unable to induce PIN1 allocation to the apical PM nor to induce retention on the basal PM despite the presence of large amounts of intracellular auxin. These data provide novel evidence that neither flux-dependent nor concentration-dependent mechanisms are sufficient to explain observed PIN1 behaviour in young tissue. Furthermore, I demonstrate that there is a clear effect of developmental stage on PIN1 behaviour, indicating that several mechanisms may in fact be in play and that those which are most relevant depend on the context in which PINs find themselves. One possible explanation that aligns with the data I obtained is that auxin gradients are important in combination with existing polarity cues as suggested previously (Jones *et al.*, 2002; Kramer, 2002, 2009; Payne and Grierson, 2009).

This age-dependent difference in PIN1 behaviour was not restricted to auxin alone, with cytokinin able to increase PIN1 allocation to the plasma membrane in young tissue, in contrast to previous data collected from mature tissue (Waldie and Leyser, 2018). Furthermore, I report that depletion and resupply of auxin is sufficient to respectively induce PIN1 depletion and re-accumulation in young stems, which is not observed in mature tissue (Bennett *et al.*, 2016). The latter is more consistent with the canalisation-like behaviour reported elsewhere (Mazur, Benková and Friml, 2016; Mazur, Gallei, *et al.*, 2020; Mazur, Kulik, *et al.*, 2020) but not observed in mature tissue (Bennett *et al.*, 2016). Whilst initially it was considered that these age-related behavioural changes may be due to increased dynamic cycling of PIN1 in young stems, no evidentiary basis for this could be established, with BFA treatment having no effect on membrane PIN1 levels. That we see an age-dependent element in relation to both CK-induced PIN1 hyper-accumulation on the membrane and its ability to re-accumulate, but that PIN1 membrane depletion due to auxin depletion or strigolactone occurs in both young and old tissue might be indicative of a role for tissue age in modulating PIN insertion but not PIN removal from the plasma membrane.

7.2 | Towards a new-old model of auxin-dependent PIN1 allocation

My results regarding PIN1 reproduce some previously characterised behaviours, such as depletion from the membrane when apical auxin is removed and remaining on the membrane when apical auxin is applied. However, there are several aspects of PIN1 behaviour in young stems which differ from those reported previously in mature stems, with PIN1 de-accumulating from the PM when apical NPA is supplied, and remaining on the membrane when simultaneously treated with NAA. The behaviour reported here is in many ways more canalisation-like than that observed previously, presenting the opportunity to explore this phenomenon in greater detail. The retention of PIN1 on the PM in the combined presence of NAA and NPA suggests that NPA-sensitive auxin flux is not required to maintain PIN1 on the membrane, yet indicates that the presence of auxin is key. However, the depletion of PIN1 from the PM when auxin is supplied basally, despite high auxin signalling as indicated by *DR5* reporters, seems to rule out a concentration-dependent mechanism as sufficient to explain the behaviours of PIN1. Given the inconsistency of presented data with either a PIN1 allocation mechanism based on auxin concentration or NPA-sensitive auxin flux (see Section 7.1), other mechanisms must be considered.

It has previously been suggested that PINs are able to sense auxin flux by responding to the amount of extracellular or intracellular auxin in their local environment, with modelling based on this able to recapitulate auxin transport canals (Garnett, 2010). As such, I assessed the relevance of an intracellular:extracellular auxin gradient to PIN membrane allocation. To do this, I deployed synthetic and natural auxins and transport inhibitors which have been demonstrated to have different affinities for auxin influx and efflux transporters. I found that, in young stems, NPA does not induce intracellular auxin accumulation despite still being able to inhibit auxin transport down the stem. I then investigated the effect of 2,4-D and 2-NOA on intracellular auxin levels and their effect on PIN1 localisation, but was unable to reproduce effects observed in isolated cell experiments. I speculate that this may be due to incomplete inhibition of influx by 2-NOA and the increased activity of *DR5* reporters in the presence of 2,4-D relative to NAA, as demonstrated previously by (Simon *et al.*, 2013). The latter does not appear to be due to increased sensitivity of the auxin signalling pathway to 2,4-D but instead, is commonly attributed to the greater stability and intracellular accumulation of 2,4-D (Kepinski and Leyser, 2005). PIN behaviour in shoots does not always correlate with that observed in roots and I have here demonstrated a difference in the action of NPA between young and mature stems. As such, it is reasonable to speculate that tissue type and developmental stage can impact the activity and action of 2,4-D and NOA, insofar as responses observed in tissue culture may not reliably represent the responses induced in stem xylem parenchyma. It would be valuable to include a positive control for the bioactivity of the NOA used here as it may have been the case that the 2-NOA was inactive. For

example, an auxin transport assay with a range of 2-NOA concentrations in order to assess whether it is effective at stopping auxin transport down the stem.

Whilst my data argues against straightforward measuring of auxin concentration or NPA-sensitive auxin flux as the drivers of PIN1 membrane localisation in young stems, I was unable to provide convincing evidence for an alternative mechanism. The data presented raises questions regarding how well we understand some of the synthetic molecules commonly used in auxin research, much of the evidence for which is based on limited single-cell data, or that from root tips. In order to satisfactorily establish what effect these various molecules are having and to determine whether auxin gradient sensing is important in controlling PIN1 localisation, we will require a direct methodology of quantifying auxin concentrations with fine resolution. Biosensors are becoming increasingly available, which can give a readout of the actual auxin concentrations within the cell (Herud-Sikimic *et al.*, 2021). It would be valuable to test the effects of the synthetic compounds deployed here using such a sensor. However, a solution to the problem of detecting extracellular auxin remains elusive and will be necessary to validate auxin gradient sensing. This might be achievable by tuning of existing biosensors to function apoplastically. Alternatively, UV Raman spectroscopy has been demonstrated as effective in detecting tryptophan and could therefore prove valuable as a complement to auxin biosensors (Asamoto and Kim, 2019).

7.3 | Demonstrating diversity in PIN responses

Previous work has shown that, even amongst the *Arabidopsis* PINs, behaviour with regard to hormones exhibits considerable differences. PIN1 and PIN7 leave the membrane in response to strigolactone whilst PIN3 and PIN4 do not, and cytokinin is able to promote the allocation of PIN3, PIN4 and PIN7 (but not PIN1) to the PM (Crawford *et al.*, 2010; Shinohara, Taylor and Leyser, 2013; Waldie and Leyser, 2018; Ticchiarelli, 2019; Van Rongen *et al.*, 2019). Furthermore PIN3, PIN4 and PIN7 are poorly expressed and not very polar in mature tissue, unlike PIN1 (Bennett *et al.*, 2016). Here I demonstrate that PIN3, PIN4 and PIN7 deplete from the membrane in the absence of apical auxin and in the presence of NPA, while PIN1 had been shown to remain on the PM when tissues are NPA treated (Bennett *et al.*, 2016). I also note that this appears to be due to differences in tissue maturity, as PIN1 in young tissue exhibits the same behaviour as PIN3, PIN4 and PIN7 in response to NPA and that this is also the case for cytokinin, with PIN1 plasma membrane allocation increasing in response to CK in young tissue whereas it appears cytokinin insensitive in mature tissue. Thus, there are clear differences in behaviour of different PINs with regard to auxin, SL, CK and this is tuneable by developmental stage.

These differences exist not only within *Arabidopsis* PINs but across species. *Brachy-*

podium PIN1b behaves analogously to *Arabidopsis* PIN1 with regard to auxin but SoPIN1 exhibits a high degree of retention on the PM in young tissue, even in the absence of apical auxin or when treated with NPA. The latter changes in mature tissue, indicating that age-related alterations in PIN behaviour are not exclusive to *Arabidopsis*. While the cytokinin sensitivity of *Arabidopsis* PIN1, but not its SL sensitivity, changes with age, *Brachypodium* SoPIN1 and PIN1b are both CK insensitive irrespective of developmental stage and SoPIN1 is only sensitive to SL in young tissue. This indicates that both the integral features of PIN proteins and the context within which they are expressed play important roles in determining their ability to respond to hormonal signals.

Clearly then, PIN behaviour in response to hormones is highly variable across time, tissue and species. It is well established that auxin transport regulation can be achieved transcriptionally, modulating transporter abundance, or post-translationally to alter activity and allocation. The results presented here highlight the importance of the latter and demonstrates that the control of PIN localisation and the auxin transport network more widely, is well positioned to act as an integrator of diverse signals involved in the regulation of a myriad of processes, including shoot branching. What is lacking however, is an understanding of just what determines these different PIN behaviours at a molecular level. Whilst some work highlights the importance of specific phosphorylation sites of PIN proteins and the role of multiple kinases in controlling not only the localisation but also the activity of PINs (Reviewed in (Tan, Luschnig and Friml, 2021)), there remain many unknowns regarding the regulation of PIN proteins and the consequences this has for the control of plant development.

7.4 | New techniques for an old hypothesis

The auxin canalisation hypothesis has long been postulated to connect auxin transport to shoot branching and explain the activity of cytokinin and strigolactone in this context. However, due to the complex interaction of multiple factors - different PINs being insensitive/sensitive to different hormones; the age-related changes I present here and the demonstrable importance of *BRC1*, it is extremely challenging to unpick the contribution of individual components. Doing so is necessary to fully understand the control of shoot branching which, in turn could play an important role in manipulating agricultural productivity. What is required is a system in which individual interactors can be made non-relevant. It has been demonstrated previously that different *Arabidopsis* PINs exhibit different behaviours with regard to hormones and I have further demonstrated an age-dependent element to this (Crawford *et al.*, 2010; Waldie and Leyser, 2018; Ticchiarelli, 2019; Van Rongen *et al.*, 2019). This knowledge, along with previous domain swap data informed the creation of chimeric PIN proteins which lack responsiveness to specific hormones, as has been done here with PIN1 and PIN3 in relation to SL (Ticchiarelli, 2019). Using these, I have shown that the central region of the PIN1

HL is necessary and sufficient for conferring SL sensitivity and that loss of this results in increased membrane accumulation and slower depletion from the PM. This further supports the role of SL in modulating PIN1 membrane levels as indicated by increased PIN1 accumulation in SL mutants and the ability of SL to induce PIN1 endocytosis (Bennett *et al.*, 2006; Crawford *et al.*, 2010; Jiang *et al.*, 2013; Shinohara, Taylor and Leyser, 2013).

The chimeric construct, PIN1::PIN1-PIN3_{L2}-GFP is able to complement the major phenotypes of *pin1* but simultaneously exhibits phenotypes reminiscent of SL perception/biosynthetic mutants in some respects. For example, loss of PIN1 SL sensitivity was correlated with subtle alterations in branching, including increased rosette branch activity and reduced branch angle. These phenotypes were intermediate between WT and SL mutants, suggesting other factors are at play. Further to this, expression of an SL insensitive PIN1-PIN3_{L2}-GFP led to changes in bud dynamics in a 2-node system, resulting in earlier activation of buds and a greater proportion of buds activating relative to controls. This in contrast to data from *brc1* and *d14* mutants which exhibit no change in these metrics (Ticchiarelli, 2019). However, there was no change in the growth rate of chimeric buds, suggesting that PIN1 SL sensitivity may be important in determining when and if AMs are released from dormancy, but less relevant to determining growth dynamics post-activation. Notably I did not observe any change in the ability of SL to enhance bud-bud competition in chimeric lines in the manner observed previously for wild type (Crawford *et al.*, 2010), suggesting SL mediates bud-bud competition by means other than membrane PIN levels. Whilst these observations are likely due to SL insensitivity of the chimeric PIN, giving insight into the relationship between SL and shoot branching, the data is made harder to interpret by the presence of SL-sensitive PIN7. It would be worthwhile to assess this chimeric PIN construct in a *pin1pin7* background and further to generate an SL-insensitive PIN7 through similar means, yielding a plant in which all the long PINs highly expressed in the stem are SL insensitive. This would effectively decouple SL-induced PIN removal from the membrane and shoot branching, revealing the role SL-induced PIN endocytosis has on bud activation.

Understanding of the hormonal responsiveness of PINs from other species could be valuable here as a resource for PINs with different hormone sensitivities. My analyses showed *Brachypodium* PIN1b & SoPIN1 to be non-responsive to CK and PIN1b SL-insensitive when expressed in *Arabidopsis*. This knowledge could be employed to generate non-responsive chimeras by performing interspecies PIN domain swaps. It would also be valuable to assess any such chimeras in lines where *BRC1* and *BRC2* activity was absent, as this would reveal whether cytokinin or SL are able to act via other pathways besides the well-established effects on transcription and PIN localisation.

Achieving these goals would be non-trivial, requiring the generation of multiple

chimeric PINs and inserting them into backgrounds where the native PIN function is absent. This may be complicated by the oft significant developmental defects of PIN mutants. If possible, it would be helpful to pinpoint the residue basis for the response/non-response of different PINs to different hormones, such that changes could be made in a more targeted manner. Whilst some evidence links individual residues to large-scale polarity changes, for example, the importance of S231, S252, S290 in regulating the apical-basal polarity switch of PIN1 (Huang *et al.*, 2010), other changes cannot be explained so simply. The current approach involving swapping large chunks of the HL, whilst effective, may be causing broader, off-target effects on PIN behaviour. In addition, data increasingly supports the notion that it is not the phosphorylation status of individual residues, but patterns of phosphorylation throughout the protein which are important to regulating PIN behaviour, making fine-tuning PIN properties a far from trivial process (Barbosa, Hammes and Schwechheimer, 2018).

7.5 | Final remarks

Here I have demonstrated that explanations previously leveraged to explain the allocation of PINs, namely NPA-sensitive auxin flux & auxin concentration, are insufficient to explain the behaviours of PIN1 in young tissues - suggesting a context dependent element to PIN behaviour. Further, I provide evidence that there is a clear role of the hydrophilic loop in controlling PIN1 behaviour in response to strigolactone, identifying that the central region of the PIN1 HL is necessary and sufficient to confer SL sensitivity. Finally, I have uncovered initial evidence that there is cross-species diversity in the behaviour of PIN1 and closely related SoPIN1 in response to cytokinin & strigolactone. Taken together, these data advance our understanding of PIN behaviour and provide significant step toward elucidating the network controlling bud activation.

Whilst the auxin transport canalisation hypothesis is simple in concept, the core mechanisms behind it, namely how PINs perceive auxin and allocate to different membranes accordingly, remain elusive. Auxin biosensors in combination with synthetic auxin analogues and transport inhibitors are likely to be key in resolving this. Unravelling the way in which CK and SL modulation of PIN membrane residency integrates with shoot branching will be vital to bettering our understanding the regulation of shoot branching.

This thesis has addressed the hormonal regulation of PIN proteins and its relation to shoot branching. It has deployed a myriad of methods from the microscopic to the macroscopic in order to shed light on the cell-level behaviours of auxin exporters and their impact on the aerial architecture of *Arabidopsis*. This research and that built upon it, could equip us in the longer term with the tools to artificially manipulate crop morphology and increase yields.

Appendix A

References

"Coming back to where you started is not the same as never leaving" - T. Pratchett

- Abas, L. *et al.* (2020) 'Naphthylphthalamic acid associates with and inhibits PIN auxin transporters', *Proceedings of the National Academy of Sciences of the United States of America*, 118(1). doi: 10.1073/pnas.2020857118.
- Abe, S. *et al.* (2014) 'Carlactone is converted to carlactonoic acid by MAX1 in Arabidopsis and its methyl ester can directly interact with AtD14 in vitro', *Proceedings of the National Academy of Sciences of the United States of America*, 111(50). doi: 10.1073/pnas.1410801111.
- Abel, S. and Theologis, A. (1996) 'Early genes and auxin action', *Plant Physiology*. doi: 10.1104/pp.111.1.9.
- Adamowski, M. and Friml, J. (2015) 'PIN-Dependent Auxin Transport: Action, Regulation, and Evolution', *The Plant Cell Online*. doi: 10.1105/tpc.114.134874.
- Aguilar-Martinez, J. A., Poza-Carrion, C. and Cubas, P. (2007) 'Arabidopsis BRANCHED1 Acts as an Integrator of Branching Signals within Axillary Buds', *The Plant Cell Online*. doi: 10.1105/tpc.106.048934.
- Agusti, J. *et al.* (2011) 'Strigolactone signaling is required for auxin-dependent stimulation of secondary growth in plants', *Proceedings of the National Academy of Sciences of the United States of America*, 108(50). doi: 10.1073/pnas.1111902108.
- Akiyama, K. and Hayashi, H. (2006) 'Strigolactones: Chemical signals for fungal symbionts and parasitic weeds in plant roots', *Handbook of Environmental Chemistry, Volume 5: Water Pollution*, 97(6). doi: 10.1093/aob/mcl063.
- Alder, A. *et al.* (2012) 'The path from beta-carotene to carlactone, a strigolactone-like plant hormone', *Science*, 335(6074). doi: 10.1126/science.1218094.
- Argyros, R. D. *et al.* (2008) 'Type B response regulators of Arabidopsis play key roles in cytokinin signaling and plant development.', *The Plant Cell*. doi: 10.1105/tpc.108.059584.
- Arite, T. *et al.* (2007) 'DWARF10, an RMS1/MAX4/DAD1 ortholog, controls lateral bud outgrowth in rice', *Plant Journal*, 51(6). doi: 10.1111/j.1365-313X.2007.03210.x.

- Arite, T. *et al.* (2009) 'D14, a strigolactone-Insensitive mutant of rice, shows an accelerated outgrowth of tillers', *Plant and Cell Physiology*. doi: 10.1093/pcp/pcp091.
- Armougom, F. *et al.* (2006) 'Expresso: Automatic incorporation of structural information in multiple sequence alignments using 3D-Coffee', *Nucleic Acids Research*, 34(WEB. SERV. ISS.). doi: 10.1093/nar/gkl092.
- Asamoto, D. A. K. and Kim, J. E. (2019) 'UV Resonance Raman Spectroscopy as a Tool to Probe Membrane Protein Structure and Dynamics', in *Methods in Molecular Biology*. doi: 10.1007/978-1-4939-9512-7_14.
- Baba, A. I. *et al.* (2019) 'AtCRK5 protein kinase exhibits a regulatory role in hypocotyl hook development during skotomorphogenesis', *International Journal of Molecular Sciences*, 20(14). doi: 10.3390/ijms20143432.
- Bailly, A. *et al.* (2008) 'Modulation of P-glycoproteins by auxin transport inhibitors is mediated by interaction with immunophilins', *Journal of Biological Chemistry*, 283(31). doi: 10.1074/jbc.M709655200.
- Bainbridge, K. *et al.* (2008) 'Auxin influx carriers stabilize phyllotactic patterning', *Genes and Development*, 22(6). doi: 10.1101/gad.462608.
- Balla, J. *et al.* (2002) 'Involvement of auxin and cytokinins in initiation of growth of isolated pea buds', *Plant Growth Regulation*, 38(2). doi: 10.1023/A:1021215728096.
- Balla, J. *et al.* (2011) 'Competitive canalization of PIN-dependent auxin flow from axillary buds controls pea bud outgrowth', *Plant Journal*. doi: 10.1111/j.1365-313X.2010.04443.x.
- Balla, J. *et al.* (2016) 'Auxin flow-mediated competition between axillary buds to restore apical dominance', *Scientific Reports*, 6. doi: 10.1038/srep35955.
- Barbez, E. and Kleine-Vehn, J. (2013) 'Divide Et Impera-cellular auxin compartmentalization', *Current Opinion in Plant Biology*. doi: 10.1016/j.pbi.2012.10.005.
- Barbosa, I. C. R., Hammes, U. Z. and Schwechheimer, C. (2018) 'Activation and

- Polarity Control of PIN-FORMED Auxin Transporters by Phosphorylation', *Trends in Plant Science*. doi: 10.1016/j.tplants.2018.03.009.
- Barbosa, I. C. R. and Schwechheimer, C. (2014) 'Dynamic control of auxin transport-dependent growth by AGCVIII protein kinases', *Current Opinion in Plant Biology*. doi: 10.1016/j.pbi.2014.09.010.
- Barratt, N. M. *et al.* (1999) 'Metabolism of exogenous auxin by *Arabidopsis thaliana*: Identification of the conjugate N(alpha)-(indol-3-ylacetyl)-glutamine and initiation of a mutant screen', *Physiologia Plantarum*, 105(2). doi: 10.1034/j.1399-3054.1999.105204.x.
- Bartel, B. and Fink, G. R. (1995) 'ILR1, an amidohydrolase that releases active indole-3-acetic acid from conjugates', *Science*, 268(5218). doi: 10.1126/science.7792599.
- Bartholomew-Began, S. and Jean, R. V. (1997) 'Phyllotaxis. A Systemic Study in Plant Morphogenesis', *The Bryologist*, 100(3). doi: 10.2307/3244517.
- Barton, M. K. and Poethig, R. S. (1993) 'Formation of the shoot apical meristem in *Arabidopsis thaliana*: An analysis of development in the wild type and in the shoot meristemless mutant', *Development*, 119(3). doi: 10.1242/dev.119.3.823.
- Bayer, E. M. *et al.* (2009) 'Integration of transport-based models for phyllotaxis and midvein formation', *Genes and Development*, 23(3). doi: 10.1101/gad.497009.
- Benjamins, R. *et al.* (2001) 'The PINOID protein kinase regulates organ development in *Arabidopsis* by enhancing polar auxin transport.', *Development* (Cambridge, England). doi: 10.1145/2076021.2048098.
- Benková, E. *et al.* (2003) 'Local, Efflux-Dependent Auxin Gradients as a Common Module for Plant Organ Formation', *Cell*. doi: 10.1016/S0092-8674(03)00924-3.
- Bennett, M. J. *et al.* (1996) 'Arabidopsis AUX1 gene: A permease-like regulator of root gravitropism', *Science*, 273(5277). doi: 10.1126/science.273.5277.948.
- Bennett, S. R. M. *et al.* (1995) 'Morphogenesis in pinoid mutants of *Arabidopsis thaliana*', *The Plant Journal*, 8(4). doi: 10.1046/j.1365-313X.1995.8040505.x.

- Bennett, T. *et al.* (2006) 'The Arabidopsis MAX pathway controls shoot branching by regulating auxin transport', *Current Biology*. doi: 10.1016/j.cub.2006.01.058.
- Bennett, T. *et al.* (2014) 'Paralogous radiations of PIN proteins with multiple origins of noncanonical PIN structure', *Molecular Biology and Evolution*. doi: 10.1093/molbev/msu147.
- Bennett, T., Hines, G., *et al.* (2016) 'Connective Auxin Transport in the Shoot Facilitates Communication between Shoot Apices', *PLoS Biology*. doi: 10.1371/journal.pbio.1002446.
- Bennett, T., Liang, Y., *et al.* (2016) 'Strigolactone regulates shoot development through a core signalling pathway', *Biology Open*. doi: 10.1242/bio.021402.
- Bennett, T., Hines, G. and Leyser, O. (2014) 'Canalization: What the flux?', *Trends in Genetics*, 30(2), pp. 41–48. doi: 10.1016/j.tig.2013.11.001.
- Van den Berg, C. *et al.* (1995) 'Cell fate in the Arabidopsis root meristem determined by directional signalling', *Nature*, 378(6552). doi: 10.1038/378062a0.
- Bergonzi, S. *et al.* (2013) 'Mechanisms of age-dependent response to winter temperature in perennial flowering of *Arabis alpina*', *Science*, 340(6136). doi: 10.1126/science.1234116.
- Bertani, G. (1951) 'Studies on lysogeny. I. The mode of phage liberation by lysogenic *Escherichia coli*.', *Journal of bacteriology*, 62(3).
- Besnard, F. *et al.* (2014) 'Cytokinin signalling inhibitory fields provide robustness to phyllotaxis', *Nature*, 505(7483). doi: 10.1038/nature12791.
- Beveridge, C. A., Ross, J. J. and Murfet, I. C. (1994) 'Branching mutant rms-2 in *Pisum sativum*: Grafting studies and endogenous indole-3-acetic acid levels', *Plant Physiology*, 104(3). doi: 10.1104/pp.104.3.953.
- Beveridge, C. A., Symons, G. M. and Turnbull, C. G. N. (2000) 'Auxin inhibition of decapitation-induced branching is dependent on graft-transmissible signals regulated by genes Rms1 and Rms2', *Plant Physiology*, 123(2). doi: 10.1104/pp.123.2.689.

- Bhalerao, R. P. *et al.* (2002) 'Shoot-derived auxin is essential for early lateral root emergence in Arabidopsis seedlings', *Plant Journal*. doi: 10.1046/j.0960-7412.2001.01217.x.
- Bhatia, N. *et al.* (2016) 'Auxin Acts through MONOPTEROS to Regulate Plant Cell Polarity and Pattern Phyllotaxis', *Current Biology*. doi: 10.1016/j.cub.2016.09.044.
- Bibikova, T. N. *et al.* (1998) 'Localized changes in apoplastic and cytoplasmic pH are associated with root hair development in Arabidopsis thaliana', *Development*, 125(15). doi: 10.1242/dev.125.15.2925.
- Bilsborough, G. D. *et al.* (2011) 'Model for the regulation of Arabidopsis thaliana leaf margin development', *Proceedings of the National Academy of Sciences of the United States of America*, 108(8). doi: 10.1073/pnas.1015162108.
- Blakeslee, J. J. *et al.* (2007) 'Interactions among PIN-FORMED and P-glycoprotein auxin transporters in Arabidopsis', *Plant Cell*, 19(1). doi: 10.1105/tpc.106.040782.
- Bleckmann, A. *et al.* (2010) 'Stem cell signaling in Arabidopsis requires CRN to localize CLV2 to the plasma membrane', *Plant Physiology*, 152(1). doi: 10.1104/pp.109.149930.
- Bleecker, A. B. and Patterson, S. E. (1997) 'Last exit: Senescence, abscission, and meristem arrest in arabidopsis', *Plant Cell*, 9(7). doi: 10.1105/tpc.9.7.1169.
- Blilou, I. *et al.* (2005) 'The PIN auxin efflux facilitator network controls growth and patterning in Arabidopsis roots', *Nature*. doi: 10.1038/nature03184.
- Booker, J. (2003) 'Auxin Acts in Xylem-Associated or Medullary Cells to Mediate Apical Dominance', *The Plant Cell Online*. doi: 10.1105/tpc.007542.
- Booker, J. *et al.* (2004) 'MAX3/CCD7 is a carotenoid cleavage dioxygenase required for the synthesis of a novel plant signaling molecule', *Current Biology*, 14(14). doi: 10.1016/j.cub.2004.06.061.
- Booker, J. *et al.* (2005) 'MAX1 encodes a cytochrome P450 family member that acts downstream of MAX3/4 to produce a carotenoid-derived branch-inhibiting hormone', *Developmental Cell*, 8(3). doi: 10.1016/j.devcel.2005.01.009.

- Boot, K. J. M. *et al.* (2016) 'Modelling the dynamics of polar auxin transport in inflorescence stems of *Arabidopsis thaliana*', *Journal of Experimental Botany*, 67(3). doi: 10.1093/jxb/erv471.
- Bouchard, R. *et al.* (2006) 'Immunophilin-like TWISTED DWARF1 modulates auxin efflux activities of *Arabidopsis* P-glycoproteins', *Journal of Biological Chemistry*, 281(41). doi: 10.1074/jbc.M604604200.
- Brand, U. *et al.* (2000) 'Dependence of stem cell fate in *Arabidopsis* on a feedback loop regulated by CLV3 activity', *Science*, 289(5479). doi: 10.1126/science.289.5479.617.
- Braun, N. *et al.* (2012) 'The pea TCP transcription factor PsBRC1 acts downstream of strigolactones to control shoot branching', *Plant Physiology*, 158(1), pp. 225–238. doi: 10.1104/pp.111.182725.
- Brewer, P. B. *et al.* (2009) 'Strigolactone acts downstream of auxin to regulate bud outgrowth in pea and *Arabidopsis*', *Plant Physiology*, 150(1). doi: 10.1104/pp.108.134783.
- Brewer, P. B. *et al.* (2015) 'Strigolactone inhibition of branching independent of polar auxin transport', *Plant Physiology*, 168(4). doi: 10.1104/pp.15.00014.
- Briggs, W. R. (1960) 'Light Dosage and Phototropic Responses of Corn and Oat Coleoptiles', *Plant Physiology*, 35(6). doi: 10.1104/pp.35.6.951.
- Brown, B. T. *et al.* (1979) 'The indirect role of 2,4-D in the maintenance of apical dominance in decapitated sunflower seedlings (*Helianthus annuus* L.)', *Planta*. doi: 10.1007/BF00380863.
- Burian, A., Barbier de Reuille, P. and Kuhlemeier, C. (2016) 'Patterns of Stem Cell Divisions Contribute to Plant Longevity', *Current Biology*, 26(11). doi: 10.1016/j.cub.2016.03.067.
- Calderón Villalobos, L. I. A. *et al.* (2012) 'A combinatorial TIR1/AFB-Aux/IAA co-receptor system for differential sensing of auxin', *Nature Chemical Biology*, 8(5). doi: 10.1038/nchembio.926.
- Cambridge, A. P. and Morris, D. A. (1996) 'Transfer of exogenous auxin from the phloem to the polar auxin transport pathway in pea (*Pisum sativum* L.)', *Planta*,

199(4). doi: 10.1007/BF00195190.

Carraro, N. *et al.* (2006) 'ZmPIN1a and ZmPIN1b encode two novel putative candidates for polar auxin transport and plant architecture determination of maize', *Plant Physiology*, 142(1). doi: 10.1104/pp.106.080119.

Casal, J. J. and Estevez, J. M. (2021) 'Auxin-Environment Integration in Growth Responses to Forage for Resources', *Cold Spring Harbor perspectives in biology*. doi: 10.1101/cshperspect.a040030.

Cecchetti, V. *et al.* (2015) 'ABCB1 and ABCB19 auxin transporters have synergistic effects on early and late Arabidopsis anther development', *Journal of Integrative Plant Biology*, 57(12). doi: 10.1111/jipb.12332.

Cecchetti, V. *et al.* (2017) 'An auxin maximum in the middle layer controls stamen development and pollen maturation in Arabidopsis', *New Phytologist*, 213(3). doi: 10.1111/nph.14207.

Chan, J. *et al.* (2020) 'Intrinsic Cell Polarity Coupled to Growth Axis Formation in Tobacco BY-2 Cells', *Current Biology*, 30(24). doi: 10.1016/j.cub.2020.09.036.

Chatfield, S. P. *et al.* (2000) 'The hormonal regulation of axillary bud growth in Arabidopsis', *Plant Journal*. doi: 10.1046/j.1365-313X.2000.00862.x.

Chevalier, F. *et al.* (2014) 'Strigolactone promotes degradation of DWARF14, an alpha/beta hydrolase essential for strigolactone signaling in Arabidopsis', *Plant Cell*, 26(3). doi: 10.1105/tpc.114.122903.

Cho, M., Lee, Z. W. and Cho, H. T. (2012) 'ATP-binding cassette B4, an auxin-efflux transporter, stably associates with the plasma membrane and shows distinctive intracellular trafficking from that of PIN-FORMED proteins', *Plant Physiology*, 159(2). doi: 10.1104/pp.112.196139.

Christensen, S. K. *et al.* (2000) 'Regulation of auxin response by the protein kinase PINOID', *Cell*, 100(4). doi: 10.1016/S0092-8674(00)80682-0.

Church, A. H. (1920) *On the interpretation of phenomena of phyllotaxis*. Oxford.

- Chute, H. M. and Maheshwari, P. (1951) 'An Introduction to the Embryology of Angiosperms.', *Bulletin of the Torrey Botanical Club*, 78(3). doi: 10.2307/2481984.
- Cieslak, M., Runions, A. and Prusinkiewicz, P. (2015) 'Auxin-driven patterning with unidirectional fluxes', in *Journal of Experimental Botany*. doi: 10.1093/jxb/erv262.
- Clark, S. E., Running, M. P. and Meyerowitz, E. M. (1993) 'CLAVATA1, a regulator of meristem and flower development in Arabidopsis', *Development*, 119(2). doi: 10.1242/dev.119.2.397.
- Clark, S. E., Running, M. P. and Meyerowitz, E. M. (1995) 'CLAVATA3 is a specific regulator of shoot and floral meristem development affecting the same processes as CLAVATA1', *Development*, 121(7). doi: 10.1242/dev.121.7.2057.
- Clough, S. J. and Bent, A. F. (1998) 'Floral dip: A simplified method for Agrobacterium-mediated transformation of Arabidopsis thaliana', *Plant Journal*, 16(6). doi: 10.1046/j.1365-313X.1998.00343.x.
- Cook, C. E. et al. (1972) 'Germination Stimulants. II. The Structure of Strigol—A Potent Seed Germination Stimulant for Witchweed (*Striga lutea* Lour.)^{1,2}', *Journal of the American Chemical Society*, 94(17). doi: 10.1021/ja00772a048.
- Coen, E. et al. (2004) 'The genetics of geometry', *Proceedings of the National Academy of Sciences of the United States of America*, 101(14). doi: 10.1073/pnas.0306308101.
- Crawford, S. et al. (2010) 'Strigolactones enhance competition between shoot branches by dampening auxin transport.', *Development* (Cambridge, England). doi: 10.1242/dev.051987.
- Dai, X. et al. (2013) 'The biochemical mechanism of auxin biosynthesis by an arabidopsis YUCCA flavin-containing monooxygenase', *Journal of Biological Chemistry*, 288(3). doi: 10.1074/jbc.M112.424077.
- Dai, Y. et al. (2006) 'Increased expression of MAP KINASE KINASE7 causes deficiency in polar auxin transport and leads to plant architectural abnormality in Arabidopsis', *Plant Cell*, 18(2). doi: 10.1105/tpc.105.037846.

Darwin, C. and Darwin, F. (1880) *The Power of Movement in Plants*. doi: 10.1017/CBO9780511693670.

Davies P.J., Lomax T.L., Muday G.K., R. P. . (1995) 'Auxin Transport', in P.J., D. (ed.) *Plant Hormones: Physiology, Biochemistry, and Molecular Biology*. Dordrecht, The Netherlands: Kluwer Academic Publishers, pp. 509–530.

Delbarre, A. *et al.* (1996) 'Comparison of mechanisms controlling uptake and accumulation of 2,4-dichlorophenoxy acetic acid, naphthalene-1-acetic acid, and indole-3-acetic acid in suspension-cultured tobacco cells', *Planta*. doi: 10.1007/BF00262639.

Depta, H. and Rubery, P. H. (1984) 'A Comparative Study of Carrier Participation in the Transport of 2,3,5-triiodobenzoic acid, indole-3-acetic acid, and 2,4-dichlorophenoxyacetic acid by *Cucurbita pepo* L. Hypocotyl Segments', *Journal of Plant Physiology*, 115(5). doi: 10.1016/S0176-1617(84)80036-X.

Dhonukshe, P. *et al.* (2007) 'Clathrin-Mediated Constitutive Endocytosis of PIN Auxin Efflux Carriers in *Arabidopsis*', *Current Biology*. doi: 10.1016/j.cub.2007.01.052.

Dhonukshe, P. *et al.* (2010) 'Plasma membrane-bound AGC3 kinases phosphorylate PIN auxin carriers at TPRXS(N/S) motifs to direct apical PIN recycling', *Development*. doi: 10.1242/dev.052456.

Doebley, J., Stec, A. and Hubbard, L. (1997) 'The evolution of apical dominance in maize', *Nature*, 386(6624). doi: 10.1038/386485a0.

Domagalska, M. A. and Leyser, O. (2011) 'Signal integration in the control of shoot branching', *Nature Reviews Molecular Cell Biology*. doi: 10.1038/nrm3088.

Dory, M. *et al.* (2018) 'Coevolving MAPK and PID phosphosites indicate an ancient environmental control of PIN auxin transporters in land plants', *FEBS Letters*, 592(1). doi: 10.1002/1873-3468.12929.

Drummond, R. S. M. *et al.* (2015) 'Environmental control of branching in *Petunia*', *Plant Physiology*, 168(2). doi: 10.1104/pp.15.00486.

Dun, E. A. *et al.* (2011) 'Antagonistic Action of Strigolactone and Cytokinin in Bud

Outgrowth Control', *Plant Physiology*. doi: 10.1104/pp.111.186783.

Dunlap, J. R. and Robacker, K. M. (1988) 'Nutrient Salts Promote Light-Induced Degradation of Indole-3-Acetic Acid in Tissue Culture Media', *Plant Physiology*, 88(2). doi: 10.1104/pp.88.2.379.

Edwards, K., Johnstone, C. and Thompson, C. (1991) 'A simple and rapid method for the preparation of plant genomic DNA for PCR analysis', *Nucleic Acids Research*. doi: 10.1093/nar/19.6.1349.

Everat-Bourbouloux, A. and Bonnemain, J.-L. (1980) 'Distribution of labelled auxin and derivatives in stem tissues of intact and decapitated broad-bean plants in relation to apical dominance', *Physiologia Plantarum*. doi: 10.1111/j.1399-3054.1980.tb04441.x.

Ferguson, B. J. and Beveridge, C. A. (2009) 'Roles for auxin, cytokinin, and strigolactone in regulating shoot branching', *Plant Physiology*, 149(4). doi: 10.1104/pp.109.135475.

Feugier, F. G. and Iwasa, Y. (2006) 'How canalization can make loops: A new model of reticulated leaf vascular pattern formation', *Journal of Theoretical Biology*, 243(2). doi: 10.1016/j.jtbi.2006.05.022.

Feugier, F. G., Mochizuki, A. and Iwasa, Y. (2005) 'Self-organization of the vascular system in plant leaves: Inter-dependent dynamics of auxin flux and carrier proteins', *Journal of Theoretical Biology*. doi: 10.1016/j.jtbi.2005.03.017.

Fletcher, J. C. (1999) 'Signaling of cell fate decisions by CLAVATA3 in Arabidopsis shoot meristems', *Science*, 283(5409). doi: 10.1126/science.283.5409.1911.

Foo, E. *et al.* (2005) 'The branching gene RAMOSUS1 mediates interactions among two novel signals and auxin in pea', *Plant Cell*, 17(2). doi: 10.1105/tpc.104.026716.

Foo, E., Turnbull, C. G. N. and Beveridge, C. A. (2001) 'Long-distance signaling and the control of branching in the rms1 mutant of pea', *Plant Physiology*, 126(1). doi: 10.1104/pp.126.1.203.

- Forestan, C., Farinati, S. and Varotto, S. (2012) 'The maize PIN gene family of auxin transporters', *Frontiers in Plant Science*, 3(FEB). doi: 10.3389/fpls.2012.00016.
- Franco-Zorrilla, J. M. *et al.* (2014) 'DNA-binding specificities of plant transcription factors and their potential to define target genes', *Proceedings of the National Academy of Sciences of the United States of America*, 111(6). doi: 10.1073/pnas.1316278111.
- Friml, J. *et al.* (2003) 'Efflux-dependent auxin gradients establish the apical-basal axis of Arabidopsis', *Nature*, 426(6963). doi: 10.1038/nature02085.
- Friml, J. *et al.* (2004) 'A PINOID-dependent binary switch in apical-basal PIN polar targeting directs auxin efflux', *Science*. doi: 10.1126/science.1100618.
- Fujita, H. and Mochizuki, A. (2006a) 'Pattern formation of leaf veins by the positive feedback regulation between auxin flow and auxin efflux carrier', *Journal of Theoretical Biology*, 241(3). doi: 10.1016/j.jtbi.2005.12.016.
- Fujita, H. and Mochizuki, A. (2006b) 'The origin of the diversity of leaf venation pattern', *Developmental Dynamics*, 235(10). doi: 10.1002/dvdy.20908.
- Galinat, W. C. (1959) 'The phytomer in relation to the floral homologies in the American *Maydea*', *Bot. Mus. Leaflet*. Harv. Univ., 19, pp. 1–32.
- Gallavotti, A. *et al.* (2008) 'sparse inflorescence1 encodes a monocot-specific YUCCA-like gene required for vegetative and reproductive development in maize', *Proceedings of the National Academy of Sciences of the United States of America*, 105(39). doi: 10.1073/pnas.0805596105.
- Gälweiler, L. *et al.* (1998) 'Regulation of polar auxin transport by AtPIN1 in Arabidopsis vascular tissue', *Science*. doi: 10.1126/science.282.5397.2226.
- Garnett, P. (2010) *Agent Based Modelling of Auxin Transport Canalisation*. University of York. Available at: <https://etheses.whiterose.ac.uk/1420/>.
- Garrison, R. (1955) 'Studies in the Development of Axillary Buds', *American Journal of Botany*, 42(3). doi: 10.2307/2438561.
- Geisler, M. *et al.* (2003) 'TWISTED DWARF1, a unique plasma membrane-

- anchored immunophilin-like protein, interacts with Arabidopsis multidrug resistance-like transporters AtPGP1 and AtPGP19', *Molecular Biology of the Cell*, 14(10). doi: 10.1091/mbc.E02-10-0698.
- Geisler, M. *et al.* (2005) 'Cellular efflux of auxin catalyzed by the Arabidopsis MDR/PGP transporter AtPGP1', *Plant Journal*, 44(2). doi: 10.1111/j.1365-313X.2005.02519.x.
- Geisler, M. and Murphy, A. S. (2006) 'The ABC of auxin transport: The role of p-glycoproteins in plant development', *FEBS Letters*. doi: 10.1016/j.febslet.2005.11.054.
- Geldner, N. *et al.* (2001) 'Auxin transport inhibitors block PIN1 cycling and vesicle trafficking', *Nature*. doi: 10.1038/35096571.
- Giulini, A., Wang, J. and Jackson, D. (2004) 'Control of phyllotaxy by the cytokinin-inducible response regulator homologue ABPHYL1', *Nature*, 430(7003). doi: 10.1038/nature02778.
- Gocal, G. F. W. *et al.* (1991) 'Changes after decapitation in concentrations of indole-3-acetic acid and abscisic acid in the larger axillary bud of *Phaseolus vulgaris* L. cv tender green', *Plant Physiology*, 95(2). doi: 10.1104/pp.95.2.344.
- Goldsmith, M. (1977) 'THE POLAR TRANSPORT OF AUXIN', *Annual Review of Plant Physiology*, 28, pp. 439–478.
- Goldsmith, M. H. M. (2003) 'The Polar Transport of Auxin', *Annual Review of Plant Physiology*. doi: 10.1146/annurev.pp.28.060177.002255.
- Gomez-Roldan, V. *et al.* (2008) 'Strigolactone inhibition of shoot branching', *Nature*. doi: 10.1038/nature07271.
- Gray, W. M. *et al.* (1999) 'Identification of an SCF ubiquitin-ligase complex required for auxin response in *Arabidopsis thaliana*', *Genes and Development*, 13(13). doi: 10.1101/gad.13.13.1678.
- Gray, W. M. *et al.* (2001) 'Auxin regulates SCFTIR1-dependent degradation of AUX/IAA proteins', *Nature*, 414(6861). doi: 10.1038/35104500.
- Greb, T. *et al.* (2003) 'Molecular analysis of the LATERAL SUPPRESSOR gene

- in Arabidopsis reveals a conserved control mechanism for axillary meristem formation', *Genes and Development*, 17(9). doi: 10.1101/gad.260703.
- Grieneisen, V. A. *et al.* (2007) 'Auxin transport is sufficient to generate a maximum and gradient guiding root growth', *Nature*, 449(7165). doi: 10.1038/nature06215.
- Grones, P. *et al.* (2018) 'PID/WAG-mediated phosphorylation of the Arabidopsis PIN3 auxin transporter mediates polarity switches during gravitropism', *Scientific Reports*. doi: 10.1038/s41598-018-28188-1.
- Guan, J. C. *et al.* (2012) 'Diverse roles of strigolactone signaling in maize architecture and the uncoupling of a branching-specific subnetwork', *Plant Physiology*, 160(3). doi: 10.1104/pp.112.204503.
- Guilfoyle, T. J. and Hagen, G. (2007) 'Auxin response factors', *Current Opinion in Plant Biology*. doi: 10.1016/j.pbi.2007.08.014.
- Guo, R. *et al.* (2021) 'Local conjugation of auxin by the GH3 amido synthetases is required for normal development of roots and flowers in Arabidopsis', *bioRxiv*, p. 2021.10.04.463114. doi: 10.1101/2021.10.04.463114.
- Haecker, A. *et al.* (2004) 'Expression dynamics of WOX genes mark cell fate decisions during early embryonic patterning in Arabidopsis thaliana', *Development*, 131(3). doi: 10.1242/dev.00963.
- Hajný, J. *et al.* (2020) 'Receptor kinase module targets PIN-dependent auxin transport during canalization', *Science*, 370(6516). doi: 10.1126/SCIENCE.ABA3178.
- Hall, S. M. and Hillman, J. R. (1975) 'Correlative inhibition of lateral bud growth in Phaseolus vulgaris L. timing of bud growth following decapitation', *Planta*. doi: 10.1007/BF00383862.
- Hamiaux, C. *et al.* (2012) 'DAD2 is an alpha/beta hydrolase likely to be involved in the perception of the plant branching hormone, strigolactone', *Current Biology*, 22(21). doi: 10.1016/j.cub.2012.08.007.
- Hao, L. *et al.* (2009) 'DWARF27, an iron-containing protein required for the biosynthesis of strigolactones, regulates rice tiller bud outgrowth', *Plant Cell*, 21(5).

doi: 10.1105/tpc.109.065987.

Hardtke, C. S. and Berleth, T. (1998) 'The Arabidopsis gene MONOPTEROS encodes a transcription factor mediating embryo axis formation and vascular development', *EMBO Journal*, 17(5). doi: 10.1093/emboj/17.5.1405.

Harrison, S. J. *et al.* (2006) 'A rapid and robust method of identifying transformed Arabidopsis thaliana seedlings following floral dip transformation', *Plant Methods*, 2(1). doi: 10.1186/1746-4811-2-19.

Hayward, A. *et al.* (2009) 'Interactions between Auxin and Strigolactone in Shoot Branching Control', *Plant Physiology*. doi: 10.1104/pp.109.137646.

Heisler, M. G. *et al.* (2005) 'Patterns of auxin transport and gene expression during primordium development revealed by live imaging of the Arabidopsis inflorescence meristem', *Current Biology*. doi: 10.1016/j.cub.2005.09.052.

Heisler, M. G. and Jönsson, H. (2006) 'Modeling auxin transport and plant development', *Journal of Plant Growth Regulation*, 25(4). doi: 10.1007/s00344-006-0066-x.

Hempel, F. D. and Feldman, L. J. (1994) 'Bi-directional inflorescence development in Arabidopsis thaliana: Acropetal initiation of flowers and basipetal initiation of paraclades', *Planta*, 192(2). doi: 10.1007/BF01089045.

Hertel, R. (1987) 'Auxin Transport: Binding of Auxins and Phytotropins to the Carriers. Accumulation into and Efflux from Membrane Vesicles', in *Plant Hormone Receptors*. doi: 10.1007/978-3-642-72779-5_8.

Hertel, R., Lomax, T. L. and Briggs, W. R. (1983) 'Auxin transport in membrane vesicles from Cucurbita pepo L.', *Planta*, 157(3). doi: 10.1007/BF00405182.

Herud-Sikimic, O. *et al.* (2021) 'A biosensor for the direct visualization of auxin', *Nature*, 592(7856). doi: 10.1038/s41586-021-03425-2.

Hofmeister, W. (1868) *Handbuch der physiologischen Botanik*. Engelmann.
Hohm, T. *et al.* (2014) 'Plasma membrane H⁺-ATPase regulation is required for auxin gradient formation preceding phototropic growth', *Molecular Systems*

Biology, 10(9). doi: 10.15252/msb.20145247.

Hohm, T. et al. (2014) 'Plasma membrane H⁺-ATPase regulation is required for auxin gradient formation preceding phototropic growth', *Molecular Systems Biology*, 10(9). doi: 10.15252/msb.20145247.

Hošek, P. et al. (2012) 'Auxin transport at cellular level: New insights supported by mathematical modelling', *Journal of Experimental Botany*. doi: 10.1093/jxb/ers074.

Huang, F. et al. (2010) 'Phosphorylation of Conserved PIN Motifs Directs Arabidopsis PIN1 Polarity and Auxin Transport', *The Plant Cell*. doi: 10.1105/tpc.109.072678.

Huijser, P. and Schmid, M. (2011) 'The control of developmental phase transitions in plants', *Development*. doi: 10.1242/dev.063511.

Hwang, I. and Sheen, J. (2001) 'Two-component circuitry in Arabidopsis cytokinin signal transduction', *Nature*. doi: 10.1038/35096500.

Inoue, T. et al. (2001) 'Identification of CRE1 as a cytokinin receptor from Arabidopsis', *Nature*. doi: 10.1038/35059117.

Irish, V. F. and Sussex, I. M. (1992) 'A fate map of the Arabidopsis embryonic shoot apical meristem', *Development*, 115(3).

Ito, H. and Gray, W. M. (2006) 'A gain-of-function mutation in the arabidopsis pleiotropic drug resistance transporter PDR9 confers resistance to auxinic herbicides', *Plant Physiology*, 142(1). doi: 10.1104/pp.106.084533.

Itoh, J. I. et al. (2012) 'Rice DECUSSATE controls phyllotaxy by affecting the cytokinin signaling pathway', *Plant Journal*, 72(6). doi: 10.1111/j.1365-313x.2012.05123.x.

Jackson, R. G. et al. (2001) 'Identification and Biochemical Characterization of an Arabidopsis Indole-3-acetic Acid Glucosyltransferase', *Journal of Biological Chemistry*, 276(6). doi: 10.1074/jbc.M006185200.

- Jackson, R. G. *et al.* (2002) 'Over-expression of an Arabidopsis gene encoding a glucosyltransferase of indole-3-acetic acid: Phenotypic characterisation of transgenic lines', *Plant Journal*, 32(4). doi: 10.1046/j.1365-313X.2002.01445.x.
- Jain, M. *et al.* (2006) 'Structure and expression analysis of early auxin-responsive Aux/IAA gene family in rice (*Oryza sativa*)', *Functional and Integrative Genomics*, 6(1). doi: 10.1007/s10142-005-0005-0.
- Jakubowska, A. and Kowalczyk, S. (2005) 'A specific enzyme hydrolyzing 6-O(4-O)-indole-3-ylacetyl-beta-D-glucose in immature kernels of *Zea mays*', *Journal of Plant Physiology*, 162(2). doi: 10.1016/j.jplph.2004.05.015.
- Jenness, M. K. *et al.* (2019) 'The arabidopsis ATP-BINDING CASSETTE transporter ABCB21 regulates auxin levels in cotyledons, the root pericycle, and leaves', *Frontiers in Plant Science*, 10. doi: 10.3389/fpls.2019.00806.
- Jeong, I. K. *et al.* (2007) 'yucca6, a dominant mutation in arabidopsis, affects auxin accumulation and auxin-related phenotypes', *Plant Physiology*, 145(3). doi: 10.1104/pp.107.104935.
- Jeong, S., Trotochaud, A. E. and Clark, S. E. (1999) 'The Arabidopsis CLAVATA2 gene encodes a receptor-like protein required for the stability of the CLAVATA1 receptor-like kinase', *Plant Cell*, 11(10). doi: 10.1105/tpc.11.10.1925.
- Jia, W. *et al.* (2016) 'Mitogen-Activated Protein Kinase Cascade MKK7-MPK6 Plays Important Roles in Plant Development and Regulates Shoot Branching by Phosphorylating PIN1 in Arabidopsis', *PLoS Biology*, 14(9). doi: 10.1371/journal.pbio.1002550.
- Jiang, L. *et al.* (2013) 'DWARF 53 acts as a repressor of strigolactone signalling in rice', *Nature*, 504(7480). doi: 10.1038/nature12870.
- Jin, S., Hou, B. and Zhang, G. (2021) 'The ectopic expression of Arabidopsis glucosyltransferase UGT74D1 affects leaf positioning through modulating indole-3-acetic acid homeostasis', *Scientific Reports*, 11(1). doi: 10.1038/s41598-021-81016-x.
- Johnson, X. *et al.* (2006) 'Branching genes are conserved across species. Genes controlling a novel signal in pea are coregulated by other long-distance signals', *Plant Physiology*, 142(3). doi: 10.1104/pp.106.087676.

- Jones, M. A. *et al.* (2002) 'The arabidopsis Rop2 GTPase is a positive regulator of both root hair initiation and tip growth', *Plant Cell*, 14(4). doi: 10.1105/tpc.010359.
- Jönsson, H. *et al.* (2006) 'An auxin-driven polarized transport model for phyllotaxis', *Proceedings of the National Academy of Sciences of the United States of America*, 103(5). doi: 10.1073/pnas.0509839103.
- Jönsson, H. *et al.* (2010) 'Alignment between PIN1 polarity and microtubule orientation in the shoot apical meristem reveals a tight coupling between morphogenesis and auxin transport', *PLoS Biology*, 8(10). doi: 10.1371/journal.pbio.1000516.
- Jurgens, G. and Mayer, U. (1994) *Arabidopsis, Embryos. Colour Atlas of Development*.
- Kalousek, P. *et al.* (2010) 'Cytokinins and polar transport of auxin in axillary pea buds', *Acta Universitatis Agriculturae et Silviculturae Mendelianae Brunensis*. doi: 10.11118/actaun201058040079.
- Kamimoto, Y. *et al.* (2012) 'Arabidopsis ABCB21 is a facultative auxin importer/exporter regulated by cytoplasmic auxin concentration', *Plant and Cell Physiology*, 53(12). doi: 10.1093/pcp/pcs149.
- Katekar, G. and Geissler, A. (1980) 'Auxin Transport Inhibitors: IV. EVIDENCE OF A COMMON MODE OF ACTION FOR A PROPOSED CLASS OF AUXIN TRANSPORT INHIBITORS: THE PHYTOTROPINS', *Plant Physiology*, 66(6). doi: 10.1104/pp.66.6.1190.
- Kawasaki, M. L. and Bell, A. D. (1991) 'Plant Form. An Illustrated Guide to Flowering Plant Morphology.', *Brittonia*, 43(3). doi: 10.2307/2807042.
- Kepinski, S. and Leyser, O. (2005) 'The Arabidopsis F-box protein TIR1 is an auxin receptor', *Nature*, 435(7041). doi: 10.1038/nature03542.
- Kim, J. Y. *et al.* (2010) 'Identification of an ABCB/P-glycoprotein-specific inhibitor of auxin transport by chemical genomics', *Journal of Biological Chemistry*, 285(30). doi: 10.1074/jbc.M110.105981.

- Kleine-Vehn, J. *et al.* (2008) 'Cellular and molecular requirements for polar PIN targeting and transcytosis in plants', *Molecular Plant*, 1(6). doi: 10.1093/mp/ssf062.
- Kleine-Vehn, J. *et al.* (2011) 'Recycling, clustering, and endocytosis jointly maintain PIN auxin carrier polarity at the plasma membrane', *Molecular Systems Biology*. doi: 10.1038/msb.2011.72.
- Knöllner, A. S. *et al.* (2010) 'Brachytic2/ZmABCB1 functions in IAA export from intercalary meristems', *Journal of Experimental Botany*, 61(13). doi: 10.1093/jxb/erq180.
- Koepfli, J., Thimann, K. and Went, F. (1938) 'Phytohormones: structure and physiological activity. I', *Journal of Biological Chemistry*. New York ; Baltimore., 122, pp. 763–780.
- Kögl, F., Haagen-Smit, A. J. and Erxleben, H. (1934) 'Über ein neues Auxin ("Hetero-auxin") aus Harn. 11. Mitteilung über pflanzliche Wachstumsstoffe', *Hoppe-Seyler's Zeitschrift für Physiologische Chemie*, 228(1–2). doi: 10.1515/bchm2.1934.228.1-2.90.
- Kowalczyk, M. and Sandberg, G. (2001) 'Quantitative analysis of indole-3-acetic acid metabolites in arabidopsis', *Plant Physiology*, 127(4). doi: 10.1104/pp.010525.
- Kramer, E. M. (2002) 'A mathematical model of pattern formation in the vascular cambium of trees', *Journal of Theoretical Biology*, 216(2). doi: 10.1006/jtbi.2002.2551.
- Kramer, E. M. (2009) 'Auxin-regulated cell polarity: an inside job?', *Trends in Plant Science*. doi: 10.1016/j.tplants.2009.02.005.
- Krecek, P. *et al.* (2009) 'The PIN-FORMED (PIN) protein family of auxin transporters', *Genome Biology*. doi: 10.1186/gb-2009-10-12-249.
- Krupinski, P. and Jönsson, H. (2010) 'Modeling auxin-regulated development.', *Cold Spring Harbor perspectives in biology*.
- Kubeš, M. *et al.* (2012) 'The Arabidopsis concentration-dependent influx/efflux transporter ABCB4 regulates cellular auxin levels in the root epidermis', *Plant*

Journal, 69(4). doi: 10.1111/j.1365-313X.2011.04818.x.

Kudo, T., Kiba, T. and Sakakibara, H. (2010) 'Metabolism and long-distance translocation of cytokinins', *Journal of Integrative Plant Biology*. doi: 10.1111/j.1744-7909.2010.00898.x.

Kuhn, A. *et al.* (2019) 'Two auxin response elements fine-tune pinoid expression during gynoecium development in *Arabidopsis thaliana*', *Biomolecules*, 9(10). doi: 10.3390/biom9100526.

Lanková, M. *et al.* (2010) 'Auxin influx inhibitors 1-NOA, 2-NOA, and CHPAA interfere with membrane dynamics in tobacco cells', *Journal of Experimental Botany*, 61(13). doi: 10.1093/jxb/erq172.

Larsson, E. *et al.* (2014) 'Polar auxin transport is essential for medial versus lateral tissue specification and vascular-mediated valve outgrowth in *Arabidopsis* gynoecia', *Plant Physiology*, 166(4). doi: 10.1104/pp.114.245951.

Larsson, E., Franks, R. G. and Sundberg, E. (2013) 'Auxin and the *Arabidopsis thaliana* gynoecium', *Journal of Experimental Botany*. doi: 10.1093/jxb/ert099.

Laufs, P. *et al.* (1998) 'Cellular parameters of the shoot apical meristem in *Arabidopsis*', *Plant Cell*, 10(8). doi: 10.1105/tpc.10.8.1375.

LeClere, S. *et al.* (2002) 'Characterization of a family of IAA-amino acid conjugate hydrolases from *Arabidopsis*', *Journal of Biological Chemistry*, 277(23). doi: 10.1074/jbc.M111955200.

Lee, H. *et al.* (2021) 'Calcium-dependent protein kinase 29 modulates PIN-FORMED polarity and *Arabidopsis* development via its own phosphorylation code', *Plant Cell*, 33(11). doi: 10.1093/plcell/koab207.

Leitner, J. *et al.* (2012) 'Lysine63-linked ubiquitylation of PIN2 auxin carrier protein governs hormonally controlled adaptation of *Arabidopsis* root growth', *Proceedings of the National Academy of Sciences of the United States of America*, 109(21). doi: 10.1073/pnas.1200824109.

Leopold, A. C. (1964) 'The Polarity of Auxin Transport.', *Brookhaven symposia in*

biology, 16, pp. 218–234.

Lewis, D. R. *et al.* (2007) 'Separating the roles of acropetal and basipetal auxin transport on gravitropism with mutations in two arabidopsis multidrug resistance-like ABC transporter genes', *Plant Cell*, 19(6). doi: 10.1105/tpc.107.051599.

Li, C. J. and Bangerth, F. (1999) 'Autoinhibition of indoleacetic acid transport in the shoots of two-branched pea (*Pisum sativum*) plants and its relationship to correlative dominance', *Physiologia Plantarum*. doi: 10.1034/j.1399-3054.1999.106409.x.

Li, H. *et al.* (2021) 'Cellular requirements for PIN polar cargo clustering in *Arabidopsis thaliana*', *New Phytologist*, 229(1). doi: 10.1111/nph.16887.

Li, J., Li, C. and Smith, S. M. (2017) *Hormone Metabolism and Signaling in Plants*, Hormone Metabolism and Signaling in Plants.

Li, L. *et al.* (2008) 'The possible action mechanisms of indole-3-acetic acid methyl ester in *Arabidopsis*', *Plant Cell Reports*, 27(3). doi: 10.1007/s00299-007-0458-9.

Liang, Y. *et al.* (2016) 'SMAX1-LIKE7 signals from the nucleus to regulate shoot development in *arabidopsis* via partially EAR motif-independent mechanisms', *Plant Cell*, 28(7). doi: 10.1105/tpc.16.00286.

Liao, C. Y. *et al.* (2015) 'Reporters for sensitive and quantitative measurement of auxin response', *Nature Methods*, 12(3). doi: 10.1038/nmeth.3279.

Liu, Z. Bin *et al.* (1994) 'Soybean GH3 promoter contains multiple auxin-inducible elements', *Plant Cell*, 6(5). doi: 10.2307/3869869.

Ljung, K., Bhalerao, R. P. and Sandberg, G. (2001) 'Sites and homeostatic control of auxin biosynthesis in *Arabidopsis* during vegetative growth', *Plant Journal*. doi: 10.1046/j.1365-313X.2001.01173.x.

Lomax, T. L., Mehlhorn, R. J. and Briggs, W. R. (1985) 'Active auxin uptake by zucchini membrane vesicles: quantitation using ESR volume and delta pH determinations.', *Proceedings of the National Academy of Sciences of the United States of America*, 82(19). doi: 10.1073/pnas.82.19.6541.

- Ludwig-Müller, J. (2011) 'Auxin conjugates: Their role for plant development and in the evolution of land plants', *Journal of Experimental Botany*, 62(6). doi: 10.1093/jxb/erq412.
- Mach, J. (2015) 'Strigolactones regulate plant growth in arabidopsis via degradation of the DWARF53-like proteins SMXL6, 7, and 8', *Plant Cell*. doi: 10.1105/tpc.15.00950.
- Mansfield, C. *et al.* (2018) 'Ectopic BASL Reveals Tissue Cell Polarity throughout Leaf Development in Arabidopsis thaliana', *Current Biology*, 28(16). doi: 10.1016/j.cub.2018.06.019.
- Marchant, A. *et al.* (1999) 'AUX1 regulates root gravitropism in Arabidopsis by facilitating auxin uptake within root apical tissues', *EMBO Journal*, 18(8). doi: 10.1093/emboj/18.8.2066.
- Marhavý, P. *et al.* (2014) 'Cytokinin controls polarity of PIN1-dependent Auxin transport during lateral root organogenesis', *Current Biology*. doi: 10.1016/j.cub.2014.04.002.
- Martinez, C. C. *et al.* (2016) 'A sister of PIN1 gene in tomato (*Solanum lycopersicum*) defines leaf and flower organ initiation patterns by maintaining epidermal auxin flux', *Developmental Biology*, 419(1). doi: 10.1016/j.ydbio.2016.08.011.
- Marzec, M. *et al.* (2020) 'Diverse roles of max1 homologues in rice', *Genes*, 11(11). doi: 10.3390/genes11111348.
- Mashiguchi, K. *et al.* (2011) 'The main auxin biosynthesis pathway in Arabidopsis', *Proceedings of the National Academy of Sciences of the United States of America*, 108(45). doi: 10.1073/pnas.1108434108.
- Mayer, K. F. X. *et al.* (1998) 'Role of WUSCHEL in regulating stem cell fate in the Arabidopsis shoot meristem', *Cell*, 95(6). doi: 10.1016/S0092-8674(00)81703-1.
- Mazur, E., Kulik, I., *et al.* (2020) 'Auxin canalization and vascular tissue formation by TIR1/AFB-mediated auxin signaling in Arabidopsis', *New Phytologist*. doi: 10.1111/nph.16446.
- Mazur, E., Gallei, M., *et al.* (2020) 'Clathrin-mediated trafficking and PIN

trafficking are required for auxin canalization and vascular tissue formation in *Arabidopsis*', *Plant Science*, 293. doi: 10.1016/j.plantsci.2020.110414.

Mazur, E., Benková, E. and Friml, J. (2016) 'Vascular cambium regeneration and vessel formation in wounded inflorescence stems of *Arabidopsis*', *Scientific Reports*. doi: 10.1038/srep33754.

McConnell, J. R. and Barton, M. K. (1998) 'Leaf polarity and meristem formation in *Arabidopsis*', *Development*, 125(15). doi: 10.1242/dev.125.15.2935.

Merks, R. M. H. *et al.* (2007) 'Canalization without flux sensors: a traveling-wave hypothesis', *Trends in Plant Science*, 12(9). doi: 10.1016/j.tplants.2007.08.004.

Michniewicz, M. *et al.* (2007) 'Antagonistic Regulation of PIN Phosphorylation by PP2A and PINOID Directs Auxin Flux', *Cell*. doi: 10.1016/j.cell.2007.07.033.

Minakuchi, K. *et al.* (2010) 'FINE CULM1 (FC1) works downstream of strigolactones to inhibit the outgrowth of axillary buds in rice', *Plant and Cell Physiology*, 51(7). doi: 10.1093/pcp/pcq083.

Mitchison, G. J. (1980) 'A model for vein formation in higher plants', *Proceedings of the Royal Society of London - Biological Sciences*, 207(1166). doi: 10.1098/rspb.1980.0015.

Mitchison, G. J., Hanke, D. E. and Sheldrake, A. R. (1981) 'The Polar Transport of Auxin and Vein Patterns in Plants [and Discussion]', *Philosophical Transactions of the Royal Society B: Biological Sciences*. doi: 10.1098/rstb.1981.0154.

Morgan, D. G. (1964) 'Influence of alpha-naphthylphthalamic acid on the movement of indolyl-3-acetic acid in plants', *Nature*, 201(4918). doi: 10.1038/201476a0.

Morris, D. A. (1977) 'Transport of exogenous auxin in two-branched dwarf pea seedlings (*Pisum sativum* L.) - Some implications for polarity and apical dominance', *Planta*. doi: 10.1007/BF00387930.

Morris, D. A. and Thomas, A. G. (1978) 'A microautoradiographic study of auxin transport in the stem of intact pea seedlings (*Pisum sativum* L.)', *Journal of Experimental Botany*, 29(1). doi: 10.1093/jxb/29.1.147.

- Morris, S. E. *et al.* (2001) 'Mutational analysis of branching in pea. Evidence that Rms1 and Rms5 regulate the same novel signal', *Plant Physiology*, 126(3). doi: 10.1104/pp.126.3.1205.
- Moubayidin, L. and Østergaard, L. (2014) 'Dynamic control of auxin distribution imposes a bilateral-to-radial symmetry switch during gynoecium development', *Current Biology*, 24(22). doi: 10.1016/j.cub.2014.09.080.
- van Mourik, S. *et al.* (2012) 'Simulation of organ patterning on the floral meristem using a polar auxin transport model', *PLoS ONE*, 7(1). doi: 10.1371/journal.pone.0028762.
- Mravec, J. *et al.* (2009) 'Subcellular homeostasis of phytohormone auxin is mediated by the ER-localized PIN5 transporter', *Nature*, 459(7250). doi: 10.1038/nature08066.
- Müller, D. *et al.* (2015) 'Cytokinin is required for escape but not release from auxin mediated apical dominance', *Plant Journal*. doi: 10.1111/tpj.12862.
- Müller, R., Bleckmann, A. and Simon, R. (2008) 'The receptor kinase CORYNE of Arabidopsis transmits the stem cell-limiting signal CLAVATA3 independently of CLAVATA1', *Plant Cell*, 20(4). doi: 10.1105/tpc.107.057547.
- Murphy, A. and Taiz, L. (1999) 'Naphthylphthalamic acid is enzymatically hydrolyzed at the hypocotyl-root transition zone and other tissues of Arabidopsis thaliana seedlings', *Plant Physiology and Biochemistry*, 37(6). doi: 10.1016/S0981-9428(99)80047-3.
- Napoli, C. (1996) 'Highly branched phenotype of the petunia dad1-1 mutant is reversed by grafting', *Plant Physiology*, 111(1). doi: 10.1104/pp.111.1.27.
- Naramoto, S. *et al.* (2010) 'ADP-ribosylation factor machinery mediates endocytosis in plant cells', *Proceedings of the National Academy of Sciences of the United States of America*, 107(50). doi: 10.1073/pnas.1016260107.
- Nelson, D. C. *et al.* (2011) 'F-box protein MAX2 has dual roles in karrikin and strigolactone signaling in Arabidopsis thaliana', *Proceedings of the National Academy of Sciences of the United States of America*, 108(21). doi: 10.1073/pnas.1100987108.

- Nimchuk, Z. L., Tarr, P. T. and Meyerowitz, E. M. (2011) 'An evolutionarily conserved pseudokinase mediates stem cell production in plants', *Plant Cell*. doi: 10.1105/tpc.110.075622.
- Nissen, S. J. and Sutter, E. G. (1990) 'Stability of IAA and IBA in Nutrient Medium to Several Tissue Culture Procedures', *HortScience*, 25(7). doi: 10.21273/hortsci.25.7.800.
- Nodzynski, T. *et al.* (2010) 'PIN phosphorylation is sufficient to mediate PIN polarity and direct auxin transport', *Proceedings of the National Academy of Sciences*. doi: 10.1073/pnas.0909460107.
- Noh, B. (2001) 'Multidrug Resistance-like Genes of Arabidopsis Required for Auxin Transport and Auxin-Mediated Development', *The Plant Cell Online*. doi: 10.1105/tpc.13.11.2441.
- Van Noorden, G. E. *et al.* (2006) 'Defective long-distance auxin transport regulation in the *Medicago truncatula* super numeric nodules mutant', *Plant Physiology*, 140(4). doi: 10.1104/pp.105.075879.
- Normanly, J., Cohen, J. D. and Fink, G. R. (1993) 'Arabidopsis thaliana auxotrophs reveal a tryptophan-independent biosynthetic pathway for indole-3-acetic acid', *Proceedings of the National Academy of Sciences of the United States of America*, 90(21). doi: 10.1073/pnas.90.21.10355.
- Notredame, C., Higgins, D. G. and Heringa, J. (2000) 'T-coffee: A novel method for fast and accurate multiple sequence alignment', *Journal of Molecular Biology*, 302(1). doi: 10.1006/jmbi.2000.4042.
- O'Connor, D. L. *et al.* (2014) 'A Division in PIN-Mediated Auxin Patterning during Organ Initiation in Grasses', *PLoS Computational Biology*. doi: 10.1371/journal.pcbi.1003447.
- O'Connor, D. L. *et al.* (2017) 'Cross-species functional diversity within the PIN auxin efflux protein family', *eLife*. doi: 10.7554/eLife.31804.
- O'Malley, R. C. *et al.* (2016) 'Cistrome and Epicistrome Features Shape the Regulatory DNA Landscape', *Cell*, 165(5). doi: 10.1016/j.cell.2016.04.038.
- O'Sullivan, O. *et al.* (2004) '3DCoffee: Combining protein sequences and

- structures within multiple sequence alignments', *Journal of Molecular Biology*, 340(2). doi: 10.1016/j.jmb.2004.04.058.
- Ogawa, M. *et al.* (2008) 'Arabidopsis CLV3 peptide directly binds CLV1 ectodomain', *Science*, 319(5861). doi: 10.1126/science.1150083.
- Okada, K. *et al.* (1991) 'Requirement of the Auxin Polar Transport System in Early Stages of Arabidopsis Floral Bud Formation.', *Plant Cell*.
- Ongaro, V. *et al.* (2008) 'Interactions between axillary branches of Arabidopsis', *Molecular Plant*. doi: 10.1093/mp/ssn007.
- Östin, A. *et al.* (1998) 'Metabolism of indole-3-acetic acid in arabidopsis', *Plant Physiology*, 118(1), pp. 285–296. doi: 10.1104/pp.118.1.285.
- Ostrowski, M., Hetmann, A. and Jakubowska, A. (2015) 'Indole-3-acetic acid UDP-glucosyltransferase from immature seeds of pea is involved in modification of glycoproteins', *Phytochemistry*, 117(1). doi: 10.1016/j.phytochem.2015.05.023.
- Paciorek, T. *et al.* (2005) 'Auxin inhibits endocytosis and promotes its own efflux from cells', *Nature*. doi: 10.1038/nature03633.
- Palmer, C. M., Bush, S. M. and Maloof, J. N. (2013) 'Phenotypic and Developmental Plasticity in Plants', in *eLS*. doi: 10.1002/9780470015902.a0002092.pub2.
- Parry, G. *et al.* (2001) 'Quick on the uptake: Characterization of a family of plant auxin influx carriers', *Journal of Plant Growth Regulation*. doi: 10.1007/s003440010030.
- Payne, R. J. H. and Grierson, C. S. (2009) 'A theoretical model for ROP localisation by auxin in arabidopsis root hair cells', *PLoS ONE*, 4(12). doi: 10.1371/journal.pone.0008337.
- Peaucelle, A. *et al.* (2008) 'Arabidopsis Phyllotaxis Is Controlled by the Methyl-Esterification Status of Cell-Wall Pectins', *Current Biology*, 18(24). doi: 10.1016/j.cub.2008.10.065.
- Peaucelle, A. *et al.* (2011) 'Pectin-induced changes in cell wall mechanics

- underlie organ initiation in Arabidopsis', *Current Biology*, 21(20). doi: 10.1016/j.cub.2011.08.057.
- Peng, J. and Chen, R. (2011) 'Auxin efflux transporter MtPIN10 regulates compound leaf and flower development in medicago truncatula', *Plant Signaling and Behaviour*, 6(10). doi: 10.4161/psb.6.10.17326.
- Perales, M. *et al.* (2016) 'Threshold-dependent transcriptional discrimination underlies stem cell homeostasis', *Proceedings of the National Academy of Sciences of the United States of America*, 113(41). doi: 10.1073/pnas.1607669113.
- Péret, B. *et al.* (2012) 'AUX/LAX genes encode a family of auxin influx transporters that perform distinct functions during arabidopsis development', *Plant Cell*, 24(7). doi: 10.1105/tpc.112.097766.
- Peterson, S. V. *et al.* (2009) 'An auxin gradient and maximum in the arabidopsis root apex shown by high-resolution cell-specific analysis of IAA distribution and synthesis', *Plant Cell*, 21(6). doi: 10.1105/tpc.109.066480.
- Petrášek, J. *et al.* (2002) 'Auxin efflux carrier activity and auxin accumulation regulate cell division and polarity in tobacco cells', *Planta*, 216(2). doi: 10.1007/s00425-002-0845-y.
- Petrášek, J. *et al.* (2003) 'Do phytohormones inhibit auxin efflux by impairing vesicle traffic?', *Plant Physiology*. doi: 10.1104/pp.012740.
- Phillips, K. A. *et al.* (2011) 'vanishing tassel2 Encodes a Grass-Specific tryptophan aminotransferase required for vegetative and reproductive development in maize', *Plant Cell*, 23(2). doi: 10.1105/tpc.110.075267.
- Poethig, R. S. (2013) 'Vegetative phase change and shoot maturation in plants', in *Current Topics in Developmental Biology*. doi: 10.1016/B978-0-12-396968-2.00005-1.
- Poirot, O. *et al.* (2004) '3DCoffee@igs: A web server for combining sequences and structures into a multiple sequence alignment', *Nucleic Acids Research*, 32(WEB SERVER ISS.). doi: 10.1093/nar/gkh382.

- Porco, S. *et al.* (2016) 'Dioxygenase-encoding AtDAO1 gene controls IAA oxidation and homeostasis in arabidopsis', *Proceedings of the National Academy of Sciences of the United States of America*, 113(39). doi: 10.1073/pnas.1604375113.
- Porter, W. and KV, T. (1965) 'Molecular requirements for auxin action – I. Halogenated indoles and indoleacetic acid', *Phytochemistry*. Oxford : Pergamon Press, 4, pp. 229–243.
- Prasad, T. K., Hosokawa, Z. and Cline, M. G. (1989) 'Effects of Auxin, Auxin-Transport Inhibitors and Mineral Nutrients on Apical Dominance in *Pharbitis nil*', *Journal of Plant Physiology*, 135(4). doi: 10.1016/S0176-1617(89)80106-3.
- Prát, T. *et al.* (2018) 'WRKY23 is a component of the transcriptional network mediating auxin feedback on PIN polarity', *PLoS Genetics*, 14(1). doi: 10.1371/journal.pgen.1007177.
- Prusinkiewicz, P. *et al.* (2009) 'Control of bud activation by an auxin transport switch', *Proceedings of the National Academy of Sciences*. doi: 10.1073/pnas.0906696106.
- Qin, G. *et al.* (2005) 'An indole-3-acetic acid carboxyl methyltransferase regulates Arabidopsis leaf development', *Plant Cell*, 17(10). doi: 10.1105/tpc.105.034959.
- R., S. (1937) 'On the Nature of Correlative Inhibition', *New Phytologist*, 36(4). doi: 10.1111/j.1469-8137.1937.tb06917.x.
- Raines, T. *et al.* (2016) 'The cytokinin response factors modulate root and shoot growth and promote leaf senescence in Arabidopsis', *Plant Journal*. doi: 10.1111/tpj.13097.
- Ramos, J. A. *et al.* (2001) 'Rapid Degradation of Auxin/Indoleacetic Acid Proteins Requires Conserved Amino Acids of Domain II and Is Proteasome Dependent', *The Plant Cell*, 13(10). doi: 10.1105/tpc.010244.
- Rampey, R. A. *et al.* (2004) 'A family of auxin-conjugate hydrolases that contributes to free indole-3-acetic acid levels during arabidopsis germination', *Plant Physiology*, 135(2). doi: 10.1104/pp.104.039677.
- Rashotte, A. M. *et al.* (2006) 'A subset of Arabidopsis AP2 transcription

- factors mediates cytokinin responses in concert with a two-component pathway', *Proceedings of the National Academy of Sciences*. doi: 10.1073/pnas.0602038103.
- Raven, J. A. (1975) 'Transport of Indoleacetic Acid in Plant Cells in Relation to pH and Electrical Potential Gradients, and its Significance for Polar IAA Transportn', *New Phytologist*, 74(2). doi: 10.1111/j.1469-8137.1975.tb02602.x.
- Reed, R. C., Brady, S. R. and Muday, G. K. (1998) 'Inhibition of auxin movement from the shoot into the root inhibits lateral root development in arabidopsis', *Plant Physiology*. doi: 10.1104/pp.118.4.1369.
- Reinhardt, D. *et al.* (2003) 'Regulation of phyllotaxis by polar auxin transport', *Nature*, 426(6964). doi: 10.1038/nature02081.
- Reinhardt, D. (2005) 'Regulation of phyllotaxis.', *The International journal of developmental biology*. Spain, 49(5–6), pp. 539–546. doi: 10.1387/ijdb.041922dr.
- Reinhardt, D., Mandel, T. and Kuhlemeier, C. (2000) 'Auxin regulates the initiation and radial position of plant lateral organs', *Plant Cell*, 12(4). doi: 10.1105/tpc.12.4.507.
- Rigó, G. *et al.* (2013) 'Inactivation of plasma membrane-localized CDPK-RELATED KINASE5 decelerates PIN2 exocytosis and root gravitropic response in Arabidopsis', *Plant Cell*, 25(5). doi: 10.1105/tpc.113.110452.
- Robert, S. *et al.* (2010) 'ABP1 mediates auxin inhibition of clathrin-dependent endocytosis in arabidopsis', *Cell*. doi: 10.1016/j.cell.2010.09.027.
- Robert, X. and Gouet, P. (2014) 'Deciphering key features in protein structures with the new ENDscript server', *Nucleic Acids Research*, 42(W1). doi: 10.1093/nar/gku316.
- Rolland-Lagan, A. G. and Prusinkiewicz, P. (2005) 'Reviewing models of auxin canalization in the context of leaf vein pattern formation in Arabidopsis', *Plant Journal*, 44(5). doi: 10.1111/j.1365-313X.2005.02581.x.
- Van Rongen, M. *et al.* (2019) 'Connective auxin transport contributes to strigolactone-mediated shoot branching control independent of the transcription factor BRC1', *PLoS Genetics*, 15(3). doi: [https:// doi.org/10.1371/journal.pgen.1007811](https://doi.org/10.1371/journal.pgen.1007811).

pgen.1008023.

Rosquete, M. R., Waidmann, S. and Kleine-Vehn, J. (2018) 'PIN7 auxin carrier has a preferential role in terminating radial root expansion in *Arabidopsis thaliana*', *International Journal of Molecular Sciences*, 19(4). doi: 10.3390/ijms19041238.

Roychoudhry, S. *et al.* (2019) 'Antagonistic and auxin-dependent phosphoregulation of columella PIN proteins controls lateral root gravitropic setpoint angle in *Arabidopsis*', *bioRxiv*. doi: 10.1101/594838.

Rubery, P. H. (1977) 'The specificity of carrier-mediated auxin transport by suspension-cultured crown gall cells', *Planta*, 135(3). doi: 10.1007/BF00384900.

Rubery, P. H. (1979) 'The effects of 2,4-dinitrophenol and chemical modifying reagents on auxin transport by suspension-cultured crown gall cells', *Planta*, 144(2). doi: 10.1007/BF00387267.

Rubery, P. H. and Sheldrake, A. R. (1973) 'Effect of pH and surface charge on cell uptake of auxin', *Nature New Biology*. doi: 10.1038/newbio244285a0.

Rubery, P. H. and Sheldrake, A. R. (1974) 'Carrier-mediated auxin transport', *Planta*. doi: 10.1007/BF00388387.

Sabater, M. and Rubery, P. H. (1987a) 'Auxin carriers in *Cucurbita* vesicles - I. Imposed perturbations of transmembrane pH and electrical potential gradients characterised by radioactive probes', *Planta*, 171(4). doi: 10.1007/BF00392298.

Sabater, M. and Rubery, P. H. (1987b) 'Auxin carriers in *Cucurbita* vesicles - III. Specificity, with particular reference to 1-naphthylacetic acid', *Planta*, 171(4). doi: 10.1007/BF00392300.

Sachs, T. (1968a) 'On the Determination of the Pattern of Vascular Tissue in Peas', *Annals of Botany*. doi: 10.1093/oxfordjournals.aob.a084249.

Sachs, T. (1968b) 'The role of the root in the induction of xylem differentiation in peas', *Annals of Botany*, 32(2). doi: 10.1093/oxfordjournals.aob.a084216.

Sachs, T. (1969) 'Polarity and the Induction of Organized Vascular Tissues', *Annals*

of Botany. doi: 10.1093/oxfordjournals.aob.a084281.

Sachs, T. (1975) 'The induction of transport channels by auxin', *Planta*. doi: 10.1007/BF00380716.

Sachs, T. (1981) 'The Control of the Patterned Differentiation of Vascular Tissues', *Advances in Botanical Research*. doi: 10.1016/S0065-2296(08)60351-1.

Sachs, T. and Thimann, K. V. (1967) 'The Role of Auxins and Cytokinins in the Release of Buds From Dominance', *American Journal of Botany*. doi: 10.2307/2440896.

de Saint Germain, A. *et al.* (2013) 'Strigolactones stimulate internode elongation independently of gibberellins', *Plant Physiology*, 163(2). doi: 10.1104/pp.113.220541.

De Saint Germain, A. *et al.* (2016) 'An histidine covalent receptor and butenolide complex mediates strigolactone perception', *Nature Chemical Biology*, 12(10). doi: 10.1038/nchembio.2147.

Sanchez Carranza, A. P. *et al.* (2016) 'Hydrolases of the ILR1-like family of *Arabidopsis thaliana* modulate auxin response by regulating auxin homeostasis in the endoplasmic reticulum', *Scientific Reports*, 6. doi: 10.1038/srep24212.

Santelia, D. *et al.* (2005) 'MDR-like ABC transporter AtPGP4 is involved in auxin-mediated lateral root and root hair development', *FEBS Letters*, 579(24). doi: 10.1016/j.febslet.2005.08.061.

Santelia, D. *et al.* (2008) 'Flavonoids redirect PIN-mediated polar auxin fluxes during root gravitropic responses', *Journal of Biological Chemistry*, 283(45). doi: 10.1074/jbc.M710122200.

Dos Santos Maraschin, F., Memelink, J. and Offringa, R. (2009) 'Auxin-induced, SCFTIR1-mediated poly-ubiquitination marks AUX/IAA proteins for degradation', *Plant Journal*, 59(1). doi: 10.1111/j.1365-313X.2009.03854.x.

Sauer, M. *et al.* (2006) 'Canalization of auxin flow by Aux/IAA-ARF-dependent feedback regulation of PIN polarity', *Genes and Development*, 20(20), pp. 2902–2911. doi: 10.1101/gad.390806.

- Scaffidi, A. *et al.* (2013) 'Carlactone-independent seedling morphogenesis in *Arabidopsis*', *Plant Journal*, 76(1). doi: 10.1111/tpj.12265.
- Scaffidi, A. *et al.* (2014) 'Strigolactone hormones and their stereoisomers signal through two related receptor proteins to induce different physiological responses in *Arabidopsis*', *Plant Physiology*, 165(3). doi: 10.1104/pp.114.240036.
- Schaller, G. E., Kieber, J. J. and Shiu, S.-H. (2008) 'Two-Component Signaling Elements and Histidyl-Aspartyl Phosphorelays', *The Arabidopsis Book*. doi: 10.1199/tab.0112.
- Scheres, B. *et al.* (1994) 'Embryonic origin of the *Arabidopsis* primary root and root meristem initials', *Development*, 120(9). doi: 10.1242/dev.120.9.2475.
- Schoof, H. *et al.* (2000) 'The stem cell population of *Arabidopsis* shoot meristems is maintained by a regulatory loop between the CLAVATA and WUSCHEL genes', *Cell*, 100(6). doi: 10.1016/S0092-8674(00)80700-X.
- Seale, M., Bennett, T. and Leyser, O. (2017) 'BRC1 expression regulates bud activation potential but is not necessary or sufficient for bud growth inhibition in *Arabidopsis*', *Development*. doi: 10.1242/dev.145649.
- Sessions, A., Weigel, D. and Yanofsky, M. F. (1999) 'The *Arabidopsis thaliana* MERISTEM LAYER 1 promoter specifies epidermal expression in meristems and young primordia', *Plant Journal*, 20(2). doi: 10.1046/j.1365-313X.1999.00594.x.
- Seto, Y. *et al.* (2019) 'Strigolactone perception and deactivation by a hydrolase receptor DWARF14', *Nature Communications*, 10(1). doi: 10.1038/s41467-018-08124-7.
- Shi, B. *et al.* (2016) 'Two-Step Regulation of a Meristematic Cell Population Acting in Shoot Branching in *Arabidopsis*', *PLoS Genetics*, 12(7). doi: 10.1371/journal.pgen.1006168.
- Shi, Q. *et al.* (2020) 'Genome-wide characterization and expression analyses of the auxin/indole-3-acetic acid (Aux/IAA) gene family in barley (*Hordeum vulgare* L.)', *Scientific Reports*, 10(1). doi: 10.1038/s41598-020-66860-7.

- Shimizu-Mitao, Y. and Kakimoto, T. (2014) 'Auxin sensitivities of all arabidopsis aux/IAAs for degradation in the presence of every TIR1/AFB', *Plant and Cell Physiology*, 55(8). doi: 10.1093/pcp/pcu077.
- Shimizu-Sato, S., Tanaka, M. and Mori, H. (2009) 'Auxin-cytokinin interactions in the control of shoot branching', *Plant Molecular Biology*. doi: 10.1007/s11103-008-9416-3.
- Shinohara, N., Taylor, C. and Leyser, O. (2013) 'Strigolactone Can Promote or Inhibit Shoot Branching by Triggering Rapid Depletion of the Auxin Efflux Protein PIN1 from the Plasma Membrane', *PLoS Biology*. doi: 10.1371/journal.pbio.1001474.
- Šimášková, M. et al. (2015) 'Cytokinin response factors regulate PIN-FORMED auxin transporters', *Nature Communications*. doi: 10.1038/ncomms9717.
- Simon, S. et al. (2013) 'Defining the selectivity of processes along the auxin response chain: A study using auxin analogues', *New Phytologist*, 200(4). doi: 10.1111/nph.12437.
- Smith, R. S. et al. (2006) 'A plausible model of phyllotaxis', *Proceedings of the National Academy of Sciences*, 103(5). doi: 10.1073/pnas.0510457103.
- Snow, M. and Snow, R. (1942) 'The Determination of Axillary Buds', *New Phytologist*, 41(1). doi: 10.1111/j.1469-8137.1942.tb07058.x.
- Snow, R. (1925) 'The correlative inhibition of the growth of axillary buds', *Annals of Botany*. doi: 10.1093/oxfordjournals.aob.a089980.
- Snow, R. (1929) 'The transmission of inhibition through dead stretches of stem', *Annals of Botany*, os-43(2). doi: 10.1093/oxfordjournals.aob.a090168.
- Snow, R. (1931) 'Experiments on growth and inhibition. Part II.-New phenomena of inhibition', *Proceedings of the Royal Society of London. Series B, Containing Papers of a Biological Character*, 108(757). doi: 10.1098/rspb.1931.0041.
- Snow, R. (1935) 'Activation of cambial growth by pure hormones [15]', *Nature*. doi: 10.1038/135876a0.

- Snow, R. and Snow, M. (1932) 'I. Experiments on Phyllotaxis. I. - The effect of isolating a Primordium', *Philosophical transactions of the Royal Society of London*. London : The Society, 221(474–482), pp. 1–43.
- Snowden, K. C. *et al.* (2005) 'The Decreased apical dominance¹/Petunia hybrida Carotenoid Cleavage Dioxygenase⁸ gene affects branch production and plays a role in leaf senescence, root growth, and flower development', *Plant Cell*, 17(3). doi: 10.1105/tpc.104.027714.
- Sorefan, K. *et al.* (2003) 'MAX4 and RMS1 are orthologous dioxygenase-like genes that regulate shoot branching in Arabidopsis and pea', *Genes and Development*, 17(12). doi: 10.1101/gad.256603.
- Staswick, P. E. *et al.* (2005) 'Characterization of an Arabidopsis enzyme family that conjugates amino acids to indole-3-acetic acid', *Plant Cell*, 17(2). doi: 10.1105/tpc.104.026690.
- Steeves, T. A. and Sussex, I. M. (1989) *Patterns in Plant Development*. doi: 10.1017/cbo9780511626227.
- Stepanova, A. N. *et al.* (2008) 'TAA1-Mediated Auxin Biosynthesis Is Essential for Hormone Crosstalk and Plant Development', *Cell*, 133(1). doi: 10.1016/j.cell.2008.01.047.
- Stirnberg, P., van de Sande, K. and Leyser, H. M. O. (2002) 'MAX1 and MAX2 control shoot lateral branching in Arabidopsis', *Development*, 129(5).
- Stoma, S. *et al.* (2008) 'Flux-based transport enhancement as a plausible unifying mechanism for auxin transport in meristem development', *PLoS Computational Biology*. doi: 10.1371/journal.pcbi.1000207.
- Su, Y. H. *et al.* (2020) 'Integration of pluripotency pathways regulates stem cell maintenance in the Arabidopsis shoot meristem', *Proceedings of the National Academy of Sciences of the United States of America*, 117(36). doi: 10.1073/pnas.2015248117.
- Sugawara, S. *et al.* (2009) 'Biochemical analyses of indole-3-acetaldoxime-dependent auxin biosynthesis in Arabidopsis', *Proceedings of the National Academy of Sciences of the United States of America*, 106(13). doi: 10.1073/pnas.0811226106.

- Sussman, M. R. and Goldsmith, M. H. M. (1981) 'The action of specific inhibitors of auxin transport on uptake of auxin and binding of N-1-naphthylphthalamic acid to a membrane site in maize coleoptiles', *Planta*, 152(1).
- Suzuki, T. *et al.* (2001) 'The Arabidopsis sensor His-kinase, AHk4, can respond to cytokinins.', *Plant & cell physiology*. doi: 10.1093/pcp/pce037.
- Swarup, R. *et al.* (2001) 'Localization of the auxin permease AUX1 suggests two functionally distinct hormone transport pathways operate in the Arabidopsis root apex', *Genes and Development*, 15(20). doi: 10.1101/gad.210501.
- Szemenyei, H., Hannon, M. and Long, J. A. (2008) 'TOPLESS mediates auxin-dependent transcriptional repression during Arabidopsis embryogenesis', *Science*, 319(5868). doi: 10.1126/science.1151461.
- Szerszen, J. B., Szczyglowski, K. and Bandurski, R. S. (1994) 'iaglu, a gene from Zea mays involved in conjugation of growth hormone indole-3-acetic acid', *Science*, 265(5179). doi: 10.1126/science.8085154.
- Takubo, E. *et al.* (2020) 'Role of Arabidopsis INDOLE-3-ACETIC ACID CARBOXYL METHYLTRANSFERASE 1 in auxin metabolism', *Biochemical and Biophysical Research Communications*, 527(4). doi: 10.1016/j.bbrc.2020.05.031.
- Tam, Y. Y., Epstein, E. and Normanly, J. (2000) 'Characterization of auxin conjugates in Arabidopsis. Low steady-state levels of indole-3-acetyl-aspartate, indole-3-acetyl-glutamate, and indole-3-acetyl-glucose', *Plant Physiology*, 123(2). doi: 10.1104/pp.123.2.589.
- Tamas, I. A. *et al.* (1989) 'Effect of plant growth substances on the growth of axillary buds in cultured stem segments of Phaseolus vulgaris L.', *Plant Growth Regulation*, 8(2). doi: 10.1007/BF00024774.
- Tan, X. *et al.* (2007) 'Mechanism of auxin perception by the TIR1 ubiquitin ligase', *Nature*, 446(7136). doi: 10.1038/nature05731.
- Tanaka, M. *et al.* (2006) 'Auxin controls local cytokinin biosynthesis in the nodal stem in apical dominance', *Plant Journal*. doi: 10.1111/j.1365-313X.2006.02656.x.
- Tanimoto, M. *et al.* (2007) 'Pax I - I partially suppresses gain-of-function mutations

- in *Arabidopsis* AXR3/IAA 17', *BMC Plant Biology*, 7. doi: 10.1186/1471-2229-7-20.
- Tao, Y. *et al.* (2008) 'Rapid Synthesis of Auxin via a New Tryptophan-Dependent Pathway Is Required for Shade Avoidance in Plants', *Cell*, 133(1). doi: 10.1016/j.cell.2008.01.049.
- Tashiro, S. *et al.* (2009) 'Changes in growth kinetics of stamen filaments cause inefficient pollination in *massugu2*, an auxin insensitive, dominant mutant of *Arabidopsis thaliana*', *Physiologia Plantarum*, 137(2). doi: 10.1111/j.1399-3054.2009.01271.x.
- Teale, W. D. *et al.* (2021) 'Flavonol-mediated stabilization of PIN efflux complexes regulates polar auxin transport', *EMBO Journal*, 40(1). doi: 10.15252/embj.2020104416.
- Teale, W. D., Paponov, I. A. and Palme, K. (2006) 'Auxin in action: Signalling, transport and the control of plant growth and development', *Nature Reviews Molecular Cell Biology*. doi: 10.1038/nrm2020.
- Teale, W. and Palme, K. (2018) 'Naphthylphthalamic acid and the mechanism of polar auxin transport', *Journal of Experimental Botany*. doi: 10.1093/jxb/erx323.
- Teh, O. K. and Moore, I. (2007) 'An ARF-GEF acting at the Golgi and in selective endocytosis in polarized plant cells', *Nature*, 448(7152). doi: 10.1038/nature06023.
- Terasaka, K. *et al.* (2005) 'PGP4, an ATP binding cassette P-glycoprotein, catalyzes auxin transport in *Arabidopsis thaliana* roots', *Plant Cell*, 17(11). doi: 10.1105/tpc.105.035816.
- Thimann, K. V., Kerckhoff, W. G. and Skoog, F. (1934) 'On the inhibition of bud development and other functions of growth substance in *vicia faba*', *Proceedings of the Royal Society B*, cxiv(789), pp. 317–339.
- Thimann, K. V. and Skoog, F. (1933) 'Studies on the Growth Hormone of Plants: III. The Inhibiting Action of the Growth Substance on Bud Development', *Proceedings of the National Academy of Sciences*. doi: 10.1073/pnas.19.7.714.

Ticchiarelli, F. (2019) The role of strigolactone and auxin in the regulation of shoot branching. University of Cambridge.

Titapiwatanakun, B. *et al.* (2009) 'ABCB19/PGP19 stabilises PIN1 in membrane microdomains in Arabidopsis', *Plant Journal*. doi: 10.1111/j.1365-313X.2008.03668.x.

Tiwari, S. B., Hagen, G. and Guilfoyle, T. J. (2004) 'Aux/IAA Proteins Contain a Potent Transcriptional Repression Domain', *Plant Cell*, 16(2). doi: 10.1105/tpc.017384.

To, J. P. C. *et al.* (2004) 'Type-A Arabidopsis response regulators are partially redundant negative regulators of cytokinin signaling.', *The Plant Cell*, 16(3). doi: 10.1105/tpc.018978.2.

Di Tommaso, P. *et al.* (2011) 'T-Coffee: A web server for the multiple sequence alignment of protein and RNA sequences using structural information and homology extension', *Nucleic Acids Research*, 39(SUPPL. 2). doi: 10.1093/nar/gkr245.

Trotochaud, A. E., Jeong, S. and Clark, S. E. (2000) 'CLAVATA3, a multimeric ligand for the CLAVATA1 receptor-kinase', *Science*, 289(5479). doi: 10.1126/science.289.5479.613.

Turnbull, C. G. N., Booker, J. P. and Leyser, H. M. O. (2002) 'Micrografting techniques for testing long-distance signalling in Arabidopsis', *Plant Journal*, 32(2). doi: 10.1046/j.1365-313X.2002.01419.x.

Ueda, H. and Kusaba, M. (2015) 'Strigolactone regulates leaf senescence in concert with ethylene in arabidopsis', *Plant Physiology*, 169(1). doi: 10.1104/pp.15.00325.

Ulmasov, T. *et al.* (1995) 'Composite structure of auxin response elements', *Plant Cell*, 7(10). doi: 10.2307/3870023.

Ulmasov, T. *et al.* (1997) 'Aux/IAA Proteins Repress Expression of Reporter Genes Containing Natural and Highly Active Synthetic Auxin Response Elements', *The Plant Cell*. doi: 10.2307/3870557.

- Ulmasov, T., Hagen, G. and Guilfoyle, T. J. (1997) 'ARF1, a transcription factor that binds to auxin response elements', *Science*, 276(5320). doi: 10.1126/science.276.5320.1865.
- Umehara, M. *et al.* (2008) 'Inhibition of shoot branching by new terpenoid plant hormones', *Nature*, 455(7210). doi: 10.1038/nature07272.
- Vernoux, T. *et al.* (2000) 'PIN-FORMED 1 regulates cell fate at the periphery of the shoot apical meristem', *Development*, 127(23). doi: 10.1242/dev.127.23.5157.
- Vernoux, T. *et al.* (2011) 'The auxin signalling network translates dynamic input into robust patterning at the shoot apex', *Molecular Systems Biology*, 7. doi: 10.1038/msb.2011.39.
- Wabnik, K. *et al.* (2010) 'Emergence of tissue polarization from synergy of intracellular and extracellular auxin signaling', *Molecular Systems Biology*, 6. doi: 10.1038/msb.2010.103.
- Waldie, T. and Leyser, O. (2018) 'Cytokinin targets auxin transport to promote shoot branching', *Plant Physiology*. Cambridge. doi: <https://doi.org/10.1104/pp.17.01691>.
- Wang, B. *et al.* (2015) 'Tryptophan-independent auxin biosynthesis contributes to early embryogenesis in Arabidopsis', *Proceedings of the National Academy of Sciences of the United States of America*, 112(15). doi: 10.1073/pnas.1503998112.
- Wang, J. *et al.* (2017) 'Cytokinin signaling activates WUSCHEL expression during axillary meristem initiation', *Plant Cell*, 29(6). doi: 10.1105/tpc.16.00579.
- Wang, L. *et al.* (2015) 'Strigolactone Signaling in Arabidopsis Regulates Shoot Development by Targeting D53-Like SMXL Repressor Proteins for Ubiquitination and Degradation', *The Plant Cell*. doi: 10.1105/tpc.15.00605.
- Wang, L. *et al.* (2020) 'Transcriptional regulation of strigolactone signalling in Arabidopsis', *Nature*, 583(7815). doi: 10.1038/s41586-020-2382-x.
- Wang, Q. *et al.* (2014) 'Auxin depletion from the leaf axil conditions competence for axillary meristem formation in Arabidopsis and tomato', *Plant Cell*, 26(5). doi: 10.1105/tpc.114.123059.

- Wang, R. and Estelle, M. (2014) 'Diversity and specificity: Auxin perception and signaling through the TIR1/AFB pathway', *Current Opinion in Plant Biology*. doi: 10.1016/j.pbi.2014.06.006.
- Wang, Y. *et al.* (2014) 'The stem cell niche in leaf axils is established by auxin and cytokinin in Arabidopsis', *Plant Cell*, 26(5). doi: 10.1105/tpc.114.123083.
- Waters, M. T., Nelson, D. C., *et al.* (2012) 'Specialisation within the DWARF14 protein family confers distinct responses to karrikins and strigolactones in Arabidopsis', *Development*, 139(7). doi: 10.1242/dev.074567.
- Waters, M. T., Brewer, P. B., *et al.* (2012) 'The Arabidopsis ortholog of rice DWARF27 acts upstream of MAX1 in the control of plant development by Strigolactones', *Plant Physiology*, 159(3). doi: 10.1104/pp.112.196253.
- Weller, B. *et al.* (2017) 'Dynamic PIN-FORMED auxin efflux carrier phosphorylation at the plasma membrane controls auxin efflux-dependent growth', *Proceedings of the National Academy of Sciences*. doi: 10.1073/pnas.1614380114.
- Went, F. (1928) 'Wuchsstoff und Wachstum', *Recueil des Travaux Botaniques Neerlandais*, 25, pp. 1–116.
- Went F. W. 1903-1990. (Frits Warmolt) (1937) *Phytohormones*. New York : Macmillan,.
- Werner, T. *et al.* (2003) 'Cytokinin-Deficient Transgenic Arabidopsis Plants Show Multiple Developmental Alterations Indicating Opposite Functions of Cytokinins in the Regulation of Shoot and Root Meristem Activity', *Plant Cell*, 15(11). doi: 10.1105/tpc.014928.
- Westfall, C. S. *et al.* (2010) 'Modulating plant hormones by enzyme action: The GH3 family of acyl acid amido synthetases', *Plant Signaling and Behavior*, 5(12). doi: 10.4161.psb.5.12.13941.
- Westfall, C. S. *et al.* (2016) 'Arabidopsis thaliana GH3.5 acyl acid amido synthetase mediates metabolic crosstalk in auxin and salicylic acid homeostasis', *Proceedings of the National Academy of Sciences of the United States of America*, 113(48). doi: 10.1073/pnas.1612635113.

- Wickson, M. and Thimann, K. V. (1958) 'The Antagonism of Auxin and Kinetin in Apical Dominance', *Physiologia Plantarum*. doi: 10.1111/j.1399-3054.1958.tb08426.x.
- Wilson, A. K. *et al.* (1990) 'A dominant mutation in *Arabidopsis* confers resistance to auxin, ethylene and abscisic acid', *MGG Molecular & General Genetics*, 222(2–3). doi: 10.1007/BF00633843.
- Wisniewska, J. *et al.* (2006) 'Polar PIN localization directs auxin flow in plants', *Science*. doi: 10.1126/science.1121356.
- Wu, M. F. *et al.* (2015) 'Auxin-regulated chromatin switch directs acquisition of flower primordium founder fate', *eLife*, 2015(4). doi: 10.7554/eLife.09269.
- Xu, X. *et al.* (2021) 'Strigolactones regulate sepal senescence in *Arabidopsis*', *Journal of Experimental Botany*, 72(15). doi: 10.1093/jxb/erab199.
- Yamada, M. *et al.* (2009) 'The TRANSPORT INHIBITOR RESPONSE2 Gene is required for auxin synthesis and diverse aspects of plant development', *Plant Physiology*, 151(1). doi: 10.1104/pp.109.138859.
- Yamada, Y. *et al.* (2014) 'Strigolactone signaling regulates rice leaf senescence in response to a phosphate deficiency', *Planta*, 240(2). doi: 10.1007/s00425-014-2096-0.
- Yamaguchi, N. *et al.* (2017) 'Fine-tuning of auxin homeostasis governs the transition from floral stem cell maintenance to gynoecium formation', *Nature Communications*, 8(1). doi: 10.1038/s41467-017-01252-6.
- Yamakawa, T. *et al.* (1979) 'Stability of indole-3-acetic acid to autoclaving, aeration and light illumination', *Agricultural and Biological Chemistry*. doi: 10.1080/00021369.1979.10863551.
- Yan, H. *et al.* (2007) 'Rice tillering dwarf mutant dwarf3 has increased leaf longevity during darkness-induced senescence or hydrogen peroxide-induced cell death', *Genes and Genetic Systems*, 82(4). doi: 10.1266/ggs.82.361.
- Yang, H. and Murphy, A. S. (2009) 'Functional expression and characterization of *Arabidopsis* ABCB, AUX 1 and PIN auxin transporters in *Schizosaccharomyces pombe*', *Plant Journal*, 59(1). doi: 10.1111/j.1365-313X.2009.03856.x.

- Yang, Y. *et al.* (2008) 'Inactive methyl indole-3-acetic acid ester can be hydrolyzed and activated by several esterases belonging to the AtMES esterase family of arabidopsis', *Plant Physiology*, 147(3). doi: 10.1104/pp.108.118224.
- Zažímalová, E. *et al.* (2007) 'Polar transport of the plant hormone auxin - The role of PIN-FORMED (PIN) proteins', *Cellular and Molecular Life Sciences*. doi: 10.1007/s00018-007-6566-4.
- Zhang, J. *et al.* (2016) 'DAO1 catalyzes temporal and tissue-specific oxidative inactivation of auxin in *Arabidopsis thaliana*', *Proceedings of the National Academy of Sciences of the United States of America*, 113(39). doi: 10.1073/pnas.1604769113.
- Zhang, J. *et al.* (2020) 'Strigolactones inhibit auxin feedback on PIN-dependent auxin transport canalization', *Nature Communications*, 11(1). doi: 10.1038/s41467-020-17252-y.
- Zhang, Y. *et al.* (2014) 'Rice cytochrome P450 MAX1 homologs catalyze distinct steps in strigolactone biosynthesis', *Nature chemical biology*, 10(12). doi: 10.1038/nchembio.1660.
- Zhang, Y. *et al.* (2018) 'A transportome-scale amiRNA-based screen identifies redundant roles of *Arabidopsis* ABCB6 and ABCB20 in auxin transport', *Nature Communications*, 9(1). doi: 10.1038/s41467-018-06410-y.
- Zhang, Y. *et al.* (2020) 'Functional innovations of PIN auxin transporters mark crucial evolutionary transitions during rise of flowering plants', *Science Advances*, 6(50). doi: 10.1126/sciadv.abc8895.
- Zhao, Y. *et al.* (2001) 'A role for flavin monooxygenase-like enzymes in auxin biosynthesis', *Science*, 291(5502). doi: 10.1126/science.291.5502.306.
- Zhao, Z. *et al.* (2010) 'Hormonal control of the shoot stem-cell niche', *Nature*, 465(7301). doi: 10.1038/nature09126.
- Zheng, Z. *et al.* (2016) 'Local auxin metabolism regulates environment-induced hypocotyl elongation', *Nature Plants*, 2(4). doi: 10.1038/NPLANTS.2016.25.
- Zhou, F. *et al.* (2013) 'D14-SCF D3 -dependent degradation of D53 regulates strigolactone signalling', *Nature*, 504(7480). doi: 10.1038/nature12878.

- Zhou, Y. *et al.* (2015) 'Control of plant stem cell function by conserved interacting transcriptional regulators', *Nature*, 517(7534). doi: 10.1038/nature13853.
- Zhou, Y. *et al.* (2018) 'Hairy meristem with wuschel confines *clavata3* expression to the outer apical meristem layers', *Science*, 361(6401). doi: 10.1126/science.aar8638.
- Zimmerman, P. W. and Wilcoxon, F. (1935) 'Several Chemical Growth Substances which Cause Initiation of Roots and Other Responses in Plants', *Contributions from Boyce Thompson Institute*, 7.
- Zou, J. *et al.* (2006) 'The rice HIGH-TILLERING DWARF1 encoding an ortholog of Arabidopsis MAX3 is required for negative regulation of the outgrowth of axillary buds', *Plant Journal*, 48(5). doi: 10.1111/j.1365-313X.2006.02916.x.
- Zourelidou, M. *et al.* (2014) 'Auxin efflux by PIN-FORMED proteins is activated by two different protein kinases, D6 PROTEIN KINASE and PINOID', *eLife*. doi: 10.7554/eLife.02860.
- Zubieta, C. *et al.* (2003) 'Structural basis for substrate recognition in the salicylic acid carboxyl methyltransferase family', *Plant Cell*, 15(8). doi: 10.1105/tpc.014548.

Appendix B

Experimental methods

Genotype	Source	Publication	Name in text
Col-0	Leyser lab stock	N/A	
<i>pin1-613</i>	Leyser lab stock	(Bennett <i>et al.</i> , 2006)	<i>pin1</i>
<i>d14 PIN1::PIN1-GFP</i>	Leyser lab stock	(Bennett <i>et al.</i> , 2016)	<i>d14 PIN1-GFP</i>
<i>max2-1</i>	Leyser lab stock	(Stirnberg, van de Sande and Leyser, 2002)	<i>max2-1</i>
<i>pin1 PIN1::PIN1-GFP</i>	Leyser lab stock	(Xu <i>et al.</i> , 2006)	PIN1-GFP
<i>pin3 PIN3::PIN3-GFP</i>	Leyser lab stock	(Blilou <i>et al.</i> , 2005)	PIN3-GFP
<i>pin4 PIN4::PIN4-GFP</i>	Leyser lab stock	(Blilou <i>et al.</i> , 2005)	PIN4-GFP
<i>pin7 PIN7::PIN7-GFP</i>	Leyser lab stock	(Blilou <i>et al.</i> , 2005)	PIN7-GFP
<i>DR5rev::GFP</i>	Leyser lab stock	(Friml <i>et al.</i> , 2003)	<i>DR5rev::GFP</i>
<i>DR5::NLS-GFP</i>	Leyser lab stock	(Heisler <i>et al.</i> , 2005)	<i>DR5::NLS-GFP</i>
<i>aux1-21 PIN1::PIN1-GFP</i>	Leyser lab stock	Van rongen, unpublished	<i>aux1-21 PIN1-GFP</i>
<i>pin1 PIN1:PIN3-PIN1_{L2}-GFP</i>	Leyser lab stock	Ticchiarelli, unpublished	<i>pin1 PIN1:PIN3-PIN1_{L2}-GFP</i>
<i>Col-0 BdSoPIN1-citrine</i>	Leyser lab stock	(O'Connor <i>et al.</i> , 2017)	SoPIN1-citrine
<i>pin1 BdSoPIN1-citrine</i>	Leyser lab stock	(O'Connor <i>et al.</i> , 2017)	<i>pin1</i> SoPIN1-citrine
<i>Col-0 BdPIN1b-citrine</i>	Leyser lab stock	(O'Connor <i>et al.</i> , 2017)	PIN1b-citrine
<i>pin1 BdPIN1b-citrine</i>	Leyser lab stock	(O'Connor <i>et al.</i> , 2017)	<i>pin1</i> PIN1b-citrine

Table B.1 | Summary of genotypes used

Primer ID	Name	Purpose	Sequence
1	344 - Citrine Seq R	PIN1b-Citrine and SoPIN1-Citrine genotyping	GAAGCACATCAGGCCG-TAG
2	524_Bradi4g26300_4230_F	SoPIN1-Citrine genotyping	CGTTCCGTGTTGATTC-CGATG
3	541_Bradi3g59520_PIN1b_5084_F	PIN1b-Citrine genotyping	TGATGCTCTTCATGTTC-GAGTACC
4	AB_1_AtPIN1 promoter_seq3_Rv	AtPIN1 promoter sequencing primer	TGAAGGTCCATGCGT-TTGTG
5	AB_2_AtPIN1TM_seq1_Rv	AtPIN1 Tm- domain sequencing primer	TGAGGTCGCCG-GAGAAATTA
6	AB_3_AtPIN1TM_seq2_Fw	AtPIN1 Tm-domain sequencing primer	GCTCCACCATGAT-TACGGC
7	AB_4_AtPIN1HL_seq1_Fw	AtPIN1 HL-domain sequencing primer	CAAGGCTTATCTGCGA-CACC
8	AB_5_AtPIN1HL_seq2_Rv	AtPIN1 HL-domain sequencing primer	AAACTCTTCCCTCTC-CACGT
9	AB_6_AtPIN1TM_seq3_F	AtPIN1 Tm-domain sequencing primer	ACAACCACTACCTGAG-CACC
10	MVR036-LBb1.3	pin-613 genotyping	ATTTTGCCGATTTG-GAAC
12	MVR086-pin1-613 LP	pin-613 genotyping	CAAAA-CACCCCCAAAATTC
13	PIN1pro-GW-F	amplification PIN1 promoter	GGGGACAACCTTGTATA-GAAAAGTTGTTACCCT-CATCCATCATTAACTT
14	PIN1pro-GW-R	amplification PIN1 promoter	GGGGACTGCTTTTTTGT-ACAACTTGTCTTTTGT-TCGCCGAGAAGAGA
15	FT_60_AtPIN1 promoter_seq1_Fw	AtPIN1 promoter sequencing primer	TTACCCTCATCCATCAT-TAACTT
16	FT_61_AtPIN1 promoter_seq2_Fw	AtPIN1 promoter sequencing primer	AAGGCCGCCTCTTTCAC-TATC
17	AB_11_AtPIN1:PIN1-P3L2-GFP_SEQ-RP	Sequencing PIN1-PIN3 chimera	CTTAGCCTGCGTCGT-TTTGT
18	AB_12_AtPIN1:PIN1-P3L2-GFP_SEQ-LP	Sequencing PIN1-PIN3 chimera	CACCGCTACGAACGAT-CATC

Table B.2 | Primers used